DEVELOPMENT OF CIRCADIAN CLOCK FUNCTIONS

EDITED BY: Daisuke Ono, Rae Silver, Jihwan Myung, Takahiro J. Nakamura and Jeff Jones

PUBLISHED IN: Frontiers in Neuroscience

frontiers Research Topics

frontiers

ISSN 1664-8714
ISBN 978-2-88971-422-3
DOI 10.3389/978-2-88971-422-3

About Frontiers

Frontiers is more than just an open-access publisher of scholarly articles: it is a pioneering approach to the world of academia, radically improving the way scholarly research is managed. The grand vision of Frontiers is a world where all people have an equal opportunity to seek, share and generate knowledge. Frontiers provides immediate and permanent online open access to all its publications, but this alone is not enough to realize our grand goals.

Frontiers Journal Series

The Frontiers Journal Series is a multi-tier and interdisciplinary set of open-access, online journals, promising a paradigm shift from the current review, selection and dissemination processes in academic publishing. All Frontiers journals are driven by researchers for researchers; therefore, they constitute a service to the scholarly community. At the same time, the Frontiers Journal Series operates on a revolutionary invention, the tiered publishing system, initially addressing specific communities of scholars, and gradually climbing up to broader public understanding, thus serving the interests of the lay society, too.

Dedication to Quality

Each Frontiers article is a landmark of the highest quality, thanks to genuinely collaborative interactions between authors and review editors, who include some of the world's best academicians. Research must be certified by peers before entering a stream of knowledge that may eventually reach the public - and shape society; therefore, Frontiers only applies the most rigorous and unbiased reviews.
Frontiers revolutionizes research publishing by freely delivering the most outstanding research, evaluated with no bias from both the academic and social point of view. By applying the most advanced information technologies, Frontiers is catapulting scholarly publishing into a new generation.

What are Frontiers Research Topics?

Frontiers Research Topics are very popular trademarks of the Frontiers Journals Series: they are collections of at least ten articles, all centered on a particular subject. With their unique mix of varied contributions from Original Research to Review Articles, Frontiers Research Topics unify the most influential researchers, the latest key findings and historical advances in a hot research area! Find out more on how to host your own Frontiers Research Topic or contribute to one as an author by contacting the Frontiers Editorial Office: frontiersin.org/about/contact

DEVELOPMENT OF CIRCADIAN CLOCK FUNCTIONS

Topic Editors:
Daisuke Ono, Nagoya University, Japan
Rae Silver, Columbia University, United States
Jihwan Myung, Taipei Medical University, Taiwan
Takahiro J. Nakamura, Meiji University, Japan
Jeff Jones, Washington University in St. Louis, United States

Citation: Ono, D., Silver, R., Myung, J., Nakamura, T. J., Jones, J., eds. (2021). Development of Circadian Clock Functions. Lausanne: Frontiers Media SA.
doi: 10.3389/978-2-88971-422-3

Table of Contents

frontiers in Neuroscience

EDITORIAL
published: 09 August 2021
doi: 10.3389/fnins.2021.735007

Editorial: Development of Circadian Clock Functions

Jihwan Myung[1,2]*, *Takahiro J. Nakamura*[3], *Jeff R. Jones*[4], *Rae Silver*[5,6] *and Daisuke Ono*[7,8]*

[1] Graduate Institute of Mind, Brain, and Consciousness, Taipei Medical University, Taipei, Taiwan, [2] Brain and Consciousness Research Center, Taipei Medical University-Shuang Ho Hospital, Ministry of Health and Welfare, Taipei, Taiwan, [3] Laboratory of Animal Physiology, School of Agriculture, Meiji University, Tokyo, Japan, [4] Department of Biology, Washington University in St Louis, St. Louis, MO, United States, [5] Department of Psychology, Columbia University, New York, NY, United States, [6] Department of Neuroscience and Behavior, Barnard College of Columbia University, New York, NY, United States, [7] Department of Neuroscience II, Research Institute of Environmental Medicine, Nagoya University, Nagoya, Japan, [8] Department of Neural Regulation, Nagoya University Graduate School of Medicine, Nagoya, Japan

Keywords: circadian rhythm, development, plasticity, neural network, aging

Editorial on the Research Topic

Development of Circadian Clock Functions

The temporal organization of physiological functions such as sleep/wakefulness or body temperature are regulated by the circadian clock. This intrinsic clock starts ticking in the embryo, matures during development, and is attenuated in the elderly. This is illustrated by weakening synchrony, entrainment, and outputs of cellular circadian rhythms in the central circadian clock, located in the suprachiasmatic nucleus (SCN) of the hypothalamus. The age-related diminution can contribute to susceptibility to diseases, such as sleep disorders, infertility, diabetes, and mental disorders. Over the course of our lives, a variety of internal and external factors come into play, under the influence of the circadian clock. The inherent developmental plasticity of the circadian system, the focus of the present issue, is critical for the establishment of normal bodily functions and their adaptation to the changing environment on earth.

At the single-cell level, the circadian clock is a transcriptional-transcriptional feedback loop (TTFL) that underlies the 24-h rhythmicity in gene expression, which is maintained even under challenges on some of the feedback components of the loop (Chiou et al. in this collection). Chiou et al. created sextuple knockout (*Cry1/2*$^{-/-}$; *Per1/2*$^{-/-}$; *Nr1d1/2*$^{-/-}$) cell lines using the CRISPR/Cas9 system and found that serum-shock inhibited CLOCK-BMAL1 in the absence of CRY, PER, and NR1D proteins. The finding lets us speculate on the TTFL during early development, where the stoichiometry of clock components is different from adults (Li and Davis, 2005). During development, the molecular components required for the emergence of the molecular circadian clock are produced *de novo* in embryonic stem cells (Yagita et al., 2010), causing time-delayed ontogenesis of tissue-level circadian clocks (Sládek et al., 2007) including the networks of the central circadian clock in the SCN (Cheng and Cheng in this collection). The network-level development confers both robustness and coding complexity to circadian clocks. Coupling among circadian clocks not only synchronizes component cellular oscillators but also provides robustness against genetic perturbations (Liu et al., 2007). The characteristics of the coupled cells [such as the peptidergic expression profile (Romero and Silver, 1990)] and the nature of coupling itself, changes through development, and can allow for unexpected circadian oscillations in the perinatal network (Ono et al., 2013; Tokuda et al., 2015). Such early developmental processes may be comparable to excessive positive coupling and subsequent pruning found in other brain regions. In the SCN, network fine-tuning occurs developmentally from single-polarity to dual-polarity coupling to facilitate the complex encoding of seasonal time in the system (Obrietan and Van den Pol, 1995; Myung et al., 2015).

OPEN ACCESS

Edited and reviewed by:
Luis de Lecea,
Stanford University, United States

***Correspondence:**
Jihwan Myung
jihwan@tmu.edu.tw
Daisuke Ono
dai-ono@riem.nagoya-u.ac.jp

Specialty section:
This article was submitted to Sleep and Circadian Rhythms, a section of the journal Frontiers in Neuroscience

Received: *01 July 2021*
Accepted: *09 July 2021*
Published: *09 August 2021*

Citation:
Myung J, Nakamura TJ, Jones JR, Silver R and Ono D (2021) Editorial: Development of Circadian Clock Functions. Front. Neurosci. 15:735007. doi: 10.3389/fnins.2021.735007

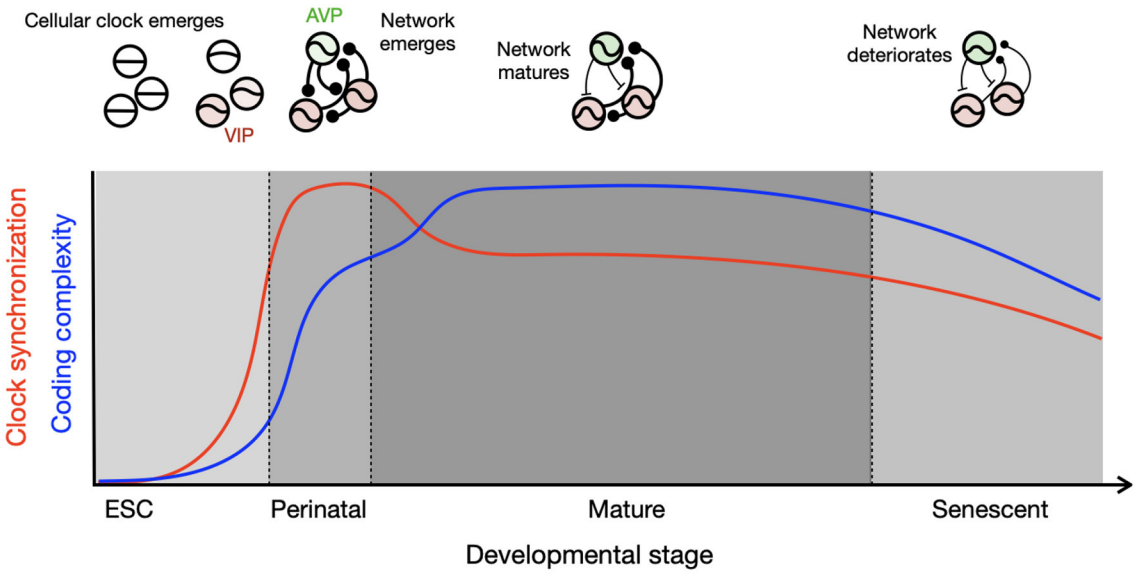

FIGURE 1 | Development of cellular and network circadian clocks characterized by clock synchronization and complexity. Single-cell molecular clocks and their inter-cellular network evolve together through the course of development, which results in divergent parallel development of synchronization (red) and complexity (blue). The circadian clock emerges in single cells after embryonic stem cell (ESC) stage and connections are made in single positive polarity (round ending) in the perinatal stage pushed by homogeneously excitatory GABA and high expression of GR, resulting in strong synchronization among the clock cells. Diversity in neuropeptidergic expression and mixture of excitatory and inhibitory GABA (T-shaped ending) develop toward maturation, which slightly lowers the degree of synchronization but allows for complexity by a wider distribution of clock phases as found during seasonal time encoding. The schematics in the upper panel illustrate oscillatory properties of single cells and network coupling for each developmental stage, with thicker connection line indicating stronger coupling.

The unique conditions in early development have clinical implications for preterm infant development in the neonatal intensive care unit (NICU) (Hazelhoff et al. in this collection). Light as the primary zeitgeber can impact perinatal development, and impairment in light entrainment has been implicated in an autism model mouse (Alamilla et al. in this collection). In this study, the authors found that Shank3$^{+/-}$ mice (an animal model linked to autism, with a deletion in the ankyrin repeat domain) showed larger light pulse-induced phase shifts and increased VIP immunoreactivity in SCN neurons. One convincing explanation for preterm mortality in the NICU comes from the absence of the placenta-fetus platform where rich circadian endocrine exchanges occur (Astiz and Oster in this collection). As a demonstration of this principle, LuŽná et al. (in this collection) reported direct alterations to the molecular clock of the fetal SCN after maternal chrono-disruption. The LuŽná et al. study and that of Caba et al. (in this collection) hint at the role of feeding entrainment in early development. At the other end of the developmental spectrum, aging is associated with a decline in circadian timekeeping (Nakamura et al., 2011). This can be caused in part by age-related changes in single cell properties of the SCN (Ashimori et al.; Rezwana et al., both in this collection). Relevant to this point, circadian feeding entrainment appears to play a role in normalizing physiological outputs despite an aging circadian clock (Aoyama et al., in this collection).

The systematic changes in circadian clocks across the lifetime may be summarized by a schematic, which tracks the co-evolution of the single-cell molecular clock and the network (**Figure 1**). Intracellular events such as the TTFL and the brain network develop with different timing. The TTFL develops during the embryonic stage, but the network matures after birth. Although the transcriptional circuits of the circadian clock in individual cells are initially incomplete, they oscillate and synchronize through intercellular coupling in the perinatal phase. The high degree of synchronization in this stage is supported by the rhythmic availability of glucocorticoids, an exceptionally strong circadian clock resetting hormone. This signal is communicated embryonically *via* the placenta and postnatally *via* maternal milk, combined with a high expression of glucocorticoid receptors in these stages (Astiz and Oster). Each clock cell is a weak oscillator at these developmental time points, so they can be influenced by non-photic cues such as those derived from feeding. At maturation, the coupled circadian clock network is organized into a heterogeneous system through a diverse expression of peptides (Varadarajan et al., 2018). The robustness of the both cellular and network of clocks declines toward the end of life, and the clocks may again become more susceptible to feeding entrainment.

In summary, the work in this issue highlights the finding that the gradual modifications that occur in cells and networks among cells shape internal circadian homeostasis and hence the temporal boundaries of events in the brain and the rest

of the body. Developmental changes throughout the life span direct the emergence and organization of circadian clocks, the clocks themselves have profound effects on development throughout life.

AUTHOR CONTRIBUTIONS

JM and DO wrote the manuscript with support of TJN, JRJ, and RS. All authors contributed to the article and approved the submitted version.

FUNDING

This work was supported by the Higher Education Sprout Project by the Taiwan Ministry of Education (DP2-109-21121-01-N-01, DP2-110-21121-01-N-01), the Taiwan Ministry of Science and Technology (110-2314-B-038-162, 110-2311-B-038-003, 109-2320-B-038-020, 109-2314-B-038-071, 109-2314-B-038-106 - MY3) (to JM), National Science Foundation (1749500) and National Institute of Health (1R01NS102962) (to RS), and JSPS KAKENHI (18H02477, 20KK0177, 21H00422, 21H00307, 21H02526) (to DO).

REFERENCES

Li, X., and Davis, F. C. (2005). Developmental expression of clock genes in the Syrian hamster. *Dev. Brain Res.* 158, 31–40. doi: 10.1016/j.devbrainres.2005.05.005

Liu, A. C., Welsh, D. K., Ko, C. H., Tran, H. G., Zhang, E. E., Priest, A. A., et al. (2007). Intercellular coupling confers robustness against mutations in the SCN circadian clock network. *Cell* 129, 605–616. doi: 10.1016/j.cell.2007.02.047

Myung, J., Hong, S., DeWoskin, D., De Schutter, E., Forger, D. B., and Takumi, T. (2015). GABA-mediated repulsive coupling between circadian clock neurons in the SCN encodes seasonal time. *Proc. Natl. Acad. Sci. U. S. A.* 112, E3920–E3929. doi: 10.1073/pnas.1421200112

Nakamura, T. J., Nakamura, W., Yamazaki, S., Kudo, T., Cutler, T., Colwell, C. S., et al. (2011). Age-related decline in circadian output. *J. Neurosci.* 31, 10201–10205. doi: 10.1523/JNEUROSCI.0451-11.2011

Obrietan, K., and Van den Pol, A. N. (1995). GABA neurotransmission in the hypothalamus: developmental reversal from Ca2+ elevating to depressing. *J. Neurosci.* 15, 5065–5077. doi: 10.1523/JNEUROSCI.15-07-05065.1995

Ono, D., Honma, S., and Honma, K. I. (2013). Cryptochromes are critical for the development of coherent circadian rhythms in the mouse suprachiasmatic nucleus. *Nat. Commun.* 4, 1–11. doi: 10.1038/ncomms2670

Romero, M. T., and Silver, R. (1990). Time course of peptidergic expression in fetal suprachiasmatic nucleus transplanted into adult hamster. *Dev. Brain Res.* 57, 1–6. doi: 10.1016/0165-3806(90)90177-Z

Sládek, M., Jindráková, Z., Bendová, Z., and Sumová, A. (2007). Postnatal ontogenesis of the circadian clock within the rat liver. *Am. J. Physiol. Regul. Integr. Comp. Physiol.* 292, R1224–R1229. doi: 10.1152/ajpregu.00184.2006

Tokuda, I. T., Ono, D., Ananthasubramaniam, B., Honma, S., Honma, K. I., and Herzel, H. (2015). Coupling controls the synchrony of clock cells in development and knockouts. *Biophys. J.* 109, 2159–2170. doi: 10.1016/j.bpj.2015.09.024

Varadarajan, S., Tajiri, M., Jain, R., Holt, R., Ahmed, Q., LeSauter, J., et al. (2018). Connectome of the suprachiasmatic nucleus: new evidence of the core-shell relationship. *eNeuro* 5:e0205-18.2018. doi: 10.1523/ENEURO.0205-18.2018

Yagita, K., Horie, K., Koinuma, S., Nakamura, W., Yamanaka, I., Urasaki, A., et al. (2010). Development of the circadian oscillator during differentiation of mouse embryonic stem cells *in vitro*. *Proc. Natl. Acad. Sci. U. S. A.* 107, 3846–3851. doi: 10.1073/pnas.0913256107

Conflict of Interest: The authors declare that the research was conducted in the absence of any commercial or financial relationships that could be construed as a potential conflict of interest.

Publisher's Note: All claims expressed in this article are solely those of the authors and do not necessarily represent those of their affiliated organizations, or those of the publisher, the editors and the reviewers. Any product that may be evaluated in this article, or claim that may be made by its manufacturer, is not guaranteed or endorsed by the publisher.

frontiers in Neuroscience

ORIGINAL RESEARCH
published: 14 December 2020
doi: 10.3389/fnins.2020.616802

A Sextuple Knockout Cell Line System to Study the Differential Roles of CRY, PER, and NR1D in the Transcription-Translation Feedback Loop of the Circadian Clock

Yi-Ying Chiou[1], Tzu-Ying Li[1], Yanyan Yang[2] and Aziz Sancar[2]*

[1] Graduate Institute of Biochemistry, National Chung Hsing University, Taichung City, Taiwan, [2] Department of Biochemistry and Biophysics, University of North Carolina School of Medicine, Chapel Hill, NC, United States

The transcription-translation feedback loop (TTFL) is the core mechanism of the circadian rhythm. In mammalian cells, CLOCK-BMAL1 proteins activate the downstream genes by binding on the E-box sequence of the clock-controlled genes. Among these gene products, CRY1, CRY2, PER1, PER2, NR1D1, and NR1D2 can regulate the CLOCK-BMAL1-mediated transcription to form the feedback loop. However, the detailed mechanism of the TTFL is unclear because of the complicated inter-regulation of these proteins. Here, we generated a cell line lacking CRY1, CRY2, PER1, PER2, NR1D1, and NR1D2 (Cry/Per/Nr1d_KO) to study TTFL. We compared the Dbp transcription after serum-shock and dexamethasone-shock between Cry/Per/Nr1d_KO cells and cells expressing endogenous CRY (Per/Nr1d_KO) or NR1D (Cry/Per_KO). Furthermore, we found that CRY1-mediated repression of Dbp could persist more than 24 h in the absence of other proteins in the negative limb of the TTFL. Our Cry/Per/Nr1d_KO cells is a suitable system for the studying of differential roles of CRY, PER, and NR1D in the TTFL.

Keywords: circadian clock, TTFL, Cryptochrome, knockout, serum shock

OPEN ACCESS

Edited by:
Jihwan Myung,
Taipei Medical University, Taiwan

Reviewed by:
Andrew C. Liu,
University of Florida, United States
Jae Kyoung Kim,
Korea Advanced Institute of Science and Technology, South Korea

****Correspondence:***
Yi-Ying Chiou
yychiou@nchu.edu.tw

Specialty section:
This article was submitted to Sleep and Circadian Rhythms, a section of the journal Frontiers in Neuroscience

Received: *13 October 2020*
Accepted: *23 November 2020*
Published: *14 December 2020*

Citation:
Chiou Y-Y, Li T-Y, Yang Y and Sancar A (2020) A Sextuple Knockout Cell Line System to Study the Differential Roles of CRY, PER, and NR1D in the Transcription-Translation Feedback Loop of the Circadian Clock. Front. Neurosci. 14:616802. doi: 10.3389/fnins.2020.616802

INTRODUCTION

Circadian rhythm is a crucial mechanism that provides a way to adapt to daily environmental changes. Many physiological functions show rhythmic oscillation with the period around 24 h (Bass, 2012; Gumz, 2016). Transcription-translation feedback loop (TTFL) is the core clock required to maintain the circadian rhythm (Reppert and Weaver, 2002; Levi and Schibler, 2007; Hardin and Panda, 2013; Partch et al., 2014). In the mammalian model of TTFL, Circadian Locomotor Output Cycles Kaput protein (CLOCK) and Brain and Muscle ARNT-Like 1 protein (BMAL1) form a heterodimer (CLOCK-BMAL1). CLOCK-BMAL1 binds to the E-box sequence in the promoters of clock-controlled genes and activates their transcription. Among these gene products, Cryptochromes (CRY1/CRY2), Periods (PER1, PER2), and Nuclear Receptor Superfamily 1 Group D (NR1D1/NR1D2) could negatively regulate the activity of CLOCK-BMAL1. CRY binds to CLOCK-BMAL1 on DNA to induce CLOCK-BMAL1-mediated transcriptional repression (Ye et al., 2011, 2014). PER removes CLOCK-BMAL1 from DNA in a CRY-dependent manner to

erase the effect of CLOCK-BMAL1 (Ye et al., 2014; Chiou et al., 2016). NR1D binds to the retinoic acid response element (RRE) of the Bmal1 and Cry1 gene to repress their transcription and thus to decrease the CLOCK-BMAL1 and CRY1 levels (Preitner et al., 2002; Ueda et al., 2005).

Studying the biochemical mechanisms of TTFL at the organismal level is challenging. Genetic disruption of these core clock genes may have other developmental problems other than the circadian-related phenotypes. For example, Bmal1 knockout mice show growth retardation, aging, and infertility phenotype (Kondratov et al., 2006). Knockout Nr1d1 also causes postnatal lethality or infertility in C57BL/6 mice (Cho et al., 2012). In another way, too many factors from physiological communications between organs contribute to the rhythmic expression of behavior in mice complicating the data interpretations for mechanism studies. For example, the circadian clock of peripheral tissue could be affected by the neural system and the hormone, which are dynamic and highly regulated (Mohawk et al., 2012). *In vitro* experiments using purified proteins have provided information about the protein-protein interaction (Ye et al., 2011; Xu et al., 2015), DNA binding (Ye et al., 2011), and structures (Huang et al., 2012; Czarna et al., 2013) of the proteins involved in TTFL. However, observations from *in vitro* experiments could not directly link to the transcriptional readouts. Cell lines have been used for the study TTFL because the rhythmic expression of circadian genes could be detected after synchronization (Balsalobre et al., 1998, 2000a). Mouse embryonic fibroblast (MEF) cells from the mice lacking specific TTFL components are suitable tools to study TTFL of the circadian clock. For example, the difference between CRY1 and CRY2 in the maintenance of TTFL has been elucidated using cells from *cry1*$^{-/-}$ *cry2*$^{-/-}$ double knockout mice (Khan et al., 2012). However, the puzzle from the crosstalk between these core clock proteins still could not be excluded. In the case of CRY, changed expression of CLOCK-BMAL1-regulated genes could be interpreted as the change of CRY activity, PER activity, or CLOCK-BMAL1 quantity (through NR1D).

Genome editing approaches provide new strategies to study TTFL of the circadian clock. Cellular studies of TTFL could be performed in the cell lines lacking multiple core clock proteins. Using the MEF cell line lacking CRY and PER (Cry/Per_KO), distinct mechanisms between CRY-mediated CLOCK-BMAL1 inhibition and PER-mediated CLOCK-BMAL1 regulation have been demonstrated (Ye et al., 2014). In another research, the MEF cell line lacking PER and NR1D (Per/Nr1d_KO) was established to study PER-mediated transcriptional activation of CLOCK-BMAL1 regulated genes without the change of CLOCK-BMAL1 level due to the inhibition of Nr1d1 and Nr1d2 by PER (Chiou et al., 2016). These successful cases prompt us to make a cell line model lacking CRY, PER, and NR1D to study TTFL. This cell line would be useful in the study of CLOCK-BMAL1 activity and the study of individual clock proteins in the negative limb of TTFL in a simplified system.

Here, we established a MEF cell line lacking endogenous CRY1, CRY2, NR1D1, NR1D2, PER1, and PER2 proteins (Cry/Per/Nr1d_KO). We performed the RNA-sequencing of Cry/Per/Nr1d_KO cells with Cry/Per_KO and Per/Nr1d_KO cells to compare the effects of endogenous NR1D and CRY on the transcriptome. We also analyzed the transcription of two representative CLOCK-BMAL1-regulated genes, Dbp, and Ciart, after serum or dexamethasone treatment of Cry/Per/Nr1d_KO, Cry/Per_KO, and Per/Nr1d_KO. The data suggested different mechanisms of serum and dexamethasone on the regulation of TTFL. Furthermore, using tamoxifen-controlled CRY1 nuclear localization in Cry/Per/Nr1d_KO cells, we found that CRY-mediated transcriptional repression of Dbp is PER-independent. However, PER is required for the reactivation of Dbp transcription.

MATERIALS AND METHODS

Generation of Mouse Embryonic Fibroblast Cell Line Lacking CRY1, CRY2, PER1, PER2, NR1D1, NR1D2 (Cry/Per/Nr1d_KO)

The Cry1/2$^{-/-}$; Per1/2$^{-/-}$; Nr1d1/2$^{-/-}$ (Cry/Per/Nr1d_KO) MEF was made by CRISPR technology using LentiCRISPRv2 (Sanjana et al., 2014) obtained from Addgene (#52961) to mutate the Nr1d1/2 alleles in Cry1/2$^{-/-}$; Per1/2$^{-/-}$ (Cry/Per_KO) MEF (Ye et al., 2014). The guide RNA sequences for Nr1d1 and Nr1d2 were identical to the sequence making Per1/2$^{-/-}$; Nr1d1/2$^{-/-}$ (Per/Nr1d_KO) MEF (Chiou et al., 2016). Lentivirus for targeting Nr1d1 and Nr1d2 were packaged in HEK293T cells separately and then were mixed for the infection of Cry/Per_KO cells. After puromycin selection, individual colonies were isolated, and the expression of NR1D1 and NR1D2 proteins were analyzed by Western blot. The genomic DNA around the targeting sites were PCR-amplified (primer information was provided in the **Supplementary Table**) and cloned into a plasmid for sequencing. After successfully isolating the Cry/Per/Nr1d_KO cells, cells were maintained in the DMEM medium supplement with 10% fetal bovine serum (FBS) without puromycin.

RNA-Sequencing Analysis of Cry/Per/Nr1d_KO, Per/Nr1d_KO, and Cry/Per_KO Cells

Cells were grown in the DMEM medium supplemented with 10% fetal bovine serum at 37°C and 5% CO_2. Total RNA was prepared when the cells were around 80% confluent using Trizol RNA reagent (Thermo Fisher Scientific) and the PureLink RNA Mini Kit (Thermo Fisher Scientific). In brief, Trizol RNA reagents were added to the cells after medium removal to lyse the cells. After phase separation steps, the fraction containing RNA was applied to the column provided in the RNA Mini Kit to purify the total RNA according to the manual of the kit. Libraries were generated using TruSeq stranded RNA preparation kit (Illumina) and sequenced using Illumina HiSeq 2000 (single-end, 50 bp) in the High Throughput Genomic Sequencing Facility at UNC_Chapel Hill. Two independent RNA preparations for each cell line were sequenced.

Sequences were mapped to the mouse genome (mm10) using RNA STAR (Galaxy 2.6.0b-1). The numbers of mapped reads

of each gene were counts using FeatureCounts (Galaxy 1.6.0.6). Data from FeatureCounts were further analyzed using Deseq2 (1.22.2) in the R program. Log2FoldChange (LFC) comparing to the CRY/PER/NR1D_KO cells was used for further analysis. The correlation analysis was performed using the "cor.test" function in the R program with the parameter "method = 'Pearson'." For visualization of the sequencing results, mapped reads were separated into two strands using Filter SAM or BAM, output SAM or BAM (Galaxy 1.8), converted to the bedgraph files using the Genome Coverage (Galaxy 2.27.0.0), and to the bigwig files using the Wig/BedGraph-to-bigWig (Galaxy 1.1.1). The raw sequencing data and the processed data were uploaded to the Gene Expression Omnibus (GSE157946).

Dbp Expression Analysis of Serum- or Dexamethasone-Synchronized Cells

For serum synchronization, cells were seeded into 60 mm dishes the day before the experiment. Serum shock was performed by replacing the medium with the DMEM medium with 50% horse serum. After 2 h, the high serum medium was replaced with the DMEM medium with 10% FBS. Cells were collected every 2 h using TriReagent (Zymo Research) and were kept at −80°C. For dexamethasone treatment, cells were treated with 100 nM dexamethasone for 2 h. Then, the medium was changed to the DMEM medium with 10% FBS, and the cells were collected as serum shock experiments.

Total RNA was purified using the DirectZol RNA Miniprep kit (Zymo Research) following the manual. RNA concentration was determined by Qubit RNA HS kit (Thermo Fisher Scientific). The same amount of RNA was reverse-transcribed into cDNA using PrimeScript RT Reagent kit (Takara Bio). Real-time PCR analysis was performed using iQ SYBR Green Supermix and CFX96 Real-Time PCR Detection System (Biorad). The relative level of RNA to the untreated sample was calculated using the $2^{\wedge}(-\Delta\Delta Cq)$ method using primary Gapdh RNA as the internal control. The primer sequences were provided in **Supplementary Table**.

Dbp Expression Analysis of in Cry/Per/Nr1d_KO Cells Expressing CRY1-ER

The DNA fragment of the ligand-binding domain of the estrogen receptor (ER) was PCR-amplified from the pWZL-blast-PER2-ER (Ye et al., 2014). This fragment was inserted to the 3′-end of mouse Cry1 cDNA in a vector by restriction enzyme digestion and ligation. The CRY1-ER was PCR-amplified and was subcloned into the pWZL-blast by restriction enzyme digestion and ligation to make pWZL-blast-CRY1-ER. Cry/Per/Nr1d_KO cells were infected by the retrovirus carrying CRY1-ER fragment. After blasticidin selection (5 μg/ml), individual colonies were isolated, and the expression of CRY1-ER protein was checked by Western blot.

The Cry/Per/Nr1d_KO-CRY1-ER cells were maintained in the DMEM medium containing 10% FBS and 2.5 μg/ml blasticidin. The cells were seeded in the DMEM medium without blasticidin when performing experiments. The addition of 4-hydroxytamoxyfen (4-OHT) into the medium to 10 nM was used to induce CRY1-ER nuclear entry. RNAs were prepared at different time courses after 4-OHT treatment and were analyzed as mentioned above.

Nuclear Fractionation and Western Blot

Antibody for detecting mouse CRY1 was provided by the laboratory of Aziz Sancar and was described previously (Ye et al., 2011). Antibodies for detection CLOCK (Bethyl Laboratories), BMAL1 (Bethyl Laboratories), CRY2 (Bethyl Laboratories), NR1D1 (Cell Signaling Technology), and NR1D2 (Santa Cruz Biotechnology) were from commercial sources.

For nuclear fractionation, cells were detached from the plate by trypsinization. After PBS wash, cells were lysed with hypotonic buffer (10 mM HEPES pH7.9, 1.5 mM $MgCl_2$, 10 mM KCl, 0.3% Igepal-CA630). After centrifugation (400 g for 5 min), the supernatants were collected as cytosol fractions. The nuclear pellets were washed with hypotonic buffer and were lysed with NUN buffer (20 mM HEPES pH7.4, 300 mM NaCl, 1 M urea, and 10% glycerol). After centrifugation (15,000 g for 15 min), the supernatants were collected as the enriched nuclear fractions.

The protein concentrations of lysates were estimated by the QuantiChrom^{TM} Total Protein Assay Kit (BioAssay System). Equal amounts of total proteins were applied to the Western blot experiments.

The Western blot results were quantified by the Image Lab software (Bio-Rad Laboratories). For estimating the relative levels of CRY1-CLOCK-BMAL1 in the nucleus, CRY1 levels in the nuclear fractions were first normalized to the BMAL1 levels and then compared to the group without 4-OHT treatment.

RESULTS

Generation of Mouse Embryonic Fibroblast Cell Line Lacking CRY1, CRY2, PER1, PER2, NR1D1, and NR1D2 (CPN_KO Cells)

To study the mechanism of TTFL without complicated interference between CRY, PER, and NR1D proteins, we attempted to generate a cell line lacking CRY1, CRY2, PER1, PER2, NR1D1, and NR1D2 (Cry/Per/Nr1d_KO). This cell line would be an advanced "*in cellulo*" biochemical system to study the function of proteins in the TTFL. We selected the MEF cell line lacking CRY1, CRY2, PER1, and PER2 (Cry/Per_KO) (Ye et al., 2014) as the parental cells. The Nr1d1 and Nr1d2 genes of the parental cells were mutated using the CRISPR/Cas9 system. Lentivirus expressing Cas9 protein and the guide RNA sequences targeting Nr1d1 and Nr1d2 was prepared as the previously published method for the generation of MEF cells lacking PER1, PER2, NR1D1, and NR1D2 (Per/Nr1d_KO) (Chiou et al., 2016). **Figure 1A** showed the relations of Cry/Per_KO, Per/Nr1d_KO, and Cry/Per/Nr1d_KO cells. We successfully isolated one clone lacking detectable NR1D1 and NR1D2 proteins from 12 clones in the first screening. We further compared the protein levels of CRY1, CRY2, NR1D1, NR1D2, CLOCK, and BMAL1 in the Cry/Per/Nr1d_KO cells with Cry/Per_KO and Per/Nr1d_KO

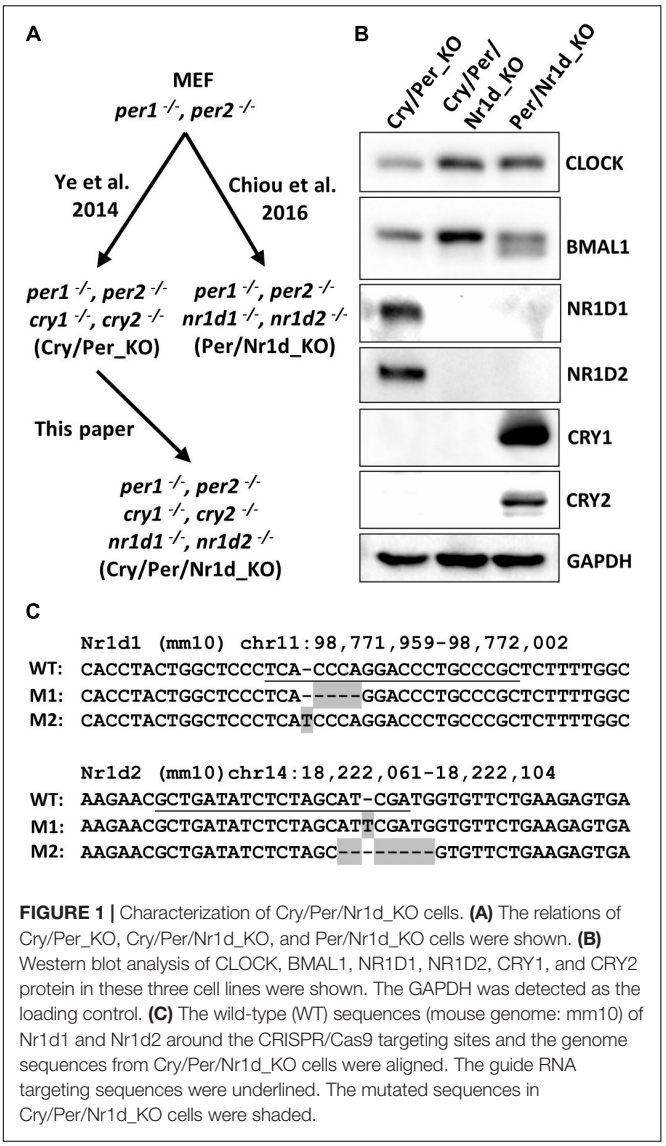

FIGURE 1 | Characterization of Cry/Per/Nr1d_KO cells. **(A)** The relations of Cry/Per_KO, Cry/Per/Nr1d_KO, and Per/Nr1d_KO cells were shown. **(B)** Western blot analysis of CLOCK, BMAL1, NR1D1, NR1D2, CRY1, and CRY2 protein in these three cell lines were shown. The GAPDH was detected as the loading control. **(C)** The wild-type (WT) sequences (mouse genome: mm10) of Nr1d1 and Nr1d2 around the CRISPR/Cas9 targeting sites and the genome sequences from Cry/Per/Nr1d_KO cells were aligned. The guide RNA targeting sequences were underlined. The mutated sequences in Cry/Per/Nr1d_KO cells were shaded.

cells (**Figure 1B**). Comparing to Cry/Per_KO cells, NR1D1 and NR1D2 proteins in Cry/Per/Nr1d_KO cells were undetectable as published Per/Nr1d_KO cells. Associated with the lack of NR1D proteins, CLOCK and BMAL1 proteins were higher in the Cry/Per/Nr1d_KO cells. Transcription of Bmal1 was repressed by NR1D proteins (Preitner et al., 2002), and thus, more BMAL1 proteins in Cry/Per/Nr1d_KO cells than in Cry/Per_KO cells was due to the increase of Bmal1 transcription in the absence of NR1D proteins. Cry/Per/Nr1d_KO cells did not express CRY1 and CRY2 proteins as the parental Cry/Per_KO cells. It has been shown that BMAL1 protein was hyperphosphorylated in Cry-deficient cells (Tamaru et al., 2003). We also observed more hyperphosphorylated BMAL1 in the Cry/Per/Nr1d_KO and the Cry/Per_KO cells than in the Per/Nr1d_KO cells expressing endogenous CRY1 and CRY2 proteins.

We also analyzed the genomic DNA sequences around the CRISPR/Cas9-targeting sites of Nr1d1 and Nr1d2 genes of the Cry/Per/Nr1d_KO cells. We got two types of Nr1d1 sequences from Cry/Per/Nr1d_KO cells with 4 bp deletion and 1 bp insertion comparing to the wild type. For Nr1d2 genes, we also got two types of sequences with 1 bp insertion and 7 bp deletion (**Figure 1C**). These data suggested that both alleles of Nr1d1 and Nr1d2 genes were frameshift-mutated in the Cry/Per/Nr1d_KO cells.

Transcriptome Analysis of Cry/Per_KO, Per/Nr1d_KO, and Cry/Per/Nr1d_KO Cells

In the TTFL model, CRY could inhibit CLOCK-BMAL1 through direct interaction on DNA, and NR1D could inhibit CLOCK-BMAL1 by decreasing the Bmal1 level. In another way, CRY could increase the BMAL1 level through inhibiting Nr1d transcription, and NR1D could activate CLOCK-BMAL1 through decreasing CRY level. However, the rhythmic Bmal1 transcription is dispensable for the intracellular circadian rhythm (Liu et al., 2008; Xu et al., 2015). To distinguish the effect of BMAL1 level change by NR1D and the effect of BMAL1 activity by CRY on the transcriptome, we analyzed the transcriptomes of Cry/Per_KO, Per/Nr1d_KO, and Cry/Per/Nr1d_KO cells by RNA-sequencing (RNA-seq). The difference of transcriptome between Cry/Per/Nr1d_KO and Cry/Per_KO cells could be explained by the expression of endogenous NR1D1 and NR1D2 proteins regardless of the expression of CRY and PER protein. Also, CRY-mediated regulation could be analyzed by comparing the transcriptome of Per/Nr1d_KO and Cry/Per/Nr1d_KO cells.

The association between RNA-seq data from two independent experiments of each cell line was analyzed by the principal component analysis (**Figure 2A**). We filtered out the genes with lower expression levels (baseMean < 100) according to the distributions of baseMean of all genes (**Figure 2B**), and compared the expression 11,912 genes in these three cell lines. The criteria we used for selecting the changed genes were described as follows: (1) the level of change was more than 75% [the absolute value of log2FoldChange $>$ log2(1.75)], and (2) the adjusted *p*-value was less than 1e-22. Comparing with Cry/Per/Nr1d_KO cells, 1,090 genes expressed differently in Cry/Per_KO cells, and 2,527 genes expressed differently in Per/Nr1d_KO cells (**Figure 2C**). From RNA-seq data, we selected circadian genes, including Clock, Arntl (Bmal1), Cry1, Cry2, Per1, Per2, Per3, Nr1d1, Nr1d2, Dbp, Hlf, Tef, Bhlh40, Bhlh41, and Ciart to compare the effect of CRY and NR1D on CLOCK-BMAL1 and its target genes (**Figure 2D**). Comparing to Cry/Per/Nr1d_KO cells, Per/Nr1d_KO cells (with CRY1 and CRY2 proteins) showed decreased RNA levels of Cry1, Cry2, Per1, Per2, Per3, Nr1d1, Nr1d2, Dbp, Hlf, Tef, Bhlh40, and Bhlh41. These genes were known CLOCK-BMAL1-regulated genes, and thus the data suggested that CRY proteins repressed CLOCK-BMAL1-mediated transcription in the absence of PER and NR1D proteins. In Per/Nr1d_KO cells, Clock mRNA was slightly lower than, and Arntl mRNA was similar to the level in Cry/Per/Nr1d_KO cells. These data indicated that CRY could not affect Clock and Bmal1 mRNA levels in the absence of NR1D proteins. In Cry/Per_KO cells (with NR1D1 and NR1D2 proteins), Arntl and Cry1 mRNAs were lower than those in the Cry/Per/Nr1d_KO cells as expected,

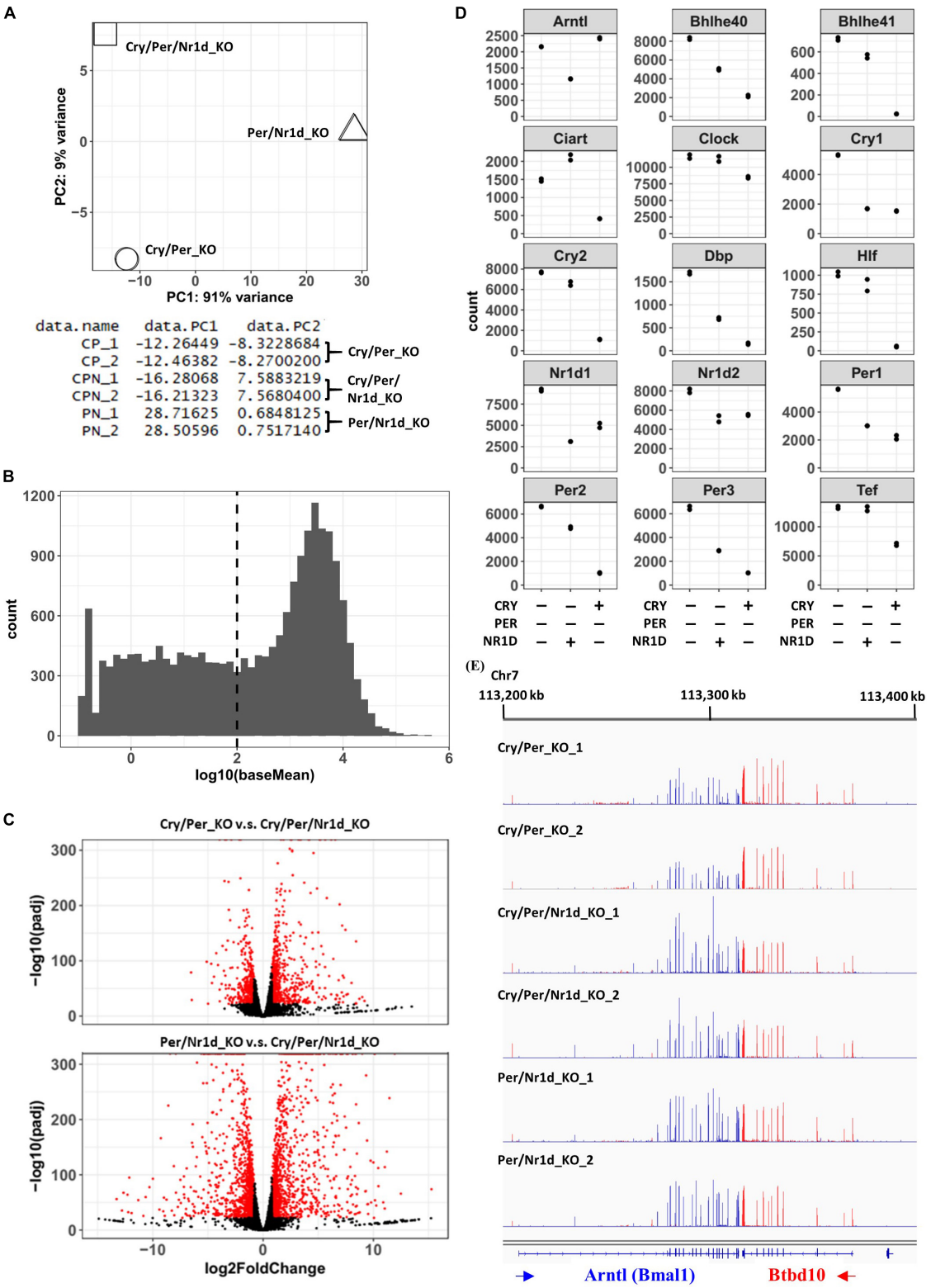

FIGURE 2 | RNA-Seq Analysis of Cry/Per_KO, Per/Nr1d_KO, and Cry/Per/Nr1d_KO Cells. **(A)** The principal component analysis was performed using Deseq2, and the data were shown and was plotted using R software. **(B)** The histogram showed the distribution of baseMean calculated by Deseq2. The dashed line indicated the position that baseMean was equal to 100. **(C)** Volcano blots of Cry/Per_KO cells vs. Cry/Per/Nr1d_KO cells and Per/Nr1d_KO cells vs. Cry/Per/Nr1d_KO cells were shown. Genes with significant differences were colored in red. **(D)** The read counts of different genes calculated by Deseq2 were extracted and were

(Continued)

FIGURE 2 | Continued
plotted. Each spot represented the value of each experiment. **(E)** The figure was the screenshot of RNA-seq data visualized by the IGV genome browser. RNA-seq datamapped to different strands of the genome were displayed in different colors, and then were overlayed to display. For better visualization quality, sample names, gene names, and the locations of the genome were added manually.

because known RRE element was identified on these two genes. However, the influences of NR1D proteins to other CLOCK-BMAL1-regulated genes were gene-specific. The mRNA levels of Nr1d1, Nr1d2, Per1, and Per3 in Cry/Per_KO cells were lower than Cry/Per/Nr1d_KO cells as the levels in Per/Nr1d_KO cells. However, the mRNA levels of Per2, Bhlh40, and Dbp in Cry/Per_KO cells were lower than Cry/Per/Nr1d_KO but were higher than Per/Nr1d_KO cells. Furthermore, the mRNA levels of Cry2, Hlf, and Tef in Cry/Per_KO cells were similar to the levels in Cry/Per/Nr1d_KO cells. RNA-seq data visualized by genome browser also presented the different expression levels of Arntl genes between Cry/Per/Nr1d_KO and Cry/Per_KO cells, but not between Cry/Per/Nr1d_KO_and Per/Nr1d_KO cells (**Figure 2E**).

To compare genes affected by the loss of CRY proteins (Per/Nr1d_KO v.s. Cry/Per/Nr1d_KO) or NR1D proteins (Cry/Per_KO v.s. Cry/Per/Nr1d_KO), we focused on the 2,918 genes that expressing differently between Cry/Per_KO and Cry/Per/Nr1d_KO (n = 1,090) or between Per/Nr1d_KO and Cry/Per/Nr1d_KO (n = 2,527) cells. Among these genes, 628 genes were affected by both CRY and NR1D in the same trend (higher or lower in both Cry/Per_KO and Per/Nr1d_KO comparing to Cry/Per/Nr1d_KO cells). This number was 57.6% of the number of NR1D affected genes and 24.1% of the number of CRY affected genes). The number of genes contrarily affected by CRY and NR1D was 71 (6.5% of NR1D affected genes, 2.8% of CRY affected genes). Others were uniquely affected by NR1D or CRY (35.9% of NR1D affected genes, 73.1% of CRY affected genes) (**Figure 3A**). We did a random sampling test (n = 100) to check whether these numbers were closed to random events. We randomly selected 1,195 (low group) and 1,332 (high group) genes as the number of genes expressing lower or higher in Per/Nr1d_KO cells and selected 444 (low group) and 646 (high group) genes as the number of genes expressing lower or higher in Cry/Per_KO cells. The mean values of the number of overlapping genes in the same group and the opposite group were 477 and 466. These data suggested that the overlapping of CRY and NR1D affected genes was not just a random event.

Because both NR1D and CRY could affect CLOCK-BMAL1-regulated genes, we selected putative CLOCK-BMAL1-regulated genes based on previously published BMAL1-chromatin immunoprecipitation sequencing data from the same Per/Nr1d_KO background (Chiou et al., 2016). Total 626 CLOCK-BMAL1-regulated genes expressing differently between Cry/Per_KO and Cry/Per/Nr1d_KO (n = 251, 40.1%) or between Per/Nr1d_KO and Cry/Per/Nr1d_KO (n = 536, 85.6%) cells. Among these genes, 157 genes were affected by both CRY and NR1D knockout in the same trend (62.5% of NR1D affected CLOCK-BMAL1-regulated genes, 29.3% of CRY affected CLOCK-BMAL1regulated genes). This number was higher than the mean value (120) from the random sampling test. Only four genes (the mean value from random sampling test was 92) were oppositely affected by CRY and NR1D (1.6% of NR1D affected CLOCK-BMAL1-regulated genes, 0.7% of CRY affected CLOCK-BMAL1-regulated genes). The numbers of CLOCK-BMAL1-regulated genes uniquely affected by NR1D or CRY were 90 (35.8% of NR1D-regulated) and 375 (59.9% of CRY-regulated) (**Figure 3B**).

We further analyzed the correlation of the CRY or NR1D-affected genes (**Figure 3C**). The expression of these genes showed a positive correlation (Pearson's correlation coefficient = 0.5108, p-value < 2.2e-16) between Cry/Per_KO and Per/Nr1d_KO cells. The correlation was increased when putative BMAL1-regulated genes were selected (Pearson's correlation coefficient = 0.6426, p-value < 2.2e-16). Reversely, the correlation was decreased when putative BMAL1-regulated genes were excluded (Pearson's correlation coefficient = 0.4940, p-value < 2.2e-16). Our RNA-seq data suggested that CRY and NR1D could regulate CLOCK-BMAL1-regulated genes independently. In another way, many genes might be regulated by CRY or NR1D in a CLOCK-BMAL1-independent manner.

Responses of Dbp and Ciart Transcription in Cry/Per_KO, Per/Nr1d_KO, and Cry/Per/Nr1d_KO Cells After Serum Shock and Dexamethasone Shock

Synchronization of cells by serum shock or dexamethasone has been used for the study of the circadian clock in the cellular model (Balsalobre et al., 1998, 2000a). However, how these treatments affected core TTFL was unclear. We have three cell lines expressing different proteins in the TTFL from the same source. Thus, we analyzed the activity of CLOCK-BMAL1 in these three different cell lines after serum shock or dexamethasone shock to find out which protein in the TTFL responded to the synchronization signals. Neither Per/Nr1d_KO, Cry/Per_KO, nor Cry/Per/Nr1d_KO cells could generate a stable oscillation of clock-controlled genes after synchronization because of the loss of complete TTFL. We focused on a shorter time course (<8 h) after the release of synchronization to analyze the direct effects of treatment on TTFL. We analyzed the primary transcript levels of two CLOCK-BMAL1 target genes, Dbp and Ciart, by RT-qPCR to represent the transcription of these genes. The primary transcript of Gapdh was selected as the internal control for possible global effect on global transcription.

Transcription of Ciart and Dbp were lower in the Per/Nr1d_KO cells expressing endogenous CRY proteins than the other two cells without treatment. However, the expression of NR1D proteins in Cry/Per_KO cells did not affect the transcription of Ciart and Dbp comparing to Cry/Per/Nr1d_KO

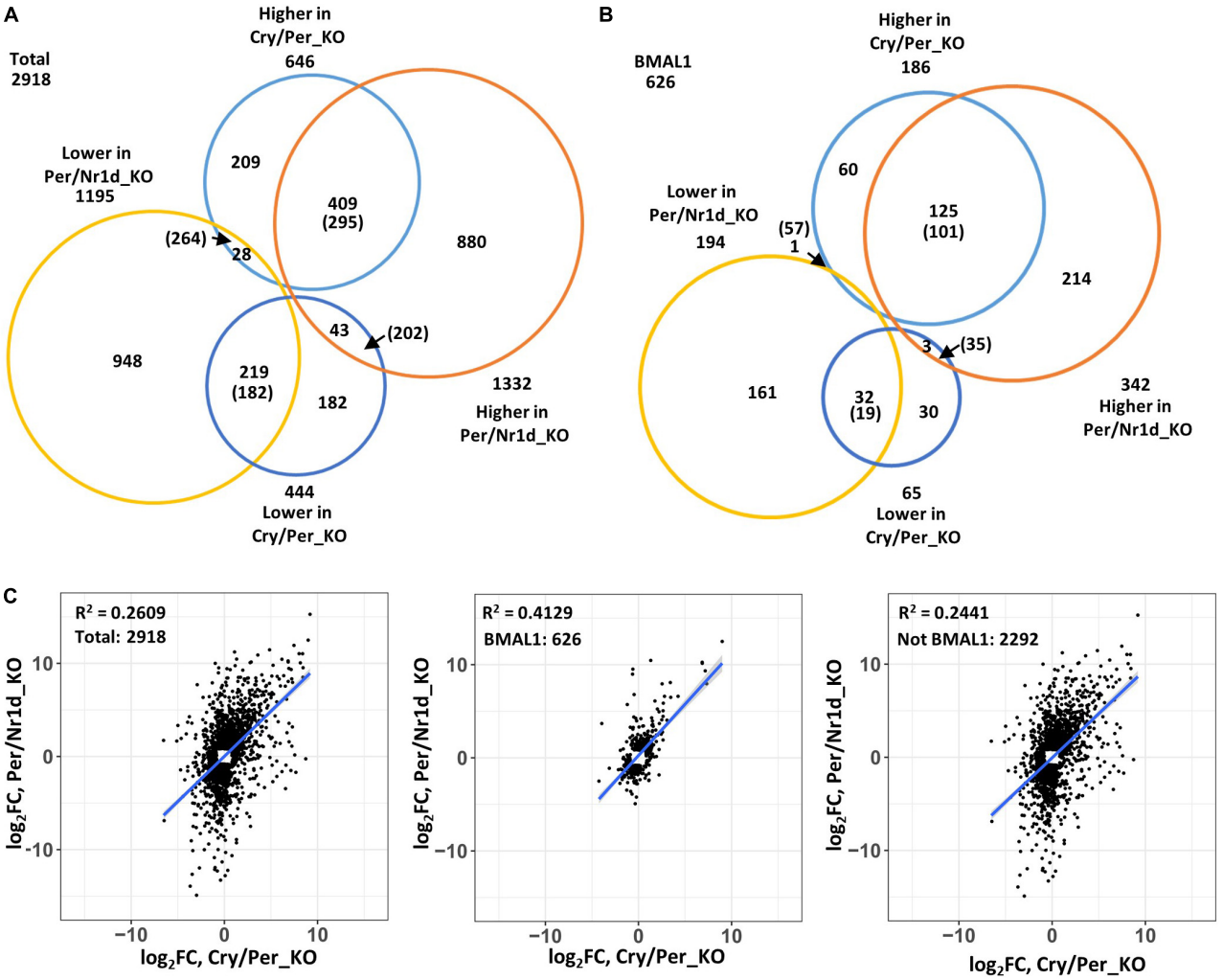

FIGURE 3 | Correlation analysis of NR1D and CRY affected genes. **(A)** Genes expressing differently to Cry/Per/Nr1d_KO cells were subgrouped based on their changes in Per/Nr1d_KO cells and Cry/Per_KO cells. The numbers indicated the numbers of genes in each group. The numbers in the parentheses were the mean values from random sampling for 100 times. Genes within the list of putative CLOCK-BMAL1-regulated genes were selected and were shown in **(B)**. **(C)** The expressional changes of individual genes in Per/Nr1d_KO (*y*-axis) and Cry/Per_KO (*x*-axis) cells were plotted. The correlation was analyzed using the linear regression model ("lm"). The R-squared values and the regression lines were shown in the figures. Data from total selected genes were plotted in the left panel or were subgrouped into BMAL1-regulated (the middle panel) or not BMAL1-regulated (the right panel).

cells (**Figure 4A**). In Cry/Per/Nr1d_KO cells, serum shock decreased the primary mRNA of Dbp and then gradually recovered. The primary RNA levels of Ciart gradually decreased after serum shock. These suggested that serum shock inhibited the activity of CLOCK-BMAL1 in the absence of CRY, PER, or NR1D proteins (**Figure 4B**, middle). In the presence of NR1D proteins (Cry/Per_KO cells), serum shock did not inhibit the transcription of Dbp or Ciart. Instead, transcription of these genes was induced by serum shock with a time delay (**Figure 4B**, left). In Per/Nr1d_KO cells, we did not observe apparent effects on the transcription of these two genes after serum shock (**Figure 4B**, right). Based on these data, we proposed that serum shock directly inhibits the activity of CLCOK-BMAL1 to decrease the transcription of target genes. For cells with high NR1D levels, decreased NR1D by decreasing CLOCK-BMAL1 activity induced the transcription of Bmal1. Increased CLOCK-BMAL1 compensated the decreased activity and caused the increase of Dbp and Ciart transcription at later time points. For cells with high CRY levels, the transcriptions of Dbp and Ciart were maintained at the lower levels (**Figure 4A**). Thus, serum shock did not cause apparent effects on Per/Nr1d_KO cells.

Horse serum contains many substances, including glucocorticoids. Dexamethasone is an agonist of glucocorticoids to activate the glucocorticoid receptor. Thus, we wanted to compare the response of dexamethasone shock to the serum shock in these three cell lines. Dexamethasone did not repress the transcription of Dbp or Ciart. Instead, we could detect the increase of Dbp transcription four hours after the release of dexamethasone in Cry/Per_KO and Cry/Per/Nr1d_KO cells (**Figure 4B,** left and middle) but not in Per/Nr1d_KO cells

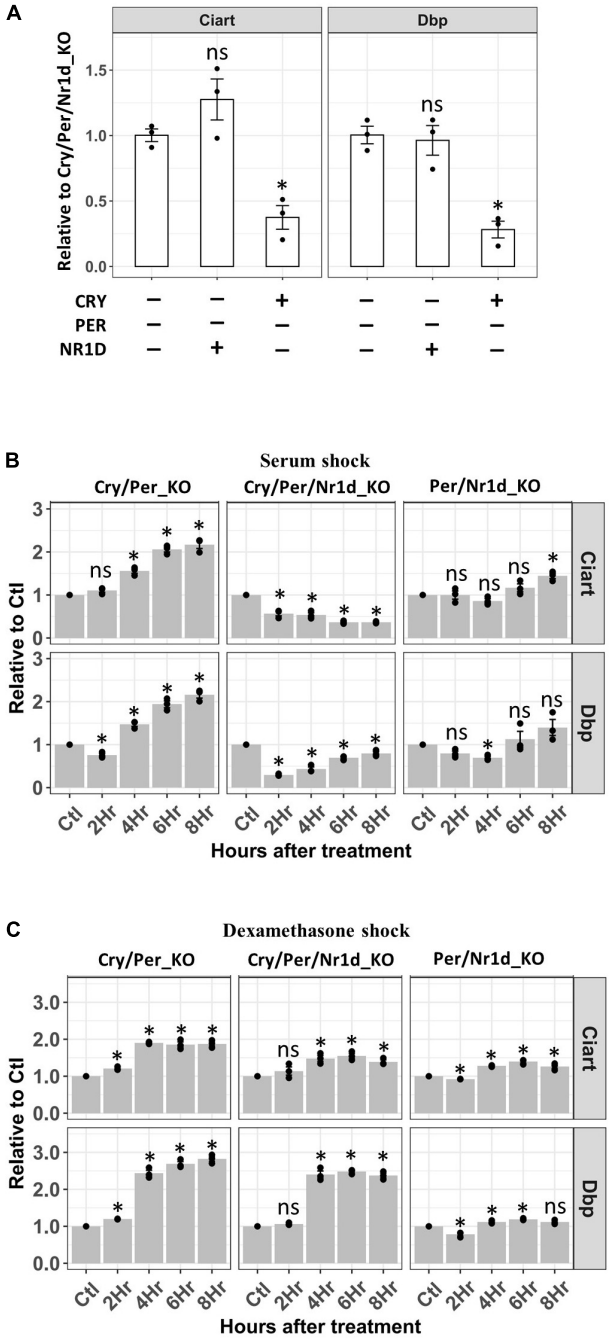

FIGURE 4 | RT-qPCR analysis of the Dbp and Ciart primary mRNA after serum or dexamethasone shock. **(A)** RT-qPCR analyzed primary mRNA levels of Ciart and Dbp in Cry/Per/Nr1d_KO, Cry/Per_KO, and Per/Nr1d_KO cellswere shown. Data were first normalized to the primary mRNA of Gapdh, then were normalized to the average in Cry/Per/Nr1d_KO cells (*y*-axis). Data were shown as mean with standard error. Data from independent experiments (point, $n = 3$) were also shown in the plot. Statistical analysis was performed using Student's *t*-test comparing to the Cry/Per/Nr1d_KO cells. *P*-values < 0.05 were considered significant. Asterisk denoted the significant difference. Data without significant difference were labeled with "ns." **(B)** RT-qPCR analyzed primary mRNA levels of Ciart and Dbp in Cry/Per/Nr1d_KO, Cry/Per_KO, and Per/Nr1d_KO cells after serum shock

(Continued)

FIGURE 4 | Continued

were shown. Data were first normalized to the primary mRNA of Gapdh, then were normalized to the values from the same cells without treatment (*y*-axis). Cells without treatment, 2, 4, 6, 8 h after treatments were analyzed (*x*-axis). Statistical analysis was performed using Student's *t*-test comparing to the untreated control of the same cells. *P*-values < 0.05 were considered significant. Asterisk (*) denoted the significant difference. Data without significant difference were labeled with "ns." **(C)** RT-qPCR analyzed primary mRNA levels of Ciart and Dbp in Cry/Per/Nr1d_KO, Cry/Per_KO, and Per/Nr1d_KO cells after dexamethasone shock were shown. Statistical analysis was performed as in **(B)**.

(**Figure 4B**, right). The effects of dexamethasone on Ciart could be observed in Cry/Per_KO cells and was weaker than the effects on Dbp. Based on our data, we concluded that the mechanisms of how serum and dexamethasone affect TTFL are different.

Study CRY1-Mediated Transcriptional Inhibition of Dbp and Ciart in Cry/Per/Nr1d_KO Cells

Lack of CRY1, CRY2, PER1, PER2, NR1D1, and NR1D2 proteins in Cry/Per/Nr1d_KO cells benefited the study of each of them individually. We combined a previously published tamoxifen-controlled nuclear entry system (Ye et al., 2014) and this unique cell line to study the transcriptional repression of Dbp by CRY1. Theoretically, if we could control the nuclear CRY1 level rhythmically, Dbp transcription would be rhythmic, too. We established Cry/Per/Nr1d_KO-CRY1-ER cells expressing CRY1 fused with an estrogen receptor ligand-binding domain. The addition of 4-hydroxytamoxifen (4-OHT) released CRY1-ER from the cytosol to the nucleus through binding to the estrogen receptor ligand-binding domain. The nuclear levels of CRY1-ER increased within 15 min after the addition of 4-OHT (**Figures 5A,C**). We could not observe the correlation between nuclear CRY1-ER and the treatment time (**Figures 5A,B**). Thus, we thought the nuclear level of CRY1-ER reached a saturated status within 15 min after adding 4-OHT. However, the effects of CRY1 on transcriptional inhibition of Dbp and Ciart showed a time-dependent manner (**Figures 5B,D**). The decrease of Dbp and Ciart primary mRNA could be observed within an hour (**Figure 5B**, right panel), and the decrease of Dbp and Ciart mature mRNA needed several hours (**Figure 5D**, left panel). We observed that the primary mRNA levels of Ciart, but not Dbp, were gradually recovered after 3 h of treatment (**Figure 5D**, right panel), representing that another regulatory mechanism independently activated the transcription of Ciart.

Next, we analyzed the nuclear distribution of CRY1-ER after the removal of 4-OHT. The cells were treated with 4-OHT for 15 min, and then the medium was changed after PBS wash. Unexpectedly, nuclear CRY1-ER was unchanged after the removal of 4-OHT for 4 h (**Figure 6A**). We extended the release time to 24 h and found that nuclear CRY1-ER after removing 4-OHT for 24 h was similar to the level just after 15 min 4-OHT treatment (**Figure 6B**). In the analysis of Dbp and Ciart mRNA, Dbp primary and mature mRNA after 24 h of the release

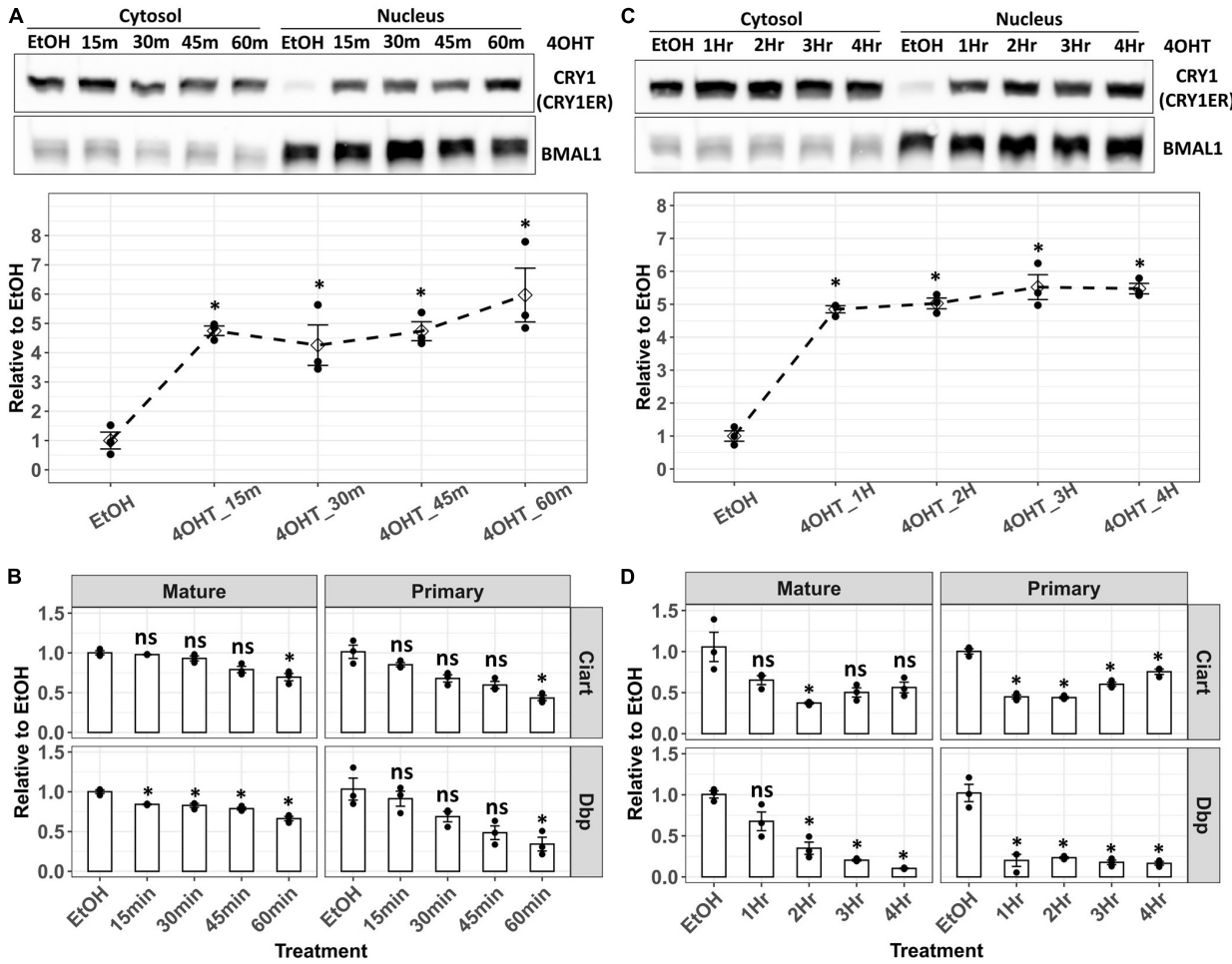

FIGURE 5 | Analysis of the Dbp and Ciart primary and mature mRNA in Cry/Per/Nr1d_KO-CRY1-ER cells after 4-OHT treatment**. (A)** Cry/Per/Nr1d_KO-CRY1-ER cells were treated with 4-OHT for 15–60 min. After the fractionation, CRY1-ER proteins were analyzed by Western blots. BMAL1 was used as the control for the nuclear fractionation and represented the total levels of CLOCK-BMAL1 (with and without CRY) in the nucleus. The lower panel was the relative levels of CRY1-ER in the nucleus to the cells treated with the vehicle (EtOH, 60 min). Data were first normalized to the BMAL1 levels, then were normalized to the average of vehicle control. The diamonds were the mean of three independent experiments. Error bars were the standard errors, and the points were the individual data. Statistical analysis was performed using Student's *t*-test comparing to the vehicle control (EtOH). $P < 0.05$ were considered significant. Asterisk (*) denoted the significant difference. **(B)** Cells were treated with 4-OHT as in **(A)**. RT-qPCR analyzed primary and mature mRNA levels were shown. Data were first normalized to the primary or mature mRNA of Gapdh, then were normalized to the average of vehicle control (y-axis). Data were shown as mean with standard error. Data from independent experiments (point, $n = 3$) were also shown in the plot. Statistical analysis was performed using Student's *t*-test comparing to the vehicle control (EtOH). *P*-values < 0.05 were considered significant. Asterisk (*) denoted the significant difference. Data without significant difference were labeled with "ns." **(C)** Cry/Per/Nr1d_KO-CRY1-ER cells were treated with 4-OHT for 1–4 h. Cells treated with EtOH for 4 h were the controls. Experiments and data analysis were the same as **(A)**. **(D)** The treatments of cells were identical to **(C)**, and the experiments and data analysis were the same as **(B)**.

of 4-OHT were as low as the levels without release (**Figure 6C**, lower panel). The results were consistent with the nuclear levels of CRY1-ER and suggested that CRY1-mediated transcriptional repression of Dbp persisted for 24 h after 4-OHT removal. The primary mRNA of Ciart was partially recovered, and the mature mRNA was fully recovered after 24 h release of 4-OHT (**Figure 6C**, upper panel). However, this may be through a TTFL-independent mechanism as the observation in **Figure 5D**.

In our previous studies, PER2 could remove CLOCK-BMAL1 from the promoter of Dbp genes and repress the transcription of Dbp (Ye et al., 2014). In another way, PER2 could also remove CLOCK-BMAL1-CRY to derepress the transcription of downstream genes, like Cry1 (Chiou et al., 2016). To understand whether PER is required for the reactivation of Dbp transcription repressed by CRY, we transiently transfected the plasmid expressing PER2 protein 24 h before 4-OHT treatment. Without 4-OHT treatment, Dbp primary mRNA in the cells expressing PER2 was lower than the cells without PER2. These data could be explained by the removal of CLOCK-BMAL1 from the promoter. The expression of PER2 did not affect the repression of Dbp by 4-OHT-induced CRY1 nuclear entry. Nevertheless, the transcriptional recovery of Dbp after 4-OHT removal could only be observed in the cells expressing PER2 (**Figure 6D**). Our data

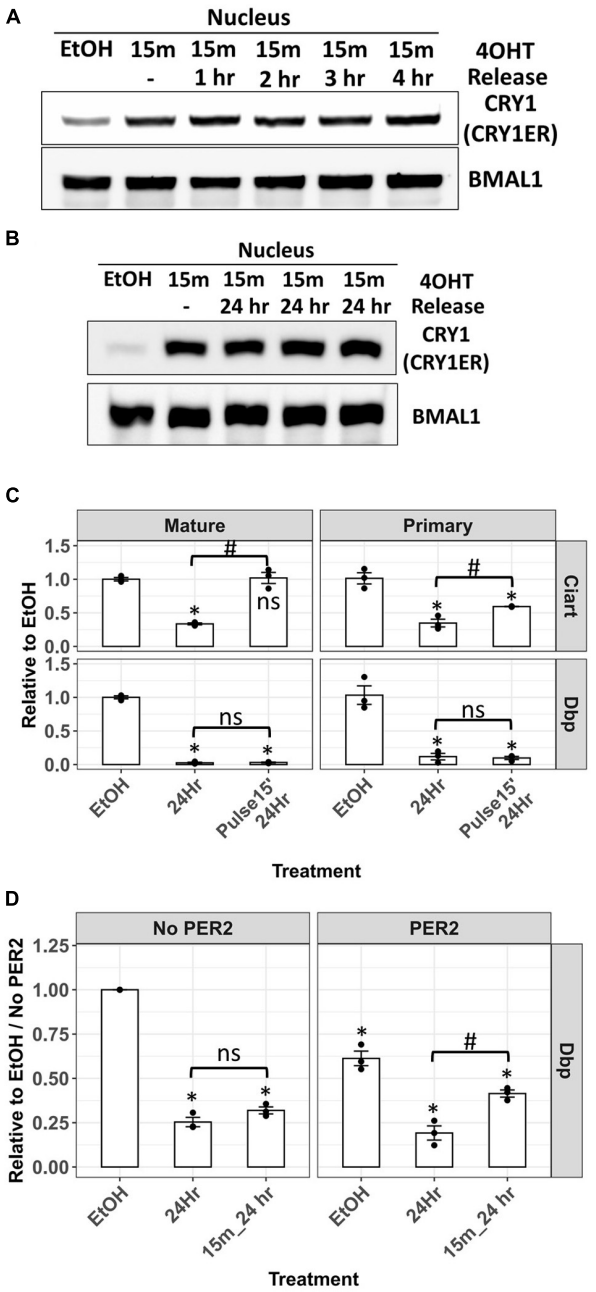

FIGURE 6 | Analysis of the Dbp primary mRNA in Cry/Per/Nr1d_KO-CRY1-ER cells after 4-OHT treatment and release. Nuclear levels of CRY1-ER in Cry/Per/Nr1d_KO-CRY1-ER cells treated with 4-OHT for 15 min and released for 1–4 h **(A)** or 24 h **(B)** were analyzed by Western blot after fractionation. BMAL1 was used as the loading control. **(C)** RT-qPCR analysis of primary and mature mRNA levels of Ciart and Dbp from cells treated with vehicle for 24 h (EtOH), 4-OHT for 24 h (24 h), and 4-OHT for 15 min and released for 24 h (pulse 15', 24 h) were shown. Statistical analysis was performed using Student's *t*-test. *P*-values < 0.05 were considered significant. Asterisk denoted the significant difference to the vehicle control. Hashtag denoted the significant difference between the 24 h treatment of 4-OHT and the 24 h release after 15 min 4-OHT treatment. Data without significant difference were labeled with "ns." **(D)** Cells were transfected with the control plasmid (pcDNA4-Myc-His) or with the plasmid expressing

(Continued)

FIGURE 6 | Continued

PER2 (pcDNA3-PER2-V5-His) 24 h before 4-OHT treatment. The 4-OHT treatment, RT-qPCR, and data analysis were the same as **(C)**. Statistical analysis was performed using Student's *t*-test. $P < 0.05$ were considered significant. Asterisk (*) denoted the significant difference to the vehicle control without PER2 expression. Hashtag (#) denoted the significant difference between the 24 h treatment of 4-OHT and the 24 h release after 15 min 4-OHT treatment. Data without significant difference were labeled with "ns."

suggested that PER is required for the release of CRY-mediated transcriptional repression.

DISCUSSION

The transcription-translation feedback loop was the core model of the circadian clock. However, studying the detailed mechanism was complicated. Experiments using purified proteins could not link to the transcription in the absence of an *in vitro* transcription system using endogenous promoter. Animals were suitable for the study of circadian regulation of physiological functions, but the detailed mechanism was hard to elucidate due to the communications between organs and tissues. Cells had a self-sustained circadian clock in the cultured condition that played a suitable model to study the mechanism. Genetic deficient mouse embryonic fibroblast cells had been used for many circadian studies. We generated a new cell line, called Cry/Per/Nr1d_KO cells, lacking CRY, PER, and NR1D proteins by CRISPR/Cas9 approach and analyzed the transcriptome of Cry/Per/Nr1d_KO, Per/Nr1d_KO, and Cry/Per_KO cells by RNA-sequencing. Using Dbp and Ciart as the readout of CLOCK-BMAL1 activity, we found that serum and dexamethasone treatment affected TTFL through different mechanisms. We found that serum, but not dexamethasone, inhibited CLOCK-BMAL1 in the absence of CRY, PER, and NR1D proteins. We studied CRY1-mediated transcriptional repression of Dbp in Cry/Per/Nr1d_KO cells and found that PER is required for the release of CRY-mediated transcriptional repression.

Cry/Per/Nr1d_KO cells provided a new tool to study the TTFL of the circadian clock biochemically. Researchers could study the regulation of CLOCK-BMAL1 and the functions of CRY, PER, and NR1D separately without the influence of feedback in Cry/Per/Nr1d_KO cells. For example, analysis of wild-type and mutant CRY1 in Cry/Per/Nr1d_KO cells helps elucidate the difference in the repression of CLOCK-BMAL1. Changes of PER activity or the CLOCK-BMAL1 quantity would not be the issue in Cry/Per/Nr1d_KO cells. However, from the biological view, Cry/Per/Nr1d_KO cells was a very extreme condition which may not exist in the physiological situation. We thought that Cry/Per/Nr1d_KO cells might mimic a situation that CLOCK-BMAL1 activity was reached the peak before the accumulation of CRY, PER, and NR1D proteins. Different situations could be mimicked by expressing different combinations of CRY, PER and NR1D proteins.

From the transcriptome analysis, we found 2,517 genes expressed differently between Cry/Per/Nr1d_KO and Per/Nr1d_KO cells. This number was around threefold

of the number of genes expressed differently between Cry/Per/Nr1d_KO and Cry/Per_KO cells (790 genes). From the data of selected CLOCK-BMAL1-regulated genes, CRY proteins showed more robust represser activities than NR1D proteins. A more potent transcriptional repressor might cause more dramatic effects on the transcriptome. We also found that the overlapping of putative CLOCK-BMAL1-regulated genes and differential expressed genes was low. Only 626 genes (21% of affected genes) closed to the BMAL1 binding site identified from a similar condition (Chiou et al., 2016). Besides CLOCK-BMAL1, CRY proteins could regulate other transcription factors. In mouse liver, CRY1 or CRY2 could bind to many positions of the genome without CLOCK-BMAL1 binding (Koike et al., 2012). Although NR1D proteins regulate the levels of CLOCK-BMAL1, genes with the RRE element would be the targets of NR1D proteins. Besides directly affected by CRY or NR1D, genes might be affected by the transcription factors or other proteins controlled by CRY or NR1D. From another viewpoint, many putative CLOCK-BMAL1 regulated genes were not affected by either CRY or NR1D. Among 3,261 putative genes, 536 genes were affected by CRY, and 251 genes were affected by NR1D. In our previous study, PER2 removed CLOCK-BMAL1 globally, but only small proportions of genes were affected by the increase of PER2 in the nucleus (Chiou et al., 2016). Thus, CLOCK-BMAL1 activity was not required for the transcription of many regulated genes. Their transcriptional levels depended more on other factors than on CLOCK-BMAL1. CLOCK-BMAL1 played another layer of regulation for the oscillation. The effect of CLOCK-BMAL1 was masked in the absence of synchronization.

Synchronization was the essential step to observe the oscillation of circadian genes. Different treatments, including serum shock (Balsalobre et al., 1998), dexamethasone (Balsalobre et al., 2000a), and forskolin (Balsalobre et al., 2000b), had been reported and been used for this purpose. We tested the response of Dbp and Ciart transcription after serum or dexamethasone treatment in cells with different circadian proteins to elucidate the mechanism of synchronization. Glucocorticoid response element (GRE) had been identified in the promoter of Per2 genes (Cheon et al., 2013). Dexamethasone might synchronize the cells by inducing the expression of Per2. The induction of Per2 by dexamethasone would inhibit the transcription of Dbp. In our system lacking PER2 protein, we could not detect the decrease of Dbp transcription after dexamethasone treatment. Instead, increased Dbp transcription could be observed 4 h after treatment in Cry/Per_KO or Cry/Per/Nr1d_KO cells (**Figure 4C**). Delayed activation of Dbp might be the secondary effect through other genes regulated by glucocorticoid signals. Serum shock inhibited the transcription of Dbp in the cells lacking CRY, PER, and NR1D proteins (Cry/Per/Nr1d_KO cells). These data suggested that CLOCK-BMAL1 activity could be directly inhibited by serum. However, in cells expressing NR1D proteins (Cry/Per_KO cells), the inhibition of Dbp transcription was compensated (**Figure 4B**). Through literature searching, we proposed the following hypothesis to explain the observation in our system. Recently, Tip60 protein was identified as the acetyltransferase of Bmal1. Tip60 protein catalyzed the K538 acetylation of BMAL1 and activated BMAL1 (Petkau et al., 2019). Tip60 protein could be phosphorylated on S86 by GSK3b to activate its acetyltransferase activity (Lin et al., 2012). Besides, serum shock induced the phosphorylation of GSK3b on S9 to inhibit the kinase activity (Yin et al., 2006). Thus, serum shock inhibited the CLOCK-BMAL1 activity probably through decreasing the activity of GSK3b and Tip60. However, NR1D1 was also the target of GSK3b. Decreased GSK3b activity by serum shock caused the decrease of NR1D1 protein and thus increased Bmal1 transcription (Yin et al., 2006), explaining why Dbp transcription in the Cry/Per_KO cells after serum shock was not decreased but was increased at later time points.

In the canonical TTFL model, transcription of CLOCK-BMAL1-regulated genes could be downregulated by CRY, PER, or NR1D proteins. Dbp transcription in the Per/Nr1d_KO cells was lower than in the Cry/Per/Nr1d_KO cells suggesting that the repressor activity of CRY is PER-independent as previously published (Ye et al., 2014). Neither serum-induced Dbp repression nor dexamethasone-induced Dbp activation in the Cry/Per/Nr1d_KO cells was observed in the Per/Nr1d_KO cells. Although CRY proteins negatively regulated their transcription, endogenous CRY1 and CRY2 in the Per/Nr1d_KO cells were sufficient to repress the Dbp transcription. CRY represses transcription through forming CLOCK-BMAL1-CRY-DNA complex. PER can remove CLOCK-BMAL1-CRY from DNA. In the absence of PER, the CLOCK-BMAL1-CRY-DNA complex might be very stable in the nucleus and persistently repress the transcription of downstream genes. CRY1-mediated inhibition of Dbp transcription persisted for 24 h in Cry/Per/Nr1d_KO cells after inducing CRY1 nuclear entry (**Figures 6B,C**). This phenomenon should not be the technical artifact from the fusion of ER to the CRY1 or the addition of 4-OHT. CRY1-mediated Dbp repression could be recovered when exogenous PER2 was expressed in the same cells (**Figure 6D**). These data also hinted that CLOCK-BMAL1 and CRY could not form a stable feedback loop. PER was required for the displacement of CLOCK-BMAL1 and CLOCK-BMAL1-CRY from DNA to reset the transcription to its basal level.

The mechanism to sustain the circadian rhythm is an exciting topic. Many mathematical models have been proposed from different viewpoints (Kim and Forger, 2012; Pett et al., 2016; Narasimamurthy et al., 2018). In different models, CRY and PER, as the central repressors in TTFL, were included but contributed differently. In the model proposed by Kim and Forger (2012), all PER and CRY forms in the nucleus were considered as the repressors. In this model, the CLOCK-BMAL1 activator became inactive when binding with the CRY-PER repressor. Thus, the stoichiometric balance between the CLOCK-BMAL1 activator and CRY-PER repressor was necessary for circadian timekeeping. Based on recent findings (Ye et al., 2014; Chiou et al., 2016) and the data in this paper, CRY and PER played different roles in the regulation of TTFL. We thought that this model could be refined by adding another repressor complex (CRY-CLOCK-BMAL1). So, the model would include three complexes, including CLOCK-BMAL1 activator, CRY-CLCOK-BMAL1 repressor and PER-CRY-CLOCK-BMAL1 inactive complex). In the model proposed by Pett et al. (2016), two activators (Dbp and Bmal1) and three repressors (Rev-erb-α (Nr1d1), Cry1 and Per2) were

included to build the model based on their mutual regulations. Cry1 and Per2 were separated because Cry1, but not Per2, was repressed by NR1D1. In this model, Cry1, Per2 and Nr1d1-mediated repressions of each other were the dominant sources in the oscillation. However, protein interactions between BMAL1, CRY1, or PER2 were not considered in this model. CRY-mediated repression also depends on the levels of PER (removing complex) and CLOCK-BMAL1 (forming complex). PER-mediated regulation also depends on the level of CRY (CRY-dependent activity).

In this paper, we found that PER is required for the reactivation of CRY-mediated transcriptional repression. Thus, PER might regulate circadian rhythm through CRY. In the phosphoswitch model (Narasimamurthy et al., 2018), PER2 was either phosphorylated at the β-TrCP site (S478) or FASP site (S659). PER2 phosphorylated at S478 was rapidly degraded. PER2 phosphorylated at S659 was further phosphorylated at neighboring sites to stabilize. In PER2 S478A mice (Masuda et al., 2020), the period of behavioral rhythm was increased. CRY1 and CRY2 protein levels were also increased in the mutant mice. Although the authors proposed that increased CRY proteins extended the repression of CLOCK-BMAL1-regulated, the promoter binding of CRY or CLOCK-BMAL1 was not analyzed. In another study (Patke et al., 2017), the exon11-deletion mutant of Cry1 identified from Delayed Sleep Phase Disorder patient showed stronger CLOCK-BMAL1 binding affinity but weaker binding on the promoter region. Besides, the CLOCK-BMAL1 displacement activity of PER required its casein kinase binding domain (Ye et al., 2014). Thus, we proposed that the ratio of PER and CRY plays critical roles in the circadian rhythm. The stoichiometric balance between CRY and PER is controlled in multiple layers, including transcription, phosphorylation and protein degradation.

DATA AVAILABILITY STATEMENT

The datasets presented in this study can be found in online repositories. The names of the repository/repositories and accession number(s) can be found below: https://www.ncbi.nlm.nih.gov/geo/query/acc.cgi?acc=GSE157946.

AUTHOR CONTRIBUTIONS

Y-YC designed the experiments, and performed the experiments, data analysis, and manuscript writing. T-YL and YY performed the experiments. AS designed experiments. All authors contributed to the article and approved the submitted version.

FUNDING

This work was supported by the Ministry of Science and Technology, Taiwan (MOST 106-2311-B-005-014 and 107-2311-B-005-012-MY3).

ACKNOWLEDGMENTS

We thank Dr. Christopher P. Selby in the AS's lab for the discussion about this work.

SUPPLEMENTARY MATERIAL

The Supplementary Material for this article can be found online at: https://www.frontiersin.org/articles/10.3389/fnins.2020.616802/full#supplementary-material

REFERENCES

Balsalobre, A., Brown, S. A., Marcacci, L., Tronche, F., Kellendonk, C., Reichardt, H. M., et al. (2000a). Resetting of circadian time in peripheral tissues by glucocorticoid signaling. *Science* 289, 2344–2347. doi: 10.1126/science.289.5488.2344

Balsalobre, A., Damiola, F., and Schibler, U. (1998). A serum shock induces circadian gene expression in mammalian tissue culture cells. *Cell* 93, 929–937. doi: 10.1016/s0092-8674(00)81199-x

Balsalobre, A., Marcacci, L., and Schibler, U. (2000b). Multiple signaling pathways elicit circadian gene expression in cultured Rat-1 fibroblasts. *Curr. Biol.* 10, 1291–1294. doi: 10.1016/s0960-9822(00)00758-2

Bass, J. (2012). Circadian topology of metabolism. *Nature* 491, 348–356. doi: 10.1038/nature11704

Cheon, S., Park, N., Cho, S., and Kim, K. (2013). Glucocorticoid-mediated Period2 induction delays the phase of circadian rhythm. *Nucleic Acids Res.* 41, 6161–6174. doi: 10.1093/nar/gkt307

Chiou, Y. Y., Yang, Y., Rashid, N., Ye, R., Selby, C. P., and Sancar, A. (2016). Mammalian Period represses and de-represses transcription by displacing CLOCK-BMAL1 from promoters in a Cryptochrome-dependent manner. *Proc. Natl. Acad. Sci. U.S.A.* 113, E6072–E6079.

Cho, H., Zhao, X., Hatori, M., Yu, R. T., Barish, G. D., Lam, M. T., et al. (2012). Regulation of circadian behaviour and metabolism by REV-ERB-alpha and REV-ERB-beta. *Nature* 485, 123–127. doi: 10.1038/nature11048

Czarna, A., Berndt, A., Singh, H. R., Grudziecki, A., Ladurner, A. G., Timinszky, G., et al. (2013). Structures of Drosophila cryptochrome and mouse cryptochrome1 provide insight into circadian function. *Cell* 153, 1394–1405. doi: 10.1016/j.cell.2013.05.011

Gumz, M. L. (2016). *Circadian Clocks : Role in Health and Disease*. New York, NY: Springer. doi: 10.1007/978-1-4939-3450-8

Hardin, P. E., and Panda, S. (2013). Circadian timekeeping and output mechanisms in animals. *Curr. Opin. Neurobiol.* 23, 724–731. doi: 10.1016/j.conb.2013.02.018

Huang, N., Chelliah, Y., Shan, Y., Taylor, C. A., Yoo, S. H., Partch, C., et al. (2012). Crystal structure of the heterodimeric CLOCK:BMAL1 transcriptional activator complex. *Science* 337, 189–194.

Khan, S. K., Xu, H., Ukai-Tadenuma, M., Burton, B., Wang, Y., Ueda, H. R., et al. (2012). Identification of a novel cryptochrome differentiating domain required for feedback repression in circadian clock function. *J. Biol. Chem.* 287, 25917–25926. doi: 10.1074/jbc.m112.368001

Kim, J. K., and Forger, D. B. (2012). A mechanism for robust circadian timekeeping via stoichiometric balance. *Mol. Syst. Biol.* 8:630. doi: 10.1038/msb.2012.62

Koike, N., Yoo, S. H., Huang, H. C., Kumar, V., Lee, C., Kim, T. K., et al. (2012). Transcriptional architecture and chromatin landscape of the core circadian clock in mammals. *Science* 338, 349–354. doi: 10.1126/science.1226339

Kondratov, R. V., Kondratova, A. A., Gorbacheva, V. Y., Vykhovanets, O. V., and Antoch, M. P. (2006). Early aging and age-related pathologies in mice deficient in BMAL1, the core componentof the circadian clock. *Genes Dev.* 20, 1868–1873. doi: 10.1101/gad.1432206

Levi, F., and Schibler, U. (2007). Circadian rhythms: mechanisms and therapeutic implications. *Annu. Rev. Pharmacol. Toxicol.* 47, 593–628. doi: 10.1146/annurev.pharmtox.47.120505.105208

Lin, S. Y., Li, T. Y., Liu, Q., Zhang, C., Li, X., Chen, Y., et al. (2012). GSK3-TIP60-ULK1 signaling pathway links growth factor deprivation to autophagy. *Science* 336, 477–481. doi: 10.1126/science.1217032

Liu, A. C., Tran, H. G., Zhang, E. E., Priest, A. A., Welsh, D. K., and Kay, S. A. (2008). Redundant function of REV-ERBalpha and beta and non-essential role for Bmal1 cycling in transcriptional regulation of intracellular circadian rhythms. *PLoS Genet.* 4:e1000023. doi: 10.1371/journal.pgen.1000023

Masuda, S., Narasimamurthy, R., Yoshitane, H., Kim, J. K., Fukada, Y., and Virshup, D. M. (2020). Mutation of a PER2 phosphodegron perturbs the circadian phosphoswitch. *Proc. Natl. Acad. Sci. U.S.A.* 117, 10888–10896. doi: 10.1073/pnas.2000266117

Mohawk, J. A., Green, C. B., and Takahashi, J. S. (2012). Central and peripheral circadian clocks in mammals. *Annu. Rev. Neurosci.* 35, 445–462. doi: 10.1146/annurev-neuro-060909-153128

Narasimamurthy, R., Hunt, S. R., Lu, Y., Fustin, J. M., Okamura, H., Partch, C. L., et al. (2018). CK1delta/epsilon protein kinase primes the PER2 circadian phosphoswitch. *Proc. Natl. Acad. Sci. U.S.A.* 115, 5986–5991. doi: 10.1073/pnas.1721076115

Partch, C. L., Green, C. B., and Takahashi, J. S. (2014). Molecular architecture of the mammalian circadian clock. *Trends Cell Biol.* 24, 90–99. doi: 10.1016/j.tcb.2013.07.002

Patke, A., Murphy, P. J., Onat, O. E., Krieger, A. C., Ozcelik, T., Campbell, S. S., et al. (2017). Mutation of the human circadian clock gene CRY1 in familial delayed sleep phase disorder. *Cell* 169, 203.e13–215.e13.

Petkau, N., Budak, H., Zhou, X., Oster, H., and Eichele, G. (2019). Acetylation of BMAL1 by TIP60 controls BRD4-P-TEFb recruitment to circadian promoters. *eLife* 8:e43235.

Pett, J. P., Korencic, A., Wesener, F., Kramer, A., and Herzel, H. (2016). Feedback loops of the mammalian circadian clock constitute repressilator. *PLoS Comput. Biol.* 12:e1005266. doi: 10.1371/journal.pcbi.1005266

Preitner, N., Damiola, F., Lopez-Molina, L., Zakany, J., Duboule, D., Albrecht, U., et al. (2002). The orphan nuclear receptor REV-ERBalpha controls circadian transcription within the positive limb of the mammalian circadian oscillator. *Cell* 110, 251–260. doi: 10.1016/s0092-8674(02)00825-5

Reppert, S. M., and Weaver, D. (2002). Coordination of circadian timing in mammals. *Nature* 418, 935–941. doi: 10.1038/nature00965

Sanjana, N. E., Shalem, O., and Zhang, F. (2014). Improved vectors and genome-wide libraries for CRISPR screening. *Nat. Methods* 11, 783–784. doi: 10.1038/nmeth.3047

Tamaru, T., Isojima, Y., van der Horst, G. T., Takei, K., Nagai, K., Takamatsu, K., et al. (2003). Nucleocytoplasmic shuttling and phosphorylation of BMAL1 are regulated by circadian clock in cultured fibroblasts. *Genes Cells* 8, 973–983. doi: 10.1046/j.1365-2443.2003.00686.x

Ueda, H. R., Hayashi, S., Chen, W., Sano, M., Machida, M., Shigeyoshi, Y., et al. (2005). System-level identification of transcriptional circuits underlying mammalian circadian clocks. *Nat. Genet.* 37, 187–192. doi: 10.1038/ng1504

Xu, H., Gustafson, C. L., Sammons, P. J., Khan, S. K., Parsley, N. C., Ramanathan, C., et al. (2015). Cryptochrome 1 regulates the circadian clock through dynamic interactions with the BMAL1 C terminus. *Nat. Struct. Mol. Biol.* 22, 476–484. doi: 10.1038/nsmb.3018

Ye, R., Selby, C. P., Chiou, Y. Y., Ozkan-Dagliyan, I., Gaddameedhi, S., and Sancar, A. (2014). Dual modes of CLOCK:BMAL1 inhibition mediated by Cryptochrome and Period proteins in the mammalian circadian clock. *Genes Dev.* 28, 1989–1998. doi: 10.1101/gad.249417.114

Ye, R., Selby, C. P., Ozturk, N., Annayev, Y., and Sancar, A. (2011). Biochemical analysis of the canonical model for the mammalian circadian clock. *J. Biol. Chem.* 286, 25891–25902. doi: 10.1074/jbc.m111.254680

Yin, L., Wang, J., Klein, P. S., and Lazar, M. A. (2006). Nuclear receptor Rev-erbalpha is a critical lithium-sensitive component of the circadian clock. *Science* 311, 1002–1005. doi: 10.1126/science.1121613

Conflict of Interest: The authors declare that the research was conducted in the absence of any commercial or financial relationships that could be construed as a potential conflict of interest.

frontiers in Neuroscience

ORIGINAL RESEARCH
published: 07 January 2021
doi: 10.3389/fnins.2020.613531

Challenging the Integrity of Rhythmic Maternal Signals Revealed Gene-Specific Responses in the Fetal Suprachiasmatic Nuclei

*Vendula Lužná, Pavel Houdek, Karolína Liška and Alena Sumová**

Laboratory of Biological Rhythms, Institute of Physiology, Czech Academy of Sciences, Prague, Czechia

During fetal stage, maternal circadian system sets the phase of the developing clock in the suprachiasmatic nuclei (SCN) via complex pathways. We addressed the issue of how impaired maternal signaling due to a disturbed environmental light/dark (LD) cycle affects the fetal SCN. We exposed pregnant Wistar rats to two different challenges – a 6-h phase shift in the LD cycle on gestational day 14, or exposure to constant light (LL) throughout pregnancy – and detected the impact on gene expression profiles in 19-day-old fetuses. The LD phase shift, which changed the maternal SCN into a transient state, caused robust downregulation of expression profiles of clock genes (*Per1*, *Per2*, and *Nr1d1*), clock-controlled (*Dbp*) genes, as well as genes involved in sensing various signals, such as *c-fos* and *Nr3c1*. Removal of the rhythmic maternal signals via exposure of pregnant rats to LL abolished the rhythms in expression of *c-fos* and *Nr3c1* in the fetal SCN. We identified *c-fos* as the gene primarily responsible for sensing rhythmic maternal signals because its expression profile tracked the shifted or arrhythmic maternal SCN clock. Pathways related to the maternal rhythmic behavioral state were likely not involved in driving the *c-fos* expression rhythm. Instead, introduction of a behavioral rhythm to LL-exposed mothers via restricted feeding regime strengthened rhythm in *Vip* expression in the fetal SCN. Our results revealed for the first time that the fetal SCN is highly sensitive in a gene-specific manner to various changes in maternal signaling due to disturbances of environmental cycles related to the modern lifestyle in humans.

Keywords: circadian clock, development, fetus, maternal entrainment, suprachiasmatic nucleus

OPEN ACCESS

Edited by:
Jihwan Myung,
Taipei Medical University, Taiwan

Reviewed by:
Yu Tahara,
Waseda University, Japan
Claudia Torres-Farfan,
Austral University of Chile, Chile
Erik D. Herzog,
Washington University in St. Louis, United States

***Correspondence:**
Alena Sumová
alena.sumova@fgu.cas.cz;
sumova@biomed.cas.cz

Specialty section:
This article was submitted to Sleep and Circadian Rhythms, a section of the journal Frontiers in Neuroscience

Received: *02 October 2020*
Accepted: *02 December 2020*
Published: *07 January 2021*

Citation:
Lužná V, Houdek P, Liška K and Sumová A (2021) Challenging the Integrity of Rhythmic Maternal Signals Revealed Gene-Specific Responses in the Fetal Suprachiasmatic Nuclei. Front. Neurosci. 14:613531. doi: 10.3389/fnins.2020.613531

INTRODUCTION

In mammalian brain, the paired suprachiasmatic nuclei of the hypothalamus (SCN) harbor principal pacemaker (central clock) (Moore and Eichler, 1972; Ralph et al., 1990) that generates rhythmic signals with a circadian ("approximately a day") period and orchestrates the phases of oscillators located throughout the body. The prominent role of the SCN among the clocks in the body is determined by 1) its unique structure, comprising a web of mutually interconnected subpopulations of cellular oscillators that ensures the production of a coherent and robust rhythmic signal (Welsh et al., 1995; Herzog et al., 2004; Liu et al., 2007; Webb et al., 2009) and 2) its ability to adjust (entrain) according to the external light/dark cycle, which is achieved via its direct connection with the retina (Zordan et al., 2001; Morin and Allen, 2006). These functions make

the SCN a key structure of predictive homeostasis that allows adaptation of physiological and behavioral processes according to expected daily and seasonal changes in external environment.

Previous research has investigated the not yet fully resolved question of when during early life the SCN begin to fulfil their role of the central clock in the body (reviewed in Sumová et al., 2012; Sumová and Čečmanová, 2020). Answering this question is important for understanding the impact of maternal chronodisruption, which may occur in pregnant women exposed to modern lifestyles, on offspring. It has been found that chronodisruption *in utero* leads to pathological phenotypes later in adulthood (Mendez et al., 2016; Richter et al., 2018; Salazar et al., 2018; Varcoe et al., 2018) that may not be rescued by quality of maternal care during postnatal period (Smarr et al., 2017). Therefore, temporal organization during fetal development seems to be important for good health in adulthood.

For experimental purposes, the development of the SCN has been mostly studied in nocturnal rodent species. Morphologically, the rodent SCN develops during the perinatal period in a gradual process, duration of which differs according to the animal species (reviewed in Bedont and Blackshaw, 2015). In rats (a rodent species used in this study), gestation lasts approximately 21–22 days and SCN neurogenesis occurs between the embryonic days 14 (E14) and E17 (Altman and Bayer, 1978). However, synapses start to be formed around E19 and the process is fully completed postnatally (Moore and Bernstein, 1989). At the level of the daily profiles of clock gene expression, which are genes whose protein products are involved in the generation of the circadian signal (reviewed in Lowrey and Takahashi, 2011), the rhythmicity also develops in the SCN gradually. This was demonstrated in the rat SCN examined *in situ* via progressively increasing amplitudes of the rhythmic profiles from the late fetal to the early postnatal stages (Sládek et al., 2004; Kováčiková et al., 2006; Houdek and Sumová, 2014). The developmental process tightly matched the progression of synaptogenesis (reviewed in Bedont and Blackshaw, 2015), which clearly suggests that the robustness of the SCN clock is dependent on its morphological maturation (reviewed in Sumová et al., 2012). Experiments using an *in vitro* approach based on detection of bioluminescence for tracking PER2 protein activity in explanted fetal SCN from mPer2^{Luc} mice confirmed the gradual prenatal development of the SCN clock (Wreschnig et al., 2014; Landgraf et al., 2015; Carmona-Alcocer et al., 2018). The gestational period in mice lasts approximately 19 days and if mouse SCN explants are harvested at E15, synchrony among the oscillators develops spontaneously after several days in culture at the time roughly corresponding to the developmental time *in vivo* (Čečmanová et al., 2019), although other studies were not able to detect this process (Landgraf et al., 2015; Carmona-Alcocer et al., 2018). Intriguingly, in contrast to the adult SCN, the immature SCN is extremely sensitive to culturing procedure itself as well as to nonspecific manipulations of the explants, which can induce robust responses of the fetal SCN clock (Nishide et al., 2008; Čečmanová et al., 2019). Therefore, the *in vitro* model does not seem to fully reflect the *in vivo* situation (Sumová and Čečmanová, 2020), and for studies targeted at investigating the impact of external environment on the fetal SCN, an *in vivo* approach, in which the state of the fetal SCN is assessed *in situ*, is more meaningful. This approach has been used to show that despite the SCN immaturity during the fetal stage, the SCN clock of newborn pups is fully entrained to that of their mother immediately after birth (Davis and Gorski, 1985a,b; Duncan et al., 1986; Reppert and Schwartz, 1986; Weaver and Reppert, 1989; Viswanathan et al., 1994; Bellavía et al., 2006). Additionally, the immature SCN was able to follow changes in the phase of the maternal SCN clock because after exposing pregnant rats to a shift in light/dark (LD) cycle during the late pregnancy, their pups were born with shifted SCN clocks (El-Hennamy et al., 2008). However, applying the shift in the LD cycle closer to delivery term was not effective because the maternal SCN did not have time to fully re-entrain (El-Hennamy et al., 2008). This clearly demonstrates that fetal SCN clock recognizes whether the maternal SCN is fully entrained or whether it is in a state of transition between the original and new LD cycle.

For adaptation to changes in the external LD cycle, the fetal SCN clock, which obviously does not receive information directly from the retina, fully depends on the rhythmic signals sent by the maternal SCN clock. The nature of these signals has previously been extensively studied, and multiple associated pathways have been identified (reviewed in Sumová et al., 2012; Bates and Herzog, 2020; Carmona-Alcocer et al., 2020; Sumová and Čečmanová, 2020). Importantly, the signals are complex and of various origins. They include the rhythmic hormonal pathways (Davis and Mannion, 1988; Viswanathan et al., 1994; Viswanathan and Davis, 1997; Houdek et al., 2015; Čečmanová et al., 2019) as well as pathways related to activity/feeding cycles (Nováková et al., 2010). Apart from their role in setting the proper phase of the fetal clock, the same maternal signals may also be significant for facilitation of fetal clock development. This is supported by our recent finding that glucocorticoid hormones (GCs), which are under control of the maternal SCN and respond to actual arousal state, are important not only for entrainment of the fetal SCN clock but may also facilitate its development (Čečmanová et al., 2019).

Altogether, the results suggest that challenging the integrity and functioning of the maternal circadian system *in vivo* may significantly impact development of the fetal SCN clock. However, knowledge on how this affects the fetal SCN clock at the level of clock and clock-related genes is lacking. To address this issue, we subjected pregnant rats to situations in which production of maternal SCN-driven rhythmic signals to their fetuses was challenged. Specifically, we aimed to manipulate maternal signaling via two different protocols, in which the SCN clock of the pregnant mother was a) in a transient state due to a phase shift in LD cycle or b) arrhythmic due to exposure to constant light (LL). Additionally, to dissect the participation of the behavioral/feeding rhythm as one of the maternal signals, we reimposed the rhythm in the LL-exposed mothers by temporally restricting access to food. Both experimental protocols used in this study were previously employed to demonstrate that in rats, maternal SCN

signaling determines the phase of the SCN clock in newborn pups (El-Hennamy et al., 2008) and that rhythmic maternal behavior resets the neonatal SCN (Nováková et al., 2010). In both studies, gene expression profiles were detected in the SCN of newborn pups just after delivery; however, the acute responses within the fetal SCN were not analyzed. Our results revealed that these challenges significantly impacted the fetal SCN in a gene-specific manner, and revealed the high and selective sensitivity of the developing SCN clock to various environmental interventions during pregnancy. The outcome of this study is important because both protocols resemble lifestyle-related challenges to the circadian system that women might be exposed to during pregnancy, such as, jet lag, shift work, an irregular daily regime, or exposure to light pollution at night.

MATERIALS AND METHODS

Animals

Adult male and female Wistar rats (Institute of Physiology, the Czech Academy of Sciences) were housed individually in a temperature-controlled facility at 23 ± 2°C with free access to food and water. All animals were originally maintained under a light/dark cycle with 12 h of light and 12 h of darkness (LD12:12). The time is expressed as Zeitgeber time (ZT); ZT0 corresponds to lights on at 06:00 h and ZT12 corresponds to lights off at 18:00 h. Vaginal smears from females were inspected to determine the estrous cycle phase. On the night of pro-estrus, females were mated with males and on the next morning, they were checked for the presence of sperm in their vaginal smears. In case of sperm positivity, the day was defined as day 0 of embryonic development (E0). Pregnant rats exposed to the experimental protocols described below were monitored for locomotor activity throughout the whole experiment.

All experiments were approved by the Animal Care and Use Committee of the Institute of Physiology and were performed in accordance with the Animal Protection Law of the Czech Republic as well as the European Community Council directives 86/609/EEC. All efforts were made to reduce the suffering of the animals.

Experimental Protocols

Experiment 1 – Effect of the Delay in the LD Cycle on Maternal and Fetal SCN Clocks

The effect of the phase-shift of the maternal signals on the fetal SCN was assessed using pregnant rats (total n = 22) that were maintained under the LD12:12 and had unlimited access to food and drinking water during the whole experiment. The pregnant rats were divided into two groups; The control group ("CTRL") (n = 11) remained under the initial LD12:12 regime throughout the whole pregnancy. Body weight (BW) and the amount of food intake were monitored in five females at the times corresponding to E0, E12 and E19. The group assigned as the "Delay" group (n = 11) was maintained under the initial LD12:12, but on E14, the LD12:12 cycle was shifted by 6 h in the direction of the phase delay so that the lights were switched off and on 6 h later in the evening and in the next morning, respectively. After the 6-h phase shift, the rats were maintained under this new light/dark regime until E19.

Nonpregnant female rats of the same age were kept under LD12:12 (n = 3) for 19 days similar to the experimental pregnant rats. They were weighed and their food consumption was monitored at E0, E12, and E19 for comparison with the pregnant rats.

Experiment 2 – Effect of Exposing Pregnant Rats to Constant Light and Restricted Feeding on the Fetuses

To ascertain the effect of maternal feeding regime on the embryonic SCN, two groups of pregnant rats (total n = 23) were exposed to constant light (LL) regime from E0 until E19. The LL regime was introduced so that the light was not switched off in the evening on E0. One group of rats was fed *ad libitum* (group "LL-ad lib") (n = 10). In this group, BW and the amount of food were monitored on E0, E14, and E19. The other group was subjected to the restricted feeding (RF) regime (group "LL-RF") from E0 until E19 (n = 13). During the RF regime, food availability was limited to only a 6-h interval from 9:00 to 15:00 (corresponding to ZT3–ZT9 based on the original LD regime). Rats in the LL-RF group were also weighed during the experiment on E0, E14, and E19. Moreover, the food in this group was weighed every day at the beginning and end of the feeding period. Both groups had unlimited access to drinking water during the whole experiment.

Nonpregnant female rats of the same age were kept under LL (n = 3) for 19 days, similar to the experimental pregnant rats. They were weighed and their food consumption was monitored on E0, E14, and E19 for comparison with that of the pregnant rats.

Locomotor Activity Monitoring

For monitoring locomotor activity, the rats were maintained individually in cages equipped with infrared movement detectors attached centrally above the top of each cage. The activity was detected using a circadian activity monitoring system (Dr. Cooper, INSERM, France). The activity was recorded every minute and double-plotted activity records were generated for visualization of the data. The resulting data were analyzed using the ClockLab toolbox (Actimetrics, Illinois, United States).

Collection of Fetal Samples

For detection of the daily gene expression profiles in the fetal SCN, the pregnant rats in all groups described above were sacrificed at gestational age E19 by decapitation under deep anesthesia by intramuscular injection of a mixture of 150 mg/kg ketamine (Vétoquinol, s.r.o., Czech Republic) and 15 mg/kg xylazine (Bioveta a.s., Czech Republic) at 3 h intervals over a 24 h period (one pregnant rat per time point). Fetuses were sacrificed by rapid decapitation, and at each time point, five fetal heads from each pregnant mother were immediately frozen on dry ice and stored at –80°C for further detection of gene expression using RT-qPCR.

Additionally, for the CTRL, LL-ad lib and LL-RF groups the whole uteruses containing embryos and placentas were extracted and weighed. The bodies without uterus as well as three dyads of embryos and the corresponding placentas from every mother in these three groups were also weighed.

Detection of mRNA Levels in the Fetal SCN Using RT-qPCR

The fetal heads from all groups in both experiments were sectioned on a cryostat into 20 μm-thick coronal sections containing the medial part of the rostro-caudal extent of the fetal SCN, which was visualized with cresyl violet staining (Sigma-Aldrich, St. Louis, United States). The SCNs were precisely separated bilaterally using a laser microdissector (LMD6000, Leica), as we previously described elsewhere (Houdek and Sumová, 2014). Dissected fetal SCN tissues were collected in a microfuge tube containing RLT buffer from the RNeasy Micro kit (Qiagen, Valencia, United States) and stored until RNA isolation was performed. Total RNA was isolated using the RNeasy Micro kit (Qiagen) according to the manufacturer's instructions. Isolated RNA samples were immediately reverse-transcribed into cDNA using the HiCapacity cDNA Synthesis Kit (Thermo Fisher, Waltham, MA, United States). The diluted cDNA was then amplified using a LightCycler 480 Real-Time PCR System (Roche, Basel, Switzerland) in 14 μl reactions using 5× HOT FIREPol Probe qPCR Mix Plus (Solis Biodyne, Tartu, Estonia) and TaqMan Gene Expression Assays (Life Technologies, California, United States) for all genes of interest (see **Table 1**). The ΔΔCt method was used for the quantification of the relative cDNA concentration using mean of three reference genes, namely *Beta-2-Microglobulin* (*B2M, Rn00560865_m1, VIC-labeled*), *Peptidylprolyl Isomerase A* (*Ppia, Rn00690933_m1, VIC*), and *Hydroxymethylbilane Synthase* (*Hmbs*, *Rn01421873_g1, VIC*).

Statistical Analyses

The t-test was used to compare the behavioral rhythm periods between the experimental groups (CTRL versus Delay groups). One-way ANOVA was used for comparisons of the behavioral rhythm periods between the LL-ad lib and LL-RF groups at two time intervals, and for comparison of maternal BW gain without the uterus and the weights of placentas and embryos among the CTRL, LL-ad lib and LL-RF groups. Two-way ANOVA was used for comparison of the profiles of BW gain and food consumption among the 5 experimental groups (CTRL, LL-ad lib, LL-RF groups, and nonpregnant CTRL and LL groups).

The daily profiles of gene expression were analyzed using 1-way ANOVA (for the detection of the significance of the effect of time) and cosinor analysis (for the detection of significance of the cosinor fit). The cosinor analysis was performed by fitting the data to one of two alternative regression models: either a horizontal straight line (null hypothesis) or a single cosine curve (alternative hypothesis) defined by the equation Y = mesor + [amplitude × cos(2 × π × (X-acrophase)/wavelength)] with a constant wavelength of 24 h. The P values, coefficient of determination R^2 (goodness of fit), amplitude, acrophase and mesor were determined (see **Table 2**). The profiles were considered rhythmic when a significant effect of time (confirmed by 1-way ANOVA) and significant cosine fit (assessed by cosinor analysis) were confirmed. Differences between two profiles processed simultaneously in the same plate during RT-qPCR were tested by 2-way ANOVA (see **Table 3**). All statistics were generated using Prism 7 software (GraphPad, CA, United States).

TABLE 1 | TaqMan probes used to detect the mRNA of genes of interest.

Gene	TaqMan probe
c-fos	Rn02396759_m1
Per1	Rn01325256_m1
Per2	Rn01427704_m1
Nr1d1	Rn01460662_m1
Rorα	Rn01173769_m1
Dbp	Rn01498425_m1
Vip	Rn00566449_m1
Avp	Rn00566449_m1
Nr3c1	Rn00561369_m1

RESULTS

Experiment 1 – Effect of the Delay in the LD Cycle on the Maternal and Fetal SCN Clocks

The Maternal SCN-Driven Locomotor Activity Rhythm Adjusts Gradually to the 6-h Phase Delay of the LD Regime

To expose the fetuses to a shift in maternal rhythmic signals, we delayed the LD cycle by 6 h starting on E14 and the pregnant rats were maintained in the new LD regime for the next 5 days (Delay group; n = 11). The actual state of the maternal SCN clock was assessed based on the adaptation of their locomotor activity rhythm to the new LD regime. The pregnant rats were fully entrained to the original LD cycle (period tau = 24 h) and after the phase shift, the activity onset and offset started to gradually become delayed via transient cycles (as shown in the representative double-plotted actogram in **Figure 1A**) with a period tau > 24 h (**Figure 1B**). The mean period was 25.17 ± 0.2 (mean ± SD), which means that the SCN clock was delayed by approximately 1 h a day. The effectiveness of the achievement of the steady-state aligned with the new LD cycle was variable among the pregnant rats, as assessed by calculating the activity/rest ratios for each rat (n = 7) before the shift (the amount of activity during the dark versus the light phase of the actual LD cycle was set as 100%) and then on each of the 4 days following the shift (**Figure 1C**). The 5th day was not included in the calculation because on that day (E19), the sampling of fetuses started; thus, for some pregnant rats, the full day record was missing. By the 4th day after the shift, out of the total

TABLE 2 | Results of cosinor analyses.

		CTRL	Delay	LL-ad lib	LL-RF
c-fos	acro ± SEM	3.26 ± 1.12	10.66 ± 0.717	–	–
	amp ± SEM	0.592 ± 0.175	0.361 ± 0.064	–	–
	mesor ± SEM	1.564 ± 0.123	0.902 ± 0.047	1.309 ± 0.08	1.078 ± 0.054
	R^2	0.219	0.437	0.070	0.082
	P	0.0063	<0.0001	0.0563	0.1745
Per1	acro ± SEM	–	–	21.69 ± 1.78	4.86 ± 1.32
	amp ± SEM	–	–	0.119 ± 0.044	0.164 ± 0.062
	mesor ± SEM	0.994 ± 0.078	0.511 ± 0.029	0.923 ± 0.031	1.288 ± 0.042
	R^2	0.029	0.042	0.174	0.149
	P	0.5598	0.4125	0.0321	0.0399
Per2	acro ± SEM	5.13 ± 1.18	10.11 ± 1.00	–	–
	amp ± SEM	0.383 ± 0.136	0.207 ± 0.053	–	–
	mesor ± SEM	1.709 ± 0.09	0.828 ± 0.038	0.718 ± 0.0186	0.72 ± 0.021
	R^2	0.166	0.280	0.131	0.052
	P	0.0268	0.0014	0.0021	0.3379
Nr1d1	acro ± SEM	–	12.16 ± 1.30	18.35 ± 0.99	1.34 ± 1.04
	amp ± SEM	–	0.12 ± 0.039	0.444 ± 0.092	0.333 ± 0.084
	mesor ± SEM	1.22 ± 0.065	0.67 ± 0.028	1.588 ± 0.055	1.666 ± 0.062
	R^2	0.012	0.196	0.195	0.285
	P	0.7907	0.0129	<0.0001	0.0012
Rorα	acro ± SEM	11.94 ± 1.36	13.35 ± 1.45	–	2.89 ± 0.96
	amp ± SEM	0.163 ± 0.055	0.137 ± 0.049	–	0.16 ± 0.041
	mesor ± SEM	0.905 ± 0.04	0.769 ± 0.039	1.005 ± 0.043	1.037 ± 0.029
	R^2	0.199	0.160	0.089	0.277
	P	0.0184	0.0281	0.0435	0.0015
Dbp	acro ± SEM	22.95 ± 1.45	–	–	0.84 ± 1.43
	amp ± SEM	0.315 ± 0.117	–	–	0.152 ± 0.053
	mesor ± SEM	1.054 ± 0.084	0.537 ± 0.023	1.22 ± 0.041	1.125 ± 0.039
	R^2	0.162	0.078	0.142	0.170
	P	0.0352	0.1886	0.0012	0.0221
Vip	acro ± SEM	16.18 ± 1.30	16.07 ± 1.16	14.87 ± 1.29	16.34 ± 0.67
	amp ± SEM	0.301 ± 0.109	0.271 ± 0.089	0.371 ± 0.093	0.658 ± 0.125
	mesor ± SEM	1.128 ± 0.075	0.968 ± 0.061	1.078 ± 0.072	1.724 ± 0.085
	R^2	0.155	0.186	0.226	0.405
	P	0.0293	0.0147	0.001	<0.0001
Avp	acro ± SEM	15.41 ± 0.81	16.36 ± 0.99	17.78 ± 0.71	20.57 ± 1.21
	amp ± SEM	0.323 ± 0.071	0.386 ± 0.105	0.452 ± 0.096	0.367 ± 0.114
	mesor ± SEM	0.731 ± 0.05	0.769 ± 0.072	1.147 ± 0.071	1.166 ± 0.081
	R^2	0.342	0.255	0.325	0.214
	P	0.0002	0.0028	0.0001	0.0091
Nr3c1	acro ± SEM	21.39 ± 1.01	–	20.45 ± 1.30	20.66 ± 1.33
	amp ± SEM	0.235 ± 0.063		0.244 ± 0.087	0.203 ± 0.07
	mesor ± SEM	1.026 ± 0.044	0.676 ± 0.034	1.44 ± 0.059	1.377 ± 0.05
	R^2	0.264	0.030	0.186	0.172
	P	0.0022	0.524	0.022	0.0211

The data show mean and SEM for acrophases (acro), amplitudes (amp), mesors (mesor), goodness of fit R^2 and significance levels (P; gray) of the daily gene expression profiles detected in the SCN of fetuses from mothers in the control group (CTRL) and the groups exposed to 6 h phase delay in LD12:12 (Delay), constant light with ad libitum feeding (LL-ad lib) and constant light with restricted feeding regime (LL-RF). The profiles are shown in the ***Figures 2****,* ***5****.*

of seven monitored pregnant rats, two fully adapted (ratio of approx. 100%; black lines) and two almost fully adapted (ratio of approx. 85%; orange lines) to the new LD regime; however, the activity of three of the rats was not entrained according to the new LD cycle (ratios approx. 25–60%; red lines). These results show that before E19, the SCN clock appeared to be in a transient state in all of the pregnant rats and full adaptation to the new LD cycle was achieved in some of them only shortly before sampling. Therefore, during the last 5 days of embryogenesis, the fetal SCN clocks of the

Delay group developed under nonstable rhythmic signals from the maternal SCN.

The Delay in the LD Cycle Dampens the Amplitudes of the Gene Expression Profiles and Shifts the *c-fos* Expression Profile in the Fetal SCN

We assessed the impact of the transient state of the maternal SCN clock on the fetal clock by comparing the gene expression profiles within the fetal SCN between the CTRL group (no shift) and the Delay group (shift in the LD cycle as described above) (**Figure 2**). We selected genes that we believed might potentially respond to altered maternal cues based on our studies and previous studies by others, namely, the immediate early gene *c-fos*, clock genes (*Per1*, *Per2*, *Nr1d1*, and *Rorα*), the clock-controlled gene *Dbp*, genes coding neurotransmitters (*Vip* and *Avp*) and the GC receptor (*Nr3c1*).

The gene expression rhythms in the fetal SCN on E19 are typically shallow, and therefore, we considered the presence of circadian rhythms based on the combination of criteria as described in the section "Materials and Methods," for which a significant cosinor fit and a significant effect of time by 1-way ANOVA were required (for the results of the cosinor analysis, see **Table 2**; for the results of 1-way ANOVA, see the significance in the graph inserts in **Figure 2**). Based on these criteria, in the CTRL group, the expression profiles of the clock genes *Per1*, *Per2*, *Nr1d1*, and *Rorα*, and the clock-controlled gene *Dbp* were arrhythmic because they did not meet both requirements for significance. In contrast, expression of *c-fos*, *Vip*, *Avp*, and *Nr3c1* exhibited shallow but significant circadian rhythms. The difference between the CTRL and Delay groups was further assessed by 2-way ANOVA (**Table 3**; the significant differences revealed by the post hoc analyses are depicted as stars at the corresponding time points in the individual graphs of **Figure 2**). Most of the expression profiles of the Delay group were significantly dampened (for all genes with the exception of *Vip, Avp*, and *Rorα*) as shown by the decrease in their mesors (**Table 2**), which was independent of whether these profiles were rhythmic in the CTRL group or not. The expression of *Per2* was one of the most robustly suppressed. Therefore, disrupting the rhythmic signaling due to transient state of the maternal SCN

TABLE 3 | Results of 2-way ANOVA analyses.

		CTRL vs delay		LL-ad lib vs LL-RF	
Gene	**Two-way ANOVA**	***P* value**	***P* value summary**	***P* value**	***P* value summary**
c-fos	Interaction	<0.0001	****	0.0022	**
	Time	<0.0001	****	0.0012	**
	Group	<0.0001	****	<0.0001	****
Per1	Interaction	0.0692	ns	0.0572	ns
	Time	0.4003	ns	0.1254	ns
	Group	<0.0001	****	<0.0001	****
Per2	Interaction	0.3168	ns	<0.0001	****
	Time	0.0205	*	<0.0001	****
	Group	<0.0001	****	0.0609	ns
Nr1d1	Interaction	0.1673	ns	<0.0001	****
	Time	0.8828	ns	0.0008	***
	Group	<0.0001	****	0.7785	ns
Rorα	Interaction	0.8877	ns	<0.0001	****
	Time	0.0072	**	0.0003	***
	Group	0.0226	*	0.4578	ns
Dbp	Interaction	0.4036	ns	0.0004	***
	Time	0.0666	ns	0.0002	***
	Group	<0.0001	****	0.0205	*
VIP	Interaction	0.0024	**	0.1359	ns
	Time	0.0006	***	<0.0001	****
	Group	0.0489	*	<0.0001	****
AVP	Interaction	0.0509	ns	0.0043	**
	Time	<0.0001	****	<0.0001	****
	Group	0.5173	ns	0.3543	ns
Nr3c1	Interaction	0.0488	*	0.6803	ns
	Time	0.2163	ns	0.0104	*
	Group	<0.0001	****	0.3721	ns

*Comparison between the gene expression profiles in the fetal SCN of the control group (CTRL) and the group exposed to 6-h phase delay in LD12:12 (Delay), and between the group exposed to constant light with ad libitum feeding (LL-ad lib) and constant light with restricted feeding regime (LL-RF). The gene expression profiles are shown in **Figures 2**, **5**. The results of significance levels (P) for the interaction between groups, the effect of time and the effect of group (gray) are shown.*

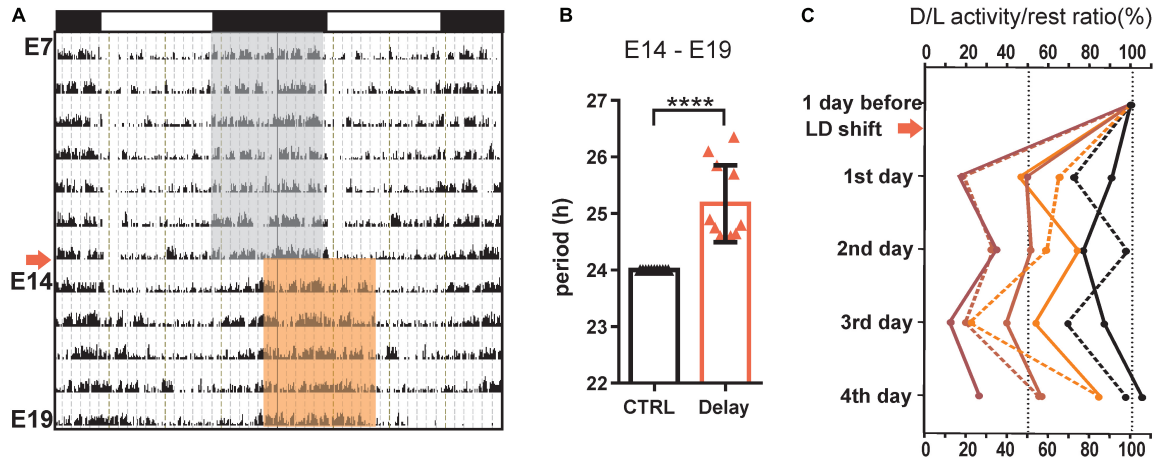

FIGURE 1 | Effect of a 6-h delay in the light/dark cycle on the maternal locomotor activity rhythm. **(A)** Representative double-plotted actogram of a pregnant Wistar rat demonstrating its locomotor activity from embryonic day (E) 7 until E19. The rats were maintained in the original light/dark cycle LD12:12 (as shown in the upper x-axis; the gray area corresponds to darkness), and they were exposed to a 6-h delay in the LD cycle (arrow) by delaying the switch to lights off on E14 (darkness in the new LD cycle is shown as the red area). The fetuses were sampled on E19. **(B)** Circadian periods of the locomotor activity rhythms of pregnant rats determined for the interval between E14 and E19. The rats maintained in the original LD12:12 cycle were assigned as the control group (CTRL; in black; $n = 11$), and those exposed to the 6-h delay in the LD cycle were assigned as the Delay group (Delay; in red; $n = 11$). Data are expressed as the mean ± SD; *t*-test $^{****}P < 0.0001$. **(C)** Percent changes in activity/rest ratios of individual pregnant rats calculated as the amount of activity during the actual dark and light phases of each day. The 1st day after the shift corresponds to E15 and the 4th day corresponds to E18. The pregnant rats were sacrificed at specific times on E19. For each pregnant rat, the activity/rest ratio before the LD shift was determined as 100%.

significantly suppressed expression of clock genes and clock-related genes in the fetal SCN but, interestingly, had no effect on the expression of genes encoding SCN neurotransmitters. Furthermore, the results reveal the recognizable role of *c-fos* in sensing the maternal signals within the fetal SCN because it was the only rhythmically expressed gene that shifted according to the maternal SCN (effect on the group by 2-way ANOVA: $P < 0.0001$). Additionally, the plausible role of GCs in maternal signaling is supported by the fact that the rhythm in expression of the GC receptor (*Nr3c1*) was abolished in the Delay group.

Altogether, the results of Experiment 1 clearly demonstrate that rhythmic maternal signals facilitate gene expression in the fetal SCN because their disruption due to the transitional state of the maternal SCN attenuates the expression levels. Additionally, the data suggest that maternal entrainment of the fetal clock is achieved by signaling pathways employing *c-fos* and GCs.

Experiment 2 – Effect of Exposing Pregnant Rats to Constant Light and Restricted Feeding on Fetuses

LL and RF Differently Affect the Body Weight, Food Consumption, and Weight of the Placentas and Fetuses of Pregnant Wistar Rat, but Not the Size of the Litter

We tested the effect of the attenuation of rhythmic signals derived from the maternal SCN on fetuses by exposing the pregnant rats to LL (LL-ad lib group). Additionally, another group of pregnant rats maintained under LL was exposed to RF (LL-RF group), which provided the fetuses with rhythmic signals derived from the maternal feeding/activity rhythm. Because the experimental protocol involved the manipulation of food access, we first tested whether it impacted BW gain and the weight of the placentas and embryos of the pregnant rats. The pregnant rats from CTRL ($n = 5$), LL-ad lib ($n = 10$), and LL-RF ($n = 13$) groups were weighed on E0, E12–14, and E19 together with a group of age-matched nonpregnant rats maintained under LD12:12 and LL ($n = 3$ in both groups). The BW gain at the time corresponding to E19 was compared between the groups (**Figure 3A**). As expected, the pregnant rats in LL-RF group gained less weight than those in the CTRL and LL-ad lib groups ($P < 0.0001$). Interestingly, exposure to the LL regime without restricting food access had no effect on BW gain because there were no significant differences between CTRL and LL-ad lib groups ($P = 0.9973$) or between the nonpregnant rats maintained on LD cycle versus LL ($P > 0.9999$) (**Figure 3A**). To assess whether the effect of RF on BW was due to a change in the amount of consumed food, we monitored the food consumption of pregnant rats from the LL-RF group by weighting the pellets every day of the RF protocol. In all other groups (CTRL, LL-ad lib and both nonpregnant groups), food consumption was determined on E0, E12–14, and E19, or at the corresponding times for the nonpregnant rats (**Figure 3B**). In accordance with the BW gain, there were no significant differences in amount of food consumed between the CTRL and LL-ad lib groups ($P > 0.9999$) or between both nonpregnant groups ($P = 0.9939$) at the end of the experiment. The pregnant rats from the LL-RF group ate less food than those from the LL-ad lib and CTRL groups (for both groups: $P < 0.0001$), but the amount of food was comparable to that consumed by both nonpregnant groups ($P_{LL-RFvsCTRLnonpregnant} > 0.9999$ and $P_{LL-RFvsLLnonpregnant} = 0.6142$) (**Figure 3B**). The lower BW gain in the LL-RF group compared to that in the LL-ad lib and

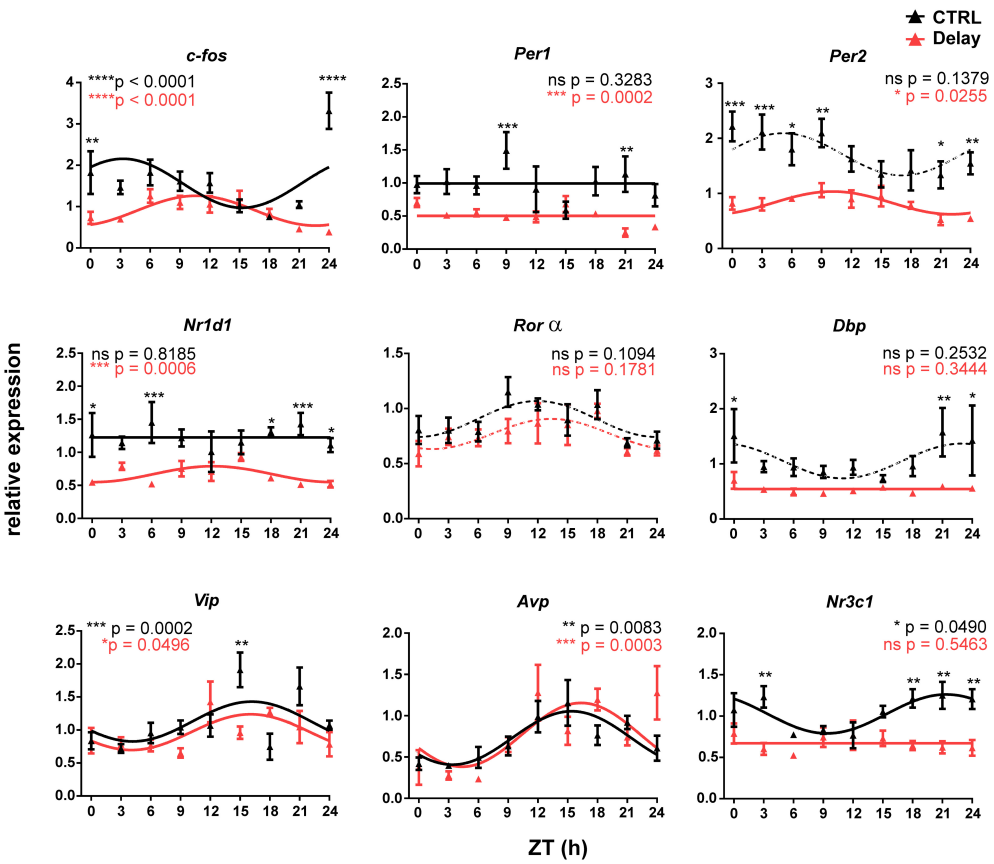

FIGURE 2 | Effect of a 6-h delay in the light/dark cycle on gene expression profiles in the fetal SCN. Pregnant Wistar rats that were maintained under the original LD12:12 cycle (CTRL group; n = 11) or exposed to a 6-h delay in the LD cycle (Delay group; n = 11) were sacrificed on E19 in 3-h intervals over 24 h period. The fetal SCN of the CTRL group (black lines and black triangles) and the Delay group (red lines and red triangles) were dissected and processed by RT-qPCR to detect the daily profiles of the relative expression of selected genes (*c-fos*, *Per1*, *Per2*, *Nr1d1*, *Rorα, Dbp*, *Vip*, *Avp,* and *Nr3c1*). Time is expressed as Zeitgeber time (ZT); ZT0 corresponds to lights on and ZT12 corresponds to lights off based on the original LD cycle. Data are expressed as the mean ± SEM; each time point corresponds to 4–5 embryos from one mother. The data were fitted with cosine curves (for the results, see **Table 2**) and analyzed by 1-way ANOVA (*P* values shown in color corresponding to each group are depicted in the upper parts of each graph); solid cosine curve means significant result of both cosinor analysis and 1-way ANOVA, dashed cosine curve means significant result of cosinor analysis but not of 1-way ANOVA, and straight line means nonsignificant result of cosinor analysis. Finally, the differences between the profiles were tested by 2-way ANOVA (results are shown in **Table 3**; the stars above the time points depict the time when the values significantly differed).

CTRL groups was due to the lower BW gain of the maternal body itself after uterus and embryo removal (**Figure 3C**). The litter sizes were comparable between the CTRL, LL-RF, and LL-ad lib groups ($P_{LL-RFvsLL-adlib}$ = 0.6657; $P_{LL-RFvsCTRL}$ = 0.9592; $P_{CTRLvsLL-adlib}$ = 0.5796) (**Figure 3D**).

Although RF decreased the BW gain due to reduced food intake in the pregnant rats of the LL-RF group, they were apparently able to compensate for it to maintain the same placenta and embryo weights as the LL-ad lib group ($P_{LL-adlibvsLL-RFgroups}$ = 0.9978 and 0.2231 for placentas and embryos, respectively) (**Figure 3E**). Importantly, LL exposure on its own significantly reduced the weights of the placentas, which were lower in both LL-exposed groups compared with those in the CTRL group ($P_{CTRLvsLL-adlib}$ = 0.0001 and $P_{CTRLvsLL-RF}$ = 0.0002). However, the weights of the embryos were slightly higher in both LL-exposed groups, although a significant difference was confirmed only between CTRL and LL-ad lib groups (P = 0.0247). Therefore, although the LL-ad lib group gained the same amount of BW as the CTRL group during pregnancy, their embryos were slightly heavier and the placentas were less well developed.

The Locomotor Activity Rhythm of Pregnant Rats Progressively Attenuates Due to Exposure to LL and Is Re-established by Concurrent Exposure to RF

The locomotor activity was monitored in pregnant rats of the LL-ad lib (n = 10) and LL-RF (n = 13) groups from E0 until E19 (representative actograms are shown in **Figures 4A,B**). Exposure to LL with *ad libitum* feeding caused immediate lengthening of the circadian periods of the locomotor activity rhythms in all mothers (**Figure 4A**); the mean period between E0 and E14 was 25.30 ± 0.38 h (**Figure 4C**). Thereafter, during the last 5 days of pregnancy, the long period-rhythms gradually weakened (see the higher variability of the estimated

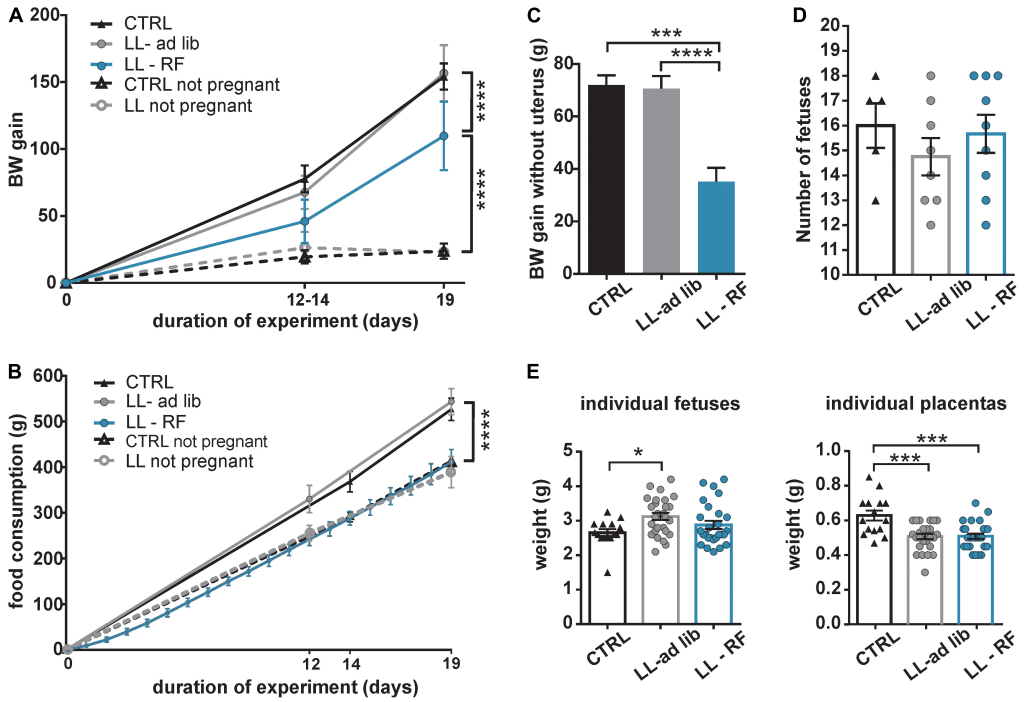

FIGURE 3 | Effect of the exposure of pregnant rats to constant light and a restricted feeding regime on the body weight, food intake, litter size and weight of placenta and fetuses. **(A)** Comparison of the body weight (BW) gain of five groups of Wistar rats over 19 days. Control pregnant (CTRL; $n = 5$) and nonpregnant (CTRL-nonpregnant; $n = 3$) rats were fed *ad libitum* and maintained under LD12:12. Additionally, pregnant (LL-ad lib; $n = 8$) and nonpregnant (LL-nonpregnant; $n = 3$) rats were exposed to constant light and fed *ad libitum*. Finally, one group of pregnant rats maintained under LL was exposed to restricted access to food (LL-RF; $n = 10$). The rats were weighed at the beginning of pregnancy (E0), on E12–E14 and at the end of the experiment on E19 or at the corresponding time intervals for the nonpregnant rats. Data are the mean ± SD. The values of BW gain after 19 days were compared between the groups by 2-way ANOVA ****$P < 0.0001$). **(B)** Comparison of food consumption (weight of the pellets in grams) between the five groups of rats described in **(A)**. Data are mean ± SD. The weights of consumed food after 19 days were compared by 2-way ANOVA (****$P < 0.0001$). **(C)** The pregnant rats in the three experimental groups described in **(A)** (CTRL, LL-ad lib, and LL-RF) were sacrificed at E19 and their bodies were weighed after the whole uterus containing embryos and placentas was removed. The weights of the separated fetuses and placentas are shown in **(E)**. For each rat, the value of BW gain was calculated relative to BW at E0. Data are the mean ± SEM. The values were compared between the groups by 1-way ANOVA (****$P < 0.0001$; ***$P = 0.0004$). **(D)** Number of fetuses (mean ± SEM) from each mother of the three groups described in **(A)** (CTRL, LL-ad lib, and LL-RF). The data were compared by 1-way ANOVA. **(E)** Weights of individual fetuses and placentas (mean ± SEM) of three groups of mothers as described in **(A)** (CTRL, LL-ad lib, and LL-RF). Three fetuses and placentas from each pregnant rat were measured. The data were compared by 1-way ANOVA (***$P_{CTRLvsLL-adlib} = 0.001$; $P_{CTRLvsLL-RF} = 0.002$; *$P = 0.025$).

periods in the interval between E14 and E19 in **Figure 4C**). Although the dynamics of the rhythm weakening were variable among the pregnant rats, all of the mothers but one became completely arrhythmic by E19, which is when the fetuses were collected. The data obtained from the single mother that remained rhythmic throughout pregnancy (shown in **Figure 4A**; actogram on the right side assigned as "rhythmic") were excluded from the study. In the pregnant rats of the LL-RF group, the activity rhythm also started to exhibit a long period up to the 5th day after exposure to LL, but then the rats reorganized their activity patterns and synchronized themselves with the time of food availability (the mean period was 24.02 and 24.14 for the E0–E14 and E14–E19 intervals, respectively; **Figure 4C**). This indicates that the pregnant rats started to be active in the expectation of food (food anticipatory activity) and ceased their activity immediately after food was removed from their cages (**Figure 4B**). Therefore, whereas in the LL-ad lib group, the SCN-driven locomotor activity rhythm was attenuated/absent during the last 5 days before the sampling of the fetuses, in the LL-RF group, the rhythm was reinforced by food availability.

Exposure of Pregnant Rats to LL and LL + RF Selectively Influences Expression of Genes in the Fetal SCN

We examined whether the LL-induced attenuation of maternal SCN-derived signals without (LL-ad lib group) and with (LL-RF group) imposed activity/feeding rhythms affected gene expression in the SCN of 19-day-old fetuses. The daily expression profiles of the same genes as those examined in Experiment 1 were analyzed (**Figure 5**). In the LL-ad lib group, the expression profiles of most genes did not meet the criteria for rhythmicity (significant cosinor fit and effect of time by 1-way ANOVA), namely the profiles of *c-fos*, *Per1*, *Per2*, *Rorα*, *Dbp*, and *Nr3c1*, although expression profile of *Nr1d1* exhibited a shallow rhythm (for the cosinor analysis data, see **Table 2**; the 1-way ANOVA results are depicted in the graph inserts of the **Figure 5**). Based on the comparison with the profiles that were rhythmic in

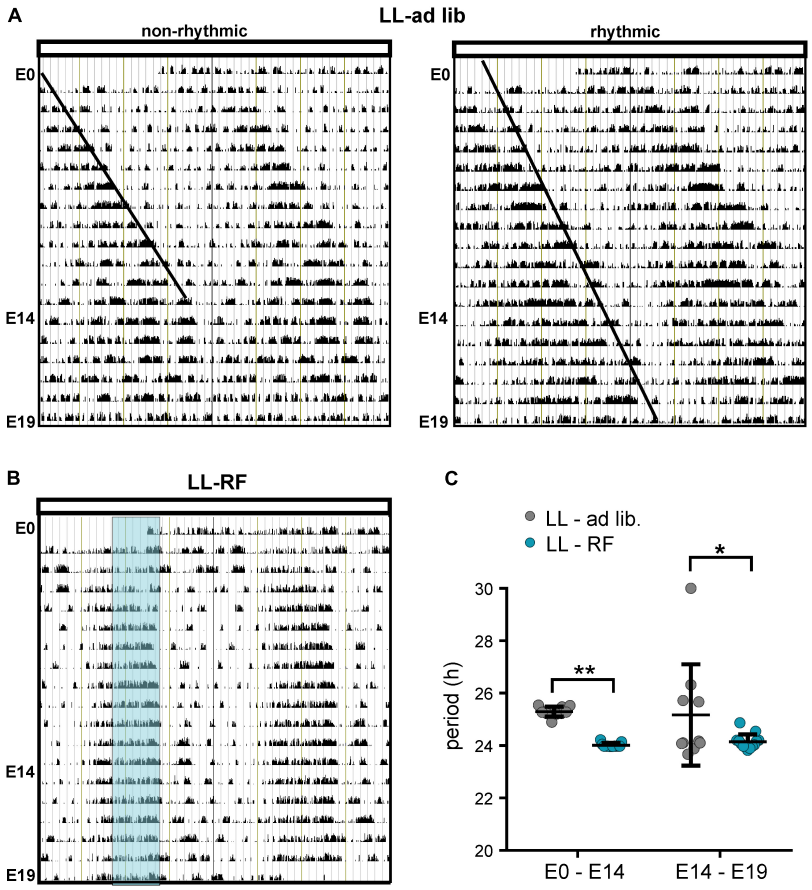

FIGURE 4 | Effect of constant light and the restricted feeding protocol on the locomotor activity of pregnant rats. **(A)** Representative double-plotted actograms of two pregnant Wistar rats kept under constant light (LL) and fed *ad libitum* during entire experiment (E0–E19) (LL-ad lib). The actogram on the left side shows an example of the activity observed in most of the pregnant rats, which became completely nonrhythmic starting before E19. The actogram on the right side is an example from one pregnant rat, which was the exception and remained rhythmic throughout the measurement (the fetal SCNs of this rat were excluded from the experiment). The lines drawn in the actograms are eye-fits of the activity offsets. **(B)** Representative double-plotted actogram of a rat exposed to LL along with the restriction of access to food for only 6 h (LL-RF group). The blue area represents the feeding time (local time 9:00–15:00). The activity of all pregnant rats in the group was adjusted according to the food availability. **(C)** Circadian periods of the locomotor activity rhythms in the LL-ad lib (n = 10) and LL-RF (n = 13) groups during the intervals E0–E14 and E14–E19. Data are expressed as individual values and means ± SD. Data were compared between both groups by 2-way ANOVA (**p = 0.0035; *p = 0.0211).

the CTRL group in Experiment 1 (**Figure 2**) it was obvious that LL exposure abolished the rhythms in *c-fos* and *Nr3c1* expression. These results were in accordance with the conclusion we had drawn based on the data from Experiment 1 that these two genes were involved in responses to maternal SCN-derived signals. Interestingly, again in accordance with the Experiment 1 data, exposure of animals fed *ad libitum* to LL had no effect on the rhythmicity of the expression of genes encoding neurotransmitters (*Vip* and *Avp*) (for the cosinor data, see **Table 2**).

Exposure of pregnant rats in which SCN signaling to fetuses was attenuated due to LL to restricted food availability (LL-RF group) had gene-specific effects within the fetal SCN (see **Table 3** for the comparison between the LL-ad lib and LL-RF profiles based on the 2-way ANOVA results). Exposure to RF did not affect the LL-induced suppression of the rhythmicity of *c-fos* and *Nr3c1* expression because their profiles in the LL-RF group were also nonrhythmic. For *c-fos*, 2-way ANOVA detected differences between the LL-ad lib and LL-RF groups only at CT0/24. Interestingly, *Per1* expression, which was nonrhythmic in the CTRL group (**Figure 2**) as well as in both LL groups (**Figure 5**), was upregulated in the LL-RF group compared to the LL-ad lib group, whereas the *Per2* expression profile did not differ. We speculate that RF restored the LL-suppressed *Per1* expression. RF exposure had a similar prominent effect on the rhythm in *Vip* expression because amplitude and mesor were increased in the LL-RF group compared to the LL-ad lib group (for the comparison of the amplitudes among the groups, see the cosinor analyses data in **Table 2**). In contrast, RF exposure had no effect on the rhythmic *Avp* expression, similar to other disruptive stimuli tested in the study. Interestingly, exposure to RF significantly shifted the rhythm of *Nr1d1* expression and induced very shallow rhythms in *Rorα* and *Dbp* expression which were all in synchrony (**Figure 5**).

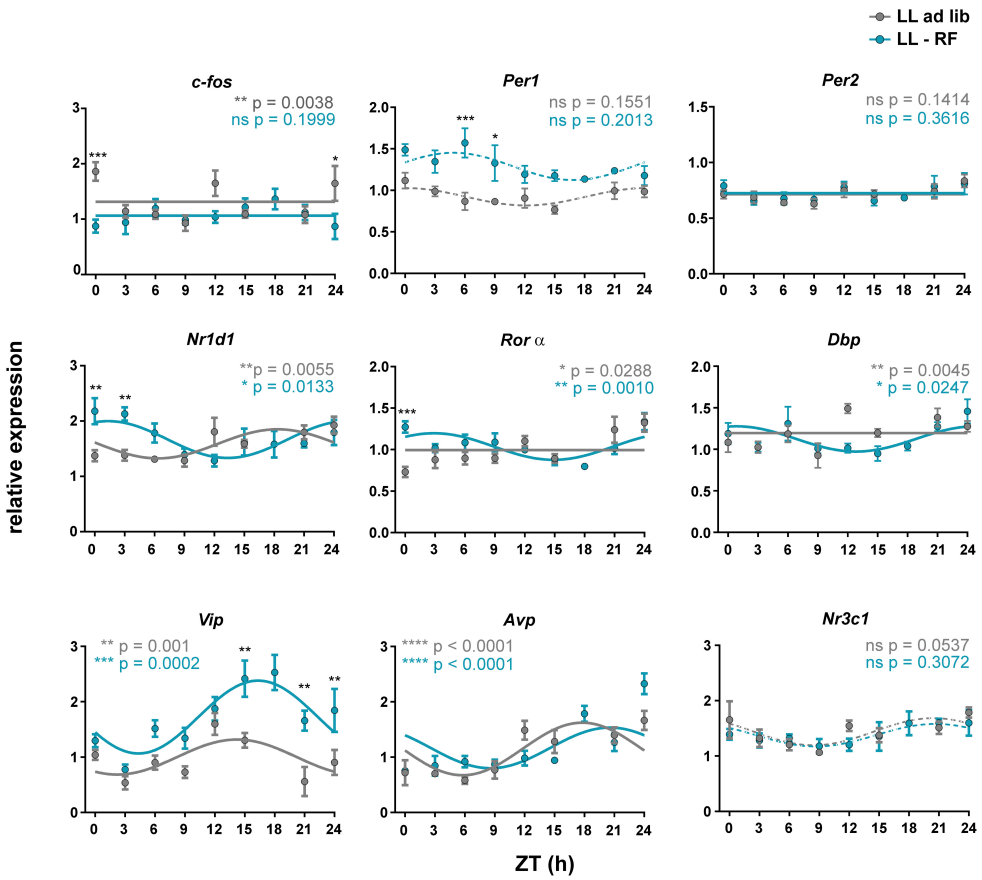

FIGURE 5 | Effect of constant light and the restricted feeding protocol on gene expression profiles in the fetal SCN. Daily profiles of the relative mRNA expression of selected genes (*c-fos*, *Per1*, *Per2*, *Nr1d1*, *Rorα, Dbp*, *Vip*, *Avp*, and *Nr3c1*) in the SCN of 19-day-old fetuses collected from pregnant rats maintained under constant light and either fed *ad libitum* (LL-ad lib group; gray lines and gray circles) or exposed to a restricted feeding regime (LL-RF group; blue lines and blue circles). The pregnant rats were sacrificed in 3 h intervals over 24 h. Time is expressed as Zeitgeber time (ZT); ZT0 corresponds to lights on and ZT12 corresponds to lights off based on the original LD cycle. Data are expressed as the mean ± SEM; each time point corresponds to 4–5 embryos from one mother. The data were fitted with cosine curves (for the results, see **Table 2**) and analyzed by 1-way ANOVA (*P* values shown in color corresponding to each group are depicted in the upper parts of each graph); solid cosine curve means significant result of both cosinor analysis and 1-way ANOVA, dashed cosine curve means significant result of cosinor analysis but not of 1-way ANOVA, and straight line means nonsignificant result of cosinor analysis. Finally, the differences between the profiles were tested by 2-way ANOVA (the results are shown in **Table 3**; the stars above the time points depict the time when the values significantly differed).

Altogether, the results of Experiment 2 demonstrated that exposure of pregnant rats fed *ad libitum* to LL impaired their circadian behavior and the development of their placentas and thus possibly influenced the maternal/fetal barrier. The SCNs of their fetuses responded to the LL-induced attenuation of the maternal rhythmic signals by abolishment of the *c-fos* and *Nr3c1* expression rhythms. Subjecting LL-exposed pregnant rats to feeding/fasting and related activity/rest rhythms had significant gene-specific effects on the fetal SCN; it restored the LL-suppressed expression levels of *Vip* and *Per1* and affected expression of genes related to sensing changes in the cellular metabolic state (*Nr1d1*, *Rorα*, and *Dbp*).

DISCUSSION

The results of our study provide the first insights into whether and how the fetal SCN clock responds to situations in which the maternal circadian system is challenged via disruption of the environmental LD regime. We demonstrate that exposure of pregnant rats to disruptions resembling situations that humans may experience in their everyday life significantly and selectively impacts gene expression in the fetal SCN. So far, the issue has not been addressed because the impact of maternal chronodisruption on the fetal SCN clock was assessed only after birth, either in newborn pups (El-Hennamy et al., 2008; Nováková et al., 2010) or during later postnatal stages (Mendez et al., 2016).

The SCN of 19-day-old fetuses of the control group, whose mothers were entrained to LD12:12, rhythmically expressed *c-fos*, *Vip*, *Avp* and *Nr3c1*, but the profiles of all other studied genes (*Per1*, *Per2*, *Nr1d1*, *Rorα*, and *Dbp*) failed to meet the requirement for a significant circadian rhythm (for more details, see section "Materials and Methods"). The presence/absence of rhythmicity in expression of these genes as well as acrophases of their rhythmic profiles were in accordance with our previous results (Sládek et al., 2004; Houdek and Sumová, 2014), with

the only exception that in the current study, the *Nr1d1* profile did not meet the significance requirements for the circadian rhythm. The abrupt 6 h-phase shift in the LD cycle induced in mothers on gestational day 14 transposed the maternal SCN clock into a transient state during which it gradually became phase-delayed by approximately 1 h a day. Over the course of the next 5 days, the activity/rest ratios calculated for each individual pregnant rat were not aligned with the new LD cycle and in some of the mothers full entrainment was not achieved even on E19, when the fetal SCN were sampled. This transient state affected the gene expression profiles in the SCN of 19-day-old fetuses. Irrespective of whether the genes were expressed rhythmically in controls or not, the expression of most of these genes was robustly suppressed, which included clock (*Per1*, *Per2*, and *Nr1d1*) and clock-controlled (*Dbp*) genes as well as genes involved in sensing various signals, such as *c-fos* and *Nr3c1*. Importantly, *c-fos* was identified as the gene primarily responsible for sensing the phase of the maternal clock because it was expressed rhythmically at E19, and its rhythm was phase-delayed according to the new phase of the maternal SCN clock. In contrast, the transient state of the maternal SCN did not change the rhythmic expression of genes encoding the neurotransmitters *Vip* and *Avp*. The result demonstrates that the rhythm of *Avp* expression, which in the adult SCN is under control of the clock as a clock-controlled gene (Jin et al., 1999), does not follow the phase of *c-fos* after the phase shift, and thus the rhythmic expression profiles of these two genes in the fetal SCN is driven by divergent signals.

To ascertain whether the effects we observed in the fetal SCN due to the transient state were caused by the abolishment or reduction in the rhythmic maternal signals, we exposed the pregnant rats to LL. Exposure to LL affects the ability of maternal SCN to transmit rhythmic signals to the fetuses because previous studies found that under LL, the SCN neuronal activity rhythm was dampened (Lucassen et al., 2016), and the cellular oscillators became mutually desynchronized (Ohta et al., 2005), which had an impact on the production of coherent rhythmic signals driving rhythms at the systemic level. Exposure of pregnant rats to LL starting on E0 caused an initial lengthening of the circadian period of locomotor activity rhythms, which was gradually followed by a complete loss of rhythmicity, as we previously showed for this rat strain (Houdek and Sumová, 2014). The timing of the beginning of arrhythmicity slightly varied among the dams and occurred after approximately 2 weeks under LL, which indicates that between E14 and E19, all but one of the pregnant rats (which was excluded from the study) completely lost behavioral rhythmicity. Therefore, the maternal signals were modulated during the same interval from E14 to E19 as in the previous experiment, in which the pregnant rats were exposed to a phase shift in the LD cycle. Exposure of rats to LL may have a more general impact on the course of pregnancy because it has previously been assigned to be a stressor (Honma and Hiroshige, 1978) and was found to potentially affect sex hormone levels (Takeo et al., 1975). Indeed, we revealed that in the LL-ad lib group, the weights of placentas were significantly reduced compared to those in the CTRL group, which was not caused by a decrease in the dams' food intake or a reduction in BW gain during pregnancy. Additionally, in our conditions the litter sizes were not affected by LL but the embryo weights were slightly higher than those in the control group. However, another study found that the weights of fetuses or newborn pups were lower in LL-exposed dams (Mendez et al., 2012; Amano et al., 2020).

In line with the results of our phase-shift experiment (as described above), we found that LL completely abolished rhythmic expression of *c-fos* in the fetal SCN but did not affect the rhythms in *Avp* and *Vip* expression. This supports the above proposed scenario of the divergence of the signals driving rhythmicity of *c-fos* and *Avp* expression in the fetal SCN. Additionally, the persistence of the *Vip* and *Avp* rhythms under LL conditions excluded the possibility that the absence of rhythmicity in the expression of genes, which were rhythmic during the LD cycle, was due to a lack of mutual synchrony among otherwise rhythmic SCN clocks in individual fetuses. Therefore, the data are in favor of the explanation that the rhythmic expression of these genes was dependent on presence of maternal signals. This conclusion is in accordance with the hypothesis we formulated earlier about the maternal origin of the rhythmicity detected at this early fetal stage in the rat SCN (Sumová et al., 2012).

Comparisons between the responses of the gene expression profiles in the fetal SCN in both experiments (**Figures 2**, **5**) revealed that they greatly differed. It appeared that the dampening of gene expression we detected under the transition state was not caused simply by the reduction/absence of signals sent from the maternal to the fetal SCN, as occurred under LL. The fetal SCN is thus responding to various maternal pathways that were plausibly specifically modulated due to exposure to these two challenges. However, identifying these mechanisms is problematic because maternal signals to the fetal SCN are complex, interconnected and convergent. They may involve hormonal levels, body temperature as well as activity/sleep and feeding/fasting rhythms (reviewed in Sumová et al., 2012). Regarding the humoral pathways, we may speculate about the involvement of at least two candidate hormones that are controlled by the maternal SCN and might thus play a role in these effects; melatonin, as a messenger of darkness (Davis and Mannion, 1988; Houdek et al., 2015), and recently discovered GCs, as messengers of the active state (Čečmanová et al., 2019). The maternal SCN provides the fetal SCN with combinatory hormonal signaling, i.e., in nocturnal rats, the simultaneously elevated levels of melatonin and GCs are signaling the time when the mother is awake and active. Importantly, these two hormones likely responded to the chronodisruptions tested in our study differently. Under the transient state due to the phase delay in the LD cycle, the maternal SCN gradually delays the timing of the elevation in melatonin levels (Humlová and Illnerová, 1992), which could theoretically drive the delay in the *c-fos* expression profile because the gene expression profile was entrained by melatonin (Houdek et al., 2015). However, the situation is not clear in case of GCs. Expression of their receptor (*Nr3c1*) exhibits circadian variation in the fetal SCN on E19, as we have shown in this study as well as our previous study (Čečmanová et al., 2019). Here, we found that the transient state abolished the circadian

rhythm in *Nr3c1* expression, suggesting impaired rhythmicity of the hormonal profile. If this is correct, the impairment of the GC rhythm due to the transient state might play a role in the downregulation of the clock gene expression profiles we detected in the fetal SCN because we have previously shown that GCs may facilitate fetal SCN development (Čečmanová et al., 2019). Therefore, we can speculate that the transient state of the SCN in pregnant rats likely affected the mutual alignment of melatonin and GC signaling to the fetal SCN, which might lead to the deregulation of convergent signaling with functional relevance for the maintenance of gene expression levels. Similar mechanism may be employed in the effect of LL on fetal SCN because it was previously found that LL exposure affects both melatonin and GC levels in pregnant rats (Mendez et al., 2012). The plasma melatonin levels in pregnant rats (Mendez et al., 2012; Houdek et al., 2015) were suppressed to the same extent as in adult males (Wideman and Murphy, 2009; Dauchy et al., 2010). Additionally, we previously confirmed that in the LL-exposed pregnant rats, melatonin injections during E17–E21 (last 5 days of pregnancy) served as a potent synchronizer of the fetal SCN clock as detected in newborn pups (Houdek et al., 2015). Under LL conditions, the amplitude of the corticosterone rhythm was significantly dampened in adult male rats (Claustrat et al., 2008; Park et al., 2013; Tapia-Osorio et al., 2013), but it was rather delayed in pregnant Sprague-Dawley rats at E18 (Mendez et al., 2012). In our Wistar rats, we found significant reduction in the amplitude of the oscillation of *Nr3c1* expression in the fetal SCN in the LL-ad lib group compared with that in the CTRL group, which suggests a significant effect of LL on the maternal GC rhythm. Theoretically, the effect might play a role in abolishment of the *c-fos* rhythm in the LL-ad lib group because we previously demonstrated that dexamethasone application to pregnant rats induced acute responses of *c-fos* expression in the fetal SCN (Čečmanová et al., 2019). Additionally, the fetal adrenal glands were suggested to play a role of a melatonin-sensitive peripheral clock in the mother (Torres-Farfan et al., 2011), providing further potential mechanism of how LL impacts the fetal SCN. Altogether, the LL-induced suppression of melatonin levels supported by a concurrent modulation of the GC rhythm seems to be a plausible mechanism for the effect we observed in the fetal SCN, although the direct connection with the regulation of the studied genes remains unclear.

The exposure of pregnant rats to LL disrupts not only hormonal levels but also other entraining signals, namely, the behavioral activity/sleep and feeding/fasting rhythms as well as the tightly related body temperature rhythm (Eastman and Rechtschaffen, 1983). Re-inducing those rhythms in pregnant rats maintained in LL via temporary restriction of access to food allowed us to ascertain their participation in the effects of LL on the fetal SCN. Previously, we showed that the same protocol was efficient in entraining the clock in newborn rats (Nováková et al., 2010). Here we found that in the fetal SCN the lack of a maternal behavioral rhythm was not involved in abolishment of *c-fos* rhythmicity due to LL exposure, further supporting the abovementioned speculations on the role of hormonal signals in the regulation of genes in the fetal SCN. Unexpectedly, we revealed participation of the maternal behavioral rhythm in maintenance of the *Vip* expression level and the amplitude of its rhythm, suggesting its role in neuronal maturation of the fetal SCN. Apart from this, less pronounced but significant effects on the expression profiles of *Per1* (slight upregulation) and *Nr1d1*, *Rorα*, and *Dbp* (by inducing shallow rhythmicity) were also detected. Interestingly, we previously observed the same effect of RF on *Nr1d1* expression in the adult SCN of rats exposed to LL (Nováková et al., 2011).

Altogether, our study revealed that the fetal SCN responds to complex maternal signals in a gene-specific manner. Importantly, disruption these maternal signals impacts the fetal SCN and affects regulation of genes that are involved in general cellular signaling as well as clock-related mechanisms. It is tempting to speculate that such effects may mediate the noxious impact of prenatal chronodisruption on the development of the SCN.

DATA AVAILABILITY STATEMENT

The raw data supporting the conclusions of this article will be made available by the authors, without undue reservation.

ETHICS STATEMENT

The animal study was reviewed and approved by the Animal Care and Use Committee of the Institute of Physiology of the Czech Academy of Sciences.

AUTHOR CONTRIBUTIONS

VL: design of the work, data acquisition, writing the draft, and final approval of the version to be published. PH: data acquisition and final approval of the version to be published. KL: data acquisition, data analysis, and final approval of the version to be published. AS: conceptualization and data interpretation, writing the manuscript, and final approval of the version to be published. All authors contributed to the article and approved the submitted version.

FUNDING

The study was supported by the Czech Science Foundation grant 19-01845S (to AS) and the Research Project RV0: 67985823.

ACKNOWLEDGMENTS

We thank Martin Sládek, Ph.D., for his methodological expertise, Mrs. Eva Suchanová for technical help, and Ms. Barbora Černá for participation in collecting samples of the fetal SCN in the phase-shift experiment.

REFERENCES

Altman, J., and Bayer, S. A. (1978). Development of the diencephalon in the rat. II. Correlation of the embryonic development of the hypothalamus with the time of origin of its neurons. *J. Comp. Neurol.* 182, 973–993. doi: 10.1002/cne.901820512

Amano, T., Ripperger, J. A., and Albrecht, U. (2020). Changing the light schedule in late pregnancy alters birth timing in mice. *Theriogenology* 154, 212–222. doi: 10.1016/j.theriogenology.2020.05.032

Bates, K., and Herzog, E. D. (2020). Maternal-fetal circadian communication during pregnancy. *Front. Endocrinol. (Lausanne)* 11:198. doi: 10.3389/fendo.2020.00198

Bedont, J. L., and Blackshaw, S. (2015). Constructing the suprachiasmatic nucleus: a watchmaker's perspective on the central clockworks. *Front. Syst. Neurosci.* 9:74. doi: 10.3389/fnsys.2015.00074

Bellavía, S. L., Carpentieri, A. R., Vaqué, A. M., Macchione, A. F., and Vermouth, N. T. (2006). Pup circadian rhythm entrainment–effect of maternal ganglionectomy or pinealectomy. *Physiol. Behav.* 89, 342–349. doi: 10.1016/j.physbeh.2006.06.018

Carmona-Alcocer, V., Abel, J. H., Sun, T. C., Petzold, L. R., Doyle, F. J., Simms, C. L., et al. (2018). Ontogeny of circadian rhythms and synchrony in the suprachiasmatic nucleus. *J. Neurosci.* 38, 1326–1334. doi: 10.1523/jneurosci.2006-17.2017

Carmona-Alcocer, V., Rohr, K. E., Joye, D. A. M., and Evans, J. A. (2020). Circuit development in the master clock network of mammals. *Eur. J. Neurosci.* 51, 82–108. doi: 10.1111/ejn.14259

Čečmanová, V., Houdek, P., Šuchmanová, K., Sládek, M., and Sumová, A. (2019). Development and entrainment of the fetal clock in the suprachiasmatic nuclei: the role of glucocorticoids. *J. Biol. Rhythms* 34, 307–322. doi: 10.1177/0748730419835360

Claustrat, B., Valatx, J.-L., Harthé, C., and Brun, J. (2008). Effect of constant light on prolactin and corticosterone rhythms evaluated using a noninvasive urine sampling protocol in the rat. *Horm. Metab. Res.* 40, 398–403. doi: 10.1055/s-2008-1065330

Dauchy, R. T., Dauchy, E. M., Tirrell, R. P., Hill, C. R., Davidson, L. K., Greene, M. W., et al. (2010). Dark-phase light contamination disrupts circadian rhythms in plasma measures of endocrine physiology and metabolism in rats. *Comp. Med.* 60, 348–356.

Davis, F. C., and Gorski, R. A. (1985a). Development of hamster circadian rhythms: prenatal entrainment of the pacemaker. *J. Biol. Rhythms* 1, 77–89. doi: 10.1177/074873048600100108

Davis, F. C., and Gorski, R. A. (1985b). Development of hamster circadian rhythms. I. Within-litter synchrony of mother and pup activity rhythms at weaning. *Biol. Reprod.* 33, 353–362. doi: 10.1095/biolreprod33.2.353

Davis, F. C., and Mannion, J. (1988). Entrainment of hamster pup circadian rhythms by prenatal melatonin injections to the mother. *Am. J. Physiol.* 255, R439–R448.

Duncan, M. J., Banister, M. J., and Reppert, S. M. (1986). Developmental appearance of light-dark entrainment in the rat. *Brain Res.* 369, 326–330. doi: 10.1016/0006-8993(86)90544-5

Eastman, C., and Rechtschaffen, A. (1983). Circadian temperature and wake rhythms of rats exposed to prolonged continuous illumination. *Physiol. Behav.* 31, 417–427. doi: 10.1016/0031-9384(83)90061-6

El-Hennamy, R., Matějů, K., Bendová, Z., Sosniyenko, S., and Sumová, A. (2008). Maternal control of the fetal and neonatal rat suprachiasmatic nucleus. *J. Biol. Rhythms* 23, 435–444. doi: 10.1177/0748730408322635

Herzog, E. D., Aton, S. J., Numano, R., Sakaki, Y., and Tei, H. (2004). Temporal precision in the mammalian circadian system: a reliable clock from less reliable neurons. *J. Biol. Rhythms* 19, 35–46. doi: 10.1177/0748730403260776

Honma, K. I., and Hiroshige, T. (1978). Endogenous ultradian rhythms in rats exposed to prolonged continuous light. *Am. J. Physiol.* 235, R250–R256.

Houdek, P., Polidarová, L., Nováková, M., Matějů, K., Kubík, Š, and Sumová, A. (2015). Melatonin administered during the fetal stage affects circadian clock in the suprachiasmatic nucleus but not in the liver. *Dev. Neurobiol.* 75, 131–144. doi: 10.1002/dneu.22213

Houdek, P., and Sumová, A. (2014). In vivo initiation of clock gene expression rhythmicity in fetal rat suprachiasmatic nuclei. *PLoS One* 9:e107360. doi: 10.1371/journal.pone.0107360

Humlová, M., and Illnerová, H. (1992). Resetting of the rat circadian clock after a shift in the light/dark cycle depends on the photoperiod. *Neurosci. Res.* 13, 147–153. doi: 10.1016/0168-0102(92)90095-t

Jin, X., Shearman, L. P., Weaver, D. R., Zylka, M. J., de Vries, G. J., and Reppert, S. M. (1999). A molecular mechanism regulating rhythmic output from the suprachiasmatic circadian clock. *Cell* 96, 57–68. doi: 10.1016/s0092-8674(00)80959-9

Kováčiková, Z., Sládek, M., Bendová, Z., Illnerová, H., and Sumová, A. (2006). Expression of clock and clock-driven genes in the rat suprachiasmatic nucleus during late fetal and early postnatal development. *J. Biol. Rhythms* 21, 140–148. doi: 10.1177/0748730405285876

Landgraf, D., Achten, C., Dallmann, F., and Oster, H. (2015). Embryonic development and maternal regulation of murine circadian clock function. *Chronobiol. Int.* 32, 416–427. doi: 10.3109/07420528.2014.986576

Liu, A. C., Welsh, D. K., Ko, C. H., Tran, H. G., Zhang, E. E., Priest, A. A., et al. (2007). Intercellular coupling confers robustness against mutations in the SCN circadian clock network. *Cell* 129, 605–616. doi: 10.1016/j.cell.2007.02.047

Lowrey, P. L., and Takahashi, J. S. (2011). Genetics of circadian rhythms in Mammalian model organisms. *Adv. Genet.* 74, 175–230. doi: 10.1016/b978-0-12-387690-4.00006-4

Lucassen, E. A., Coomans, C. P., van Putten, M., de Kreij, S. R., van Genugten, J. H. L. T., Sutorius, R. P. M., et al. (2016). Environmental 24-hr cycles are essential for health. *Curr. Biol.* 26, 1843–1853. doi: 10.1016/j.cub.2016.05.038

Mendez, N., Abarzua-Catalan, L., Vilches, N., Galdames, H. A., Spichiger, C., Richter, H. G., et al. (2012). Timed maternal melatonin treatment reverses circadian disruption of the fetal adrenal clock imposed by exposure to constant light. *PLoS One* 7:e42713. doi: 10.1371/journal.pone.0042713

Mendez, N., Halabi, D., Spichiger, C., Salazar, E. R., Vergara, K., Alonso-Vasquez, P., et al. (2016). Gestational chronodisruption impairs circadian physiology in rat male offspring, increasing the risk of chronic disease. *Endocrinology* 157, 4654–4668. doi: 10.1210/en.2016-1282

Moore, R. Y., and Bernstein, M. E. (1989). Synaptogenesis in the rat suprachiasmatic nucleus demonstrated by electron microscopy and synapsin I immunoreactivity. *J. Neurosci.* 9, 2151–2162. doi: 10.1523/jneurosci.09-06-02151.1989

Moore, R. Y., and Eichler, V. B. (1972). Loss of a circadian adrenal corticosterone rhythm following suprachiasmatic lesions in the rat. *Brain Res.* 42, 201–206. doi: 10.1016/0006-8993(72)90054-6

Morin, L. P., and Allen, C. N. (2006). The circadian visual system, 2005. *Brain Res. Rev.* 51, 1–60. doi: 10.1016/j.brainresrev.2005.08.003

Nishide, S. Y., Honma, S., and Honma, K. I. (2008). The circadian pacemaker in the cultured suprachiasmatic nucleus from pup mice is highly sensitive to external perturbation. *Eur. J. Neurosci.* 27, 2686–2690. doi: 10.1111/j.1460-9568.2008.06231.x

Nováková, M., Polidarová, L., Sládek, M., and Sumová, A. (2011). Restricted feeding regime affects clock gene expression profiles in the suprachiasmatic nucleus of rats exposed to constant light. *Neuroscience* 197, 65–71. doi: 10.1016/j.neuroscience.2011.09.028

Nováková, M., Sládek, M., and Sumová, A. (2010). Exposure of pregnant rats to restricted feeding schedule synchronizes the SCN clocks of their fetuses under constant light but not under a light-dark regime. *J. Biol. Rhythms* 25, 350–360. doi: 10.1177/0748730410377967

Ohta, H., Yamazaki, S., and McMahon, D. G. (2005). Constant light desynchronizes mammalian clock neurons. *Nat. Neurosci.* 8, 267–269. doi: 10.1038/nn1395

Park, S. Y., Walker, J. J., Johnson, N. W., Zhao, Z., Lightman, S. L., and Spiga, F. (2013). Constant light disrupts the circadian rhythm of steroidogenic proteins in the rat adrenal gland. *Mol. Cell Endocrinol.* 371, 114–123. doi: 10.1016/j.mce.2012.11.010

Ralph, M. R., Foster, R. G., Davis, F. C., and Menaker, M. (1990). Transplanted suprachiasmatic nucleus determines circadian period. *Science* 247, 975–978. doi: 10.1126/science.2305266

Reppert, S. M., and Schwartz, W. J. (1986). Maternal suprachiasmatic nuclei are necessary for maternal coordination of the developing circadian system. *J. Neurosci.* 6, 2724–2729. doi: 10.1523/jneurosci.06-09-02724.1986

Richter, H. G., Mendez, N., Abarzua-Catalan, L., Valenzuela, G. J., Seron-Ferre, M., and Torres-Farfan, C. (2018). Developmental programming of capuchin monkey adrenal dysfunction by gestational chronodisruption. *Biomed. Res. Int.* 2018:9183053.

Salazar, E. R., Richter, H. G., Spichiger, C., Mendez, N., Halabi, D., Vergara, K., et al. (2018). Gestational chronodisruption leads to persistent changes in the rat fetal and adult adrenal clock and function. *J. Physiol.* 596, 5839–5857. doi: 10.1113/jp276083

Sládek, M., Sumová, A., Kováčiková, Z., Bendová, Z., Laurinová, K., and Illnerová, H. (2004). Insight into molecular core clock mechanism of embryonic and early postnatal rat suprachiasmatic nucleus. *Proc. Natl. Acad. Sci. U.S.A.* 101, 6231–6236. doi: 10.1073/pnas.0401149101

Smarr, B. L., Grant, A. D., Perez, L., Zucker, I., and Kriegsfeld, L. J. (2017). Maternal and early-life circadian disruption have long-lasting negative consequences on offspring development and adult behavior in mice. *Sci. Rep.* 7:3326.

Sumová, A., and Čečmanová, V. (2020). Mystery of rhythmic signal emergence within the suprachiasmatic nuclei. *Eur. J. Neurosci.* 51, 300–309. doi: 10.1111/ejn.14141

Sumová, A., Sládek, M., Polidarová, L., Nováková, M., and Houdek, P. (2012). Circadian system from conception till adulthood. *Prog. Brain Res.* 199, 83–103. doi: 10.1016/b978-0-444-59427-3.00005-8

Takeo, Y., Shirama, K., Shimizu, K., and Maekawa, K. (1975). Correlation between sexual maturation and induction of persistent estrus by continuous illumination. *Endocrinol. Jpn.* 22, 453–456. doi: 10.1507/endocrj1954.22.453

Tapia-Osorio, A., Salgado-Delgado, R., Angeles-Castellanos, M., and Escobar, C. (2013). Disruption of circadian rhythms due to chronic constant light leads to depressive and anxiety-like behaviors in the rat. *Behav. Brain Res.* 252, 1–9. doi: 10.1016/j.bbr.2013.05.028

Torres-Farfan, C., Mendez, N., Abarzua-Catalan, L., Vilches, N., Valenzuela, G. J., and Seron-Ferre, M. (2011). A circadian clock entrained by melatonin is ticking in the rat fetal adrenal. *Endocrinology* 152, 1891–1900. doi: 10.1210/en.2010-1260

Varcoe, T. J., Gatford, K. L., and Kennaway, D. J. (2018). Maternal circadian rhythms and the programming of adult health and disease. *Am. J. Physiol. Regul. Integr. Comp. Physiol.* 314, R231–R241.

Viswanathan, N., and Davis, F. C. (1997). Single prenatal injections of melatonin or the D1-dopamine receptor agonist SKF 38393 to pregnant hamsters sets the offsprings' circadian rhythms to phases 180 degrees apart. *J. Comp. Physiol. A* 180, 339–346. doi: 10.1007/s003590050053

Viswanathan, N., Weaver, D. R., Reppert, S. M., and Davis, F. C. (1994). Entrainment of the fetal hamster circadian pacemaker by prenatal injections of the dopamine agonist SKF 38393. *J. Neurosci.* 14, 5393–5398. doi: 10.1523/jneurosci.14-09-05393.1994

Weaver, D. R., and Reppert, S. M. (1989). Periodic feeding of SCN-lesioned pregnant rats entrains the fetal biological clock. *Dev. Brain Res.* 46, 291–295. doi: 10.1016/0165-3806(89)90292-7

Webb, A. B., Angelo, N., Huettner, J. E., and Herzog, E. D. (2009). Intrinsic, nondeterministic circadian rhythm generation in identified mammalian neurons. *Proc. Natl. Acad. Sci. U.S.A.* 106, 16493–16498. doi: 10.1073/pnas.0902768106

Welsh, D. K., Logothetis, D. E., Meister, M., and Reppert, S. M. (1995). Individual neurons dissociated from rat suprachiasmatic nucleus express independently phased circadian firing rhythms. *Neuron* 14, 697–706. doi: 10.1016/0896-6273(95)90214-7

Wideman, C. H., and Murphy, H. M. (2009). Constant light induces alterations in melatonin levels, food intake, feed efficiency, visceral adiposity, and circadian rhythms in rats. *Nutr. Neurosci.* 12, 233–240. doi: 10.1179/147683009x423436

Wreschnig, D., Dolatshad, H., and Davis, F. C. (2014). Embryonic development of circadian oscillations in the mouse hypothalamus. *J. Biol. Rhythms* 29, 299–310. doi: 10.1177/0748730414545086

Zordan, M. A., Rosato, E., Piccin, A., and Foster, R. (2001). Photic entrainment of the circadian clock: from *Drosophila* to mammals. *Semin. Cell Dev. Biol.* 12, 317–328. doi: 10.1006/scdb.2001.0259

Conflict of Interest: The authors declare that the research was conducted in the absence of any commercial or financial relationships that could be construed as a potential conflict of interest.

frontiers in Neuroscience

MINI REVIEW
published: 12 January 2021
doi: 10.3389/fnins.2020.631687

Feto-Maternal Crosstalk in the Development of the Circadian Clock System

Mariana Astiz and Henrik Oster*

Center of Brain, Behavior and Metabolism, Institute of Neurobiology, University of Lübeck, Lübeck, Germany

The circadian (24 h) clock system adapts physiology and behavior to daily recurring changes in the environment. Compared to the extensive knowledge assembled over the last decades on the circadian system in adults, its regulation and function during development is still largely obscure. It has been shown that environmental factors, such as stress or alterations in photoperiod, disrupt maternal neuroendocrine homeostasis and program the offspring's circadian function. However, the process of circadian differentiation cannot be fully dependent on maternal rhythms alone, since circadian rhythms in offspring from mothers lacking a functional clock (due to SCN lesioning or genetic clock deletion) develop normally. This mini-review focuses on recent findings suggesting that the embryo/fetal molecular clock machinery is present and functional in several tissues early during gestation. It is entrained by maternal rhythmic signals crossing the placenta while itself controlling responsiveness to such external factors to certain times of the day. The elucidation of the molecular mechanisms through which maternal, placental and embryo/fetal clocks interact with each other, sense, integrate and coordinate signals from the early life environment is improving our understanding of how the circadian system emerges during development and how it affects physiological resilience against external perturbations during this critical time period.

Keywords: pregnancy, fetus, circadian clock, placenta, gating

OPEN ACCESS

Edited by:
Daisuke Ono,
Nagoya University, Japan

Reviewed by:
Martin Sládek,
The Czech Academy of Sciences, Czechia
Claudia Torres-Farfan,
Austral University of Chile, Chile

****Correspondence:***
Mariana Astiz
m.astiz@uni-luebeck.de;
marianaastiz@gmail.com

Specialty section:
This article was submitted to Sleep and Circadian Rhythms, a section of the journal Frontiers in Neuroscience

Received: *20 November 2020*
Accepted: *18 December 2020*
Published: *12 January 2021*

Citation:
Astiz M and Oster H (2021) Feto-Maternal Crosstalk in the Development of the Circadian Clock System. Front. Neurosci. 14:631687. doi: 10.3389/fnins.2020.631687

INTRODUCTION

The circadian system is required to anticipate and adapt physiology to daily recurring changes in the environment over 24 h (Dibner et al., 2010). It coordinates complex behaviors such as sleep (Collins et al., 2020), activity (Moore and Eichler, 1972; Stephan and Zucker, 1972), food intake (Hatori et al., 2012; Koch et al., 2020), and stress responses (Oster et al., 2006). In mammals, a master circadian pacemaker is located in the hypothalamic suprachiasmatic nucleus (SCN) and subordinated clocks are present throughout the brain and the periphery (Ralph et al., 1990). The SCN perceives time of day via direct photic input from the retina and subsequently relays temporal information through coordination of the neuroendocrine system. Therefore, several SCN efferent connections are found within the medial hypothalamus where key cell groups are involved in organizing hormone release and autonomic nervous system tone (Kalsbeek et al., 2006, 2011). A plethora of humoral and neuronal signals convey time-of-day information to the periphery to elicit rhythmic regulation of the local clock gene machinery and, in turn, of a set of tissue-specific downstream clock-controlled genes (Buhr and Takahashi, 2013).

During pregnancy, the maternal neuroendocrine system adapts to support fetal development and growth (Tal et al., 2000; Russell and Brunton, 2019). Circadian coordination likely plays a fundamental role in this adaptation during the whole period of pregnancy, parturition, and lactation (Wharfe et al., 2016a). However, compared to the extensive knowledge gained over the last decades on the adult circadian system, its regulation and function during pregnancy remains largely obscure (Wharfe et al., 2011, 2016a,b; Papacleovoulou et al., 2017). The placenta is the only organ that is formed by the interaction of, both, maternal and fetal/embryonic tissues. It forms the interface between the two circulatory systems. The circadian clock is strongly involved in regulating functions such as hormone synthesis and immunity in the adult, then it might be involved in the diurnal regulation of these functions also during embryogenesis and in the placenta. And, last but not least, the fetal/embryo circadian system develops and gains autonomy toward term (Wharfe et al., 2011; Landgraf et al., 2015) under the influence of endogenous and exogenous entrainment signals crossing the placenta (Serón-Ferré et al., 2012; Čečmanová et al., 2019). However, little is known about fetal/neonate clock functions that might be relevant during this period of development.

Understanding circadian coordination during pregnancy requires an assessment of the interaction of three clocks—maternal, placental and fetal—plus taking into account that this interaction undergoes dynamic changes over the course of pregnancy (Mark et al., 2017). After birth, maternal behavior, body temperature and signals from breast milk further affect neonate circadian system development until weaning (Nozhenko et al., 2015) (**Figure 1**).

The Maternal Circadian System During Pregnancy and Early Postnatal Life

The role of the maternal clock during perinatal life has been studied by SCN lesion experiments in rodents, using clock deficient models and by exposing the pregnant mother to environmental conditions such as constant light (LL), chronic phase shifts or mistimed food availability, at different phases of gestation (Varcoe et al., 2011, 2013, 2018; Vilches et al., 2014; Houdek et al., 2015; Mendez et al., 2016; Smarr et al., 2017; Carmona et al., 2019). In the short term, the impact of maternal chonodisruption has been assessed using within-litter synchrony of the fetal/neonate central and peripheral clocks, metabolic rhythms, and activity as readouts. Interestingly, all different manipulations seems to have similar effects depending on the time of gestation when the chonodisruption was induced (Reppert and Schwartz, 1984; Davis and Gorski, 1988; Jud and Albrecht, 2006; Mendez et al., 2012, 2016; Varcoe et al., 2016; Salazar et al., 2018). Maternal chronodisruption also induces long term effects in the offspring such as memory and learning deficits (Vilches et al., 2014), increased anxiety, anhedonia, and depressive-like behavior (Voiculescu et al., 2016; Zhang et al., 2017) and metabolic effects such as adiposity and impaired glucose tolerance (Mendez et al., 2016).

Several maternal signals have been proposed as candidates to cross the placenta and reach the fetal clock. Melatonin is secreted by the pineal gland at night controlled through neuronal connections from the SCN (Lehman et al., 1987). Melatonin levels increase gradually toward the end of pregnancy returning to non-pregnant levels shortly after birth (Tamura et al., 2008). Melatonin is also found at considerable amounts in breast milk (Illnerová et al., 1993; Rowe and Kennaway, 2002). Experiments in rats have demonstrated that some of the short- and long-term effects of maternal LL exposure (Mendez et al., 2012; Houdek et al., 2015; Voiculescu et al., 2015, 2016), pinealectomy (Bellavía et al., 2006; Motta-Teixeira et al., 2018) or SCN lesions (Davis and Mannion, 1988) can be rescued by the administration of melatonin (recently reviewed by Hsu and Tain, 2020). Interestingly, the central and peripheral clocks of the fetus/newborn seem to respond differently to melatonin replacement in arrhythmic mothers (Mendez et al., 2012; Houdek et al., 2015). Despite that melatonin receptors have been found in several fetal tissues and in different species (Torres-Farfan et al., 2006) as previously reviewed by Voiculescu et al. (2014), the melatonin secretion pathway is suppressed in most inbred mouse strains. Considering that the offspring of these mice shows robust rhythms, melatonin might be a synchronizing signal for the fetal/neonate clock, but it is likely not essential for the normal development of the circadian system.

Dopamine has been proposed as a "light-phase" entrainment signal—i.e., antiphasic and functionally antagonistic to melatonin—during the development of the circadian system (Iuvone and Gan, 1995). Dopamine is able to cross placental barrier freely and is also found in breast milk (Watanabe et al., 1990). Moreover, dopamine receptors are widely expressed in the fetal/neonate brain (Weaver et al., 1992; Rivkees and Lachowicz, 1997). The exposure of neonates to the dopamine receptor 1 (D1R) agonist SKF38393 increases c-fos expression in the SCN (Weaver and Reppert, 1995). However, there is no substantial evidence of a direct role of dopamine programing the long-term function of the circadian system.

Glucocorticoids (GCs) have strong circadian entrainment functions (Oster et al., 2017). In humans and rodents, maternal GCs are released rhythmically anticipating the active phase during whole pregnancy with a gradual increase of baseline levels toward the end (Wharfe et al., 2016a). GCs are essential for fetal tissue maturation, especially in the lung, and GR (glucocorticoid receptor), or CRH (corticotrophin releasing hormone) deficiency is lethal for the fetus (Goldfeld et al., 1983; Muglia et al., 1995). Therefore, while low GC concentrations seem to be necessary for pregnancy success, epidemiological studies and animal experiments suggest that high GC levels during pregnancy increase the risk of developing behavioral and metabolic disorders later in life (Moisiadis and Matthews, 2014a; Coleman et al., 2016; Marín, 2016; Busada and Cidlowski, 2017; Van den Bergh et al., 2017; Logan and McClung, 2019). Interestingly, most rodent prenatal stress paradigms entail some degree of circadian disruption because the animals are manipulated during their normal rest phase. We have recently demonstrated that the offspring from mothers exposed to GCs during the rest phase show worse circadian and stress-related behavioral phenotypes than those from mothers exposed to the same GC concentration, but during the active phase (Astiz et al., 2020).

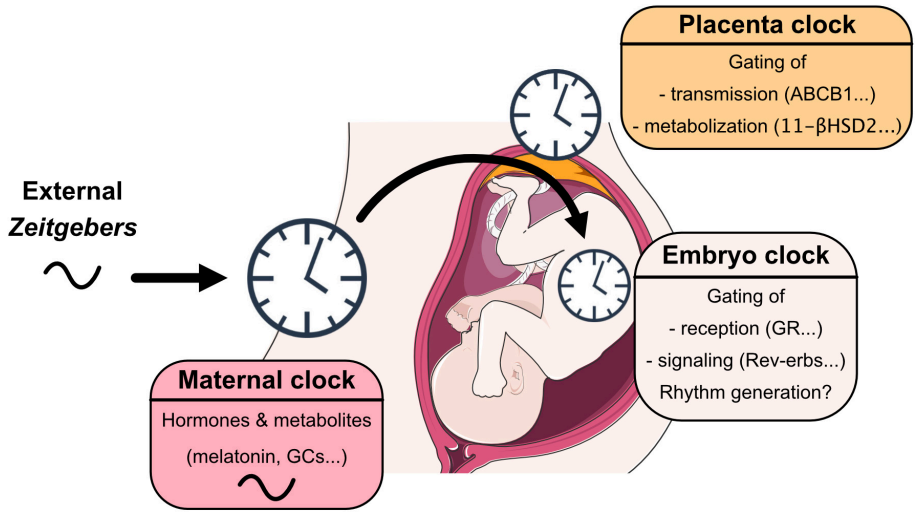

FIGURE 1 | View on mechanisms through which maternal, placental and embryo/fetal clocks interact with each other, sense, integrate, and coordinate signals from the early life environment.

Much less is known about other signals that are also rhythmic in the mother and are known to cross the placenta or to impact on fetus development such as leptin. Transplacental transport of leptin increases during the last week of gestation in rats, together with an increase in expression of leptin receptor in the placenta, likely due to increasing energy requirements (Herrid et al., 2014; Vlahos et al., 2020). Interestingly, transplacental leptin passage is reduced after maternal GCs exposure, whereas treatment with metyrapone (an inhibitor of GCs synthesis) has the opposite effect (Smith and Waddell, 2002, 2003). Other signals such as placental lactogen, prolactin, progesterone, estradiol, and insulin are less likely candidates for fetal circadian entrainment. Serum levels of human chorionic gonadotropin (hCG) and placental lactogen (hPL) were measured over 24 h, but no clear rhythms were detected (Houghton et al., 1982). Progesterone, estradiol, and insulin show rhythmic oscillations in non-pregnant rodents but there is not enough evidence for such rhythms during pregnancy.

Circadian rhythms in maternal core body temperature were also investigated as a possible entrainment signal, however, the reduced amplitude of these rhythms argues against a significant role as time-giver (Wharfe et al., 2016b).

Taking together these data suggest that the effect of maternal signals on the developing circadian system depend on concentration, circadian phase, the interaction with other signals, and gestational/postnatal age.

Placental Clocks and the Circadian Regulation of Feto-Maternal Crosstalk

In order to reach the developing embryonic/fetal clock, entrainment signals will have to pass through the placenta—as process, which could be by itself gated by the circadian clock. The placenta provides the interface between both circulatory systems. It controls the exchange of nutrients, hormones, xenobiotics, metabolites, and waste between mother and fetus (Han et al., 2018; Staud and Karahoda, 2018). Some maternal signals such as melatonin or dopamine freely cross the placenta and convey external time to the fetus (Naitoh et al., 1998; Okatani et al., 1998). Others, such as glucocorticoids, are metabolized by enzymes expressed in the labyrinth zone (LZ) of the placenta (Okatani et al., 1998; Krozowski et al., 1999; Mark et al., 2009, 2017; Christ et al., 2012; Waddell et al., 2012; Houdek et al., 2015). The LZ of rodents consists of maternal blood spaces separated from the fetal vasculature by trophoblasts and fetal connective tissue. It is of fetal origin and analog to the chorionic villi in humans (Han et al., 2018; Staud and Karahoda, 2018). Enzymes such as 11-βHSD2 (11-β-hydroxysteroid dehydrogenase 2) and ABCB1 (ATP-Binding Cassette Subfamily B Member 1) are highly abundant in the LZ and protect the fetus from excessive levels of GCs. The expression of these enzymes is rhythmic in the circadian range in the LZ and other tissues (Waddell et al., 2012). For instance, ABCB1 has drug-efflux functions in placenta with a broad substrate specificity, a diurnal regulation might have implications when considering the optimal treatment time of pregnant mothers aiming at either maximal or minimal availability to the fetus. Therefore, it would be interesting to assess whether the local clock is responsible for the rhythmic regulation of these or other transporters.

In mice, the junctional zone (JZ) of the placenta secretes monoamines and steroids with endocrine, paracrine, and autocrine functions modulating maternal and fetal physiology throughout pregnancy (Longhi and Kulay, 1974; Napso et al., 2018). Placental hormones such as hCG (human chorionic gonadotropin), hPL (placental lactogen) show no significant diurnal variation in maternal serum (Houghton et al., 1982) which is probably explained by the absence of a robust rhythmic expression of the clock gene machinery in the JZ (Wharfe et al., 2011). The placental decidua mediates the maternal immune tolerance to the embryo (Arck and Hecher, 2013). Since, several

immune processes are strongly regulated by the circadian system, it would be interesting to assess whether either the maternal or the placental clock influence this aspect of immune adaptation.

Fetal and Neonate Clock Development and Their Function as Gatekeepers of Circadian Entrainment Signals

Besides maternal signals and their passage through the placenta, the entrainment of the fetal circadian system will depend on a third factor, the reception of those signals at embryonic target tissues. The expression of receptors for dopamine and glucocorticoids shows dynamic changes in the developing SCN with high levels during the prenatal phase followed by downregulation during postnatal stages (Rosenfeld et al., 1988; Weaver and Reppert, 1995). The exposure of neonates to the dopamine receptor 1 (D1R) agonist SKF38393 increases c-fos expression in the SCN during the first 3 days of postnatal life, but receptor expression is downregulated by post-natal day 4—and so is the response of the SCN to the D1R agonist (Weaver and Reppert, 1995). GCs influence the development of many hypothalamic nuclei including the SCN (Moisiadis and Matthews, 2014b; Čečmanová et al., 2019) but the GR is not expressed in the adult nuclei (Rosenfeld et al., 1988). Consequently, the adult master clock becomes insensitive to dopamine, GCs and, potentially, other peripheral signals, which may be an essential condition for the SCN to keep the time under conditions of conflicting environmental signals.

When exactly and how the circadian clock starts ticking is still an open question. In mice, neuronal division in the developing SCN takes place between gestational day (GD) 10–15 peaking at GD12 (Kabrita and Davis, 2008). Intra-SCN circuits differentiate during the following days and retinal projections reach the SCN mediating photic entrainment shortly after birth (Sekaran et al., 2005). In contrast, the molecular clock machinery in the SCN and peripheral tissues is already expressed earlier (Landgraf et al., 2015; Čečmanová et al., 2019) and daily changes in metabolic activity are detectable in the SCN during late gestation (Reppert and Schwartz, 1984). Recent data from our lab show that the circadian phase of GCs that reach fetal tissues determines their effectiveness in programing the offspring's circadian behavior. This temporal gating originates from the embryonic clock system and may involve rhythmic expression of the negative GR modulator *Reverse erythroblastoma (REV-ERB*α/β aka *Nr1d1/2*) (Astiz et al., 2020).

Taken together, these results indicate that an intrinsic genetic programs, at the level of fetal tissues, interact with maternal signals. The outcome of this interaction not only affects acute responses of the embryo to external stimuli, but may also determine the physiological programing of circadian behavior and energy metabolism.

DISCUSSION

Circadian clocks have a pervasive influence on all aspects of physiology and behavior and, not surprisingly, they also influence embryonic development and the interaction between the embryo and its prenatal environment. Potent players in this context are timing signals perceived by the mother and transmitted to the unborn. On the other hand, the fetal circadian system is gradually evolving toward the end of gestation, thus more and more impinging on how maternal signals are interpreted and translated. Placental rhythmic programs have an important function in this crosstalk by gating which signals actually reach the embryo and how much of them at a given time.

The downregulation of receptors (such as GR) in the fetal SCN and the partial loss of rhythmicity of some of the maternal signals toward term indicate an emancipatory step of the prenatal pacemaker from maternal zeitgebers. It also highlights dynamics in the interaction between maternal signals and developmental programs during pregnancy in general. Metabolomic approaches may help to further decipher these kinetics allowing more straightforward strategies to manipulate genes and pathways during different stages of fetal development. From a clinical perspective, a better comprehension of these interactions will allow to improve existing therapeutic paradigms targeting disorders of the pregnant mother or the developing child with regard to efficiency or unwanted side effects.

AUTHOR CONTRIBUTIONS

MA and HO discussed the concept and wrote the manuscript. Both authors contributed to the article and approved the submitted version.

FUNDING

This work was supported by the German Research Foundation (DFG) grants AS547-1/1 (to MA), OS353-7/1, GRK1957, and OS353-10/1 (to HO).

REFERENCES

Arck, P. C., and Hecher, K. (2013). Fetomaternal immune cross-talk and its consequences for maternal and offspring's health. *Nat. Med.* 19, 548–556. doi: 10.1038/nm.3160

Astiz, M., Heyde, I., Fortmann, M. I., Bossung, V., Roll, C., Stein, A., et al. (2020). The circadian phase of antenatal glucocorticoid treatment affects the risk of behavioral disorders. *Nat. Commun.* 11:3593. doi: 10.1038/s41467-020-17429-5

Bellavía, S. L., Carpentieri, A. R., Vaqué, A. M., Macchione, A. F., and Vermouth, N. T. (2006). Pup circadian rhythm entrainment–effect of maternal ganglionectomy or pinealectomy. *Physiol. Behav.* 89, 342–349. doi: 10.1016/j.physbeh.2006.06.018

Buhr, E. D., and Takahashi, J. S. (2013). Molecular components of the mammalian circadian clock. *Handb. Exp. Pharmacol.* 2013, 3–27. doi: 10.1007/978-3-642-25950-0_1

Busada, J. T., and Cidlowski, J. A. (2017). Mechanisms of glucocorticoid action during development. *Curr. Top. Dev. Biol.* 125, 147–170. doi: 10.1016/bs.ctdb.2016.12.004

Carmona, P., Pérez, B., Trujillo, C., Espinosa, G., Miranda, F., Mendez, N., et al. (2019). Long-term effects of altered photoperiod during pregnancy on liver

gene expression of the progeny. *Front. Physiol.* 10:1377. doi: 10.3389/fphys.2019.01377

Čečmanová, V., Houdek, P., Šuchmanová, K., Sládek, M., and Sumová, A. (2019). Development and entrainment of the fetal clock in the suprachiasmatic nuclei: the role of glucocorticoids. *J. Biol. Rhythms* 34, 307–322. doi: 10.1177/0748730419835360

Christ, E., Korf, H.-W., and von Gall, C. (2012). When does it start ticking? Ontogenetic development of the mammalian circadian system. *Prog. Brain Res.* 199, 105–118. doi: 10.1016/B978-0-444-59427-3.00006-X

Coleman, G., Gigg, J., and Canal, M. M. (2016). Postnatal light alters hypothalamic-pituitary-adrenal axis function and induces a depressive-like phenotype in adult mice. *Eur. J. Neurosci.* 44, 2807–2817. doi: 10.1111/ejn.13388

Collins, B., Pierre-Ferrer, S., Muheim, C., Lukacsovich, D., Cai, Y., Spinnler, A., et al. (2020). Circadian VIPergic neurons of the suprachiasmatic nuclei sculpt the sleep-wake cycle. *Neuron* 108, 486.e5–499.e5. doi: 10.1016/j.neuron.2020.08.001

Davis, F. C., and Gorski, R. A. (1988). Development of hamster circadian rhythms: role of the maternal suprachiasmatic nucleus. *J. Comp. Physiol. A* 162, 601–610. doi: 10.1007/BF01342635

Davis, F. C., and Mannion, J. (1988). Entrainment of hamster pup circadian rhythms by prenatal melatonin injections to the mother. *Am. J. Physiol.* 255, R439–R448. doi: 10.1152/ajpregu.1988.255.3.R439

Dibner, C., Schibler, U., and Albrecht, U. (2010). The mammalian circadian timing system: organization and coordination of central and peripheral clocks. *Annu. Rev. Physiol.* 72, 517–549. doi: 10.1146/annurev-physiol-021909-135821

Goldfeld, A. E., Firestone, G. L., Shaw, P. A., and Gluecksohn-Waelsch, S. (1983). Recessive lethal deletion on mouse chromosome 7 affects glucocorticoid receptor binding activities. *Proc. Natl. Acad. Sci. U.S.A.* 80, 1431–1434. doi: 10.1073/pnas.80.5.1431

Han, L. W., Gao, C., and Mao, Q. (2018). An update on expression and function of P-gp/ABCB1 and BCRP/ABCG2 in the placenta and fetus. *Expert Opin. Drug Metab. Toxicol.* 14, 817–829. doi: 10.1080/17425255.2018.1499726

Hatori, M., Vollmers, C., Zarrinpar, A., DiTacchio, L., Bushong, E. A., Gill, S., et al. (2012). Time-restricted feeding without reducing caloric intake prevents metabolic diseases in mice fed a high-fat diet. *Cell Metab.* 15, 848–860. doi: 10.1016/j.cmet.2012.04.019

Herrid, M., Palanisamy, S. K. A., Ciller, U. A., Fan, R., Moens, P., Smart, N. A., et al. (2014). An updated view of leptin on implantation and pregnancy: a review. *Physiol. Res.* 63, 543–557. doi: 10.33549/physiolres.932674

Houdek, P., Polidarová, L., Nováková, M., Matějů, K., Kubík, Š, and Sumová, A. (2015). Melatonin administered during the fetal stage affects circadian clock in the suprachiasmatic nucleus but not in the liver. *Dev. Neurobiol.* 75, 131–144. doi: 10.1002/dneu.22213

Houghton, D. J., Newnham, J. P., Lo, K., Rice, A., and Chard, T. (1982). Circadian variation of circulating levels of four placental proteins. *Br. J. Obstet. Gynaecol.* 89, 831–835. doi: 10.1111/j.1471-0528.1982.tb05035.x

Hsu, C.-N., and Tain, Y.-L. (2020). Light and circadian signaling pathway in pregnancy: programming of adult health and disease. *Int. J. Mol. Sci.* 21:2232. doi: 10.3390/ijms21062232

Illnerová, H., Buresová, M., and Presl, J. (1993). Melatonin rhythm in human milk. *J. Clin. Endocrinol. Metab.* 77, 838–841. doi: 10.1210/jcem.77.3.8370707

Iuvone, P. M., and Gan, J. (1995). Functional interaction of melatonin receptors and D1 dopamine receptors in cultured chick retinal neurons. *J. Neurosci.* 15, 2179–2185. doi: 10.1523/jneurosci.15-03-02179.1995

Jud, C., and Albrecht, U. (2006). Circadian rhythms in murine pups develop in absence of a functional maternal circadian clock. *J. Biol. Rhythms* 21, 149–154. doi: 10.1177/0748730406286264

Kabrita, C. S., and Davis, F. C. (2008). Development of the mouse suprachiasmatic nucleus: determination of time of cell origin and spatial arrangements within the nucleus. *Brain Res.* 1195, 20–27. doi: 10.1016/j.brainres.2007.12.020

Kalsbeek, A., Palm, I. F., La Fleur, S. E., Scheer, F. A. J. L., Perreau-Lenz, S., Ruiter, M., et al. (2006). SCN outputs and the hypothalamic balance of life. *J. Biol. Rhythms* 21, 458–469. doi: 10.1177/0748730406293854

Kalsbeek, A., Yi, C.-X., Cailotto, C., la Fleur, S. E., Fliers, E., and Buijs, R. M. (2011). Mammalian clock output mechanisms. *Essays Biochem.* 49, 137–151. doi: 10.1042/bse0490137

Koch, C. E., Begemann, K., Kiehn, J. T., Griewahn, L., Mauer, J., and Hess, M. E. (2020). Circadian regulation of hedonic appetite in mice by clocks in dopaminergic neurons of the VTA. *Nat. Commun.* 11:3071. doi: 10.1038/s41467-020-16882-6

Krozowski, Z., Li, K. X., Koyama, K., Smith, R. E., Obeyesekere, V. R., Stein-Oakley, A., et al. (1999). The type I and type II 11beta-hydroxysteroid dehydrogenase enzymes. *J. Steroid Biochem. Mol. Biol.* 69, 391–401. doi: 10.1016/s0960-0760(99)00074-6

Landgraf, D., Achten, C., Dallmann, F., and Oster, H. (2015). Embryonic development and maternal regulation of murine circadian clock function. *Chronobiol. Int.* 32, 416–427. doi: 10.3109/07420528.2014.986576

Lehman, M. N., Silver, R., Gladstone, W. R., Kahn, R. M., Gibson, M., and Bittman, E. L. (1987). Circadian rhythmicity restored by neural transplant. Immunocytochemical characterization of the graft and its integration with the host brain. *J. Neurosci.* 7, 1626–1638. doi: 10.1523/jneurosci.07-06-01626.1987

Logan, R. W., and McClung, C. A. (2019). Rhythms of life: circadian disruption and brain disorders across the lifespan. *Nat. Rev. Neurosci.* 20, 49–65. doi: 10.1038/s41583-018-0088-y

Longhi, L., and Kulay, L. (1974). Optical and electron histochemistry of epinephrine, monoamine oxidase and glycogen in junctional zone of rat placenta during the functional period. *Ann. Histochim.* 19, 1–5.

Marín, O. (2016). Developmental timing and critical windows for the treatment of psychiatric disorders. *Nat. Med.* 22, 1229–1238. doi: 10.1038/nm.4225

Mark, P. J., Augustus, S., Lewis, J. L., Hewitt, D. P., and Waddell, B. J. (2009). Changes in the placental glucocorticoid barrier during rat pregnancy: impact on placental corticosterone levels and regulation by progesterone. *Biol. Reprod.* 80, 1209–1215. doi: 10.1095/biolreprod.108.073650

Mark, P. J., Crew, R. C., Wharfe, M. D., and Waddell, B. J. (2017). Rhythmic three-part harmony: the complex interaction of maternal, placental and fetal circadian systems. *J. Biol. Rhythms* 32, 534–549. doi: 10.1177/0748730417728671

Mendez, N., Abarzua-Catalan, L., Vilches, N., Galdames, H. A., Spichiger, C., Richter, H. G., et al. (2012). Timed maternal melatonin treatment reverses circadian disruption of the fetal adrenal clock imposed by exposure to constant light. *PLoS One* 7:e42713. doi: 10.1371/journal.pone.0042713

Mendez, N., Halabi, D., Spichiger, C., Salazar, E. R., Vergara, K., Alonso-Vasquez, P., et al. (2016). Gestational chronodisruption impairs circadian physiology in rat male offspring, increasing the risk of chronic disease. *Endocrinology* 157, 4654–4668. doi: 10.1210/en.2016-1282

Moisiadis, V. G., and Matthews, S. G. (2014a). Glucocorticoids and fetal programming part 1: outcomes. *Nat. Rev. Endocrinol.* 10, 391–402. doi: 10.1038/nrendo.2014.73

Moisiadis, V. G., and Matthews, S. G. (2014b). Glucocorticoids and fetal programming part 2: mechanisms. *Nat. Rev. Endocrinol.* 10, 403–411. doi: 10.1038/nrendo.2014.74

Moore, R. Y., and Eichler, V. B. (1972). Loss of a circadian adrenal corticosterone rhythm following suprachiasmatic lesions in the rat. *Brain Res.* 42, 201–206. doi: 10.1016/0006-8993(72)90054-6

Motta-Teixeira, L. C., Machado-Nils, A. V., Battagello, D. S., Diniz, G. B., Andrade-Silva, J., Silva, S., et al. (2018). The absence of maternal pineal melatonin rhythm during pregnancy and lactation impairs offspring physical growth, neurodevelopment, and behavior. *Horm. Behav.* 105, 146–156. doi: 10.1016/j.yhbeh.2018.08.006

Muglia, L., Jacobson, L., Dikkes, P., and Majzoub, J. A. (1995). Corticotropin-releasing hormone deficiency reveals major fetal but not adult glucocorticoid need. *Nature* 373, 427–432. doi: 10.1038/373427a0

Naitoh, N., Watanabe, Y., Matsumura, K., Murai, I., Kobayashi, K., Imai-Matsumura, K., et al. (1998). Alteration by maternal pinealectomy of fetal and neonatal melatonin and dopamine D1 receptor binding in the suprachiasmatic nuclei. *Biochem. Biophys. Res. Commun.* 253, 850–854. doi: 10.1006/bbrc.1998.9819

Napso, T., Yong, H. E. J., Lopez-Tello, J., and Sferruzzi-Perri, A. N. (2018). The role of placental hormones in mediating maternal adaptations to support pregnancy and lactation. *Front. Physiol.* 9:1091. doi: 10.3389/fphys.2018.01091

Nozhenko, Y., Asnani-Kishnani, M., Rodríguez, A. M., and Palou, A. (2015). Milk leptin surge and biological rhythms of leptin and other regulatory proteins in breastmilk. *PLoS One* 10:e0145376. doi: 10.1371/journal.pone.0145376

Okatani, Y., Okamoto, K., Hayashi, K., Wakatsuki, A., Tamura, S., and Sagara, Y. (1998). Maternal-fetal transfer of melatonin in pregnant women near term. *J. Pineal Res.* 25, 129–134. doi: 10.1111/j.1600-079x.1998.tb00550.x

Oster, H., Challet, E., Ott, V., Arvat, E., de Kloet, E. R., Dijk, D.-J., et al. (2017). The functional and clinical significance of the 24-hour rhythm of circulating glucocorticoids. *Endocr. Rev.* 38, 3–45. doi: 10.1210/er.2015-1080

Oster, H., Damerow, S., Kiessling, S., Jakubcakova, V., Abraham, D., Tian, J., et al. (2006). The circadian rhythm of glucocorticoids is regulated by a gating mechanism residing in the adrenal cortical clock. *Cell Metab.* 4, 163–173. doi: 10.1016/j.cmet.2006.07.002

Papacleovoulou, G., Nikolova, V., Oduwole, O., Chambers, J., Vazquez-Lopez, M., Jansen, E., et al. (2017). Gestational disruptions in metabolic rhythmicity of the liver, muscle, and placenta affect fetal size. *FASEB J.* 31, 1698–1708. doi: 10.1096/fj.201601032R

Ralph, M. R., Foster, R. G., Davis, F. C., and Menaker, M. (1990). Transplanted suprachiasmatic nucleus determines circadian period. *Science* 247, 975–978. doi: 10.1126/science.2305266

Reppert, S. M., and Schwartz, W. J. (1984). The suprachiasmatic nuclei of the fetal rat: characterization of a functional circadian clock using 14C-labeled deoxyglucose. *J. Neurosci.* 4, 1677–1682. doi: 10.1523/jneurosci.04-07-01677.1984

Rivkees, S. A., and Lachowicz, J. E. (1997). Functional D1 and D5 dopamine receptors are expressed in the suprachiasmatic, supraoptic, and paraventricular nuclei of primates. *Synapse* 26, 1–10. doi: 10.1002/(sici)1098-2396(199705)26:1<1::aid-syn1>3.0.co;2-d

Rosenfeld, P., Van Eekelen, J. A. M., Levine, S., and De Kloet, E. R. (1988). Ontogeny of the Type 2 glucocorticoid receptor in discrete rat brain regions: an immunocytochemical study. *Dev. Brain Res.* 42, 119–127. doi: 10.1016/0165-3806(88)90207-6

Rowe, S. A., and Kennaway, D. J. (2002). Melatonin in rat milk and the likelihood of its role in postnatal maternal entrainment of rhythms. *Am. J. Physiol. Regul. Integr. Comp. Physiol.* 282, R797–R804. doi: 10.1152/ajpregu.00228.2001

Russell, J. A., and Brunton, P. J. (2019). Giving a good start to a new life via maternal brain allostatic adaptations in pregnancy. *Front. Neuroendocrinol.* 53:100739. doi: 10.1016/j.yfrne.2019.02.003

Salazar, E. R., Richter, H. G., Spichiger, C., Mendez, N., Halabi, D., Vergara, K., et al. (2018). Gestational chronodisruption leads to persistent changes in the rat fetal and adult adrenal clock and function. *J. Physiol.* 596, 5839–5857. doi: 10.1113/JP276083

Sekaran, S., Lupi, D., Jones, S. L., Sheely, C. J., Hattar, S., Yau, K.-W., et al. (2005). Melanopsin-dependent photoreception provides earliest light detection in the mammalian retina. *Curr. Biol.* 15, 1099–1107. doi: 10.1016/j.cub.2005.05.053

Serón-Ferré, M., Mendez, N., Abarzua-Catalan, L., Vilches, N., Valenzuela, F. J., Reynolds, H. E., et al. (2012). Circadian rhythms in the fetus. *Mol. Cell. Endocrinol.* 349, 68–75. doi: 10.1016/j.mce.2011.07.039

Smarr, B. L., Grant, A. D., Perez, L., Zucker, I., and Kriegsfeld, L. J. (2017). Maternal and Early-Life Circadian Disruption Have Long-Lasting Negative Consequences on Offspring Development and Adult Behavior in Mice. *Sci. Rep.* 7:3326. doi: 10.1038/s41598-017-03406-4

Smith, J. T., and Waddell, B. J. (2002). Leptin receptor expression in the rat placenta: changes in ob-ra, ob-rb, and ob-re with gestational age and suppression by glucocorticoids. *Biol. Reprod.* 67, 1204–1210. doi: 10.1095/biolreprod67.4.1204

Smith, J. T., and Waddell, B. J. (2003). Leptin distribution and metabolism in the pregnant rat: transplacental leptin passage increases in late gestation but is reduced by excess glucocorticoids. *Endocrinology* 144, 3024–3030. doi: 10.1210/en.2003-0145

Staud, F., and Karahoda, R. (2018). Trophoblast: the central unit of fetal growth, protection and programming. *Int. J. Biochem. Cell Biol.* 105, 35–40. doi: 10.1016/j.biocel.2018.09.016

Stephan, F. K., and Zucker, I. (1972). Circadian rhythms in drinking behavior and locomotor activity of rats are eliminated by hypothalamic lesions. *Proc. Natl. Acad. Sci. U.S.A.* 69, 1583–1586. doi: 10.1073/pnas.69.6.1583

Tal, R., Taylor, H. S., Burney, R. O., Mooney, S. B., and Giudice, L. C. (2000). "Endocrinology of pregnancy," in *Endotext*, eds K. R. Feingold, B. Anawalt, A. Boyce, G. Chrousos, W. W. de Herder, K. Dungan, et al. (South Dartmouth, MA: MDText.com, Inc).

Tamura, H., Takayama, H., Nakamura, Y., Reiter, R. J., and Sugino, N. (2008). Fetal/placental regulation of maternal melatonin in rats. *J. Pineal Res.* 44, 335–340. doi: 10.1111/j.1600-079X.2007.00537.x

Torres-Farfan, C., Rocco, V., Monsó, C., Valenzuela, F. J., Campino, C., Germain, A., et al. (2006). Maternal melatonin effects on clock gene expression in a nonhuman primate fetus. *Endocrinology* 147, 4618–4626. doi: 10.1210/en.2006-0628

Van den Bergh, B. R. H., van den Heuvel, M. I., Lahti, M., Braeken, M., de Rooij, S. R., Entringer, S., et al. (2017). Prenatal developmental origins of behavior and mental health: the influence of maternal stress in pregnancy. *Neurosci. Biobehav. Rev.* 117, 26–64. doi: 10.1016/j.neubiorev.2017.07.003

Varcoe, T. J., Boden, M. J., Voultsios, A., Salkeld, M. D., Rattanatray, L., and Kennaway, D. J. (2013). Characterisation of the maternal response to chronic phase shifts during gestation in the rat: implications for fetal metabolic programming. *PLoS One* 8:e53800. doi: 10.1371/journal.pone.0053800

Varcoe, T. J., Gatford, K. L., and Kennaway, D. J. (2018). Maternal circadian rhythms and the programming of adult health and disease. *Am. J. Physiol. Regul. Integr. Comp. Physiol.* 314, R231–R241. doi: 10.1152/ajpregu.00248.2017

Varcoe, T. J., Voultsios, A., Gatford, K. L., and Kennaway, D. J. (2016). The impact of prenatal circadian rhythm disruption on pregnancy outcomes and long-term metabolic health of mice progeny. *Chronobiol. Int.* 33, 1171–1181. doi: 10.1080/07420528.2016.1207661

Varcoe, T. J., Wight, N., Voultsios, A., Salkeld, M. D., and Kennaway, D. J. (2011). Chronic phase shifts of the photoperiod throughout pregnancy programs glucose intolerance and insulin resistance in the rat. *PLoS One* 6:e18504. doi: 10.1371/journal.pone.0018504

Vilches, N., Spichiger, C., Mendez, N., Abarzua-Catalan, L., Galdames, H. A., Hazlerigg, D. G., et al. (2014). Gestational chronodisruption impairs hippocampal expression of NMDA receptor subunits Grin1b/Grin3a and spatial memory in the adult offspring. *PLoS One* 9:e91313. doi: 10.1371/journal.pone.0091313

Vlahos, A., Mansell, T., Burgner, D., Collier, F., Novakovic, B., Saffery, R., et al. (2020). Determinants of placental leptin receptor gene expression and association with measures at birth. *Placenta* 100, 89–95. doi: 10.1016/j.placenta.2020.08.010

Voiculescu, S. E., Le Duc, D., Roşca, A. E., Zeca, V., Chiţimuş, D. M., Arsene, A. L., et al. (2016). Behavioral and molecular effects of prenatal continuous light exposure in the adult rat. *Brain Res.* 1650, 51–59. doi: 10.1016/j.brainres.2016.08.031

Voiculescu, S. E., Rosca, A. E., Zeca, V., Zagrean, L., and Zagrean, A. M. (2015). Impact of maternal melatonin suppression on forced swim and tail suspension behavioral despair tests in adult offspring. *J. Med. Life* 8, 202–206.

Voiculescu, S. E., Zygouropoulos, N., Zahiu, C. D., and Zagrean, A. M. (2014). Role of melatonin in embryo fetal development. *J. Med. Life* 7, 488–492.

Waddell, B. J., Wharfe, M. D., Crew, R. C., and Mark, P. J. (2012). A rhythmic placenta? Circadian variation, clock genes and placental function. *Placenta* 33, 533–539. doi: 10.1016/j.placenta.2012.03.008

Watanabe, T., Matsuhashi, K., and Takayama, S. (1990). Placental and blood-brain barrier transfer following prenatal and postnatal exposures to neuroactive drugs: relationship with partition coefficient and behavioral teratogenesis. *Toxicol. Appl. Pharmacol.* 105, 66–77. doi: 10.1016/0041-008x(90)90359-3

Weaver, D. R., and Reppert, S. M. (1995). Definition of the developmental transition from dopaminergic to photic regulation of c-fos gene expression in the rat suprachiasmatic nucleus. *Brain Res. Mol. Brain Res.* 33, 136–148. doi: 10.1016/0169-328x(95)00117-b

Weaver, D. R., Rivkees, S. A., and Reppert, S. M. (1992). D1-dopamine receptors activate c-fos expression in the fetal suprachiasmatic nuclei. *Proc. Natl. Acad. Sci. U.S.A.* 89, 9201–9204. doi: 10.1073/pnas.89.19.9201

Wharfe, M. D., Mark, P. J., and Waddell, B. J. (2011). Circadian variation in placental and hepatic clock genes in rat pregnancy. *Endocrinology* 152, 3552–3560. doi: 10.1210/en.2011-0081

Wharfe, M. D., Mark, P. J., Wyrwoll, C. S., Smith, J. T., Yap, C., Clarke, M. W., et al. (2016a). Pregnancy-induced adaptations of the central circadian clock

and maternal glucocorticoids. *J. Endocrinol.* 228, 135–147. doi: 10.1530/JOE-15-0405

Wharfe, M. D., Wyrwoll, C. S., Waddell, B. J., and Mark, P. J. (2016b). Pregnancy suppresses the daily rhythmicity of core body temperature and adipose metabolic gene expression in the mouse. *Endocrinology* 157, 3320–3331. doi: 10.1210/en.2016-1177

Zhang, P., Li, G., Li, H., Tan, X., and Cheng, H.-Y. M. (2017). Environmental perturbation of the circadian clock during pregnancy leads to transgenerational mood disorder-like behaviors in mice. *Sci. Rep.* 7:12641. doi: 10.1038/s41598-017-13067-y

Conflict of Interest: The authors declare that the research was conducted in the absence of any commercial or financial relationships that could be construed as a potential conflict of interest.

frontiers in Neuroscience

BRIEF RESEARCH REPORT
published: 25 January 2021
doi: 10.3389/fnins.2021.638122

Cellular Senescence Triggers Altered Circadian Clocks With a Prolonged Period and Delayed Phases

Rezwana Ahmed[1,2,3], Yasukazu Nakahata[1,2], Kazuyuki Shinohara[2] and Yasumasa Bessho[1]*

[1] Laboratory of Gene Regulation Research, Division of Biological Science, Graduate School of Science and Technology, Nara Institute of Science and Technology (NAIST), Ikoma, Japan, [2] Department of Neurobiology and Behavior, Nagasaki University Graduate School of Biomedical Sciences, Nagasaki, Japan, [3] Department of Pharmaceutical Sciences, North South University, Dhaka, Bangladesh

Senescent cells, which show the permanent growth arrest in response to various forms of stress, accumulate in the body with the progression of age, and are associated with aging and age-associated diseases. Although the senescent cells are growth arrested, they still demonstrate high metabolic rate and altered gene expressions, indicating that senescent cells are still active. We recently showed that the circadian clock properties, namely phase and period of the cells, are altered with the establishment of replicative senescence. However, whether cellular senescence triggers the alteration of circadian clock properties in the cells is still unknown. In this study we show that the oxidative stress-induced premature senescence induces the alterations of the circadian clock, similar to the phenotypes of the replicative senescent cells. We found that the oxidative stress-induced premature senescent cells display the prolonged period and delayed phases. In addition, the magnitude of these changes intensified over time, indicating that cellular senescence changes the circadian clock properties. Our current results corroborate with our previous findings and further confirm that cellular senescence induces altered circadian clock properties, irrespective of the replicative senescence or the stress-induced premature senescence.

Keywords: circadian, clock, senescence, aging, oxidative stress

OPEN ACCESS

Edited by:
Takahiro J. Nakamura, Meiji University, Japan

Reviewed by:
Hikari Yoshitane, The University of Tokyo, Japan
Yu Tahara, Waseda University, Japan

***Correspondence:**
Yasukazu Nakahata
yasu-nakahata@nagasaki-u.ac.jp

Specialty section:
This article was submitted to Sleep and Circadian Rhythms, a section of the journal Frontiers in Neuroscience

Received: *05 December 2020*
Accepted: *04 January 2021*
Published: *25 January 2021*

Citation:
Ahmed R, Nakahata Y, Shinohara K and Bessho Y (2021) Cellular Senescence Triggers Altered Circadian Clocks With a Prolonged Period and Delayed Phases. Front. Neurosci. 15:638122. doi: 10.3389/fnins.2021.638122

INTRODUCTION

Cellular senescence is the state of permanent growth arrest of cells. The senescent cells have been found to be accumulated in the body with aging, and have been associated with various age-related diseases, for example, atherosclerosis (Wang and Bennett, 2012; Childs et al., 2018; Cho et al., 2020), osteoarthritis (Jeon et al., 2017, 2019; Xu et al., 2017), alveolar lung diseases (Hashimoto et al., 2016; Schafer et al., 2017; Houssaini et al., 2018), and cancer (Parrinello et al., 2005; Bavik et al., 2006; Liu and Hornsby, 2007; Bhatia et al., 2008; Campisi et al., 2011; Castro-Vega et al., 2015; Ortiz-Montero et al., 2017). Removal of the senescent cells from the body, either using the pharmacologic interventions (Chang et al., 2016; Yosef et al., 2016; Baar et al., 2017; Lehmann et al., 2017; Schafer et al., 2017; Bussian et al., 2018; Zhang et al., 2019) or genetic ablations (Baker et al., 2011, 2016; Childs et al., 2016; Hashimoto et al., 2016; Bussian et al., 2018), have recently been reported to lead to the extended healthspan of prematurely and naturally aged mice and

also attenuated the already existing diseases in mouse models of disease. Various forms of stress such as excessive cell proliferation, oncogenic stress and extreme DNA damage induce cellular senescence. These different forms of stress lead to the cells having the different types of the cellular senescence, such as the replicative senescence, oncogene-induced senescence and the stress-induced premature senescence. Despite the fact that the various types of the senescent cells are permanently growth arrested, they still have their individual differential transcriptome signatures, and secretory phenotype (Maciel-Baron et al., 2016; Hernandez-Segura et al., 2017; Nakao et al., 2020). Hence it can be postulated that the presence of the replicative senescent cells, oncogene-induced senescent cells, and stress-induced premature senescent cells may affect the physiological systems differentially. *In vivo* it is currently impossible to distinguish between the different types of the senescent cells and the effects they exert (Hernandez-Segura et al., 2017). Recently, we found that circadian clock properties are altered with replicative senescence. However, whether the alteration of the circadian clock is specific for the replicative senescent cells or is also observed in the other types of senescence programs is still largely known.

The circadian clock, which is an intrinsic time-keeping system of almost all living systems on earth, possesses robust and flexible mechanisms against environmental light/dark condition (Partch et al., 2014; Bass and Lazar, 2016; Takahashi, 2017; Honma, 2018). However, it has been found that the circadian clock becomes less robust and flexible with aging, both at the animal level (Valentinuzzi et al., 1997) and also at the tissue levels (Nakamura et al., 2015). Also, at the cellular level, we recently found that the circadian clock is altered with the establishment of replicative senescence; the circadian period becomes longer, and the peak phases are delayed compared with the proliferative cells (Ahmed et al., 2019). We assume that cellular senescence affects the circadian clock mechanism, but not *vice versa*, since we have reported that the fibroblast cells derived from *Bmal1* knockout mice embryo in which circadian clock is completely disrupted, show the normal senescence process (Nakahata et al., 2018). Although in our previous paper, we showed that the circadian clock is altered with the establishment of replicative senescence, till date, no evidence has directly demonstrated that cellular senescence *per se* affects the circadian clock mechanism. Hence, in this study, we induce oxidative stress-induced premature senescence of human primary fibroblasts, to investigate whether other types of senescence affect the circadian clock and therefore, confirm that cellular senescence affects the circadian clock, irrespective of the type of senescence.

MATERIALS AND METHODS

Cell Culture and H_2O_2 Treatment

Primary human lung fetal fibroblasts (TIG-3) of Japanese origin were kindly provided by Drs. T. Takumi and T. Akagi. The cells were cultured in DMEM-4.5 g/L glucose (Nacalai Tesque, Japan) supplemented with 10% FBS (Sigma) and antibiotics (100 units/mL penicillin, 100 μg/mL streptomycin, Nacalai Tesque, Japan) at 37°C and 5% CO_2 in a humidified incubator. The proliferative cells used in this study were established in our previous report (Ahmed et al., 2019) which consisted of cells in the passage range of P25-29.

For the induction of oxidative stress-induced premature senescence H_2O_2 was used as the stressor. The proliferative cells were plated on 6-well plates at the seeding density of 8.5×10^4 cells/well on Day-0 (**Figure 1A**). On Day-1, (i.e., 24 h after plating) cells were incubated with various concentrations of H_2O_2 (Wako, Japan) as indicated, for 2 h, then rinsed with DMEM twice and incubated for 22 h. Cells treated with equivalent volumes of dH_2O as H_2O_2 were considered as controls. This process was repeated on Day-2 and Day-3. Then cells were cultured until Day-9, splitting on Day-4 and Day-7, each time with the seeding density at 8.5×10^4 cells/well.

Lentivirus Production and TIG-3 Cells Infection

Lentivirus production was performed as described previously (Ahmed et al., 2019). For infection of the target TIG-3 cells, cells in the Passage range of 25–29 in the previous study (Ahmed et al., 2019) were used. The culture medium was replaced with the lentivirus suspension supplemented with 8 μg/ml protamine sulfate (Nacalai Tesque, Japan). 24 h later the cells were washed with PBS once and cultured 2 more days with fresh medium. Infected cells were kept in liquid nitrogen until cells were subjected to experiments.

Senescence-Associated β-Galactosidase Assay (SA-β-Gal Assay), RNA Extraction, qPCR, Real-Time Luciferase Monitoring Assay, and Cosinor Analysis

These methods were described preciously (Ahmed et al., 2019).

Statistics

Values are reported as mean ± SEM. Statistical differences were determined by a Student's two-tailed *t* test. Statistical significance is displayed as $^*p < 0.05$, $^{**}p < 0.01$, or $^{***}p < 0.001$.

RESULTS

Oxidative Stress-Induced Premature Senescence in TIG-3 Cells

In our previous study, we obtained the proliferative and replicative senescent TIG-3 cells by serial passaging and found that senescent TIG-3 cells possess altered circadian clock properties with prolonged period and delayed phase (Ahmed et al., 2019). To address whether the senescence process triggers the alteration of circadian clock properties, we induced the oxidative stress-induced premature senescence using the proliferative cells, which consisted of cells in the Passage range of 25–29 in the previous study (Ahmed et al., 2019). In order to induce oxidative stress-induced premature senescence, we chose H_2O_2, as it is one of the most widely used stressors and also because it is thought of as

a natural inducer of oxidative stress (Toussaint et al., 2000). To optimize the concentration of H_2O_2, we first exposed the cells to varying concentrations of H_2O_2 for 2 h, performing 3 consecutive H_2O_2 treatments every 24 h (**Figure 1A**). Senescent cells are known to exhibit a plethora of features such as enlarged, flattened morphology, increased senescence-associated β-galactosidase (SA-β-Gal) activity (Debacq-Chainiaux et al., 2009; Khaidizar et al., 2017), and increased expressions of cell cycle inhibitors ($p16^{INK4a}$, $p19^{ARF}$, and $p21^{CIP1}$) (Stein et al., 1999; Krishnamurthy et al., 2004; Khaidizar et al., 2017). Hence on Day-8, the cells were checked for some of the aforementioned features. Starting at 300 μM, the cells appeared to be larger in size and flattened and showed significantly higher percentage of the SA-β-Gal-positive cells compared to the control cells (**Figures 1B,C**). Higher concentrations also gave correspondingly higher percentage of SA-β-Gal-positive cells, however, increasing number of cell deaths also occurred. As such, we determined that the optimum concentration that could induce significant SA-β-Gal activity was 300 μM (49.3% ± 2.9), and this percentage of SA-β-Gal-positive cells was in the same range to that found in the replicative senescent cells, as reported previously (Ahmed et al., 2019).

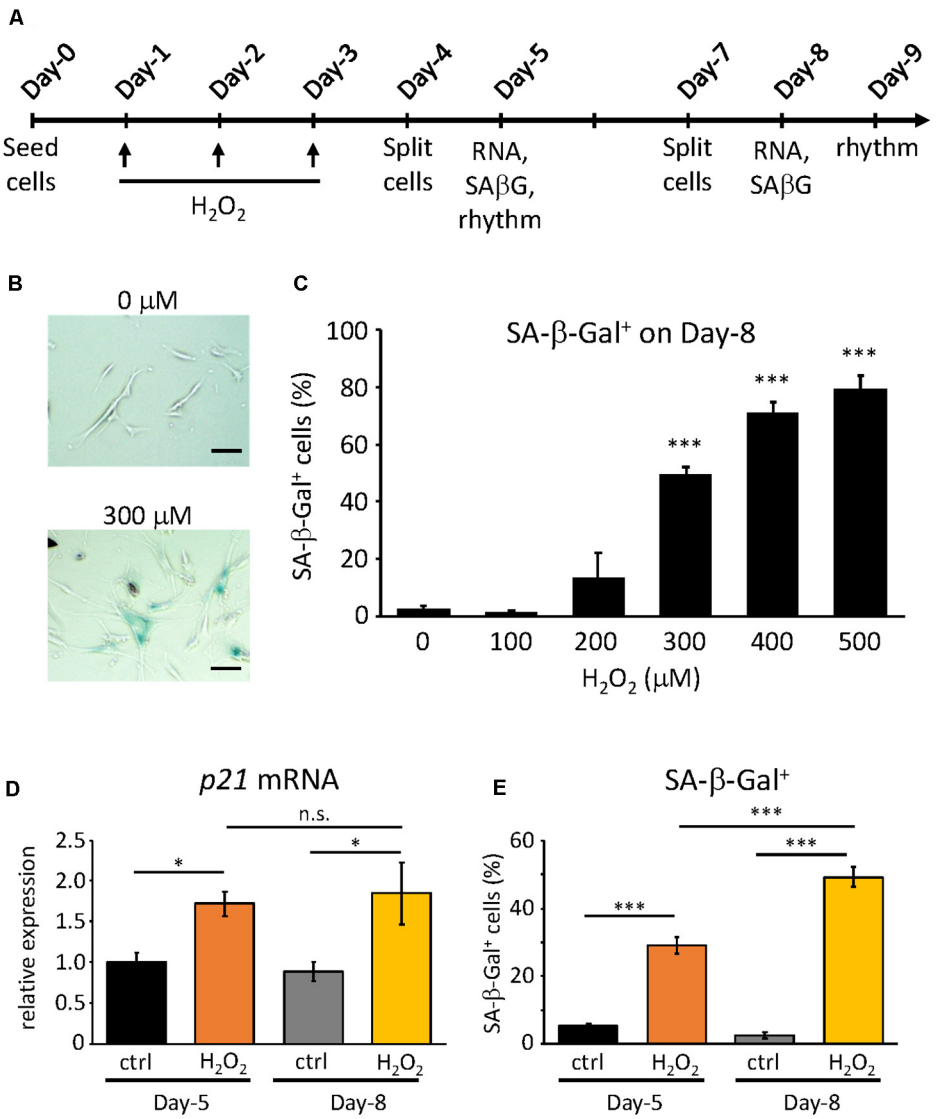

FIGURE 1 | Confirmation of H_2O_2-induced premature senescence. **(A)** Scheme of this study. RNA, SA-β-Gal and rhythm mean RNA extraction, SA-β-Gal assay and real-time luciferase monitoring assay, respectively **(B)** Representative pictures of SA-β-Gal positive cells (blue) at Day-9 under control (upper) and 300 μM H_2O_2-treated conditions. Scale bars represent 100 μm (micrometer). **(C)** The percentage of SA-β-Gal positive cells were quantified at different concentrations. **(D)** $p21^{CIP1}$ gene expressions under control or 300 μM H_2O_2-treated conditions at indicated days were analyzed by qPCR. The expression level of control condition at Day-5 was set to 1. **(E)** The percentage of SA-β-Gal positive cells under control or 300 μM H_2O_2-treated conditions at indicated days were quantified. n.s., not significant, $*p < 0.05$, $***p < 0.001$, by Student's two-tailed *t* test.

Next, we sought to characterize the process of the oxidative stress-induced premature senescence after the exposure of TIG-3 cells to H_2O_2. To this end, we checked the two senescence features, the cell cycle inhibitor *p21* mRNA expression level and SA-β-Gal activity, at two time points i.e., on Day-5 and Day-8 at 300 μM of H_2O_2. On Day-5, both *p21* mRNA expression ($p = 0.02$) and SA-β-Gal positive cells ($p = 4.8 \times 10^{-8}$) in the H_2O_2-treated cells were increased compared to the control cells (**Figures 1D,E**). As expected, on Day-8 both senescence features were significantly higher in H_2O_2-treated cells ($p = 0.01$ and 5.5×10^{-5} for *p21* mRNA expression and SA-β-Gal positive cells, respectively). Intriguingly, *p21* expression levels were comparable in H_2O_2-treated cells between Day-5 and Day-8 ($p = 0.77$, **Figure 1D**), whereas SA-β-Gal positive cells on Day-8 was significantly higher than that on Day-5 ($p = 1.6 \times 10^{-12}$, **Figure 1E**). These results indicate that the cells start ceasing proliferation almost immediately after exposure to the stressor H_2O_2, however, the development of the oxidative stress-induced premature senescence process is gradual, the intensity of which increases with time.

Alteration of Circadian Clock Characteristics in the Oxidative Stress-Induced Premature Senescent TIG-3 Cells

Next we assessed the changes in the circadian clock properties of the cells, both at Day-5 and Day-9, compared to the control cells. For this purpose, we used the TIG-3 cells lentivirally infected with the *bmal1* promoter-driven luciferase gene (Brown et al., 2005). The infected cells were synchronized with dexamethasone and were subjected to real-time luciferase assay. As shown in **Figure 2A**, the circadian oscillation patterns of the control cells both on Day-5 and Day-9 were very close to each other (see **Supplementary Figure 1** for raw data of oscillation patterns). Intriguingly, the oscillation pattern of H_2O_2-treated cells on Day-5, which have already shown senescent features (**Figures 1D,E**), was similar to those of control cells, suggesting that circadian clock is intact in Day-5 senescent cells. On the contrary, the oscillation pattern of the H_2O_2-treated cells on Day-9 was shifted to the right (**Figure 2A**), suggesting the alteration of the circadian clock i.e., a delay in their clock timings. In order to more precisely check the timings of the cells, the trough times of the cells on Day-5 and Day-9 were extracted. For the cells on Day-5, the 1st trough times were 28.87 ± 0.35 h and 29.57 ± 0.39 h for the control cells and H_2O_2-treated cells, respectively, with no statistically significant difference ($p = 0.19$, **Figure 2B**). For the cells on Day-9, the 1st trough times were 29.65 ± 0.17 h and 32.34 ± 0.11 h for the control cells and H_2O_2-treated cells, respectively, with statistically significant difference ($p = 1.5 \times 10^{-11}$). For the 2nd trough times, the control cells at Day-5 showed 53.15 ± 0.37 h while the H_2O_2-treated cells showed 54.78 ± 0.48 h, with statistically significant difference ($p = 0.01$). For the Day-9 cells, the 2nd trough times were 53.94 ± 0.23 h and 59.09 ± 0.60 h, for the control cells and H_2O_2-treated cells, respectively, with statistically significant difference ($p = 4.4 \times 10^{-8}$). We then compared intra-group trough times of the cells between Day-5 and Day-9. As expected, there were no differences of 1st and 2nd trough times in the control cells. On the other hand, for 1st trough times in H_2O_2-treated cells, the cells at Day-5 showed 29.57 ± 0.39 h while the cells at Day-9 showed 32.34 ± 0.11 h, with statistically significant difference ($p = 1.9 \times 10^{-6}$). Also, for 2nd trough times in H_2O_2-treated cells, the cells at Day-5 showed 54.78 ± 0.48 h and the cells at Day-9 showed 59.09 ± 0.60 h, with statistically significant difference ($p = 1.0 \times 10^{-5}$). These results indicate that the H_2O_2-treated cells on Day-9, with the higher level of the senescent features, consistently displayed the delayed trough timings, which is in accordance with the replicative senescent cells reported in our previous study (Ahmed et al., 2019). Meanwhile, the trough timings of H_2O_2-treated cells on Day-5, with the milder level of the senescent features, were similar to those of control cells, which suggests that the alteration of circadian clock by H_2O_2 on Day-5 is much milder than that on Day-9.

We further checked the period and damping rate of the cells on Day-5 and Day-9 (**Figures 2C,D**). Period was calculated as time difference between 1st and 2nd trough times. For the cells on Day-5, the period length of the control cells was 24.25 ± 0.17 h and that of the H_2O_2-treated cells was 25.21 ± 0.21 h, $p = 0.002$, with a period extension of 0.96 h in the H_2O_2-treated cells. For the cells at Day-9, the period of the control cells was 24.29 ± 0.19 h while that of the H_2O_2-treated cells was 26.74 ± 0.55 h, $p = 2.8 \times 10^{-4}$, with a period extension of 2.45 h. Furthermore, the period of the H_2O_2-treated cells on Day-9 was 1.53 h longer than that on Day-5, with statistically significant different ($p = 0.011$). In case of the damping rate of the circadian oscillation patterns of the cells, Day-5 cells did not show any significant difference in their damping rates, for both the control and H_2O_2-treated cells (**Figure 2D**). For the cells of Day-9, the oscillation pattern of the H_2O_2-treated cells damped down more than the control cells, $p = 0.015$. Also, the damping of the H_2O_2-treated cells on Day-9 damped down more than that on Day-5, $p = 0.044$. Collectively, the period changes and damping rates suggest that the H_2O_2-treated cells on Day-9 display the higher intensity alterations of the circadian clock properties, although period changes start with the initiation of the process of oxidative stress-induced premature senescence.

To confirm the above results, we also analyzed the data of **Figure 2** mathematically using the Cosinor software (**Supplementary Figure 2**). For the period, control cells on Day-5 had the period of 23.70 ± 0.21 h while the H_2O_2-treated cells had period of 25.99 ± 0.14 h, $p = 2.6 \times 10^{-9}$; for Day-9 cells, the period of the control cells was 25.03 ± 0.16 h while that of the H_2O_2-treated cells was 26.85 ± 0.19 h, $p = 2.5 \times 10^{-7}$ (**Supplementary Figure 2A**), both of which are consistent with the manual extraction of the period data (**Figure 2**). Again, the period of H_2O_2-treated cells on Day-9 was significantly longer than that on Day-5, $p = 0.001$. In case of the acrophase, on Day-5, the control cells had an acrophase of -320.00 ± 5.76 while the H_2O_2-treated cells had an acrophase of -317.69 ± 5.00, with no statistically significant difference ($p = 0.77$, **Supplementary Figure 2B**), indicating that there is no phase delay between the cells at the beginning of the oxidative senescence development.

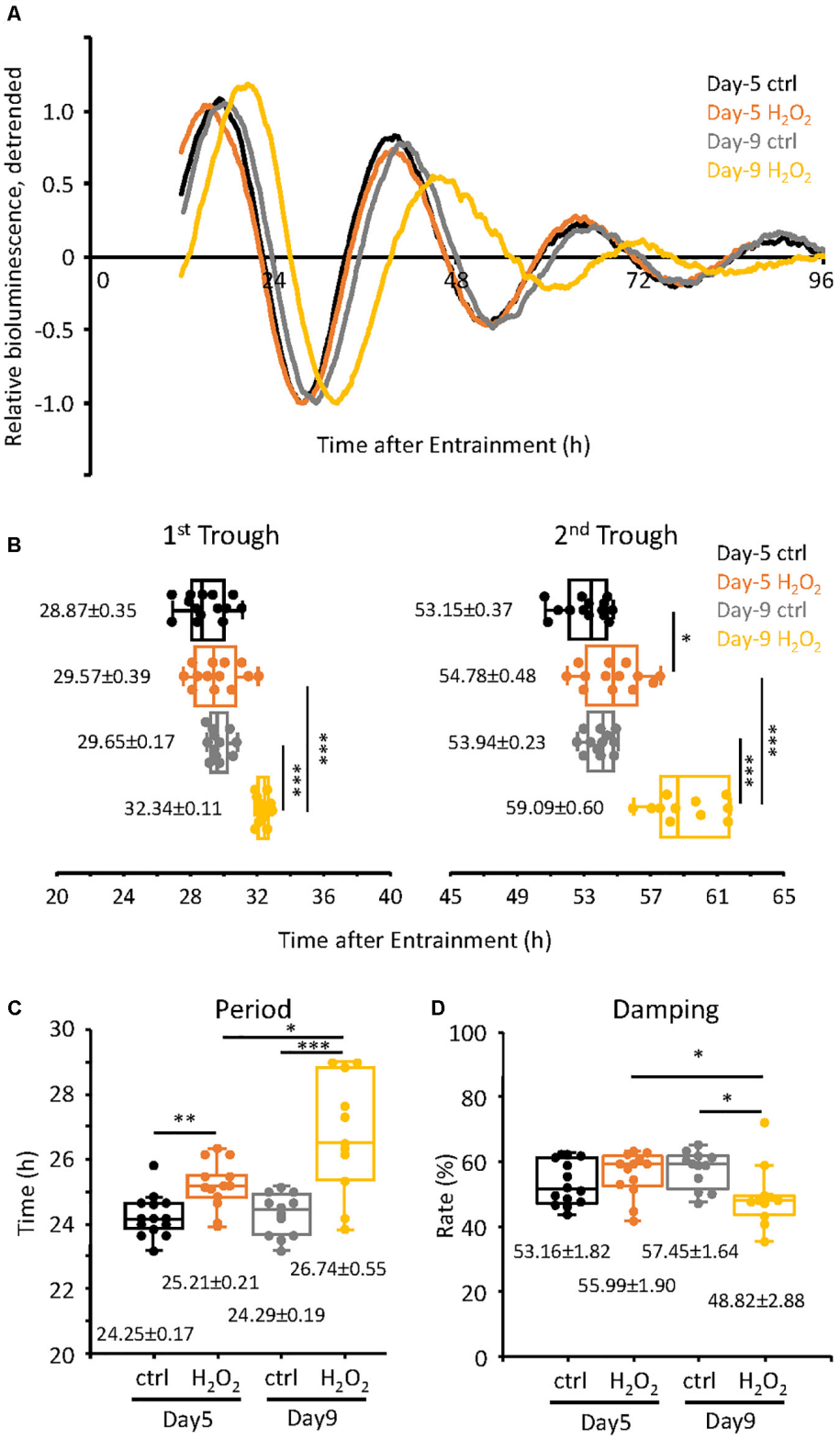

FIGURE 2 | Alteration of circadian clock in H_2O_2-induced premature senescent cells at Day-9 was observed. **(A)** Relative oscillation patterns of luciferase of control and 300 μM H_2O_2-treated cells at Day-5 and -9 were monitored by using a real-time luciferase monitoring system. Lowest intensity of each sample was set to −1. **(B)** Box-whisker plots of trough-times are displayed. Values are mean ± SEM. **(C,D)** Box-whisker plots of period lengths **(C)** and damping ratio **(D)** in cells with control and H_2O_2-treated cells at Day-5 and -9 are displayed. Values are mean ± SEM. *$p < 0.05$, **$p < 0.01$, and ***$p < 0.001$, by Student's two-tailed t test.

On Day-9, the control cells had an acrophase of -322.25 ± 2.36, which was comparable to those of Day-5, while the H_2O_2-treated cells had an acrophase of -356.64 ± 1.06, $p = 2.0 \times 10^{-11}$ (**Supplementary Figure 2B**), indicating phase delay on Day-9 in accordance with **Figure 2B**. Also, the acrophase of H_2O_2-treated cells on Day-9 was significantly different from that on Day-5, $p = 0.001$.

$3xH_2O_2$ treatment induced the initiation of cellular senescence easily, however, it altered all the circadian clock properties gradually. Therefore, we conclude that the circadian changes observed in the H_2O_2-treated cells are a result of the oxidative stress-induced premature senescence of the cells, not simply an effect of the H_2O_2 on the cells *per se*.

Finally, endogenous circadian gene expressions in H_2O_2-induced senescent cells on Day-9 were analyzed. Similar to our previous results in replicative senescent cells (Ahmed et al., 2019), *PER1*, *PER2,* and *CRY1* mRNAs were downregulated in senescent cells, however, *CRY2*, *REV-ERBa*, and *BMAL1* mRNAs were comparable to control non-senescent cells (**Figure 3**). These results suggest that not only circadian phenotypes, but also molecular regulations for circadian clock are similar, irrespective of the type of cellular senescence.

DISCUSSION

In this study, we revealed that the oxidative stress-induced premature senescence triggers the alteration of circadian clock properties, that is, the delayed phase and period extension. Also, we have recently reported that the period and phase of circadian clock in the replicative senescent cells was prolonged and delayed compared to the proliferative cells, respectively (Ahmed et al., 2019). Based on our findings, we propose that cellular senescence induces the period extension and delayed phase of circadian clock properties by similar molecular mechanisms, irrespective of the replicative senescence or the oxidative stress-induced premature senescence.

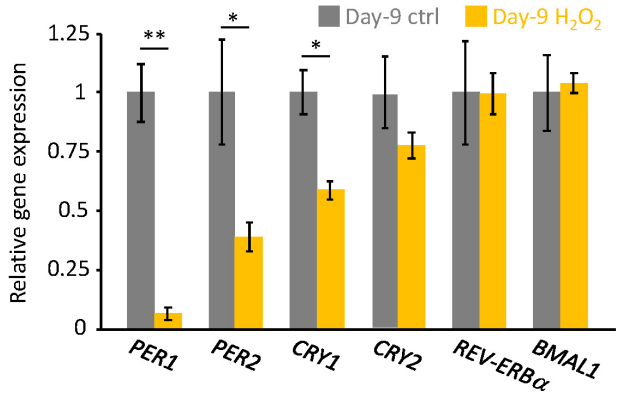

FIGURE 3 | The endogenous circadian clock genes expression level was downregulated in the senescent cells. *PER1*, *PER2*, *CRY1*, *CRY2*, *REV-ERBa*, and *BMAL1* mRNAs in unsynchronized cells were analyzed by qPCR. Each sample was normalized by 18S rRNA. Expression levels of each gene in control cells were set to 1. $*p < 0.05$, $***p < 0.01$, by Student's two-tailed *t* test.

In aged organisms, in addition to the replicative senescent cells, the stress-induced premature senescent cells occupy a major portion of the senescent cells (Campisi, 2005; Khapre et al., 2011). Oxidative stress is one of the strongest contributors of stress-induced premature senescence and is likely one of the major mediators of stress-induced premature senescence *in vivo* (Chen et al., 1995; Campisi, 2005; Khapre et al., 2011). Interestingly, several studies from model animals and humans have demonstrated that aging can also lead to alteration of the circadian clock (Pittendrigh and Daan, 1974; Witting et al., 1994; Valentinuzzi et al., 1997; Van Someren, 2000; Davidson et al., 2008; Sellix et al., 2012; Mattis and Sehgal, 2016). These evidence suggest that the attenuation of circadian clock functions with aging is in accordance with the accumulation of the senescent cells *in vivo*. Senolytic drugs (Chang et al., 2016; Yosef et al., 2016; Lehmann et al., 2017) which selectively eliminate senescent cells, or transgenic mice, such as INK-ATTAC (Baker et al., 2011) and p16-3MR mice (Demaria et al., 2014), in which senescent cells can be selectively eliminated in an inducible fashion, will be good strategies to address this hypothesis.

As already discussed in our previous study (Ahmed et al., 2019), the altered circadian clock properties have also been reported by Nakamura et al. (2015) using *ex vivo* SCN tissue of old mice. Compared to the consistent results from cellular and tissue levels, results at the organismal level have been controversial, some reports demonstrate prolonged period (Valentinuzzi et al., 1997), but others show shortened period (Pittendrigh and Daan, 1974; Witting et al., 1994). Aging phenotype is the result of complex intra- and inter-organ communications and individual contributions of different factors to total aging phenotype are still unknown. This is probably the reason for the controversial reports at the organismal level. Further investigations to unravel individual factors affecting total aging phenotype will be required.

We concluded in this study that $3\times H_2O_2$-treated cells on Day-5 have already entered the senescent phase, because of the high expression and level of *p21* mRNA and SA-b-Gal activity, respectively (**Figures 1D,E**), and H_2O_2-treated cells on Day-9 were more maturated. Meanwhile the alteration of circadian clock properties in H_2O_2-treated cells on Day-5 occurred only in terms of the period prolongation, and on Day-9 the period was much longer than that on Day-5. Intriguingly, phase and damping rate were altered only on Day-9, suggesting that molecular mechanisms of the period prolongation and delayed-phase/damping are independent. These results also suggest that the molecular mechanisms in circadian period regulations are vulnerable to cellular senescence, while the molecular mechanisms in circadian phase regulations are more robust than those in period regulations. Compared to our $3xH_2O_2$ treatment, acute single H_2O_2 treatment with high dose has been reported to alter circadian clock properties; H_2O_2 treatment resets circadian clock mediated by the dimerization of BMAL1 and HSF1 (Tamaru et al., 2013), induces phase changes of circadian clock in mouse embryonic fibroblast (MEF) cells and mouse peripheral tissues (Tahara et al., 2016), increases the amplitude of circadian clock by activating NRF2 following *Cry1* expression in stable

Per2:Luc reporter MEF cells (Wible et al., 2018), elicits phase-dependent PER2 degradation and circadian phase shifts in mouse fibroblasts (Putker et al., 2018), and shortens the circadian period by downregulating *Rev-erva/b* mRNAs via the activation of PRX2/STAT3 pathway in stable Bmal1:dLuc reporter NIH3T3 cells (Ji et al., 2019). These circadian phenotypes triggered by acute H_2O_2 are different from our current results, thereby indicating that the circadian phenotypes observed in our study are a result of the oxidative stress-induced premature senescence of the cells, not simply an effect of the H_2O_2 on circadian clock *per se*.

Li et al. (2020) have recently reported that increased non-genetic variation in gene expression predominantly drives circadian period prolongation in clonal cell lines (Li et al., 2020). Our studies demonstrated that variations in trough times and periods are larger in replicative/stress-induced premature senescent cells, compared to those in proliferative/control cells. Meanwhile, senescent cells are not homogeneous, they are heterogenous mixture of cells, for example, the percentage of SA-b-Gal positive cells was not 100% (**Figure 1D**). These data support that variation in circadian gene expression among senescent cells is greater. Furthermore, aging has been associated with increased stochastic transcriptional noise (Bahar et al., 2006; Enge et al., 2017; Martinez-Jimenez et al., 2017; Tang et al., 2019), therefore, increased transcriptional noise in senescent cells might be one of the causes to induce prolonged circadian period. Analyses of circadian period in single cells and single-cell RNA-sequence will provide an answer for this possibility.

Senescent cells are metabolically active, and increase in the AMP/ATP ratio and decrease in NAD^+ amount have been reported during senescence (James et al., 2015; Khaidizar et al., 2017). Increase in the AMP/ATP ratio promotes AMP-activated protein kinase (AMPK), which acts as a sensor of the reduced energetic state and further activates catabolic pathways while inhibiting anabolic ones (Hardie, 2003; Garcia and Shaw, 2017). Meanwhile it has been reported that mTOR, which is an intracellular nutrient sensor for high cellular energy state and associated with autophagy, is also upregulated during senescence (Herranz et al., 2015; Laberge et al., 2015; Nacarelli and Sell, 2017). Decrease in NAD^+ amount attenuates enzymatic activities of NAD^+-dependent enzymes, such as sirtuin family deacetylase (SIRT1-7) and poly (ADP-ribose) polymerases (PARPs) (Imai and Guarente, 2014, 2016; Schultz and Sinclair, 2016). Many of aforementioned signaling molecules are reported to regulate circadian clock properties. AMPK is a rhythmically expressed kinase and phosphorylates CK1ε, resulting in enhanced phosphorylation and degradation of PER2 (Um et al., 2007; Sahar and Sassone-Corsi, 2012) and CRY1 (Lamia et al., 2009; Sahar and Sassone-Corsi, 2012; Jordan and Lamia, 2013). AMPK activation by AMPK agonist, AICAR, or glucose deprivation, increased the circadian period and decreased the amplitude (Lamia et al., 2009), which are consistent with our finding in senescent cells, although another AMPK agonist metformin shortened circadian period (Um et al., 2007). mTOR perturbation, such as RNAi knockdown or mTOR inhibitors, lengthened circadian period in fibroblast, SCN, and animal behaviors (Zhang et al., 2009; Ramanathan et al., 2018), these reports show opposite effects to our findings. NAD^+ shows rhythmic 24 h oscillation and post-translationally modifies histone H3, BMAL1, PER2 and CLOCK by SIRT1 and PARP1 (Nakahata et al., 2008; Ramsey et al., 2009; Asher et al., 2010). Decrease in NAD^+ by FK866 treatment amplified E-box-regulated circadian genes, such as *per2* and *dbp* mRNAs (Nakahata et al., 2009). Current study demonstrated that the amplitude of circadian oscillation driven by *bmal1*-promoter was damped more in senescent cells (**Figure 2D**), which is probably due to the increase in E-box-regulated circadian gene, *rev-erb*, the repressor for *bmal1* gene regulation. Intriguingly, it has been demonstrated that H_2O_2 decreases intracellular NAD^+ in some primary cells, suggesting that senescent cells in our study also possesses low NAD^+ (Furukawa et al., 2007; Han et al., 2016). Evidences mentioned here imply that altered signaling pathways during senescence affects circadian clock properties, however, as far as we know, molecular connections between cellular senescence and circadian clock remain largely uncovered. Therefore, further investigations addressing this will be required to understand, maintain and cure the circadian clock mechanisms in the elderly.

In summary, our results indicate that cellular senescence alters the circadian clock, irrespective of the type of cellular senescence. In aged individuals, disruption of the circadian clock functions has been associated with many age-related diseases, however, the underlying cause of this disruption of the circadian clock was largely unknown. Our novel findings, therefore, open up new avenues to investigate the underlying mechanisms that lead to the disruption of the circadian clock function in aged organisms.

DATA AVAILABILITY STATEMENT

The original contributions presented in the study are included in the article/**Supplementary Material**, further inquiries can be directed to the corresponding author.

AUTHOR CONTRIBUTIONS

RA performed experiments and drafted the manuscript. YN performed experiments, designed the overall approach, coordinated the study, and wrote the manuscript. KS contributed to coordination of the study. YB contributed to design and coordination of the study. All authors contributed to the article and approved the submitted version.

FUNDING

This work was supported by JSPS KAKENHI Grant Number 17K08569 (YN).

SUPPLEMENTARY MATERIAL

The Supplementary Material for this article can be found online at: https://www.frontiersin.org/articles/10.3389/fnins.2021.638122/full#supplementary-material

REFERENCES

Ahmed, R., Ashimori, A., Iwamoto, S., Matsui, T., Nakahata, Y., and Bessho, Y. (2019). Replicative senescent human cells possess altered circadian clocks with a prolonged period and delayed peak-time. *Aging* (Albany Ny) 11, 950–973. doi: 10.18632/aging.101794

Asher, G., Reinke, H., Altmeyer, M., Gutierrez-Arcelus, M., Hottiger, M. O., and Schibler, U. (2010). Poly(ADP-ribose) polymerase 1 participates in the phase entrainment of circadian clocks to feeding. *Cell* 142, 943–953. doi: 10.1016/j.cell.2010.08.016

Baar, M. P., Brandt, R. M., Putavet, D. A., Klein, J. D., Derks, K. W., Bourgeois, B. R., et al. (2017). Targeted *Apoptosis* of senescent cells restores tissue homeostasis in response to chemotoxicity and aging. *Cell* 169, 132–147.e116.

Bahar, R., Hartmann, C. H., Rodriguez, K. A., Denny, A. D., Busuttil, R. A., Dolle, M. E., et al. (2006). Increased cell-to-cell variation in gene expression in ageing mouse heart. *Nature* 441, 1011–1014. doi: 10.1038/nature04844

Baker, D. J., Childs, B. G., Durik, M., Wijers, M. E., Sieben, C. J., Zhong, J., et al. (2016). Naturally occurring p16(Ink4a)-positive cells shorten healthy lifespan. *Nature* 530, 184–189. doi: 10.1038/nature16932

Baker, D. J., Wijshake, T., Tchkonia, T., Lebrasseur, N. K., Childs, B. G., Van De Sluis, B., et al. (2011). Clearance of p16Ink4a-positive senescent cells delays ageing-associated disorders. *Nature* 479, 232–236. doi: 10.1038/nature10600

Bass, J., and Lazar, M. A. (2016). Circadian time signatures of fitness and disease. *Science* 354, 994–998. doi: 10.1126/science.aah4965

Bavik, C., Coleman, I., Dean, J. P., Knudsen, B., Plymate, S., and Nelson, P. S. (2006). The gene expression program of prostate fibroblast senescence modulates neoplastic epithelial cell proliferation through paracrine mechanisms. *Cancer Res.* 66, 794–802. doi: 10.1158/0008-5472.can-05-1716

Bhatia, B., Multani, A. S., Patrawala, L., Chen, X., Calhoun-Davis, T., Zhou, J., et al. (2008). Evidence that senescent human prostate epithelial cells enhance tumorigenicity: cell fusion as a potential mechanism and inhibition by p16INK4a and hTERT. *Int. J. Cancer* 122, 1483–1495. doi: 10.1002/ijc.23222

Brown, S. A., Fleury-Olela, F., Nagoshi, E., Hauser, C., Juge, C., Meier, C. A., et al. (2005). The period length of fibroblast circadian gene expression varies widely among human individuals. *PLoS Biol.* 3:e338. doi: 10.1371/journal.pbio.0030338

Bussian, T. J., Aziz, A., Meyer, C. F., Swenson, B. L., Van Deursen, J. M., and Baker, D. J. (2018). Clearance of senescent glial cells prevents tau-dependent pathology and cognitive decline. *Nature* 562, 578–582. doi: 10.1038/s41586-018-0543-y

Campisi, J. (2005). Senescent cells, tumor suppression, and organismal aging: good citizens, bad neighbors. *Cell* 120, 513–522. doi: 10.1016/j.cell.2005.02.003

Campisi, J., Andersen, J. K., Kapahi, P., and Melov, S. (2011). Cellular senescence: a link between cancer and age-related degenerative disease? *Semin. Cancer Biol.* 21, 354–359.

Castro-Vega, L. J., Jouravleva, K., Ortiz-Montero, P., Liu, W. Y., Galeano, J. L., Romero, M., et al. (2015). The senescent microenvironment promotes the emergence of heterogeneous cancer stem-like cells. *Carcinogenesis* 36, 1180–1192. doi: 10.1093/carcin/bgv101

Chang, J., Wang, Y., Shao, L., Laberge, R. M., Demaria, M., Campisi, J., et al. (2016). Clearance of senescent cells by ABT263 rejuvenates aged hematopoietic stem cells in mice. *Nat. Med.* 22, 78–83. doi: 10.1038/nm.4010

Chen, Q., Fischer, A., Reagan, J. D., Yan, L. J., and Ames, B. N. (1995). Oxidative DNA damage and senescence of human diploid fibroblast cells. *Proc. Natl. Acad. Sci. U.S.A.* 92, 4337–4341. doi: 10.1073/pnas.92.10.4337

Childs, B. G., Baker, D. J., Wijshake, T., Conover, C. A., Campisi, J., and Van Deursen, J. M. (2016). Senescent intimal foam cells are deleterious at all stages of atherosclerosis. *Science* 354, 472–477. doi: 10.1126/science.aaf6659

Childs, B. G., Li, H., and Van Deursen, J. M. (2018). Senescent cells: a therapeutic target for cardiovascular disease. *J. Clin. Invest.* 128, 1217–1228. doi: 10.1172/jci95146

Cho, J. H., Kim, E. C., Son, Y., Lee, D. W., Park, Y. S., Choi, J. H., et al. (2020). CD9 induces cellular senescence and aggravates atherosclerotic plaque formation. *Cell Death Differ.* 27, 2681–2696. doi: 10.1038/s41418-020-0537-9

Davidson, A. J., Yamazaki, S., Arble, D. M., Menaker, M., and Block, G. D. (2008). Resetting of central and peripheral circadian oscillators in aged rats. *Neurobiol. Aging* 29, 471–477. doi: 10.1016/j.neurobiolaging.2006.10.018

Debacq-Chainiaux, F., Erusalimsky, J. D., Campisi, J., and Toussaint, O. (2009). Protocols to detect senescence-associated beta-galactosidase (SA-betagal) activity, a biomarker of senescent cells in culture and in vivo. *Nat. Protoc.* 4, 1798–1806. doi: 10.1038/nprot.2009.191

Demaria, M., Ohtani, N., Youssef, S. A., Rodier, F., Toussaint, W., Mitchell, J. R., et al. (2014). An essential role for senescent cells in optimal wound healing through secretion of PDGF-AA. *Dev. Cell* 31, 722–733. doi: 10.1016/j.devcel.2014.11.012

Enge, M., Arda, H. E., Mignardi, M., Beausang, J., Bottino, R., Kim, S. K., et al. (2017). Single-cell analysis of human pancreas reveals transcriptional signatures of aging and somatic mutation patterns. *Cell* 171:e314.

Furukawa, A., Tada-Oikawa, S., Kawanishi, S., and Oikawa, S. (2007). H2O2 accelerates cellular senescence by accumulation of acetylated p53 via decrease in the function of SIRT1 by NAD+ depletion. *Cell Physiol. Biochem.* 20, 45–54.

Garcia, D., and Shaw, R. J. (2017). AMPK: mechanisms of cellular energy sensing and restoration of metabolic balance. *Mol. Cell* 66, 789–800. doi: 10.1016/j.molcel.2017.05.032

Han, X., Tai, H., Wang, X., Wang, Z., Zhou, J., Wei, X., et al. (2016). AMPK activation protects cells from oxidative stress-induced senescence via autophagic flux restoration and intracellular NAD(+) elevation. *Aging Cell* 15, 416–427. doi: 10.1111/acel.12446

Hardie, D. G. (2003). Minireview: the AMP-activated protein kinase cascade: the key sensor of cellular energy status. *Endocrinology* 144, 5179–5183. doi: 10.1210/en.2003-0982

Hashimoto, M., Asai, A., Kawagishi, H., Mikawa, R., Iwashita, Y., Kanayama, K., et al. (2016). Elimination of p19ARF-expressing cells enhances pulmonary function in mice. *JCI Insight* 1:e87732.

Hernandez-Segura, A., De Jong, T. V., Melov, S., Guryev, V., Campisi, J., and Demaria, M. (2017). Unmasking transcriptional heterogeneity in senescent cells. *Curr. Biol.* 27, 2652–2660.e2654.

Herranz, N., Gallage, S., Mellone, M., Wuestefeld, T., Klotz, S., Hanley, C. J., et al. (2015). mTOR regulates MAPKAPK2 translation to control the senescence-associated secretory phenotype. *Nat. Cell Biol.* 17, 1205–1217. doi: 10.1038/ncb3225

Honma, S. (2018). The mammalian circadian system: a hierarchical multi-oscillator structure for generating circadian rhythm. *J. Physiol. Sci.* 68, 207–219. doi: 10.1007/s12576-018-0597-5

Houssaini, A., Breau, M., Kebe, K., Abid, S., Marcos, E., Lipskaia, L., et al. (2018). mTOR pathway activation drives lung cell senescence and emphysema. *JCI Insight* 3:e93203.

Imai, S., and Guarente, L. (2014). NAD+ and sirtuins in aging and disease. *Trends Cell Biol.* 24, 464–471. doi: 10.1016/j.tcb.2014.04.002

Imai, S., and Guarente, L. (2016). It takes two to tango: NAD+ and sirtuins in aging/longevity control. *npj Aging Mechanisms Dis.* 2:16017.

James, E. L., Michalek, R. D., Pitiyage, G. N., De Castro, A. M., Vignola, K. S., Jones, J., et al. (2015). Senescent human fibroblasts show increased glycolysis and redox homeostasis with extracellular metabolomes that overlap with those of irreparable DNA damage, aging, and disease. *J. Proteome Res.* 14, 1854–1871. doi: 10.1021/pr501221g

Jeon, O. H., Kim, C., Laberge, R. M., Demaria, M., Rathod, S., Vasserot, A. P., et al. (2017). Local clearance of senescent cells attenuates the development of post-traumatic osteoarthritis and creates a pro-regenerative environment. *Nat. Med.* 23, 775–781. doi: 10.1038/nm.4324

Jeon, O. H., Wilson, D. R., Clement, C. C., Rathod, S., Cherry, C., Powell, B., et al. (2019). Senescence cell-associated extracellular vesicles serve as osteoarthritis disease and therapeutic markers. *JCI Insight* 4:e125019.

Ji, G., Lv, K., Chen, H., Wang, Y., Zhang, Y., Li, Y., et al. (2019). Hydrogen peroxide modulates clock gene expression via PRX2-STAT3-REV-ERBalpha/beta pathway. *Free Radic. Biol. Med.* 145, 312–320. doi: 10.1016/j.freeradbiomed.2019.09.036

Jordan, S. D., and Lamia, K. A. (2013). AMPK at the crossroads of circadian clocks and metabolism. *Mol. Cell Endocrinol.* 366, 163–169. doi: 10.1016/j.mce.2012.06.017

Khaidizar, F. D., Nakahata, Y., Kume, A., Sumizawa, K., Kohno, K., Matsui, T., et al. (2017). Nicotinamide phosphoribosyltransferase delays cellular senescence by upregulating SIRT1 activity and antioxidant gene expression in mouse cells. *Genes Cells* 22, 982–992. doi: 10.1111/gtc.12542

Khapre, R. V., Kondratova, A. A., Susova, O., and Kondratov, R. V. (2011). Circadian clock protein BMAL1 regulates cellular senescence in vivo. *Cell Cycle* 10, 4162–4169. doi: 10.4161/cc.10.23.18381

Krishnamurthy, J., Torrice, C., Ramsey, M. R., Kovalev, G. I., Al-Regaiey, K., Su, L., et al. (2004). Ink4a/Arf expression is a biomarker of aging. *J. Clin. Invest.* 114, 1299–1307. doi: 10.1172/jci22475

Laberge, R. M., Sun, Y., Orjalo, A. V., Patil, C. K., Freund, A., Zhou, L., et al. (2015). MTOR regulates the pro-tumorigenic senescence-associated secretory phenotype by promoting IL1A translation. *Nat. Cell Biol.* 17, 1049–1061. doi: 10.1038/ncb3195

Lamia, K. A., Sachdeva, U. M., Ditacchio, L., Williams, E. C., Alvarez, J. G., Egan, D. F., et al. (2009). AMPK regulates the circadian clock by cryptochrome phosphorylation and degradation. *Science* 326:5951.

Lehmann, M., Korfei, M., Mutze, K., Klee, S., Skronska-Wasek, W., Alsafadi, H. N., et al. (2017). Senolytic drugs target alveolar epithelial cell function and attenuate experimental lung fibrosis ex vivo. *Eur. Respir. J.* 50:1602367. doi: 10.1183/13993003.02367-2016

Li, Y., Shan, Y., Desai, R. V., Cox, K. H., Weinberger, L. S., and Takahashi, J. S. (2020). Noise-driven cellular heterogeneity in circadian periodicity. *Proc. Natl. Acad. Sci. U.S.A.* 117, 10350–10356. doi: 10.1073/pnas.1922388117

Liu, D., and Hornsby, P. J. (2007). Senescent human fibroblasts increase the early growth of xenograft tumors via matrix metalloproteinase secretion. *Cancer Res.* 67, 3117–3126. doi: 10.1158/0008-5472.can-06-3452

Maciel-Baron, L. A., Morales-Rosales, S. L., Aquino-Cruz, A. A., Triana-Martinez, F., Galvan-Arzate, S., Luna-Lopez, A., et al. (2016). Senescence associated secretory phenotype profile from primary lung mice fibroblasts depends on the senescence induction stimuli. *Age (Dordr)* 38:26.

Martinez-Jimenez, C. P., Eling, N., Chen, H. C., Vallejos, C. A., Kolodziejczyk, A. A., Connor, F., et al. (2017). Aging increases cell-to-cell transcriptional variability upon immune stimulation. *Science* 355, 1433–1436. doi: 10.1126/science.aah4115

Mattis, J., and Sehgal, A. (2016). Circadian rhythms, sleep, and disorders of aging. *Trends Endocrinol. Metab.* 27, 192–203. doi: 10.1016/j.tem.2016.02.003

Nacarelli, T., and Sell, C. (2017). Targeting metabolism in cellular senescence, a role for intervention. *Mol. Cell Endocrinol.* 455, 83–92. doi: 10.1016/j.mce.2016.08.049

Nakahata, Y., Kaluzova, M., Grimaldi, B., Sahar, S., Hirayama, J., Chen, D., et al. (2008). The NAD+-dependent deacetylase SIRT1 modulates CLOCK-mediated chromatin remodeling and circadian control. *Cell* 134, 329–340. doi: 10.1016/j.cell.2008.07.002

Nakahata, Y., Sahar, S., Astarita, G., Kaluzova, M., and Sassone-Corsi, P. (2009). Circadian control of the NAD+ salvage pathway by CLOCK-SIRT1. *Science* 324, 654–657. doi: 10.1126/science.1170803

Nakahata, Y., Yasukawa, S., Khaidizar, F. D., Shimba, S., Matsui, T., and Bessho, Y. (2018). Bmal1-deficient mouse fibroblast cells do not provide premature cellular senescence in vitro. *Chronobiol. Int.* 35, 730–738. doi: 10.1080/07420528.2018.1430038

Nakamura, T. J., Nakamura, W., Tokuda, I. T., Ishikawa, T., Kudo, T., Colwell, C. S., et al. (2015). Age-related changes in the circadian system unmasked by constant conditions. *eNeuro* 2:ENEURO.0064-15.2015.

Nakao, M., Tanaka, H., and Koga, T. (2020). Cellular senescence variation by metabolic and epigenomic remodeling. *Trends Cell Biol.* 30, 919–922. doi: 10.1016/j.tcb.2020.08.009

Ortiz-Montero, P., Londono-Vallejo, A., and Vernot, J. P. (2017). Senescence-associated IL-6 and IL-8 cytokines induce a self- and cross-reinforced senescence/inflammatory milieu strengthening tumorigenic capabilities in the MCF-7 breast cancer cell line. *Cell Commun. Signal.* 15:17.

Parrinello, S., Coppe, J. P., Krtolica, A., and Campisi, J. (2005). Stromal-epithelial interactions in aging and cancer: senescent fibroblasts alter epithelial cell differentiation. *J. Cell Sci.* 118, 485–496. doi: 10.1242/jcs.01635

Partch, C. L., Green, C. B., and Takahashi, J. S. (2014). Molecular architecture of the mammalian circadian clock. *Trends Cell Biol.* 24, 90–99. doi: 10.1016/j.tcb.2013.07.002

Pittendrigh, C. S., and Daan, S. (1974). Circadian oscillations in rodents: a systematic increase of their frequency with age. *Science* 186, 548–550. doi: 10.1126/science.186.4163.548

Putker, M., Crosby, P., Feeney, K. A., Hoyle, N. P., Costa, A. S. H., Gaude, E., et al. (2018). Mammalian circadian period, but not phase and amplitude, is robust against redox and metabolic perturbations. *Antioxid. Redox Signal.* 28, 507–520. doi: 10.1089/ars.2016.6911

Ramanathan, C., Kathale, N. D., Liu, D., Lee, C., Freeman, D. A., Hogenesch, J. B., et al. (2018). mTOR signaling regulates central and peripheral circadian clock function. *PLoS Genet.* 14:e1007369. doi: 10.1371/journal.pgen.1007369

Ramsey, K. M., Yoshino, J., Brace, C. S., Abrassart, D., Kobayashi, Y., Marcheva, B., et al. (2009). Circadian clock feedback cycle through NAMPT-mediated NAD+ biosynthesis. *Science* 324, 651–654. doi: 10.1126/science.1171641

Sahar, S., and Sassone-Corsi, P. (2012). Regulation of metabolism: the circadian clock dictates the time. *Trends Endocrinol. Metab.* 23, 1–8. doi: 10.1016/j.tem.2011.10.005

Schafer, M. J., White, T. A., Iijima, K., Haak, A. J., Ligresti, G., Atkinson, E. J., et al. (2017). Cellular senescence mediates fibrotic pulmonary disease. *Nat. Commun.* 8:14532.

Schultz, M. B., and Sinclair, D. A. (2016). Why NAD+ declines during aging: it's destroyed. *Cell Metab.* 23, 965–966. doi: 10.1016/j.cmet.2016.05.022

Sellix, M. T., Evans, J. A., Leise, T. L., Castanon-Cervantes, O., Hill, D. D., Delisser, P., et al. (2012). Aging differentially affects the re-entrainment response of central and peripheral circadian oscillators. *J. Neurosci.* 32, 16193–16202. doi: 10.1523/jneurosci.3559-12.2012

Stein, G. H., Drullinger, L. F., Soulard, A., and Dulić, V. (1999). Differential roles for cyclin-dependent kinase inhibitors p21 and p16 in the mechanisms of senescence and differentiation in human fibroblasts. *Mol. Cell Biol.* 19, 2109–2117. doi: 10.1128/mcb.19.3.2109

Tahara, Y., Yokota, A., Shiraishi, T., Yamada, S., Haraguchi, A., Shinozaki, A., et al. (2016). In vitro and in vivo phase changes of the mouse circadian clock by oxidative stress. *J. Circadian Rhythms* 14, 4.

Takahashi, J. S. (2017). Transcriptional architecture of the mammalian circadian clock. *Nat. Rev. Genet.* 18, 164–179. doi: 10.1038/nrg.2016.150

Tamaru, T., Hattori, M., Ninomiya, Y., Kawamura, G., Vares, G., Honda, K., et al. (2013). ROS stress resets circadian clocks to coordinate pro-survival signals. *PLoS One* 8:e82006. doi: 10.1371/journal.pone.0082006

Tang, H., Geng, A., Zhang, T., Wang, C., Jiang, Y., and Mao, Z. (2019). Single senescent cell sequencing reveals heterogeneity in senescent cells induced by telomere erosion. *Protein Cell* 10, 370–375. doi: 10.1007/s13238-018-0591-y

Toussaint, O., Dumont, P., Dierick, J. F., Pascal, T., Frippiat, C., Chainiaux, F., et al. (2000). Stress-induced premature senescence. Essence of life, evolution, stress, and aging. *Ann. N. Y. Acad. Sci.* 908, 85–98. doi: 10.1111/j.1749-6632.2000.tb06638.x

Um, J. H., Yang, S., Yamazaki, S., Kang, H., Viollet, B., Foretz, M., et al. (2007). Activation of 5′-AMP-activated kinase with diabetes drug metformin induces casein kinase Iepsilon (CKIepsilon)-dependent degradation of clock protein mPer2. *J. Biol. Chem.* 282, 20794–20798. doi: 10.1074/jbc.c700070200

Valentinuzzi, V. S., Scarbrough, K., Takahashi, J. S., and Turek, F. W. (1997). Effects of aging on the circadian rhythm of wheel-running activity in C57BL/6 mice. *Am. J. Physiol.* 273, R1957–R1964.

Van Someren, E. J. W. (2000). Circadian and sleep disturbances in the elderly. *Exp. Gerontol.* 35, 1229–1237. doi: 10.1016/s0531-5565(00)00191-1

Wang, J. C., and Bennett, M. (2012). Aging and atherosclerosis: mechanisms, functional consequences, and potential therapeutics for cellular senescence. *Circ. Res.* 111, 245–259. doi: 10.1161/circresaha.111.261388

Wible, R. S., Ramanathan, C., Sutter, C. H., Olesen, K. M., Kensler, T. W., Liu, A. C., et al. (2018). NRF2 regulates core and stabilizing circadian clock loops, coupling redox and timekeeping in Mus musculus. *eLife* 7:e31656.

Witting, W., Mirmiran, M., Bos, N. P., and Swaab, D. F. (1994). The effect of old age on the free-running period of circadian rhythms in rat. *Chronobiol. Int.* 11, 103–112. doi: 10.3109/07420529409055896

Xu, M., Bradley, E. W., Weivoda, M. M., Hwang, S. M., Pirtskhalava, T., Decklever, T., et al. (2017). Transplanted senescent cells induce an osteoarthritis-like condition in mice. *J. Gerontol. A Biol. Sci. Med. Sci.* 72, 780–785.

Yosef, R., Pilpel, N., Tokarsky-Amiel, R., Biran, A., Ovadya, Y., Cohen, S., et al. (2016). Directed elimination of senescent cells by inhibition of BCL-W and BCL-XL. *Nat. Commun.* 7:11190.

Zhang, E. E., Liu, A. C., Hirota, T., Miraglia, L. J., Welch, G., Pongsawakul, P. Y., et al. (2009). A genome-wide RNAi screen for modifiers of the circadian clock in human cells. *Cell* 139, 199–210. doi: 10.1016/j.cell.2009.08.031

Zhang, P., Kishimoto, Y., Grammatikakis, I., Gottimukkala, K., Cutler, R. G., Zhang, S., et al. (2019). Senolytic therapy alleviates Abeta-associated oligodendrocyte progenitor cell senescence and cognitive deficits in an Alzheimer's disease model. *Nat. Neurosci.* 22, 719–728. doi: 10.1038/s41593-019-0372-9

Conflict of Interest: The authors declare that the research was conducted in the absence of any commercial or financial relationships that could be construed as a potential conflict of interest.

frontiers in Neuroscience

ORIGINAL RESEARCH
published: 18 February 2021
doi: 10.3389/fnins.2021.604165

Altered Light Sensitivity of Circadian Clock in Shank3$^{+/-}$ Mouse

Javier Alamilla[1†], Yazmín Ramiro-Cortés[2†], Adriana Mejía-López[2], José-Luis Chavez[2], Dulce Olivia Rivera[2], Víctor Felipe[2] and Raúl Aguilar-Roblero[2]*

[1] Centro Universitario de Investigaciones Biomédicas, Consejo Nacional de Ciencia y Tecnología (CONACYT)-Universidad de Colima, Colima, Mexico, [2] División de Neurociencias, Instituto de Fisiología Celular, Universidad Nacional Autónoma de México, Mexico

Autism spectrum disorder (ASD) is a neurodevelopmental disorder characterized by impairment in communication and social interaction, repetitive or stereotypical behaviors, altered sensory perception, and sleep disorders. In general, the causes of ASD remain unknown, but in Phelan–McDermid syndrome, it is known that the disorder is related to the haploinsufficiency of the Shank3 gene. We used an autism model with compromised glutamatergic signaling, the Shank3$^{+/-}$ mouse, to study the circadian rhythm architecture of locomotion behavior and its entrainment to light. We also analyzed the synapse between the retinohypothalamic tract (RHT) and the suprachiasmatic nucleus (SCN), employing tract tracing and immunohistochemical techniques. We found that Shank3$^{+/-}$ mice were not impaired in the SCN circadian clock, as indicated by a lack of differences between groups in the circadian architecture in entrained animals to either long or short photoperiods. Circadian rhythm periodicity (tau) was unaltered between genotypes in constant darkness (DD, dim red light). Similar results were obtained in the re-entrainment to shifts in the light–dark cycle and in the entrainment to a skeleton photoperiod from DD. However, Shank3$^{+/-}$ mice showed larger phase responses to light pulses, both delays and advances, and rhythm disorganization induced by constant bright light. Immunohistochemical analyses indicated no differences in the RHT projection to the SCN or the number of SCN neurons expressing the *N*-methyl-D-aspartate (NMDA) receptor subunit NR2A, whereas the Shank3$^{+/-}$ animals showed decreased c-Fos induction by brief light pulses at CT14, but increased number of vasoactive intestinal polypeptide (VIP)-positive neurons. These results indicate alterations in light sensitivity in Shank3$^{+/-}$ mice. Further studies are necessary to understand the mechanisms involved in such increased light sensitivity, probably involving VIP neurons.

Keywords: phase response curve (PRC), ASD, autism, SCN, RHT, NMDA receptor GluN2A, receptor GluN2A, constant light

OPEN ACCESS

Edited by:
Daisuke Ono,
Nagoya University, Japan

Reviewed by:
Alun Thomas Lloyd Hughes,
Liverpool John Moores University, United Kingdom
Yu Tahara,
Waseda University, Japan

***Correspondence:**
Raúl Aguilar-Roblero
raguilar@ifc.unam.mx

[†] These authors have contributed equally to this work

Specialty section:
This article was submitted to Sleep and Circadian Rhythms, a section of the journal Frontiers in Neuroscience

Received: *08 September 2020*
Accepted: *12 January 2021*
Published: *18 February 2021*

Citation:
Alamilla J, Ramiro-Cortés Y, Mejía-López A, Chavez J-L, Rivera DO, Felipe V and Aguilar-Roblero R (2021) Altered Light Sensitivity of Circadian Clock in Shank3$^{+/-}$ Mouse. Front. Neurosci. 15:604165. doi: 10.3389/fnins.2021.604165

INTRODUCTION

Circadian rhythms are behavioral and physiological processes with a periodicity close to 24h generated by the suprachiasmatic nuclei (SCN), the circadian clock of the hypothalamus (Marcheva et al., 2013). The SCN synchronizes to environmental light *via* a subpopulation of ganglia cells in the retina expressing the photopigment melanopsin (Hattar et al., 2003; Hankins et al., 2008),

whose unmyelinated axons form the retinohypothalamic tract (RHT) (Moore and Lenn, 1972). The RHT terminals release glutamate and pituitary adenylate cyclase-activating peptide to SCN ventral neurons (Abrahamson and Moore, 2001; Hannibal, 2002, 2006). Glutamate activates *N*-methyl-D-aspartate (NMDA) and α-amino-3-hydroxyl-5-methyl-4-isoxazole-propionate (AMPA)–kainate postsynaptic receptors (Kim and Dudek, 1991), which increase intracellular calcium in SCN neurons and activate signaling cascades necessary for the synchronization of the circadian clock to light (Ding et al., 1994, 1997).

Autism spectrum disorder (ASD) is a neurodevelopmental disorder characterized by core symptoms of impaired communication and social interaction, repetitive or stereotyped behaviors, and altered sensory perception (Klintwall et al., 2011; Carbonetto, 2014; Baum et al., 2015; Bourgeron, 2015; Robertson and Baron-Cohen, 2017; Schroeder et al., 2017). It is estimated that, worldwide, one in 160 children has ASD (World Health Organization, 2013). The core symptoms are associated with secondary comorbid conditions including intellectual disability, anxiety, gastrointestinal problems, and sleep troubles (Bourgeron, 2015). The causes of ASD remain unknown; however, there are indications of a genetic basis linked to genes of proteins related to synaptic structure and function (Zoghbi and Bear, 2012). One of the best characterized examples is Phelan–McDermid syndrome (PMS), which is caused by a deletion of the Shank3 gene in a single allele in the chromosome 22q13. The main features of PMS are neonatal hypotonia, absent or severely delayed speech, intellectual disability, and autism spectrum disorder (Phelan and McDermid, 2012). The Shank3 gene encodes for the protein SHANK3, a scaffolding protein localized at the postsynaptic of excitatory synapses. SHANK3 scaffold ionotropic and metabotropic glutamate receptors are considered to be key regulators, either directly or indirectly, of synaptic transmission and plasticity (Monteiro and Feng, 2017).

A remarkable feature of ASD is that children manifest a high incidence of sleep problems, of around 53% (Wiggs and Stores, 2004). Interestingly, children with PMS also present an elevated incidence of sleep disturbances, ∼90% of the cases (Bro et al., 2017). Sleep problems and ASD suggest an unexplored link between autism and circadian rhythms. For instance, a circadian oscillation of the SHANK3 in the hippocampus and striatum, which correlates with melatonin serum levels (Sarowar et al., 2016), was recently discovered. Furthermore, it has been reported that knockout mice lacking exon 21 of Shank3 exhibit differences in non-REM sleep and slight differences in free-running circadian rhythms in constant darkness (DD) in comparison to wild-type controls (Ingiosi et al., 2019).

Despite this evidence, the role of the circadian system in autism is unknown. Since SHANK proteins are necessary *via* the PSD-95/GKAP complex, for the organization of NMDA receptors in the postsynaptic density (Lim et al., 1999), and NMDA receptors are crucial for light-induced phase shifts (Colwell and Menaker, 1992; Ding et al., 1994, 1997), we tested whether a compromised glutamatergic signaling in Shank3$^{+/-}$ mice (an animal model linked to autism, with a deletion in the ankyrin repeat domain which encodes for one of the major Shank3 isoforms, Shank3α) affects the circadian rhythm in locomotion, its entrainment to light, the fiber density from the RHT to the SCN, and the number of neurons expressing vasoactive intestinal polypeptide (VIP), NMDA2A subunit, and c-Fos photoinduction in the SCN.

MATERIALS AND METHODS

Animals and Housing

B6(Cg)-Shank3tm1.1Bux/J heterozygous mice (Jax, no. 017889) were bred with C57BL/6J wild-type mice. For aims of housing and breeding but not experimental, the animals were housed under a cycle of 12-h light/dark in a conventional temperature and humidity vivarium, with *ad libitum* access to food and water. Shank3$^{+/+}$ (wild type, WT) and Shank3$^{+/-}$ (HET) littermates including male and female mice were 16weeks old at the beginning of the behavioral experiments. The animals were genotyped at the beginning and again at the end of the experimental procedures to confirm the subject genotype. Data collection and analysis were performed blind with regard to the genotype of the animals until the end of the experiments. All experimental protocols were conducted according to current Mexican legislation NOM-062-ZOO-1999 (SAGARPA), the internal ethical institutional committee guidelines (authorization CICUAL RA-58-15), and the guidelines on the use of animals from the Society for Neuroscience.

We defined DD as the constant exposition to dim red light (5lx) and LD as the exposition to bright light (300 lx, LL) followed by constant dim red light (5 lx).

Before the experiments, the mice were housed for habituation at least for 10 days in groups of four, in the vivarium of the Chronobiology Laboratory, with water and food *ad libitum*. The habituation room was kept at a temperature of 24°C (± 1) under a 14:10-h photoperiod (LD 14:10, lights on at 07:00 hours).

Behavioral Recordings

At the beginning of the experiment, mice were transferred to individual acrylic boxes in cabinets with controlled light–dark daily cycles. Dim red light (5 lx) was constantly present as background throughout the experiment. The circadian rhythm of locomotion was continuously monitored by a computerized system described by Mercado et al. (2009). Briefly, each time the animal moved, electric pulses were generated through pressure sensors placed beneath the floor; these events were computed at 1-min intervals and stored in magnetic media for later analysis. Pairs of animals from both groups (WT and Shank3$^{+/-}$) were monitored simultaneously under the same lighting conditions.

In the first experiment, 22 animals (11 WT and 11 HET) were recorded in different lighting conditions to describe the circadian architecture under long (LD 14:10) and short (LD 10:14) photoperiods. In this experiment, re-entrainment to a 6-h LD advance phase shift was performed. In the second experiment, we analyzed the circadian rhythms under the skeleton photoperiod (SKP) that consisted of two light pulses (1 h, 300 lx) separated by a long (13 h) and a short (9 h) interval

of DD (Pittendrigh and Daan, 1976). In SKP, animals are kept in DD for 2 weeks and then two short light pulses per circadian cycle were applied to the DD for at least 21 days. This condition resembles closely the natural conditions of nocturnal animals living in a burrow in the wild. We also analyzed the response to a brief light pulse (15 min, 400 lx) in three characteristic zones (CT06 dead, CT14 delays, and CT22 advances) of the phase response curve (PRC), as previously described for C57BL/6 mice (Schwartz and Zimmerman, 1990).

Data Analysis

Graphic display of double plots and χ^2 periodogram analysis of the data were made by the Digital Analysis System Applied to Chronobiology (Omnialva/SPAD9) developed and validated in our laboratory (Instituto de Fisiología Celular, Universidad Nacional Autónoma de México). To analyze the architecture of the circadian rhythm, the durations in minutes of activity (α), rest (ρ), and period (τ) were calculated for the different lighting conditions to which the individuals were exposed. For each of the last 10 cycles in each lighting condition, the times of activity onset and offset were recorded. Activity onset was considered as the first point of upward inflection of activity counts in at least five consecutive bins. Activity offset was marked as the first point of downward inflection of activity counts in at least five consecutive bins. The durations of α, ρ, and τ were then calculated for each of the 10 days, with the mean values of these measures being used as individual values for further statistical analysis. For constant lighting conditions, either DD or LL, the period of rhythmicity was estimated from the χ^2 periodogram obtained from the last 10 days of each segment of the experiment. The period of rhythmicity was read from the peak in the range from 15 to 30 h that reached an α level of 0.0001; loss of rhythmicity was considered to occur when the amplitude of the peaks did not reach an α level of 0.01. Period stability was defined as the inverse of the variance ($1/s^2$) from several tau estimates, computed from 10-day intervals, as described in Aschoff (1984). We also computed the days it took to synchronize the animals to 6-h advances in the LD cycle. We considered that the subject was entrained when the duration of α was similar to the mean value before the LD shift.

To analyze the circadian rhythms under the SKP and the PRC, the recordings were conducted in dim red light (5 lx) for at least 10 basal days. In nocturnal rodents, circadian time 12 (CT12) is designated as the beginning of the subjective night indicated by the onset of the active phase. CT12 was estimated by adjusting a line to the onset of activity of at least 10 cycles; τ was then calculated from the slope of this line. To analyze the characteristic zones of the PRC, on day 11, a 15-min light pulse was applied either at CT06, CT14, or CT22, each one projected from CT12 on day 10, and the recordings continued in DD for at least 14 days. The phase shifts in the activity onset were estimated on the day of the light pulse by comparing the line adjusted to CT12 from the last 10 days of recording projected to the day the light pulse was applied with the corresponding line adjusted before the light pulse. To analyze the circadian rhythms under SKP, on day 11, the recordings continue for at least 21 days under a DD background on which two 1-h light pulses are separated by long (13 h) and short (9 h) DD intervals.

RHT Tracing

After the behavioral recordings were finished, subsets of animals from both groups were anesthetized with fluothane vapors. Cholera toxin β-subunit (CTB, List Biological) was injected into the vitreous of one eye (1.5 μl of 0.2% CTB in 2% dimethyl sulfoxide/0.9% saline solution at a rate of about 0.3 μl/min). Forty-eight hours later, the animals were further processed for immunohistochemical staining, as described below.

c-Fos Photoinduction

In order to establish the SCN response to brief light pulses, different subsets of animals (from both groups) were recorded in DD for at least 7 days and CT12 was determined as previously described. A 15-min light pulse was applied the next day at CT14 projected from CT12. Another set of WT animals received a 15-min light pulse at CT06 and were used as baseline to compare the c-Fos photoinduction at CT14. Both sets of animals were contrasted with animals manipulated at the same circadian times (CTs) but did not receive light pulses. All animals were further processed for immunohistochemistry, as described next.

Histological Procedures

At the conclusion of the previous experiments, the animals received a lethal dose of pentobarbital sodium (60 mg/kg body weight) and were transcardially perfused with 50 ml of 0.9% saline solution followed by 100 ml of paraformaldehyde–lysine–periodate fixative, consisting of a solution of 4% paraformaldehyde in phosphate-buffered saline (PBS; 0.1 M, pH 7.2) added with lysine (75 mM) and *m*-periodate (10 mM). Brains were dissected and post-fixed for 1 h at 4°C with paraformaldehyde–lysine–periodate and then cryoprotected by successively immersing the brain in 10%, 20%, and 30% sucrose solutions. Coronal sections 30 μm thick were obtained using a cryostat at −23°C. All sections obtained throughout the SCN were collected in three sets in ice-cold PBS (0.1 M, 0.15 M NaCl, pH 7.2), then processed for immunohistochemistry according to the avidin–biotin method. All the primary antibodies used in this research have been previously used and tested. Primary antibodies were diluted as indicated in 0.1 M PBS containing 1.0% normal serum in 0.3% Triton X-100 [anti-VIP raised in rabbit, CAT 20077, Incstar, 1:2,000 (Patton et al., 2020); anti-CTB subunit raised in goat, CAT 703, List Biological Laboratories, 1:2,000 (Zhao et al., 2015); anti-NMDAR2A (GluN2A) raised in rabbit, CAT ACG 002, Alomone Labs, 1:400 (Atkin et al., 2015); and anti c-FOS raised in rabbit, CAT SC-52, Santa Cruz, 1:1,000 (Li and Spitzer, 2020)]. Sections from each bin were incubated with one of the primary antibodies for 72 h at 4°C, then rinsed in PBS and incubated for 2 h at room temperature in biotinylated secondary antibodies (goat anti-rabbit, rabbit anti-goat, and goat anti-rabbit immunoglobulin G), respectively, rinsed in PBS, and incubated for 2 h at room temperature in avidin–biotin–peroxidase complex, rinsed again in PBS, and pre-incubated for 5 min in 0.05% diaminobenzidine (DAB) in Tris buffer (pH 7.2). Of 30% hydrogen peroxide, 35 μl was then

added to each set of sections and left to react for an additional 5 min. These procedures were done simultaneously in control and experimental tissues. Secondary antibodies (Alexa Fluor 488: donkey anti-goat and goat anti-rabbit, both from Abcam, Cambridge, UK) were used at a 1:200 dilution. Sections were then mounted with PBS (pH 7.2), air dehydrated, and covered with Permount (Fisher Scientific, Hampton, NH) and stored until inspected by microscopy. In an additional set of sections, the primary antibody was omitted as a control for nonspecific binding of the secondary antibody (**Supplementary Figure 1**).

Image Acquisition

SCN slices stained with DAB were visualized in an Olympus BX51 microscope (Shinjuku City, Tokyo, Japan), whereas immunofluorescence staining was imaged in two different confocal microscopes: a TCS-SP5 II (Leica, Heidelberg, Germany) and a LSM710 (Carl Zeiss, Oberkochen, Germany). Only complete and undamaged sets of sections were used for imaging analysis. The software used for image acquisition were Image-Pro Plus v.4.1 (Media Cybernetics, Silver Spring, United States) and Zen 12 (Carl Zeiss). A panoramic view was obtained with a ×10 objective. Subsequently, ×20 and ×40 were used to analyze SCN neuronal populations by stereology.

For light microscopy, steps of 10 μm were employed to capture at least three micrographs from each section, with at least three sections used from each brain. For confocal microscopy, steps of 1 μm were employed to capture optical slices (around 20 optical slices were gathered per image). A minimum of three SCN sections were acquired for each brain. Parameters such as laser intensity, resolution, gain, and digital offset were adjusted with the WT group, taking care to ensure there was no saturation and the parameter adjustments were maintained constant for subsequent images across both genotypes.

Image Analysis

SCN neurons immunolabeled for c-Fos, VIP, NMDAR2A, and CTB-labeled RHT fibers were counted by stereology using the optical fractionator method of Gundersen (Mouton, 2011) according to:

$$\text{Total } N = \Sigma Q^*(F_1)^*(F_2)^*(F_3)$$

where Total N is the total neuronal number, ΣQ is the number of objects actually counted, F_1 = 1/(number of sections analyzed/total number of sections), F_2 = 1/(area of the dissector frame/area of the x–y step), and F_3 = 1/(dissector height/section

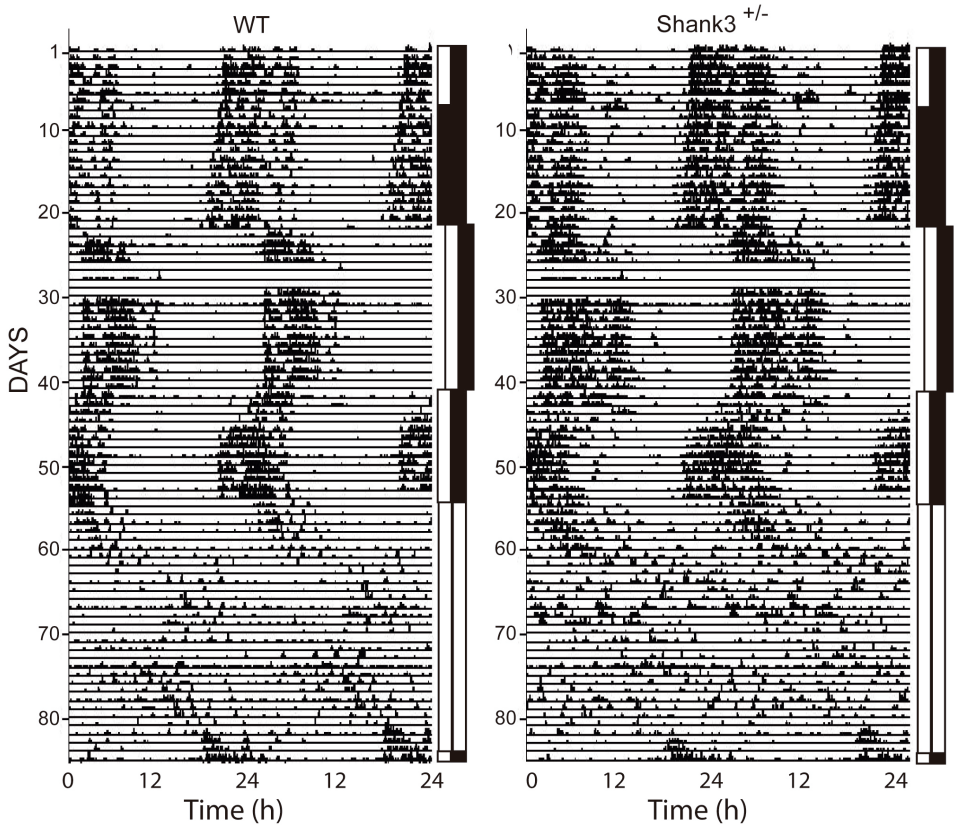

FIGURE 1 | Representative examples of double-plot actograms from wild-type (WT) and Shank3$^{+/-}$ mice. The different lighting conditions are indicated as *vertical bars beside each actogram*. The LD condition is represented by *black* and *white bars*; DD, *double black bars*; and LL, *double white bars*. In these actograms, animals were submitted to a long photoperiod (14:10). The *shift to the right in the bars*, approx. recording days 20–40, indicates a 6-h delay in lights-on time. The 6-h advance is shown as a shift back in the lights-off time. The days of recording are on the *left* and the time of recording (in hours) at the *bottom*.

thickness). The SCN on one side of the brain was photographed by light or confocal microscopy, as described above. Using ImageJ software (1.53c), the numbers of neuronal somata within an unbiased optical dissector (volume = 105 μm^3) were counted from photographs of three out of 11–12 SCN sections (which comprise its rostrocaudal extent). The dissectors were distributed at an *x*–*y* step of 120 μm with the aid of a Grid tool from ImageJ. For the CTB-labeled RHT fibers, a cycloid grid from ImageJ was used as the unbiased dissector.

Statistical Analysis

The data from the circadian architecture are given as the mean ± standard error of the mean (SEM). Latency to entrain to phase shifts, SKP, and the labeled RHT fibers are shown as box and whisker (5–95 percentiles) bars. Characteristic PRC regions are shown as the mean and SEM. Normal distribution (Shapiro–Wilk) and the homogeneity of variances (Levene test) were evaluated before the use of parametric statistics. To analyze differences between the experimental groups, Students *t* test for independent samples was used. Statistical analyses for c-Fos were performed with a three-way ANOVA with Tukey's *post hoc*. All statistical analyses were done using GraphPad Prism 7.0 (GraphPad Software, La Jolla, CA, United States). The α level was set at 0.05.

RESULTS

Behavior

Examples of double-plot actograms under different lighting conditions from the first experiment are shown in **Figure 1**;

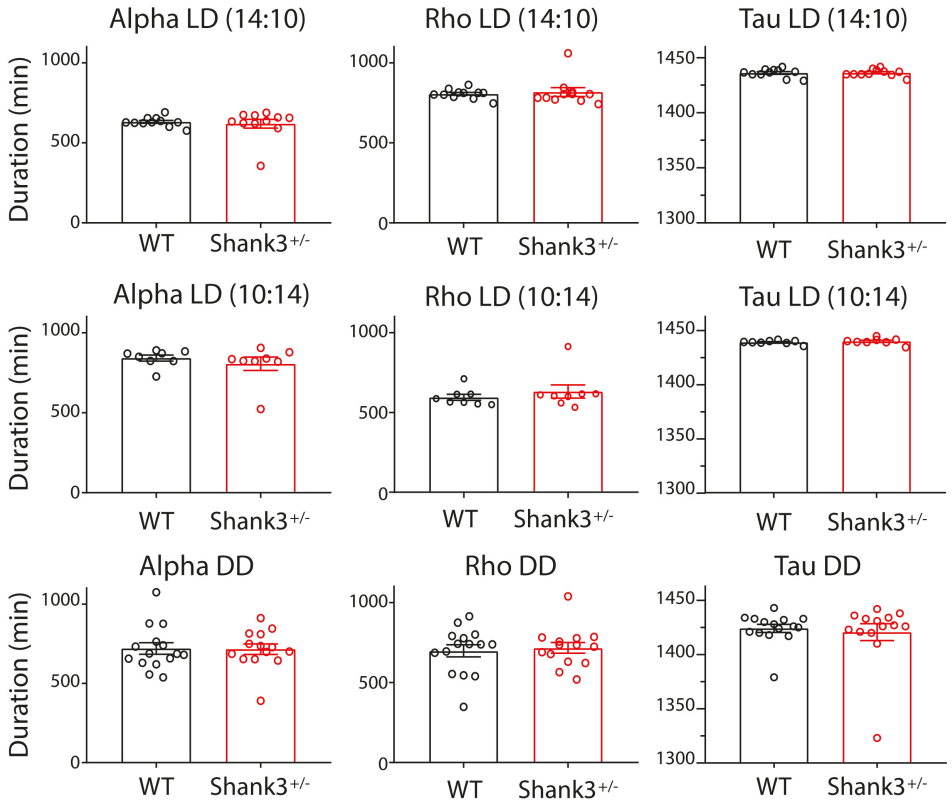

FIGURE 2 | Architecture of circadian rhythms for wild type (WT) and Shank$^{+/-}$ under different lighting schedules. Bar graphs (mean ± SEM) and individual dots of the circadian rhythm architecture from WT (*black*) and Shank3$^{+/-}$ (*red*). The *columns* indicate (from *left to right*) the durations (in minutes) of activity (α), rest (ρ), and period (τ) estimated from 10 days of recording. The *rows* indicate the lighting schedules (from *top to bottom*): long photoperiod, short photoperiod, and DD (constant dim red light).

TABLE 1 | Phase angle of activity (α) and rest (ρ) for animals maintained in two different photoperiods.

Photoperiod	ψα			ψρ		
	WT	Shank3$^{+/-}$		WT	Shank3$^{+/-}$	
14:10	5.5 ± 3.2	0.3 ± 6.1	t=0.75, df=14, p=0.5	81.6 ± 22.0	23.8 ± 38.0	t=1.3, df=14, p=0.2
10:14	12 ± 2.1	7.6 ± 5.4	t=0.75, df=14, p=0.5	93.0 ± 20.0	59.0 ± 48.8	t=0.63, df=14, p=0.5

No significant differences between groups were found. Positive values indicate that α or ρ, begin before light was off or on, respectively.

the left and right panels are representative examples for WT and Shank3$^{+/-}$. No significant differences were found in the circadian architecture of WT and Shank3$^{+/-}$ mice under different lighting conditions (**Figure 2**).

Under the long photoperiod (LD 14:10), the durations of activity (α), rest (ρ), and period under entrained conditions (τ*) for WT were (mean ± SEM in minutes, for this and subsequent photoperiods): 631 ± 9, 806 ± 9, and 1,436 ± 1, respectively, and for Shank3$^{+/-}$ were 619 ± 28, 818 ± 28, and 1,436 ± 1, respectively (**Figure 2**, top). The inter-individual period stability was lower in WT with respect to Shank3$^{+/-}$ (0.07 and 0.1, respectively).

As expected, under the short photoperiod (LD 10:14), the α, ρ, and τ for WT were (in minutes) 842 ± 19, 595 ± 19, and 1,437 ± 1, respectively; in Shank3$^{+/-}$, α, ρ, and τ were 806 ± 42, 632 ± 42, and 1,438 ± 1, respectively (**Figure 2**, center, and **Supplementary Figure 2**). Period stability under the short photoperiod decreased from 0.36 in WT to 0.13 in Shank3$^{+/-}$.

As α, ρ, and τ were not significantly different between WT and Shank3$^{+/-}$ animals, in the long (14:10) and short (10:14) photoperiods, therefore, we did not further evaluate such parameters in a regular 12:12 photoperiod.

Additional phase angles of activity (ψα) and rest (ψρ) were evaluated for the long and short photoperiods in WT and Shank3$^{+/-}$ animals. No significant differences were found in ψα and ψρ between the different groups of animals at the different photoperiods analyzed (**Table 1**).

In DD, the α, ρ, and τ for WT were, respectively 719.7 ± 36.7; 698.5 ± 37.9, and 1424 ± 3.7, while those for Shank3$^{+/-}$ were 715.6 ± 32.9, 716.9 ± 33.1, and 1421 ± 7.9, respectively (**Figure 2**,

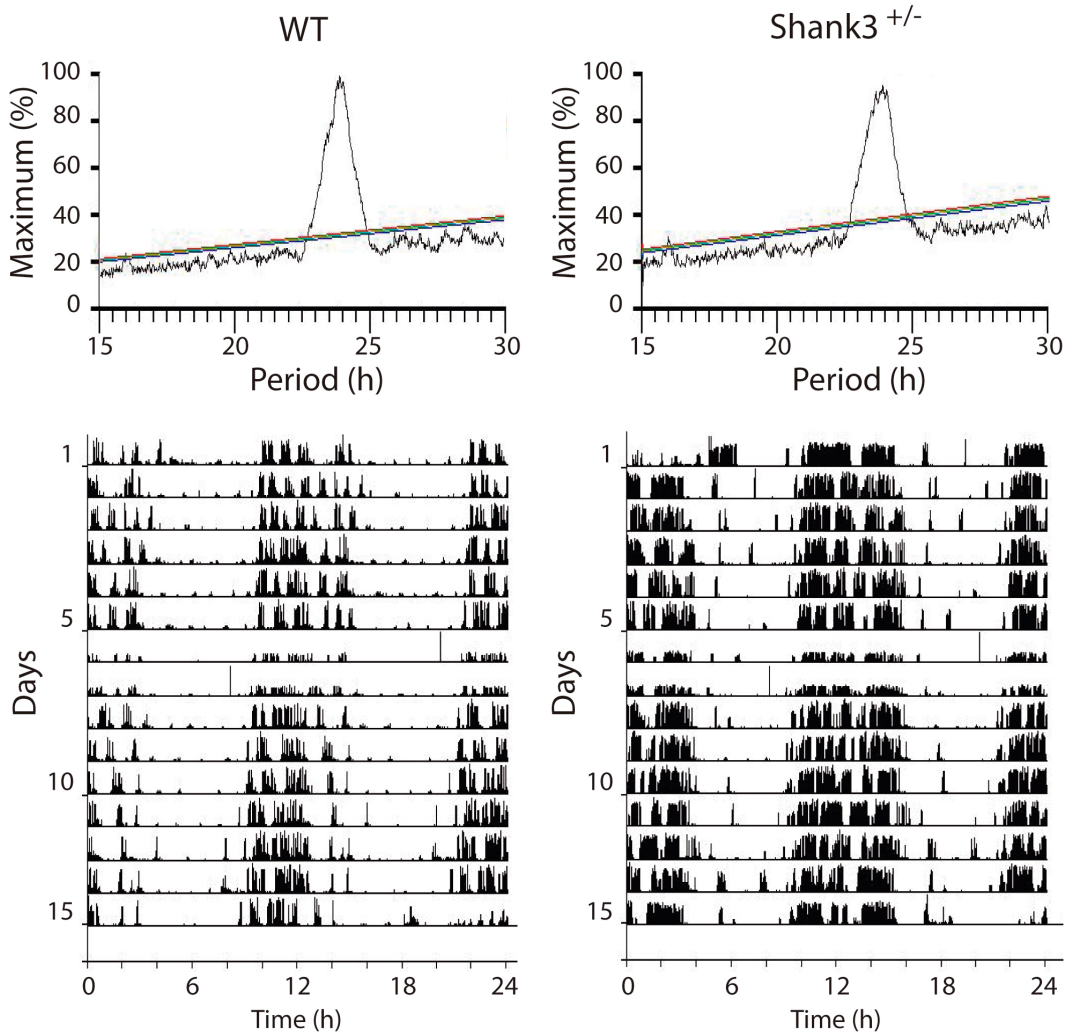

FIGURE 3 | Representative examples of the χ^2 periodograms from wild-type (WT) and Shank3$^{+/-}$ mice in DD. There were no differences between groups in the endogenous period. The actograms at the *bottom* show the data segments used to calculate the χ^2 periodogram. QP is normalized as a percentage of the maximal peak value. For **Figures 3**, **4**: *different color diagonal lines* indicate statistical significance ($p < 0.05, 0.01, 0.001$).

bottom). The period stability in DD was higher in WT with respect to Shank3$^{+/-}$ (0.005 and 0.001, respectively). The χ^2 periodogram for all days in DD showed one peak, 1,428.0 ± 6.1 and 1,438.2 ± 1.2 for each group, respectively. Representative χ^2 periodograms under DD from each group are shown in **Figure 3**.

Under LL, both groups of animals showed an initial increase in τ to 1,482.1 ± 12.0 h for WT and 1,506.2 ± 18.1 h for Shank3$^{+/-}$; after ∼6 days, an additional increase to 1,536 ± 2.4 for WT and 1,590.2 ± 48.3 for Shank3$^{+/-}$ was observed. After ∼13 days in LL, one WT (1/12, 8.3%) and all Shank3$^{+/-}$ mice (11/11, 100%) were behaviorally arrhythmic ($p < 0.0001$, Fisher's exact test) (**Supplementary Figure 3**). Overall, the χ^2 periodogram for all days recorded under LL showed that both groups showed two main peaks (τ), 1,471.8 ± 6.1 and 1,531.8 ± 7.2 for WT and 1,471.2 ± 6.6 and 1,578.1 ± 5.4 for Shank3$^{+/-}$. A statistical difference was found when we only compared the longer τ between groups ($t = 5.2$, $p = 0.0002$, unpaired t test). Additional minor peaks were found in some animals from both groups. In WT animals, a third peak was found in 50% of the cases, whereas in Shank3$^{+/-}$ mice a similar phenomenon was detected in 30% (**Figure 4**).

Under the long photoperiod, the latency (in days) to entrain to LD advances were, for WT and Shank3$^{+/-}$ (median ± minimum–maximum), 6 ± 4–8 and 8 ± 4–9, respectively (**Figure 5** and **Supplementary Figure 4**).

Remarkably, significant differences between WT and Shank3$^{+/-}$ animals were found in the PRC (**Figure 6**). Light pulses applied at CT6 either in WT (−0.1 ± 5.2 min) or Shank3$^{+/-}$ (−2.4 ± 7 min) had no effect on the phase of the rhythm [$t_{(12)} = 0.27$, $p = 0.79$, unpaired t test with Welch's correction]. At CT14, phase delays were −66 ± 14 min in WT and −109 ± 14 min in Shank3$^{+/-}$ [$t_{(29)} = 2.2$, $p = 0.035$,

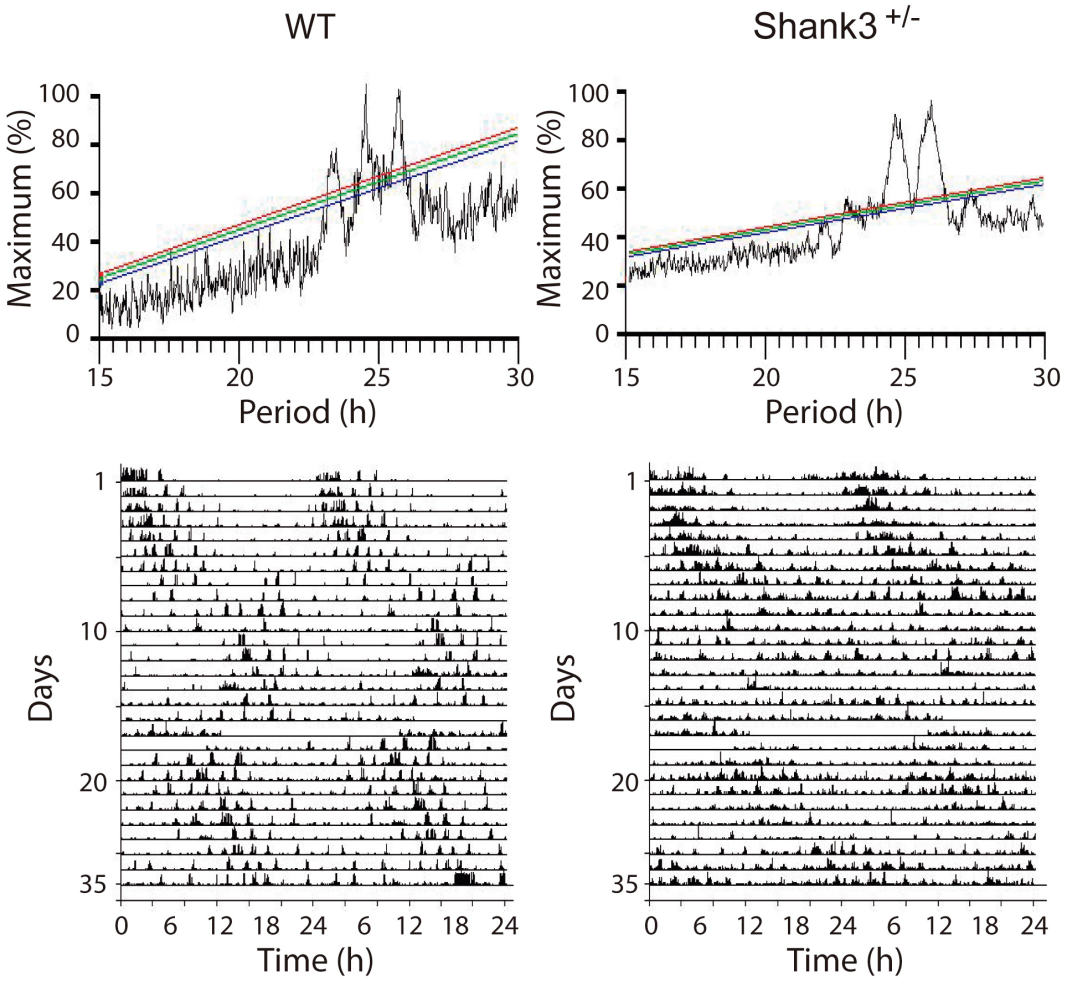

FIGURE 4 | Representative examples of the χ^2 periodograms from wild-type (WT) and Shank3$^{+/-}$ mice in LL. Constant light induces a clear disruption of the architecture of circadian rhythms in both groups characterized for showing at least two peaks in the QP values. The actograms at the *bottom* show the data segments used to calculate the χ^2 periodogram. The QP amplitude is normalized as a percentage of the maximal peak value.

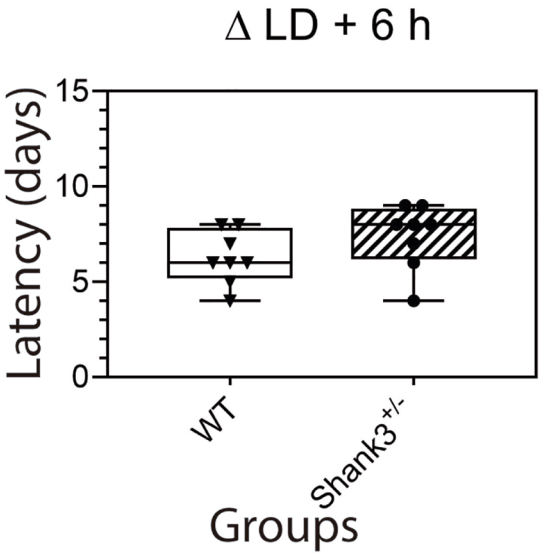

FIGURE 5 | Latency to re-entrain to LD 6-h shifts. There were no differences between groups in the number of days to re-entrain to a 6-h advance in the lights-on time. Box and whiskers (5–95 percentiles) from wild type (WT, *open box*) and Shank3$^{+/-}$ (*hatched box*). Individual data are also plotted.

unpaired *t* test with Welch's correction]. At CT22, phase advances were 23.8 ± 16 min for WT and 69 ± 11 min for Shank3$^{+/-}$ [$t_{(16)} = 2.72$, $p = 0.037$, unpaired *t* test with Welch's correction].

Histology

Figure 7 shows representative examples of immunostaining to CTB and the NMDAR2A. Our results indicated no important differences in the number of retinal axons impinging on SCN neurons using DAB (**Figure 7**, left panels) and the fluorescence expression coming from such terminals [96.8 ± 38.4 and 130.5 ± 42.7 AU × mm^2 for WT and Shank3$^{+/-}$, respectively, six animals in each group (data not shown)]. Similarly, no differences were found in the amount of SCN neurons expressing the NMDAR2A subunit (**Figure 7**, bottom left panel).

On the other hand, the expressions of c-Fos and VIP were analyzed in WT and Shank3$^{+/-}$ animals. Immunopositive SCN neurons to c-Fos were counted in WT and Shank3$^{+/-}$ animals, at two times of assessment (CT6 and CT14) and in the presence or absence of the light pulse (**Figure 8A**). Analyses performed with three-way ANOVA on the data (**Table 2**) indicated a significant interaction as a result of the CT of experimentation [$F_{(1,26)} = 13.2$, $p = 0.001$]. Also, the CT of experimentation and the genotypes of the animals showed a relevant interaction [$F_{(1,26)} = 5.8$, $p = 0.02$]. Finally, the CT of experimentation and the presence or absence of the light pulse had a significant interaction [$F_{(1,26)} = 9.8$, $p = 0.004$]. It is worth noticing that at CT6, the numbers of SCN neurons with c-Fos immunostaining were not different in both genotypes of animals with and without the light pulse (**Figure 8B**). However, at CT14, WT animals showed higher numbers of c-Fos-immunopositive neurons induced by the light pulse in comparison to the Shank3$^{+/-}$ mice that received the light pulse. The animals that did not receive the light pulse showed significantly lower numbers of ventrolateral SCN neurons in comparison to their counterparts that received the light pulse (**Figure 8C**).

Regarding VIP expression, we found higher numbers of VIP-immunopositive neurons in Shank3$^{+/-}$ animals (1,423 ± 129) in relation to WT mice [996 ± 120; $t_{(8)} = 2.4$, $p = 0.04$, unpaired *t* test] (**Figure 9**).

DISCUSSION

At the behavioral level, here, we report that Shank3$^{+/-}$ mice did not show modifications in the circadian rhythm functioning, implying no alteration in the SCN physiology, as indicated by the lack of differences between groups in the circadian architecture: the tau was unaltered in DD, the durations of alpha and rho were similar between genotypes in entrained animals to either the long or short photoperiod, the re-entrainment to shifts in the L/D cycle, and in the SKP. However, we did find differences in the response to light between groups, as indicated by the larger phase responses induced by 15-min bright light pulses, both delays and advances, and the differences in rhythm dynamics (progress to overt arrhythmic pattern) induced by constant bright light. Moreover, our histological analysis indicated changes in WT and Shank3$^{+/-}$ in c-Fos expression and in the amount of VIP-immunoreactive SCN neurons. These differences indicate alterations in light sensitivity in Shank3$^{+/-}$ mice with respect to their WT siblings.

It is worth noting that Shank3$^{+/-}$ mice did not show changes in the duration of the activity/resting phase and the period of the circadian rhythm of locomotion, in the short and long photoperiods, as well as the time taken to reach synchronization to a 6-h shift. Moreover, Shank3$^{+/-}$ mice did not present any disturbance in the above-mentioned parameters when they were under DD, which is consistent with the data reported for SHANK3$^{\Delta C}$ mice, which do not show a disruption in the circadian rhythms specifically in alpha or period length during the DD period (Ingiosi et al., 2019). Nevertheless, in that study, the authors described reduced wheel-running activity as well as differences in the architecture of sleep in SHANK3$^{\Delta C}$ animals. We think that these contrasting results in relation to our study may be due to our use of heterozygous mice instead of knockout mice. In addition, the differences can be related to the fact that the wheel-running activity is considered a self-motivated rewarding behavior (Janik and Mrosovsky, 1993; Marchant and Mistlberger, 1996; Pendergast et al., 2014) that can differ from the parameters of the circadian rhythm and its synchronization to light analyzed in the present research.

We found no evident differences between Shank3$^{+/-}$ and WT mice in the immunohistochemical staining of the RHT projections and the NMDA receptor subunit 2A in SCN neurons. However, Shank3$^{+/-}$ animals showed a decreased c-Fos photoinduction at CT14 in SCN neurons, whereas VIP-positive neurons were augmented. c-Fos expression is used to detect neuronal trans-synaptic activation (Morgan and Curran, 1991). Therefore, it is tempting to consider that a lower c-Fos

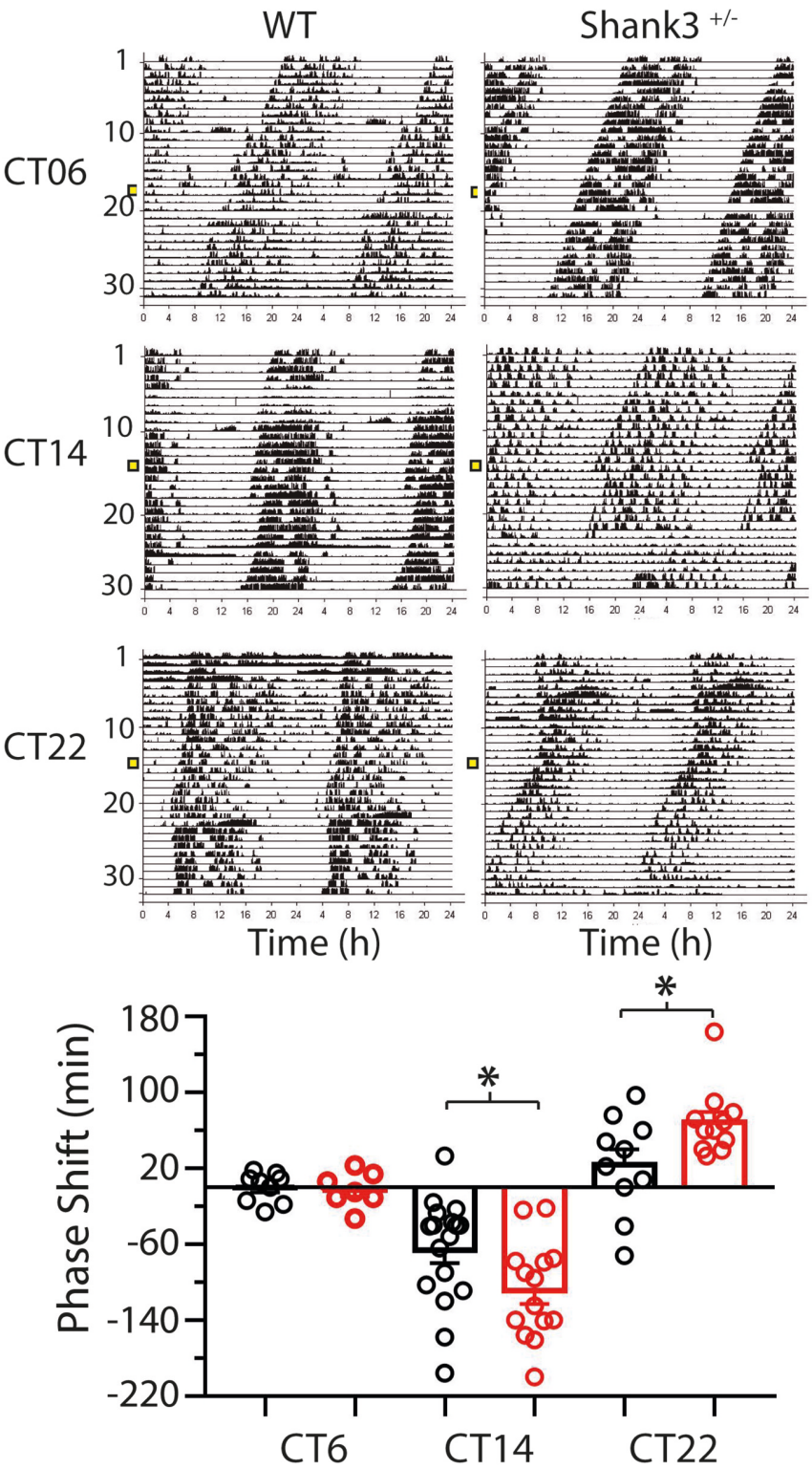

FIGURE 6 | Differences in the phase shifts at two characteristic times of the phase response curve (PRC) between wild-type (WT) and Shank3$^{+/-}$ mice. Fifteen-minute light pulses of white light (400 lx) given to mice kept in DD induce either a delay or an advance in the onset of activity depending on the time of presentation (CT14 or CT22, respectively), except at CT6 when no phase response was induced. In all cases, Shank3$^{+/-}$ (*red bars*) show larger responses than WT (*black bars*) mice. Positive values correspond to phase advances and negative values correspond to delays. Mean ± SEM in minutes are plotted. *$p < 0.05$, *t* test with Welch's correction.

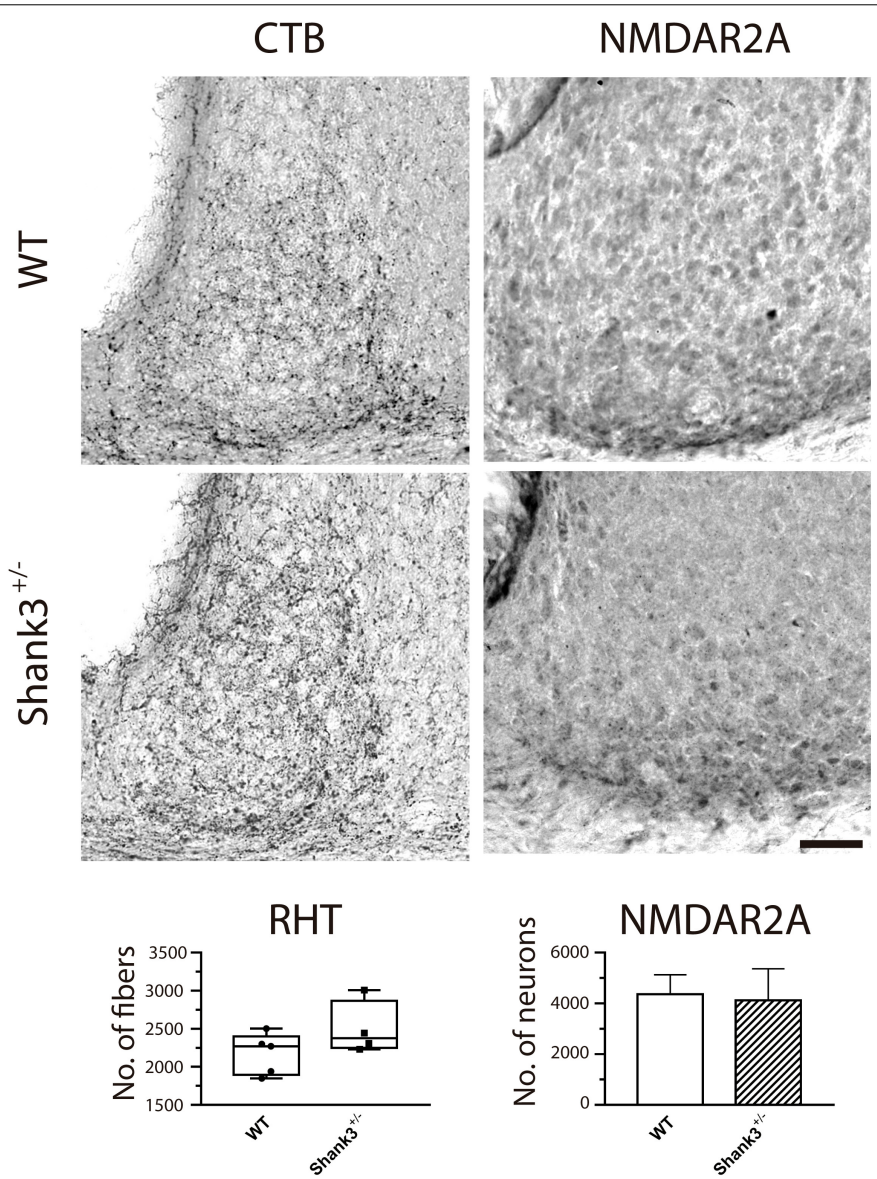

FIGURE 7 | Immunostaining for cholera toxin β-subunit (CTB) and NMDAR2A in the suprachiasmatic nucleus (SCN) from wild-type (WT) and Shank3$^{+/-}$ mice. CTB (diaminobenzidine, DAB, *left column*) and NMDAR2A (*right column*) did not show obvious differences in the immunoreactivity between groups (WT, *top micrographs*; Shank3$^{+/-}$, *bottom micrographs*). For this and subsequent figures (**Figures 8**, **9**), *scale bar* = 50 μm.

immunoreactivity in Shank3$^{+/-}$ animals after a light pulse may indicate reduced glutamatergic signaling in some point of the RHT–SCN pathway. Moreover, an increase in SCN VIP neurons, which are essential for the light-mediated resetting (Jones et al., 2018; Mazuski et al., 2018), may be the result of a compensatory mechanism.

Since SHANK3 is a scaffold protein for AMPA, NMDA, and the metabotropic glutamate receptors in the postsynaptic density (Sheng and Kim, 2000), the reduced c-Fos expression in Shank3$^{+/-}$ SCN neurons may be an expected outcome. Nevertheless, it is likely that corrective mechanisms take place in the Shank3$^{+/-}$ circadian system to maintain constant synaptic functions, such as the increase in VIP neurons in Shank3$^{+/-}$ animals. Some studies manipulating the Shank3 gene show an increase in the frequency of miniature glutamatergic events in the Schaffer collateral-CA1 in the hippocampus (Bozdagi et al., 2010). Other studies show that spine length is increased at 4 weeks of age but decreased at 10 weeks in dendrites of hippocampal CA1 neurons, but no differences in miniature inhibitory postsynaptic potentials were found (Wang et al., 2011). Still other studies show a decrease in the amplitude of miniature glutamatergic events in cortico-striatal connections (Peça et al., 2011; Zhou et al., 2016). A plausible explanation for our results is that the higher behavioral response of the Shank3$^{+/-}$ mice to brief light

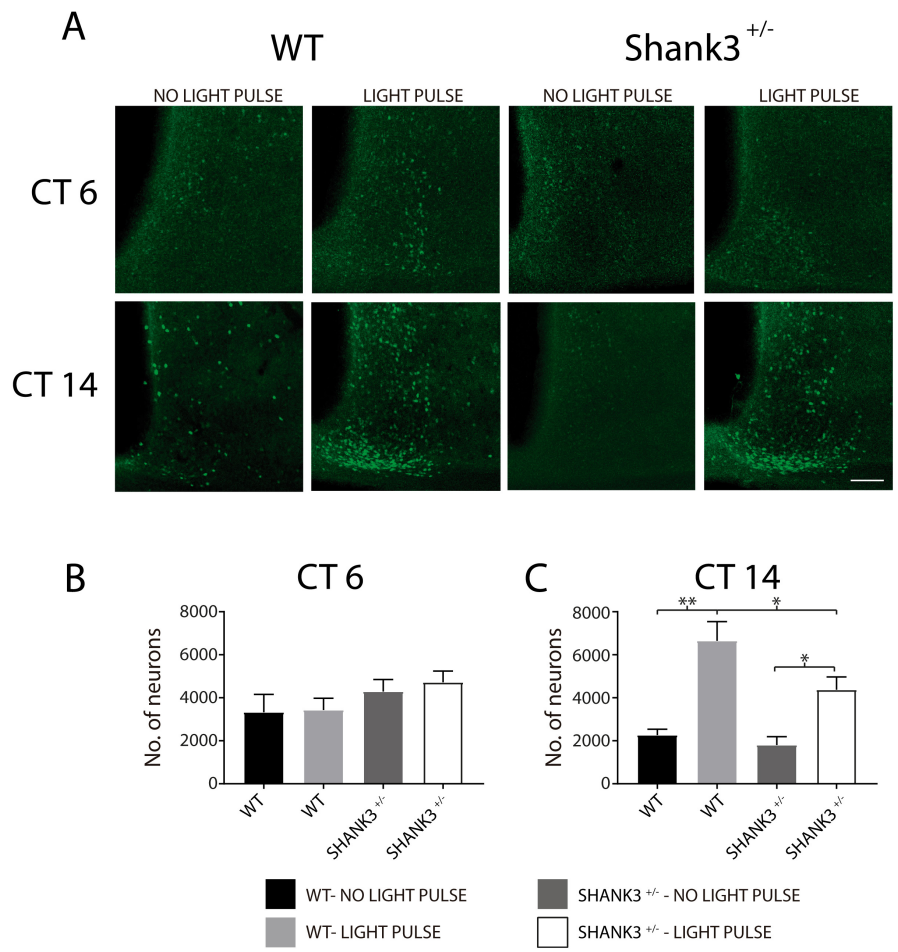

FIGURE 8 | c-Fos immunoreactivity of suprachiasmatic nucleus (SCN) neurons in wild-type (WT) and Shank3$^{+/-}$ mice. **(A)** Micrographs of c-Fos immunostaining in WT and Shank3$^{+/-}$ animals, with and without light pulse, and analyzed in two circadian times (6 and 14). Graphs depict the number of SCN neurons immunopositive to c-Fos at CT6 **(B)** and CT 14 **(C)**. For (**C**): *$p < 0.05$, **$p < 0.01$, Tukey's multiple comparisons test.

TABLE 2 | SCN neurons expressing C-Fos immunoreactivity in WT and Shank3$^{+/-}$ animals (*n*), at two CT of experimentation (CT6, CT14).

	WT-No light pulse	*n*	WT-Light pulse	*n*	Shank3$^{+/-}$ No light pulse	*n*	Shank3$^{+/-}$ Light pulse	*n*
CT6	3333 ± 827	7	3428 ± 549	4	4293 ± 557	3	4720 ± 525	3
CT14	2260 ± 278	4	6653 ± 891$^{\#}$	4	1801 ± 389*	4	4378 ± 593*	5

Tukey's multiple comparisons test: WT (#) $p < 0.01$ presence vs. absence of light pulse; Shank3+/- (*) $p < 0.05$ presence vs. absence of light pulse.

pulses in DD at CT14 and CT22 is the result of an augmented sensibility to light related to the augmented expression of VIP-positive neurons in the SCN that might have resulted from a compensatory mechanism of an impairment in the retinal communication to the SCN.

The period stability index found in WT and Shank3$^{+/-}$ mice in different photoperiods is interesting. Our results suggest that Shank3$^{+/-}$ animals had more stable periods in long photoperiods (14:10), whereas this situation was reversed in short photoperiods (10:14). However, it is worth noting that the stability found in Shank3$^{+/-}$ mice is quite similar in both photoperiods (0.1 and 0.13, long and short, respectively), but in WT animals, the short photoperiod shows higher variability (0.07 and 0.36, long and short photoperiods, respectively). Perhaps the higher stability found in the periods of Shank3$^{+/-}$ mice, along different photoperiods, is a result of a greater responsivity to light, which may be related to the result that Shank3$^{+/-}$ mice showed an increased response to light in the PRC.

It should be mentioned that even though the constant dim red light (CDRL) exposition is a broadly used experimental approach to solve maintenance and experimental procedures, it is not a perfect equivalent alternative to complete darkness; given

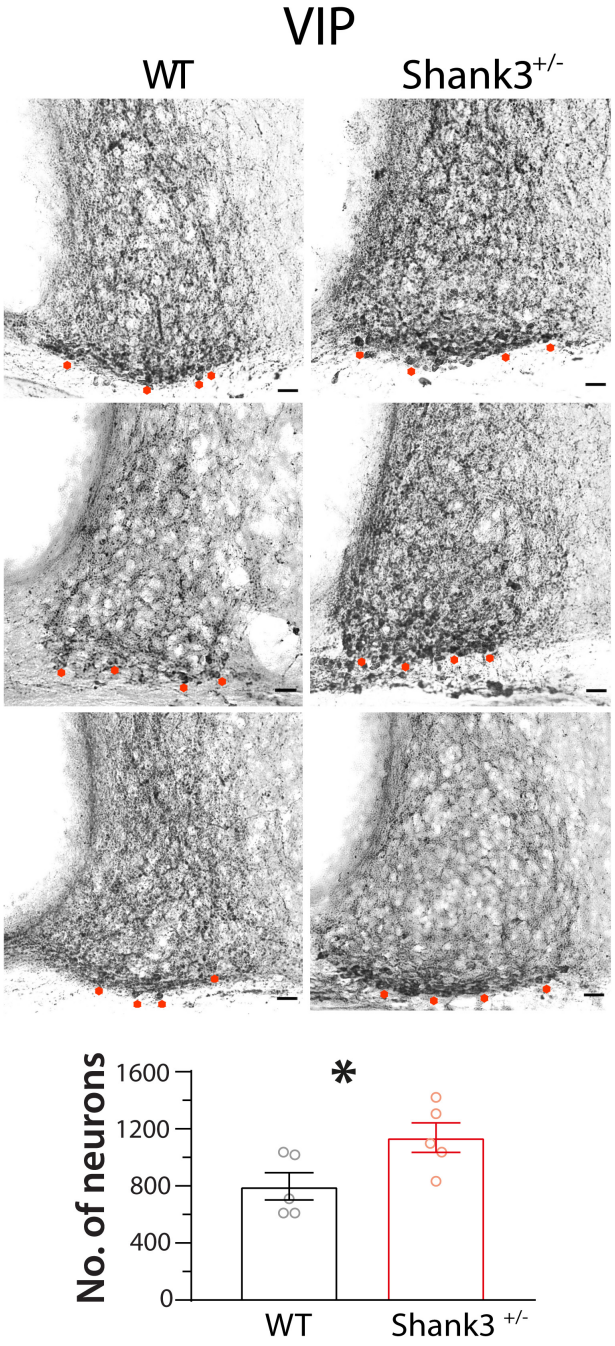

FIGURE 9 | Vasoactive intestinal polypeptide (VIP) immunostaining in suprachiasmatic nucleus (SCN) neurons of wild-type (WT) and Shank3$^{+/-}$ mice. Shank3$^{+/-}$ animals (*right column*) showed higher numbers of VIP-immunopositive SCN neurons than WT mice (*left column*, five animals in each group). *Asterisks* indicate SCN neurons immunopositive to VIP. *$p < 0.05$, unpaired *t* test.

that, CDRL has physiological effects on the circadian rhythms in comparison to DD (Gonzalez, 2018). However, we consider unlikely that the exposure of Shank3$^{+/-}$ mice to CDRL instead of DD can hide modifications in circadian rhythms because both groups of animals were exposed to similar light environmental conditions in concurrent times.

The increased light sensitivity in Shank3$^{+/-}$ could also be related to the increased latency of the pupillary light reflex reported in children with ASD and in the Shank3 macaque (Daluwatte et al., 2013; Zhou et al., 2019). Furthermore, several lines of evidence indicate high levels of glutamate in serum and brain structures (using proton magnetic resonance spectroscopy) in children diagnosed with autism (Rojas, 2014). The decreased c-Fos photoinduction at CT14 found in Shank3$^{+/-}$ SCN neurons is contradictory to the overreaction of Shank3$^{+/-}$ mice to the light pulse in the PRC, which may indicate that c-Fos photoinduction is not directly related to the direction (either advance or delay) of the behavioral phase shifts. This could be related also to the common sleep problems shown by children with this developmental pathology (Wiggs and Stores, 2004; Bro et al., 2017; Veatch et al., 2017), which consist of long sleep latencies and delayed or advanced sleep onset or offset. It is likely that a small amount of light is sufficient to synchronize children with autism to a new schedule, whereas a similar amount of light is impotent to synchronize a regular person.

A caveat of the present research is that we did not explore sex differences in this research. Autism spectrum disorder has a higher prevalence in males than females in a magnitude of 2:1–3:1 (Halladay et al., 2015). Moreover, it is likely that the existence of a sexual dimorphism in the circadian rhythms of autism models, such as the Shank3$^{+/-}$ mice, awaits being addressed.

CONCLUSION

In conclusion, Shank3$^{+/-}$ mice showed a higher response in the PRC than their wild-type littermates. However, no changes were evident in the general architecture of the circadian rhythms. Histological analyses indicated a decrease in c-Fos photoinduction in Shank3$^{+/-}$ SCN neurons at CT14, whereas augmented VIP-positive neurons were found in such animals. In this regard, we hypothesize that the circadian system of Shank3$^{+/-}$ mice compensates the impairment of the RHT–SCN communication with an overexpression of VIP SCN neurons, which may result in larger phase shifts induced by light. More research is necessary to understand the cellular processes that affect synchronization in Shank3$^{+/-}$ animals, which may shed light on the problems related to circadian rhythm in patients diagnosed with this developmental pathology.

DATA AVAILABILITY STATEMENT

The raw data supporting the conclusions of this article will be made available by the authors, without undue reservation.

ETHICS STATEMENT

The animal study was reviewed and approved by Internal ethical committee from the Instituto de Fisiología Celular de la Universidad Nacional Autónoma de México (authorization

CICUAL RA-58-15) in accordance to the guidelines on the use of animals from the Society for Neuroscience.

AUTHOR CONTRIBUTIONS

JA, YR-C, and RA-R contributed to generate the hypothesis, provide animals and materials, design the study, analyze the data, and wrote the manuscript. AM-L, J-LC, DR, and VF conducted the experiments and analyze the data. All authors contributed to the article and approved the submitted version.

FUNDING

RA-R is supported by grants IN205917 and IN205720 from Programa de Apoyo a Proyectos de Investigación e Inovación Tecnológica/UNAM and YR-C by grant IN207429 from Programa de Apoyo a Proyectos de Investigación e Inovación Tecnológica/UNAM and grant 254878 from Consejo Nacional de Ciencia y Tecnología, Mexico.

ACKNOWLEDGMENTS

We thank the skillful technical assistance of Karina Galindo, Ana Escalante, and Francisco Pérez.

SUPPLEMENTARY MATERIAL

The Supplementary Material for this article can be found online at: https://www.frontiersin.org/articles/10.3389/fnins.2021.604165/full#supplementary-material

REFERENCES

Abrahamson, E. E., and Moore, R. Y. (2001). Suprachiasmatic nucleus in the mouse: retinal innervation, intrinsic organization and efferent projections. *Brain Research*. 916, 172–191. doi: 10.1016/s0006-8993(01)02890-6

Atkin, G., Moore, S., Lu, Y., Nelson, R. F., Tipper, N., Rajpal, G., et al. (2015). Loss of F-box only protein 2 (Fbxo2) disrupts levels and localization of select NMDA receptor subunits, and promotes aberrant synaptic connectivity. *J. Neurosci.* 35, 6165–6178. doi: 10.1523/jneurosci.3013-14.2015

Baum, S. H., Stevenson, R. A., and Wallace, M. T. (2015). Behavioral, perceptual, and neural alterations in sensory and multisensory function in autism spectrum disorder. *Prog.ress in Neurobiology.* 134, 140–160. doi: 10.1016/j.pneurobio.2015.09.007

Bourgeron, T. (2015). From the genetic architecture to synaptic plasticity in autism spectrum disorder. *Nat.ure Rev.iews Neuroscience.* 16:, 551. doi: 10.1038/nrn3992

Bozdagi, O., Sakurai, T., Papapetrou, D., Wang, X., Dickstein, D. L., Takahashi, N., et al. (2010). Haploinsufficiency of the autism-associated Shank3 gene leads to deficits in synaptic function, social interaction, and social communication. *Mol. Autism.* 1:, 15. doi: 10.1186/2040-2392-1-15

Bro, D., O'Hara, R., Primeau, M., Hanson-Kahn, A., Hallmayer, J., and Bernstein, J. A. (2017). Sleep disturbances in individuals with Phelan-McDermid syndrome: correlation with caregivers' sleep quality and daytime functioning. *Sleep.* 40:, zsw062.

Carbonetto, S. (2014). A blueprint for research on Shankopathies: a view from research on autism spectrum disorder. *Dev.elopmental Neurobiology.* 74, 85–112. doi: 10.1002/dneu.22150

Colwell, C. S., and Menaker, M. (1992). Nmda as well as Non-Nmda receptor antagonists can prevent the phase-shifting effects of light on the circadian system of the golden-hamster. *J.ournal of Biol.ogical Rhythms.* 7, 125–136. doi: 10.1177/074873049200700204

Daluwatte, C., Miles, J. H., Christ, S. E., Beversdorf, D. Q., Takahashi, T. N., and Yao, G. (2013). Atypical pupillary light reflex and heart rate variability in children with autism spectrum disorder. *J. Autism. Dev. Disord.* 43, 1910–1925. doi: 10.1007/s10803-012-1741-3

Ding, J., Chen, D., Weber, E., Faiman, L., Rea, M., and Gillette, M. (1994). Resetting the biological clock: mediation of nocturnal circadian shifts by glutamate and NO. *Science.* 266, 1713–1717. doi: 10.1126/science.7527589

Ding, J. M., Faiman, L. E., Hurst, W. J., Kuriashkina, L. R., and Gillette, M. U. (1997). Resetting the biological clock: mediation of nocturnal CREB phosphorylation via light, glutamate, and Nitric Oxide. *The J.ournal of Neuroscience.* 17, 667–675. doi: 10.1523/jneurosci.17-02-00667.1997

Gonzalez, M. M. C. (2018). Dim light at night and constant darkness: two frequently used lighting conditions that jeopardize the health and well-being of laboratory rodents. *Front. Neurol.* 9:609.

Halladay, A. K., Bishop, S., Constantino, J. N., Daniels, A. M., Koenig, K., Palmer, K., et al. (2015). Sex and gender differences in autism spectrum disorder: summarizing evidence gaps and identifying emerging areas of priority. *Mol. Autism.* 6:, 36.

Hankins, M. W., Peirson, S. N., and Foster, R. G. (2008). Melanopsin: an exciting photopigment. *Trends in Neurosciences.* 31, 27–36. doi: 10.1016/j.tins.2007.11.002

Hannibal, J. (2002). Neurotransmitters of the retino-hypothalamic tract. *Cell Tissue Res.* 309, 73–88. doi: 10.1007/s00441-002-0574-3

Hannibal, J. (2006). Roles of PACAP-containing retinal ganglion cells in circadian timing. *Int. Rev. Cytol.* 251, 1–39. doi: 10.1016/s0074-7696(06)51001-0

Hattar, S., Lucas, R. J., Mrosovsky, N., Thompson, S., Douglas, R. H., Hankins, M. W., et al. (2003). Melanopsin and rod-cone photoreceptive systems account for all major accessory visual functions in mice. *Nature.* 424, 76–81.

Ingiosi, A. M., Schoch, H., Wintler, T., Singletary, K. G., Righelli, D., Roser, L. G., et al. (2019). Shank3 modulates sleep and expression of circadian transcription factors. *Elife.* 8:, e42819.

Janik, D., and Mrosovsky, N. (1993). Nonphotically induced phase shifts of circadian rhythms in the golden hamster: activity-response curves at different ambient temperatures. *Physiol. Behav.* 53, 431–436. doi: 10.1016/0031-9384(93)90135-3

Jones, J. R., Simon, T., Lones, L., and Herzog, E. D. (2018). SCN VIP neurons are essential for normal light-mediated resetting of the circadian system. *J. Neurosci.* 38, 7986–7995. doi: 10.1523/jneurosci.1322-18.2018

Kim, Y. I., and Dudek, F. E. (1991). Intracellular electrophysiological study of suprachiasmatic nucleus neurons in rodents: excitatory synaptic mechanisms. *The J.ournal of Physiology.* 444, 269–287. doi: 10.1113/jphysiol.1991.sp018877

Klintwall, L., Holm, A., Eriksson, M., Carlsson, L. H., Olsson, M. B., Hedvall, A., et al. (2011). Sensory abnormalities in autism. A brief report. *Res.earch in Dev.elopmental Disabilities.* 32, 795–800.

Li, H. Q., and Spitzer, N. C. (2020). Exercise enhances motor skill learning by neurotransmitter switching in the adult midbrain. *Nat. Commun.* 11:2195.

Lim, S., Naisbitt, S., Yoon, J., Hwang, J.-I., Suh, P.-G., Sheng, M., et al. (1999). Characterization of the shank family of synaptic proteins: multiple genes, alternative splicing, and differential expression in brain and development. *J.ournal of Biol.ogical Chemistry.* 274, 29510–29518. doi: 10.1074/jbc.274.41.29510

Marchant, E. G., and Mistlberger, R. E. (1996). Entrainment and phase shifting of circadian rhythms in mice by forced treadmill running. *Physiol. Behav.* 60, 657–663. doi: 10.1016/s0031-9384(96)80045-x

Marcheva, B., Ramsey, K. M., Peek, C. B., Affinati, A., Maury, E., and Bass, J. (2013). "Circadian clocks and metabolism," in *Circadian Clocks*, eds A. Kramer and M. Merrow (Berlin: Springer Berlin Heidelberg), 127–155. doi: 10.1007/978-3-642-25950-0_6

Mazuski, C., Abel, J. H., Chen, S. P., Hermanstyne, T. O., Jones, J. R., Simon, T., et al. (2018). Entrainment of circadian rhythms depends on firing rates and neuropeptide release of VIP SCN Neurons. *Neuron* 99, 555–563e5.

Mercado, C., Diaz-Munoz, M., Alamilla, J., Valderrama, K., Morales-Tlalpan, V., and Aguilar-Roblero, R. (2009). Ryanodine-sensitive intracellular Ca2+ channels in rat suprachiasmatic nuclei are required for circadian clock control of behavior. *J.ournal of Biol.ogical Rhythms.* 24, 203–210. doi: 10.1177/0748730409333354

Monteiro, P., and Feng, G. (2017). SHANK proteins: roles at the synapse and in autism spectrum disorder. *Nat.ure Rev.iews Neuroscience.* 18:, 147. doi: 10.1038/nrn.2016.183

Moore, R. Y., and Lenn, N. J. (1972). A retinohypothalamic projection in the rat. *J. Comp. Neurol.* 146, 1–14. doi: 10.1002/cne.901460102

Morgan, J. I., and Curran, T. (1991). Stimulus-Transcription coupling in the nervous system: involvement of the inducible proto-oncogenes fos and jun. *Ann.ual Rev.iew of Neuroscience.* 14, 421–451. doi: 10.1146/annurev.ne.14.030191.002225

Mouton, P. (2011). *Unbiased Stereology: A Concise Guide*. Baltimore: Johns Hopkins University Press.

Patton, A. P., Edwards, M. D., Smyllie, N. J., Hamnett, R., Chesham, J. E., Brancaccio, M., et al. (2020). The VIP-VPAC2 neuropeptidergic axis is a cellular pacemaking hub of the suprachiasmatic nucleus circadian circuit. *Nat. Commun.* 11:, 3394.

Peça, J., Feliciano, C., Ting, J. T., Wang, W., Wells, M. F., Venkatraman, T. N., et al. (2011). Shank3 mutant mice display autistic-like behaviours and striatal dysfunction. *Nature.* 472:, 437. doi: 10.1038/nature09965

Pendergast, J. S., Branecky, K. L., Huang, R., Niswender, K. D., and Yamazaki, S. (2014). Wheel-running activity modulates circadian organization and the daily rhythm of eating behavior. *Front. Psychol.* 5:177.

Phelan, K., and McDermid, H. E. (2012). The 22q13.3 deletion syndrome (Phelan-McDermid Syndrome). *Mol. Syndromol.* 2, 186–201.

Pittendrigh, C. S., and Daan, S. (1976). A functional analysis of circadian pacemakers in nocturnal rodents. *J. Comp. Physiol.* 106, 291–331. doi: 10.1007/bf01417859

Robertson, C. E., and Baron-Cohen, S. (2017). Sensory perception in autism. *Nat.ure Rev.iews Neuroscience.* 18, 671–684. doi: 10.1038/nrn.2017.112

Rojas, D. C. (2014). The role of glutamate and its receptors in autism and the use of glutamate receptor antagonists in treatment. *J.ournal of Neural Transmission.* 121, 891–905. doi: 10.1007/s00702-014-1216-0

Sarowar, T., Chhabra, R., Vilella, A., Boeckers, T. M., Zoli, M., and Grabrucker, A. M. (2016). Activity and circadian rhythm influence synaptic Shank3 protein levels in mice. *J.ournal of Neurochemistry.* 138, 887–895. doi: 10.1111/jnc.13709

Schroeder, J. C., Reim, D., Boeckers, T. M., and Schmeisser, M. J. (2017). "Genetic animal models for autism spectrum disorder," in *Social Behavior from Rodents to Humans: Neural Foundations and Clinical Implications*, eds M. Wöhr and S. Krach (Cham: Springer International Publishing), 311–324.

Schwartz, W., and Zimmerman, P. (1990). Circadian timekeeping in BALB/c and C57BL/6 inbred mouse strains. *J. Neurosci.* 10, 3685–3694. doi: 10.1523/jneurosci.10-11-03685.1990

Sheng, M., and Kim, E. (2000). The Shank family of scaffold proteins. *J. Cell Sci.* 113(Pt 11), 1851–1856.

Veatch, O. J., Sutcliffe, J. S., Warren, Z. E., Keenan, B. T., Potter, M. H., and Malow, B. A. (2017). Shorter sleep duration is associated with social impairment and comorbidities in ASD. *Autism. Res.* 10, 1221–1238. doi: 10.1002/aur.1765

Wang, X., McCoy, P. A., Rodriguiz, R. M., Pan, Y., Je, H. S., Roberts, A. C., et al. (2011). Synaptic dysfunction and abnormal behaviors in mice lacking major isoforms of Shank3. *Hum.an Mol.ecular Genetics.* 20, 3093–3108. doi: 10.1093/hmg/ddr212

Wiggs, L., and Stores, G. (2004). Sleep patterns and sleep disorders in children with autistic spectrum disorders: insights using parent report and actigraphy. *Dev.elopmental Med.icine And Child Neurology.* 46, 372–380. doi: 10.1017/s0012162204000611

World Health Organization (2013). *Meeting Report: Autism Spectrum Disorders and Other Developmental Disorders: From Raising Awareness to Building Capacity: World Health Organization, Geneva, Switzerland 16–18 September 2013*. Geneva: World Health Organization, 36.

Zhao, W. J., Sun, Q. J., Guo, R. C., and Pilowsky, P. M. (2015). Catecholamine inputs to expiratory laryngeal motoneurons in rats. *J. Comp. Neurol.* 523, 381–390. doi: 10.1002/cne.23677

Zhou, Y., Kaiser, T., Monteiro, P., Zhang, X., Van der Goes, M. S., Wang, D., et al. (2016). Mice with Shank3 mutations associated with ASD and schizophrenia display both shared and distinct defects. *Neuron.* 89, 147–162. doi: 10.1016/j.neuron.2015.11.023

Zhou, Y., Sharma, J., Ke, Q., Landman, R., Yuan, J., Chen, H., et al. (2019). Atypical behaviour and connectivity in SHANK3-mutant macaques. *Nature.* 570, 326–331. doi: 10.1038/s41586-019-1278-0

Zoghbi, H. Y., and Bear, M. F. (2012). Synaptic dysfunction in neurodevelopmental disorders associated with autism and intellectual disabilities. *Cold Spring Harb.or Perspect.ives in Biology.* 4:a009886. doi: 10.1101/cshperspect.a009886

Conflict of Interest: The authors declare that the research was conducted in the absence of any commercial or financial relationships that could be construed as a potential conflict of interest.

frontiers in Neuroscience

MINI REVIEW
published: 17 March 2021
doi: 10.3389/fnins.2021.636764

Food Entrainment, Arousal, and Motivation in the Neonatal Rabbit Pup

Mario Caba[1], Michael N. Lehman[2] and Mario Daniel Caba-Flores[3]*

[1] Centro de Investigaciones Biomédicas, Universidad Veracruzana, Xalapa, Mexico, [2] Brain Health Research Institute, Kent State University, Kent, OH, United States, [3] Doctorado en Ciencias Biomédicas, CIB, Universidad Veracruzana, Xalapa, Mexico

In the newborn rabbit, the light entrainable circadian system is immature and once a day nursing provides the primary timing cue for entrainment. In advance of the mother's arrival, pups display food anticipatory activity (FAA), and metabolic and physiological parameters are synchronized to this daily event. Central structures in the brain are also entrained as indicated by expression of Fos and Per1 proteins, GFAP, a glial marker, and cytochrome oxidase activity. Under fasting conditions, several of these rhythmic parameters persist in the periphery and brain, including rhythms in the olfactory bulb (OB). Here we provide an overview of these physiological and neurobiological changes and focus on three issues, just beginning to be examined in the rabbit. First, we review evidence supporting roles for the organum vasculosum of lamina terminalis (OVLT) and median preoptic nucleus (MnPO) in homeostasis of fluid ingestion and the neural basis of arousal, the latter which also includes the role of the orexigenic system. Second, since FAA in association with the daily visit of the mother is an example of conditioned learning, we review evidence for changes in the corticolimbic system and identified nuclei in the amygdala and extended amygdala as part of the neural substrate responsible for FAA. Third, we review recent evidence supporting the role of oxytocinergic cells of the paraventricular hypothalamic nucleus (PVN) as a link to the autonomic system that underlies physiological events, which occur in preparation for the upcoming next daily meal. We conclude that the rabbit model has contributed to an overall understanding of food entrainment.

Keywords: food entrainment, paraventricular nucleus, oxytocin, corticosterone, sympathetic system, parasympathetic system, reward, median preoptic nucleus

OPEN ACCESS

Edited by:
Jihwan Myung,
Taipei Medical University, Taiwan

Reviewed by:
Danica Patton,
Kwantlen Polytechnic University, Canada
Andrew Steele,
California State Polytechnic University, Pomona, United States
Alfonso Abizaid,
Carleton University, Canada

****Correspondence:***
Mario Caba
mcaba@uv.mx

Specialty section:
This article was submitted to Sleep and Circadian Rhythms, a section of the journal Frontiers in Neuroscience

Received: *02 December 2020*
Accepted: *01 March 2021*
Published: *17 March 2021*

Citation:
Caba M, Lehman MN and Caba-Flores MD (2021) Food Entrainment, Arousal, and Motivation in the Neonatal Rabbit Pup. Front. Neurosci. 15:636764. doi: 10.3389/fnins.2021.636764

INTRODUCTION

Mammals usually forage and consume food during their period of activity, which is controlled by the biological clock in the brain, the suprachiasmatic nucleus (SCN), with light serving as their main entraining signal (Finger et al., 2020). Thus, nocturnal rodents rest during the day but at evening increase their locomotor activity. However, when food is withheld and provided for a short period at a fixed time during the day, the normal activity pattern of animals shift from that controlled by the SCN and animals show now intense locomotor behavior, termed food anticipatory activity (FAA; Mistlberger, 1994) before food availability. In addition, a number of other physiological and

neural parameters also are entrained. Early studies proposed that this phenomenon was controlled by an oscillatory system entrained by food, named the food-entrainable oscillator (Stephan, 2002). Now there is general agreement that FAA is controlled by a diffuse system of central and peripheral structures (Mistlberger, 2020) but the precise mechanism of their action it is not well understood. In contrast, rabbit pups in nature eat once a day for a few minutes. They have been recognized as a model of FAA, and offer an opportunity to study food entrainment with little manipulation. Here we first review what is known about the SCN in rabbit pups, including its responsiveness to light, as well as review evidence about peripheral parameters and central structures that are entrained by periodic food ingestion. Then we focus on three aspects of food entrainment that have been relatively unexplored in the rabbit. First, we focus on forebrain areas activated during arousal at the time of FAA, considering evidence supporting a role of the median preoptic nucleus (MnPO) in neural control of FAA and related peripheral events. Second, since periodic food ingestion implicates a conditioning process we also propose a neural substrate of motivational conditioning underlying FAA. Third, finally we address recent evidence in the rabbit pup regarding a population of oxytocinergic cells in the brain that may play a central role in coordinating mechanisms between central and peripheral structures in FAA. Finally, we compare results in the rabbit with those seen in other species and consider the usefulness of the rabbit pup for the study of food entrainment in an evolutionary context.

IMMATURE LIGHT ENTRAINABLE OSCILLATOR

Altricial mammals, such as the hamster and the rat, at postnatal day 1 (PD1) possess few or no retinal projections from the retinohypothalamic tract to the SCN (Speh and Moore, 1993). The rabbit pup is also altricial and spends all its time in a dark nest without receiving light. Tract tracing studies using Cholera toxin B subunit, revealed that, contrary to rodents, the SCN of the rabbit at PD1 receives a dense innervation of retinal projections with a predominantly contralateral pattern throughout the entire SCN (Juárez et al., 2013). A light pulse induces robust expression of the protein FOS, a marker of neural activity, in the SCN of the rabbit pup at PD1 although the adult pattern is not reached until PD19, after opening of the eyelids (Juárez et al., 2013). However, in this period before reaching the adult capacity to be entrained by light the neonatal rabbit exhibits a remarkable characteristic, it presents robust entrainment periodic to food.

FOOD, A STRONG SYNCHRONIZER OF LOCOMOTOR BEHAVIOR

Rabbit pups are alone in the nest in darkness and spend most part of the time huddled with little movement (Jilge, 1993), which helps to maintain their core body temperature (Bautista et al., 2008). In nature (Lloyd and McCowan, 1968) and in laboratory conditions, the mother nurses her pups with circadian periodicity and pups show a sharp increase in locomotor behavior at around 3 h before daily suckling of milk (Caba and González-Mariscal, 2009; González-Mariscal et al., 2016). Nursing lasts around 5 min and immediately after locomotor behavior sharply decreases and thereafter pups exhibit low activity until expectancy of next nursing bout (Jilge, 1993, 1995; González-Mariscal et al., 2016). This behavioral pattern persists when pups remain un-nursed for 48 h and is evident starting around postnatal day 2 (Caba et al., 2008; Trejo-Muñoz et al., 2012).

PHYSIOLOGICAL, METABOLIC, AND HORMONAL PARAMETERS ASSOCIATED WITH FAA

Core body temperature increases 2–3 h prior to nursing which persists in un-nursed pups (Jilge et al., 2000; Trejo-Muñoz et al., 2012). Upon nursing stomach weight sharply increases and induces a sequential use of fuels, first glucose, then liver glycogen and finally free fatty acids in fasted subjects (Escobar et al., 2000; Morgado et al., 2008, 2010). We explored the patterns of the secretion of corticosterone (CORT) and ghrelin under these conditions. In contrast to rat pups (Levine, 2002), rabbit pups show a CORT rhythm entrained by nursing, which persist in un-nursed pups (Rovirosa et al., 2005; Morgado et al., 2008, 2010). With respect to ghrelin, 12 h after milk ingestion there is a sharp increase, which coincides with the emptying of most parts of the stomach (Morgado et al., 2008, 2010). This is interesting as ghrelin increases before meal ingestion in several species when subjects start to be hungry (Williams and Cummings, 2005); in addition, there is a premeal activation of ghrelin in oxyntic cells (LeSauter et al., 2009). However, ghrelin by itself it is not necessary for FAA in mice (Gunapala et al., 2011).

RHYTHMS IN OLFACTORY BULB AND OTHER BRAIN STRUCTURES ASSOCIATED WITH FAA

The behavioral response of rabbit pups to the nipple's mammary pheromone (2-methyl-but-2-enal; 2MB2) is highest during FAA (Schaal et al., 2003; Coureaud et al., 2004; Montigny et al., 2006), which suggests that changes also occur in the olfactory bulb (OB). Indeed, expression of FOS, by immunocytochemistry, used as neural marker of activity, shows rhythms entrained by the time of suckling of milk (Nolasco et al., 2012). At this time both Fos and cytochrome oxidase activity, a marker of metabolic activity (Wong-Riley, 1989), are highest and persist in fasted subjects (Nolasco et al., 2012; Olivo et al., 2014). Also Per1, an indicator of circadian oscillation, shows robust rhythms in the OB, entrained by nursing (Nolasco et al., 2012; Montúfar-Chaveznava et al., 2013). In addition, astrocytes in the OB also show daily changes in the length of radial processes and in expression of glial fibrillary acidic protein, which are

associated to nursing time (Vázquez et al., 2020). It is necessary to explore the role of glia in the circadian rhythmicity in the OB. In contrast the SCN at this age is immature (Montúfar-Chaveznava et al., 2013). This suggests that the OB may be of major importance for the entrainment to daily nursing, and is also supported by evidence that the OB in adult rodents displays daily changes in sensitivity to odors (Amir et al., 1999; Granados-Fuentes et al., 2006), can be entrained by daily meals (Caba et al., 2014), and contains a circadian clock independent of the SCN (Granados-Fuentes et al., 2006). However, while bilateral destruction of the OB in the rabbit disrupts FAA (Navarrete et al., 2016) it has no or little effect on FAA in adult rats (Davidson et al., 2001).

Other brain areas have also been implicated in FAA in the rabbit pup. Similar to the OB, the dorsomedial hypothalamic nucleus (Caba et al., 2008) and the parabrachial nucleus (Juárez et al., 2012) are entrained, as indicated by PER1, reaching a peak 4–8 h after nursing, and their oscillations persist during fasting. In contrast the dorsal vagal complex (Juárez et al., 2012) only express FOS after nursing. Taken together, these results suggest that rabbit pups depend on multiple brain structures to entrain to daily food intake.

ROLE OF THE ORGANUM VASCULOSUM OF LAMINA TERMINALIS, THIRST AND AROUSAL

Rabbit pups ingest a large volume of milk at the time of suckling and do not drink additional fluids for the remaining 24 h. To better understand this continuous cycle of fluid balance in the brain we explored the role of the organum vasculosum of lamina terminalis (OVLT). This organ contains osmoreceptors and their destruction together with the adjacent MNPO significantly disrupts thirst and fluid balance (Johnson and Buggy, 1978; McKinley et al., 1999). In the rabbit pup, we saw a marked increase of FOS protein expression in the OVLT at 4 h before nursing (**Figure 1**) likely reflecting a signal of thirst. In support of this, pharmacological induction of thirst in rats produces a large increase of Fos in the OVLT (Thunhorst et al., 1998). Additionally, we also observed a large postprandial increase of Fos protein, which is consistent with the large volume of milk ingested (**Figure 1**), and 8 h. After nursing Fos reaches its lowest levels (**Figure 1**; Moreno et al., 2013) and stomach weight steadily decreases. At the time of next FAA, the stomach is almost empty (Morgado et al., 2008, 2010) and Fos increases again in the OVLT. In contrast, under fasting conditions, Fos levels remain high at all times (Moreno et al., 2013). In a further study we examined Per1 protein and found a clear rhythm with a peak 8 h after nursing indicating that this rhythm was entrained by this event; as in the case of Fos, no rhythm was observed in fasted pups (**Figure 1**). Overall, we conclude that the OVLT actively participates in the osmoregulatory control of milk ingestion and perhaps its activation before nursing contributes to the expression of FAA though connections with other brain areas, particularly the MnPO where thirst signals are integrated and in the cerebral cortex induce drinking behavior (McKinley et al., 2015).

MEDIAL PREOPTIC AREA AND CORE BODY TEMPERATURE

At the time of FAA, the core body temperature of rabbit pups also increases. Neurons in the preoptic area (POA) receive ascending peripheral thermosensory signals that are integrated in this nucleus and *via* projections then regulate the dorsomedial hypothalamic nucleus to promote thermogenesis (Morrison, 2016). In the rabbit we found an increase of Fos protein in the POA at the time of nursing coinciding with the increase in core body temperature at the same time. Lower values were found at other time points of the cycle (Moreno et al., 2013). However, no rhythm of Fos was observed in un-nursed pups, and also no rhythm in Per1 protein was observed in nursed and fasted pups (Moreno et al., 2014). In contrast the rhythm of body temperature persists in un-nursed pups (Jilge et al., 2000; Trejo-Muñoz et al., 2012). Thus the observed effect on Fos at the time of nursing in the POA seems not to be related to the rhythm of temperature.

ROLE OF THE MEDIAN PREOPTIC NUCLEUS AND THE OREXINERGIC SYSTEM IN FAA

Immediately after FAA and milk ingestion, the rabbit pup's activity sharply decreases and pups remain huddled with very little movement for around next 20 h. In considering this change from a heightened state of alertness to an almost quiescent state suggestive of sleep, we decided to explore regions in the POA that integrate information related to the control of the sleep/wake cycle. We centered our attention in the MnPO, which is an integrative center in the rostral wall of the third ventricle in the forebrain that plays a key role in the sleep/wake cycle (Suntsova et al., 2007; Sakai, 2011; McKinley et al., 2015). In nursed pups we found an anticipatory increase of Fos at the time of nursing and low levels before and after that event (**Figure 1**). A similar pattern, with a delayed increase 1.5 after nursing, was found in fasted pups (Moreno et al., 2013). In addition, we explored Per1 protein and found a clear rhythm in both nursed and fasted pups with higher values at the time and thereafter nursing and lowest levels 16 h after (**Figure 1**). Notably, in the same study we determined possible rhythms of Per1 in the OVLT, MPOA, and the MnPO and only in this latter structure did the rhythm persist in un-nursed pups (Moreno et al., 2014). MnPO activation seen as increases in Fos protein had previously been associated with sleep or sleep pressure (McKinley et al., 2015). As pups remains quiescent, perhaps sleeping, after FAA it is possible that this increase in Fos indicates sleep pressure. However, activation of this nucleus at the time of nursing could be related also to FAA. Electrophysiological studies revealed that MnPO contained similar proportion of neurons that showed increased discharge during either sleep or waking state (Sakai, 2011). The author of that study suggested that in contrast to the classical view that the MnPO plays a role only in sleep, this nucleus might modulate a differential role between sleep and wake states. This proposal is consistent with the observed persistence of Per1 rhythms. In

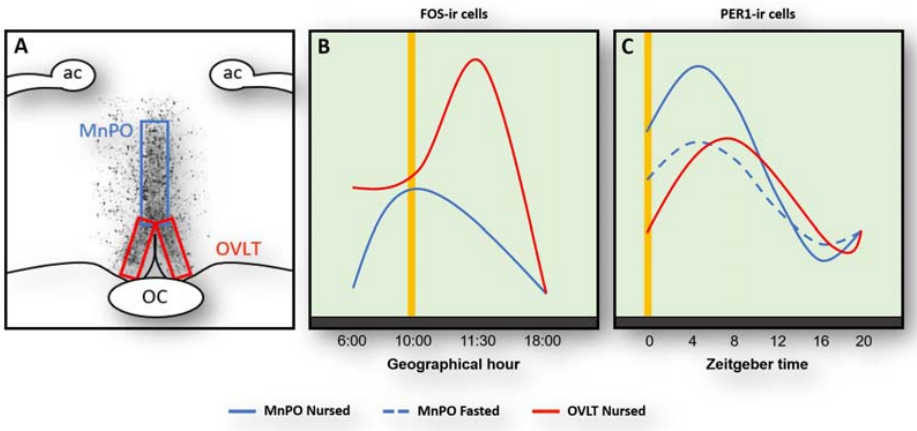

FIGURE 1 | Activation of Fos- **(A,B)** and Per1**(C)**-ir cells in the median preoptic nucleus (MnPO) and in the organum vasculosum of lamina terminalis (OVLT) in relation to nursing (yellow vertical line). Panel **(A)** shows the location of the MnPO and OVLT. **(B)** At the time of nursing Fos increases in both OVLT (red line) and MnPO (blue) with a further increase 1.5 h after in the MnPO. **(C)** Per1 increases in both OVLT and MnPO 4–8 after nursing, but this rhythm persists in un-nursed pups only in the MnPO (dashed blue line). Modified from Moreno et al., 2013, 2014. ac, anterior commissure; OC, optic chiasma.

support of this the MnPO send projections to the orexinergic cells in the perifornical area of the lateral hypothalamus to modulate sleep/awake states (Uschakov et al., 2007; Sakai, 2011; McKinley et al., 2015). These orexinergic cells are active at the time of FAA in mice (Mieda et al., 2004) in adult rats (Jiménez et al., 2013), and in the rabbit (Moreno et al., 2013). To our knowledge the MnPO has not been analyzed in relation to food entrainment in other species and this is an area worthy of further study.

MOTIVATION AND THE EXTENDED AMYGDALA IN FAA

In the adult rat, FAA shows features that implicate a process of conditioned learning (Silver et al., 2011). In order to explore brain mechanisms associated with conditioned learning of FAA, we analyzed several nuclei of the amygdala and the extended amygdala related to alertness and emotional arousal by using CO histochemistry (Olivo et al., 2017). During the period of FAA, we found activation in the basolateral, medial and central nuclei of the amygdala, bed nucleus of the terminalis, lateral septum, and nucleus accumbens core. This is interesting as the basolateral amygdala mediates the acquisition of associative learning and together with other nuclei of the extended amygdala participates in the emotional processing of stimuli (Davis and Whalen, 2001; Namburi et al., 2015). Also, in food-restricted rats, the basolateral amygdala, as well as other regions of the corticolimbic system, is entrained as indicated by Fos and Per1 proteins (Angeles-Castellanos et al., 2007). After food ingestion in the rabbit there was an increase in metabolic activity in the nucleus accumbens shell, caudate, putamen and cortical amygdala (Olivo et al., 2017), which further support a functional role in FAA for the circuit of food reward (Morales and Berridge, 2020). Overall, these results indicate a neural substrate for the conditioned learning in subjects that is induced by the nursing event and suggests that rabbit pups are motivationally aroused in expectation of receiving food.

OXYTOCIN AND A CENTRAL AND PERIPHERAL NETWORK IN FOOD ENTRAINMENT

After food ingestion there is an oxytocin (OT) release to the periphery and in several brain regions (Swanson and Kuypers, 1980; Olson et al., 1991; Verbalis et al., 1996; Spetter and Hallschmid, 2017), and OT projections to the brainstem are thought to be critical in a circuit underlying feeding and satiety (rev Swanson and Kuypers, 1980; McCormack et al., 2020). In the rabbit pup, milk ingestion induces an activation of OT neurons in both the SON and paraventricular hypothalamic nucleus (PVN) (Caba et al., 2003; Morgado et al., 2011). Peripheral OT plays a role in energy intake and expenditure processes including gastric emptying and distention, carbohydrate and lipid intake, fat oxidation, insulin secretion and glucose homeostasis (revs. Spetter and Hallschmid, 2017; McCormack et al., 2020). However, in the main body of the PVN, specifically in its dorsal and ventral portion and in its caudal region, we found an activation of OT cells *before* milk ingestion in the rabbit (Caba et al., 2020). In **Figure 2**, we show this effect in the two subregions of the main body of the PVN. This result suggests a differential activation of OT neurons in this nucleus related to preparatory actions for the upcoming meal. In the rat under food restriction, and in the rabbit pup before their daily period of milk intake, there is an increase in corticosterone, free fatty acids and glucagon indicating a catabolic state, and in parallel there is a decrease in glycogen and insulin (Díaz-Muñoz et al., 2000; Escobar et al., 2000; Morgado et al., 2008, 2010). We proposed (Caba et al., 2020) that the subpopulation of activated neurons

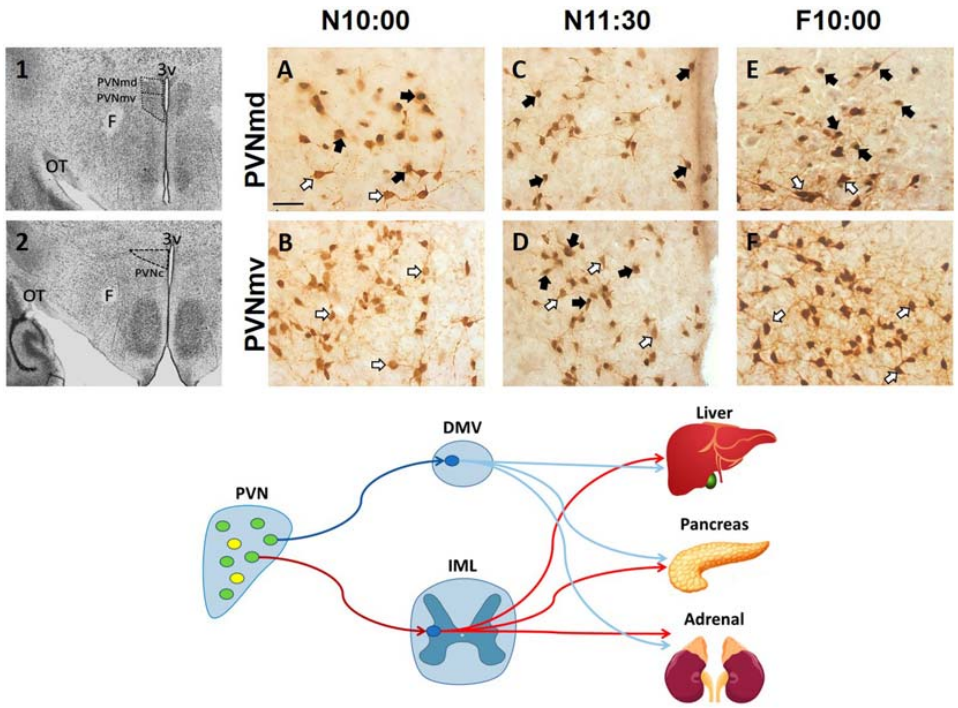

FIGURE 2 | Activation of oxytocinergic cells in the paraventricular hypothalamic nucleus (PVN) that coincides with food anticipatory activity in rabbit pups. 1, 2: Photomicrographs showing the location of the dorsal (PVNmd) and ventral (PVNmv) portions of the main body of the PVN **(A)** and their caudal portion (PVNc) **(B)**. A-F: Expression of oxytocin (white arrows) and double-labeled oxytocin and Fos (black arrows)-ir cells in the PVNmd **(A,C,E)** and PVNmv **(B,D,F)** just before nursing at 10:00 am (N10:00), 1.5 h after (N11:30) and in fasted subjects at the time of the previous scheduled nursing (F10:00). Note the increase in Fos/OT-ir cells before nursing **(A)** that persist in fasted subjects **(E)** only in the PVNmd. In contrast, the PVNmv only shows an increase in FOS/OT-ir cells after suckling of milk **(D)**. OT, optic tract. Modified from Caba et al. (2020). Bottom panel. Schematic of non-OT cells (yellow) and interaction of PVN OT (green) pre-autonomic sympathetic (red) and parasympathetic (blue) neurons that project to the preganglionic sympathetic system (red) in the intermediolateral (IML) column of the spinal cord, or to the preganglionic parasympathetic system (blue) of the dorsal motor nucleus of the vagus (DMV) in the medulla, that control the neural outflow to peripheral organs. Adapted from Buijs et al. (2001, 2003).

in the PVN are related to these peripheral effects through identified preganglionic OT cells from the sympathetic and parasympathetic system that project from the PVN to the liver, pancreas, and adrenals (**Figure 1**, bottom panel; Buijs et al., 2001, 2003). It seems likely that this activation is associated with both central and peripheral roles of these cells in the context of food entrainment. Future studies need to explore the differential activation of these OT cells and their receptors to projected areas in order to determine their physiological importance for FAA.

CONCLUSION

Although animals usually forage and eat during their period of activity, food is usually only available at a specific time either during the active or rest phase. In this respect, FAA represents an adaptive strategy in response to a limited, ecological resource. Although this phenomenon had been studied mainly in a few species of mammals, it had also been described in bees (rev. in Antle and Silver, 2009), and under laboratory conditions in zebrafish *Danio rerio* and in cavefish *Phreatichthys andruzzii* (Cavallari et al., 2011). Cavefish have evolved to live in darkness and although they express rhythmic clock genes they do not respond to light/dark cycles. On the other hand, under conditions of food restriction, cavefish show an increase in locomotor behavior before food availability indicative of FAA, as well as robust circadian rhythms of clock genes (Cavallari et al., 2011). This suggests that the ability for food entrainment is preserved across diverse taxa. Finally, it is evident that food is more important for survival than light. The rabbit pup presents an extraordinary opportunity to study FAA with little manipulation because this species shows this important evolutionary strategy only during the first 2 weeks of life before they open their eyes and start to be entrained by light.

AUTHOR CONTRIBUTIONS

MC, MNL, and MDC-F conceived and wrote the manuscript. All authors contributed to the article and approved the submitted version.

FUNDING

CONACYT scholarship to MDC-F #451898.

REFERENCES

Amir, S., Cain, S., Sullivan, J., Robinson, B., and Stewart, J. (1999). In rats, odor-induced fos in the olfactory pathways depends on the phase of the circadian clock. *Neurosci. Lett.* 272, 175–178. doi: 10.1016/s0304-3940(99)00609-6

Angeles-Castellanos, M., Mendoza, J., and Escobar, C. (2007). Restricted feeding schedules phase shift daily rhythms of c-fos and protein Per1 immunoreactivity in corticolimbic regions in rats. *Neuroscience* 144, 344–355. doi: 10.1016/j.neuroscience.2006.08.064

Antle, M. C., and Silver, R. (2009). Neural basis of timing and anticipatory behaviors. *Eur. J. Neurosci.* 30, 1643–1649. doi: 10.1111/j.1460-9568.2009.06959.x

Bautista, A., García-Torres, E., Martínez-Gómez, M., and Hudson, R. (2008). Do newborn domestic rabbits Oryctolagus cuniculus compete for thermally advantageous positions in the litter huddle? *Behav. Ecol. Sociobiol.* 62, 331–339. doi: 10.1007/s00265-007-0420-4

Buijs, R. M., Chun, S. J., Niijima, A., Romijn, H. J., and Nagai, K. (2001). Parasympathetic and sympathetic control of the pancreas: a role for the suprachiasmatic nucleus and other hypothalamic centers that are involved in the regulation of food intake. *J. Comp. Neurol.* 431, 405–423.

Buijs, R. M., La Fleur, S. E., Wortel, J., Van Heyningen, C., Zuiddam, L., Mettenleiter, T. C., et al. (2003). The suprachiasmatic nucleus balances sympathetic and parasympathetic output to peripheral organs through separate preautonomic neurons. *J. Comp. Neurol.* 464, 36–48. doi: 10.1002/cne.10765

Caba, M., and González-Mariscal, G. (2009). The rabbit pup, a natural model of nursing-anticipatory activity. *Eur. J. Neurosci.* 30, 1697–1706. doi: 10.1111/j.1460-9568.2009.06964.x

Caba, M., Huerta, C., Meza, E., Hernández, M., and Rovirosa-Hernández, M. J. (2020). Oxytocinergic cells of the hypothalamic paraventricular nucleus are involved in food entrainment. *Front. Neurosci.* 14:49. doi: 10.3389/fnins.2020.00049

Caba, M., Pabello, M., Moreno, M. L., and Meza, E. (2014). Main and accessory olfactory bulbs and their projections in the brain anticipate feeding in food-entrained rats. *Chronobiol. Int.* 31, 869–877. doi: 10.3109/07420528.2014.918625

Caba, M., Rovirosa, M. J., and Silver, R. (2003). Suckling and genital stroking induces fos expression in hypothalamic oxytocinergic neurons of rabbit pups. *Dev. Brain Res.* 143:119–128. doi: 10.1016/S0165-3806(03)00064-6

Caba, M., Tovar, A., Silver, R., Mogado, E., Meza, E., Zavaleta, Y., et al. (2008). Nature's food anticipatory experiment: entrainment of locomotor behavior, suprachiasmatic and dorsomedial hypothalamic nuclei by suckling in rabbit pups. *Eur. J. Neurosci.* 27, 432–443. doi: 10.1111/j.1460-9568.2008.06017.x

Cavallari, N., Frigato, E., Vallone, D., Fröhlich, N., Lopez-Olmeda, J. F., Foà, A., et al. (2011). A blind circadian clock in cavefish reveals that opsins mediate peripheral clock photoreception. *PLoS Biol.* 9:e1001142. doi: 10.1371/journal.pbio.1001142

Coureaud, G., Langlois, D., Sicard, G., and Schaal, B. (2004). Newborn rabbit responsiveness to the mammary pheromone is concentration-dependent. *Chem. Senses* 29, 341–350. doi: 10.1093/chemse/bjh037

Davidson, A. J., Aragona, B. J., Werner, R. M., Schroeder, E., Smith, J. C., and Stephan, F. K. (2001). Food-anticipatory activity persists after olfactory bulb ablation in the rat. *Physiol. Behav.* 72, 231–235. doi: 10.1016/s0031-9384(00)00417-0

Davis, M., and Whalen, P. J. (2001). The amygdala: vigilance and emotion. *Mol. Psychiatry* 6, 13–34. doi: 10.1038/sj.mp.4000812

Díaz-Muñoz, M., Vázquez-Martínez, O., Aguilar-Roblero, R., and Escobar, C. (2000). Anticipatory changes in liver metabolism and entrainment of insulin, glucagon, and corticosterone in food-restricted rats. *Am. J. Physiol. Regul. Integr. Comp. Physiol.* 279, R2048–R2056. doi: 10.1152/ajpregu.2000.279.6.R2048

Escobar, C., Hudson, R., Martínez-Gómez, R., and Aguilar-Roblero, R. (2000). Metabolic correlates of the circadian pattern of suckling-associated arousal in young rabbits. *J. Comp. Physiol. A.* 186, 33–38. doi: 10.1007/s003590050004

Finger, A.-M., Dibner, C., and Kramer, A. (2020). Coupled network of the circadian clocks: a driving force of rhythmic physiology. *FEBS Lett.* 594, 2734–2769. doi: 10.1002/1873-3468.13898

González-Mariscal, G., Caba, M., Martínez-Gómez, M., Bautista, A., and Hudson, R. (2016). Mothers and offspring: the rabbit as a model system in the study of mammalian maternal behavior and sibling interactions. *Horm. Behav.* 77, 30–41. doi: 10.1016/j.yhbeh.2015.05.011

Granados-Fuentes, D., Tseng, A., and Herzog, E. D. (2006). A circadian clock in the olfactory bulb controls olfactory responsivity. *J. Neurosci.* 26, 12219–12225. doi: 10.1523/JNEUROSCI.3445-06.2006

Gunapala, K. M., Gallardo, C. M., Hsu, C. T., and Steele, A. D. (2011). Single gene deletions of orexin, leptin, neuropeptide Y, and ghrelin do not appreciably alter food anticipatory activity in mice. *PLoS One* 6:e18377. doi: 10.1371/journal.pone.0018377

Jilge, B. (1993). The ontogeny of circadian rhythms in the rabbit. *J. Biol. Rhythm.* 8, 247–260. doi: 10.1177/074873049300800307

Jilge, B. (1995). Ontogeny of the rabbit's circadian rhythms without an external zeitgeber. *Physiol. Behav.* 58, 131–140. doi: 10.1016/0031-9384(95)00006-5

Jilge, B., Kuhnt, B., Landerer, W., and Rest, S. (2000). Circadian thermoregulation in suckling rabbit pups. *J. Biol. Rhythm.* 15, 329–335. doi: 10.1177/074873000129001431

Jiménez, A., Caba, M., and Escobar, C. (2013). Food-entrained patterns in orexin cells reveal subregion differential activation. *Brain Res.* 1531, 41–50. doi: 10.1016/j.brainres.2013.03.031

Johnson, A. K., and Buggy, J. (1978). Periventricular preoptic hypothalamus is vital for thirst and normal water economy. *Am. J. Physiol.* 234, R122–R129. doi: 10.1152/ajpregu.1978.234.3.R122

Juárez, C., Morgado, E., Meza, E., Waliszewski, S. M., Aguilar-Roblero, R., and Caba, M. (2013). Development of retinal projections and response to photic input in the suprachiasmatic nucleus of New Zealand White Rabbits. *Brain Res.* 1499, 21–28. doi: 10.1016/j.brainres.2013.01.010

Juárez, C., Morgado, E., Waliszewski, S. M., Martínez, A. J., Meza, E., and Caba, M. (2012). Synchronization of PER1 protein in parabrachial nucleus in a natural model of food anticipatory activity. *Eur. J. Neurosci.* 35, 1458–1465. doi: 10.1111/j.1460-9568.2012.08051.x

LeSauter, J., Hoque, N., Weintraub, M., Pfaff, D. W., and Silver, R. (2009). Stomach ghrelin-secreting cells as food-entrainable circadian clocks. *Proc. Natl. Acad. Sci. U.S.A.* 106, 13582–13587. doi: 10.1073/pnas.0906426106

Levine, S. (2002). Regulation of the hypothalamic–pituitary–adrenal axis in the neonatal rat: the role of maternal behaviour. *Neurotox. Res.* 4, 557–564. doi: 10.1080/10298420290030569

Lloyd, H. G., and McCowan, D. (1968). Some observations on the breeding burrows o the wild rabbit. *Oryctol. cunic. Island Skokholm. J. Zool.* 156, 540–554. doi: 10.1111/j.1469-7998.1968.tb04376.x

McCormack, S. E., Blevins, J. E., and Lawson, E. A. (2020). Metabolic effects of oxytocin. *Endocr. Rev.* 41, 121–145. doi: 10.1210/endrev/bnz

McKinley, M. J., Mathai, M. L., Pennington, G., Rundgren, M., and Vivas, L. (1999). Effect of individual or combined ablation of the nuclear groups of the lamina terminalis on water drinking in sheep. *Am. J. Physiol.* 276, R673–R683. doi: 10.1152/ajpregu.1999.276.3.R673

McKinley, M. J., Yao, S. T., Uschakov, A., McAllen, R. M., Rundgren, M., and Martelli, D. (2015). The median preoptic nucleus: front and centre for the regulation of body fluid, sodium, temperature, sleep and cardiovascular homeostasis. *Acta Physiol.* 214, 8–32. doi: 10.1111/apha.12487

Mieda, M., Clay, W. S., Sinton, C. M., Richardson, J. A., Sakurai, T., and Yanagisawa, M. (2004). Orexin neurons function in an efferent pathway of a food-entrainable circadian oscillator in eliciting food-anticipatory activity and wakefulness. *J. Neurosci.* 24, 10493–10501. doi: 10.1523/JNEUROSCI.3171-04.2004

Mistlberger, R. E. (1994). Circadian food-anticipatory activity: formal models and physiological mechanisms. *Neurosci. Biobehav. Rev.* 18, 171–195. doi: 10.1016/0149-7634(94)90023-X

Mistlberger, R. E. (2020). Food as circadian time cue for appetitive behavior. *F1000 Res.* 9:61. doi: 10.12688/f1000research.20829.1

Montigny, D., Coureaud, G., and Schaal, B. (2006). Rabbit pup response to the mammary pheromone: from automatism to prandial control. *Physiol. Behav.* 89, 742–749. doi: 10.1016/j.physbeh.2006.08.022

Montúfar-Chaveznava, R., Hernández-Campos, O., Hudson, R., and Caldelas, I. (2013). Differential maturation of the molecular clockwork in the olfactory bulb and suprachiasmatic nucleus of the rabbit. *Neuroscience* 207, 198–207. doi: 10.1016/j.neuroscience.2012.01.025

Morales, I., and Berridge, K. C. (2020). 'Liking' and 'wanting' in eating and food reward: brain mechanisms and clinical implications. *Physiol. Behav.* 227, 113152. doi: 10.1016/j.physbeh.2020.113152

Moreno, M. L., Meza, E., Morgado, E., Juárez, C., Ramos-Ligonio, A., Ortega, A., et al. (2013). Activation of organum vasculosum of lamina terminalis, median preoptic nucleus, and medial preoptic area in anticipation of nursing in rabbit pups. *Chronobiol. Int.* 30, 1272–1282. doi: 10.3109/07420528.2013.823980

Moreno, M. L., Meza, E., Ortega, A., and Caba, M. (2014). The median preoptic nucleus exhibits circadian regulation and is involved in food anticipatory activity in rabbit pups. *Chronobiol. Int.* 31, 515–522. doi: 10.3109/07420528.2013.874354

Morgado, E., Gordon, M. K., Miñana-Solís, M., Meza, E., Levine, S., Escobar, C., et al. (2008). Hormonal and metabolic rhythms associated with the daily scheduled nursing in rabbit pups. *Am. J. Physiol. Regul. Integr. Comp. Physiol.* 295, R690–R695. doi: 10.1152/ajpregu.00162.2008

Morgado, E., Juárez, C., Melo, A. I., Domínguez, B., Lehman, M. N., Escobar, C., et al. (2011). Artificial feeding synchronizes behavioral, hormonal, metabolic and neural parameters inmother-deprived neonatal rabbit pups. *Eur. J. Neurosci.* 34, 1807–1816. doi: 10.1111/j.1460-9568.2011.07898.x

Morgado, E., Meza, E., Gordon, M. K., Pau, F. K. Y., Juárez, C., and Caba, M. (2010). Persistence of hormonal and metabolic rhythms during fasting in 7- to 9-day old rabbits entrained by nursing during the night. *Horm. Behav.* 58, 465–472. doi: 10.1016/j.yhbeh.2010.05.003

Morrison, S. F. (2016). Central control of body temperature. *F1000 Res.* 5:880. doi: 10.12688/f1000research.7958.1

Namburi, P., Beyeler, A., Yorozu, S., Calhoon, G. G., Halbert, S. A., Wichmann, R., et al. (2015). A circuit mechanism for differentiating positive and negative associations. *Nature* 520, 675–678. doi: 10.1038/nature14366

Navarrete, E., Ortega-Bernal, J. R., Trejo-Muñoz, L., Díaz, G., Montúfar-Chaveznava, R., and Caldelas, I. (2016). Participation of the olfactory bulb in circadian organization during early postnatal life in rabbits. *PLoS One* 11:e0156539. doi: 10.1371/journal.pone.0156539

Nolasco, N., Juárez, C., Morgado, E., Meza, E., and Caba, M. (2012). A circadian clock in the olfactory bulb anticipates feeding during food anticipatory activity. *PLoS One* 7:e47779. doi: 10.1371/journal.pone.0047779

Olivo, D., Caba, M., Gonzalez-Lima, F., Rodríguez-Landa, J. F., and Corona-Morales, A. A. (2017). Metabolic activation of amygdala, lateral septum and accumbens circuits during food anticipatory behavior. *Behav. Brain Res.* 316, 261–270. doi: 10.1016/j.bbr.2016.09.015

Olivo, D., Caba, M., Gonzalez-Lima, F., Vázquez, A., and Corona-Morales, A. (2014). Circadian feeding entrains anticipatory metabolic activity in piriform cortex and olfactory tubercle, but not in suprachiasmatic nucleus. *Brain Res.* 1592, 11–21. doi: 10.1016/j.brainres.2014.09.054

Olson, B. R., Drutarosky, M. D., Chow, M. S., Hruby, V. J., Stricker, E. M., and Verbalis, J. G. (1991). Oxytocin and an oxytocin agonist administered centrally decrease food intake in rats. *Peptides* 12, 113–118. doi: 10.1016/0196-9781(91)90176-P

Rovirosa, M. J., Levine, S., Gordon, M. K., and Caba, M. (2005). Circadian rhythm of corticosterone secretion in the neonatal rabbit. *Dev. Brain Res.* 158, 92–96. doi: 10.1016/j.devbrainres.2005.06.007

Sakai, K. (2011). Sleep-waking discharge profiles of median preoptic and surrounding neurons in mice. *Neuroscience.* 182, 144–161. doi: 10.1016/j.neuroscience.2011.03.010

Schaal, B., Coureaud, G., Langlois, D., Giniès, C., Sémon, E., and Perrier, G. (2003). Chemical and behavioural characterization of the rabbit mammary pheromone. *Nature* 424, 68–72. doi: 10.1038/nature01739

Silver, R., Balsam, P. D., Butler, M. P., and LeSauter, J. (2011). Food anticipation depends on oscillators and memories in both body and brain. *Physiol. Behav.* 104, 562–571. doi: 10.1016/j.physbeh.2011.05.034

Speh, J. C., and Moore, R. Y. (1993). Retinohypothalamic tract development in the hamster and rat. *Dev. Brain Res.* 76, 171–181. doi: 10.1016/0165-3806(93)90205-o

Spetter, M. S., and Hallschmid, M. (2017). Current findings on the role of oxytocin in the regulation of food intake. *Physiol. Behav.* 176, 31–39. doi: 10.1016/j.physbeh.2017.03.007

Stephan, F. K. (2002). The "other" circadian system: food as a Zeitgeber. *J. Biol. Rhythms* 17, 284–292. doi: 10.1177/074873040201700402

Suntsova, N., Guzman-Marin, R., Kumar, S., Alam, M. N., Szymusiak, R., and McGinty, D. (2007). The median preoptic nucleus reciprocally modulates activity of arousal-related and sleep-related neurons in the perifornical lateral hypothalamus. *J. Neurosci.* 27, 1616–1630. doi: 10.1523/JNEUROSCI.3498-06.2007

Swanson, L. W., and Kuypers, H. G. (1980). The paraventricular nucleus of the hypothalamus: cytoarchitectonic subdivisions and organization of projections to the pituitary, dorsal vagal complex, and spinal cord as demonstrated by retrograde fluorescence double-labeling methods. *J. Comp. Neurol.* 194, 555–570. doi: 10.1002/cne.901940306

Thunhorst, R. L., Xu, Z., Cicha, M. Z., Zardetto-Smith, A. M., and Johnson, A. K. (1998). Fos expression in rat brain during depletion-induced thirst and salt appetite. *Am. J. Physiol.* 274, R1807–R1814. doi: 10.1152/ajpregu.1998.274.6.r1807

Trejo-Muñoz, L., Navarrete, E., Montúfar-Chaveznava, R., and Caldelas, I. (2012). Determining the period, phase and anticipatory component of activity and temperature patterns in newborn rabbits that were maintained under a daily nursing schedule and fasting conditions. *Physiol. Behav.* 106, 587–596. doi: 10.1016/j.physbeh.2012.04.005

Uschakov, A., Gong, H., McGinty, D., and Szymusiak, R. (2007). Efferent projections from the median preoptic nucleus to sleep-and arousal regulatory nuclei in the rat brain. *Neuroscience* 150, 104–120. doi: 10.1016/j.neuroscience.2007.05.055

Vázquez, A., Hernández-Oliveras, A., Santiago-García, J., Caba, M., Gonzalez-Lima, F., Olivo, D., et al. (2020). Daily changes in GFAP expression in radial glia of the olfactory bulb in rabbit pups entrained to circadian feeding. *Physiol. Behav.* 217, 112824. doi: 10.1016/j.physbeh.2020.112824

Verbalis, J. G., Blackburn, R. E., Hoffman, G. E., and Stricker, E. M. (1996). Establishing behavioral and physiological functions of central oxytocin: insights from studies of oxytocin and ingestive behaviors. *Adv. Exp. Med. Biol.* 395, 209–225.

Williams, D. L., and Cummings, D. E. (2005). Regulation of ghrelin in physiologic and pathophysiologic states. *J. Nutr.* 135, 1320–1325. doi: 10.1093/jn/135.5.1320

Wong-Riley, M. T. (1989). Cytochrome oxidase: an endogenous metabolic marker for neuronal activity. *Trends. Neurosci.* 12, 94–101. doi: 10.1016/0166-2236(89)90165-3

Conflict of Interest: The authors declare that the research was conducted in the absence of any commercial or financial relationships that could be construed as a potential conflict of interest.

frontiers in Neuroscience

MINI REVIEW
published: 18 March 2021
doi: 10.3389/fnins.2021.634034

Beginning to See the Light: Lessons Learned From the Development of the Circadian System for Optimizing Light Conditions in the Neonatal Intensive Care Unit

*Esther M. Hazelhoff[1], Jeroen Dudink[2], Johanna H. Meijer[1] and Laura Kervezee[1]**

[1] Laboratory for Neurophysiology, Department of Cellular and Chemical Biology, Leiden University Medical Center, Leiden, Netherlands, [2] Department of Neonatology, Wilhelmina Children's Hospital and Brain Centre Rudolf Magnus, University Medical Centre Utrecht, Utrecht, Netherlands

OPEN ACCESS

Edited by:
Daisuke Ono,
Nagoya University, Japan

Reviewed by:
Jennifer Anne Evans,
Marquette University, United States
Ethan Buhr,
University of Washington,
United States

***Correspondence:**
Laura Kervezee
l.kervezee@lumc.nl

Specialty section:
This article was submitted to Sleep and Circadian Rhythms, a section of the journal Frontiers in Neuroscience

Received: 26 November 2020
Accepted: 19 February 2021
Published: 18 March 2021

Citation:
Hazelhoff EM, Dudink J, Meijer JH and Kervezee L (2021) Beginning to See the Light: Lessons Learned From the Development of the Circadian System for Optimizing Light Conditions in the Neonatal Intensive Care Unit. Front. Neurosci. 15:634034. doi: 10.3389/fnins.2021.634034

The circadian timing system optimizes health by temporally coordinating behavior and physiology. During mammalian gestation, fetal circadian rhythms are synchronized by the daily fluctuations in maternal body temperature, hormones and nutrients. Circadian disruption during pregnancy is associated with negative effects on developmental outcomes in the offspring, highlighting the importance of regular and robust 24-h rhythms over gestation. In the case of preterm birth (before 37 weeks of gestation), maternal cues no longer synchronize the neonate's circadian system, which may adversely affect the neonate. There is increasing evidence that introducing robust light-dark cycles in the Neonatal Intensive Care Unit has beneficial effects on clinical outcomes in preterm infants, such as weight gain and hospitalization time, compared to infants exposed to constant light or constant near-darkness. However, the biological basis for these effects and the relationship with the functional and anatomical development of the circadian system is not fully understood. In this review, we provide a concise overview of the effects of light-dark cycles on clinical outcomes of preterm neonates in the NICU and its alignment with the development of the circadian system.

Keywords: cycled light, development, preterm infants, circadian system, Neonatal Intensive Care Unit, chronobiology, eye development and function

INTRODUCTION

During pregnancy, a highly controlled uterine environment provides the best possible conditions for optimal fetal development in preparation for a successful transition to postnatal life. The mother supplies oxygen, hormones, and nutrients via the placenta. In addition to these substrates, the mother conveys circadian timing cues to the fetus through her own daily rhythms in body temperature, physical activity, feeding behavior, and hormonal levels (Serón-Ferré et al., 2001, 2012; Bates and Herzog, 2020). Several lines of evidence show that maternal circadian

rhythms are important for the offspring. For example, pregnant women on shift work, which may lead to circadian disruption, have an increased risk of adverse reproductive outcomes (Kervezee et al., 2018). A recent meta-analysis reported an increased odds of preterm birth (odds ratio [OR]: 1.13; 95% confidence interval [CI]: 1.00–1.28) and of having a small-for-gestational-age neonate (OR: 1.18; 95% CI: 1.01–1.38) in rotating night shift work compared to fixed day shift work (Cai et al., 2019). Research in animal models supports these findings, showing that environmental disruption of circadian rhythms during pregnancy leads to adverse pregnancy outcomes (Summa et al., 2012) as well as to negative effects in the offspring later in life, such as altered adrenal function, impaired adaptive immune system, social avoidance and depressive like behavior (Borniger et al., 2014; Cissé et al., 2017a,b; Man et al., 2017; Smarr et al., 2017; Salazar et al., 2018).

In case of preterm birth (i.e., babies born before 37 weeks of gestation), the period that the fetus spends in the controlled intrauterine environment comes to an end prematurely. The preterm baby is typically admitted to a Neonatal Intensive Care Unit (NICU), where clear environmental 24-h rhythms are usually absent, exposing the infant to a constant temperature and irregular or continuous illumination (Fielder and Moseley, 2000; White et al., 2013; Bueno and Menna-Barreto, 2016; Hay, 2017). There is a growing concern that the absence of temporal cues in the NICU may not be optimal for the development of premature infants (Symington and Pinelli, 2006; van den Hoogen et al., 2017). The postnatal environment is especially important given the critical period of development that occurs *ex utero* following extreme preterm birth (i.e., born before 28 weeks of gestation). For example, between 18 and 39 weeks of gestation, fetal brain volume usually increases 10 to 34-fold, depending on the brain region (Andescavage et al., 2017; Matthews et al., 2018). In addition, during the stay in the NICU, the immature and rapidly developing brain is particularly vulnerable to environmental stressors, which might compromise neurobehavioral development (Aucott et al., 2002; Ward and Beachy, 2003; Symington and Pinelli, 2006; Santos et al., 2016; Matthews et al., 2018; Twilhaar et al., 2018). Indeed, as the survival rate of premature infants has improved (Zeitlin et al., 2010; World Health Organization, 2012; Platt, 2014), we have to acknowledge that the potential complications of prematurity, both experienced in the NICU and in later life, become increasingly important (Ward and Beachy, 2003). Designing a NICU environment from a chronobiological perspective might be desirable for improving preterm outcomes.

There is accumulating evidence that introducing a robust light-dark cycle in the NICU environment is beneficial for postnatal development (as reviewed below). However, to better understand the biological basis for these effects, it is important to take into consideration the different critical periods of fetal development. For the light-dark cycle to be beneficial for postnatal development, a premature infant should be able to perceive light and confer this light information to the biological clock. In this review we aim to provide an overview of the potential effects of a light-dark cycle in a NICU in the context of the development of the visual and circadian systems.

THE CIRCADIAN TIMING SYSTEM

Over the course of evolution organisms have adapted to alternating light-dark cycles due to the rotation of the earth on its axis by developing a circadian clock, which controls the daily timing of biological processes ranging from gene expression to behavior (Dibner et al., 2010). In mammals, circadian rhythms are orchestrated by a central clock located in the suprachiasmatic nuclei (SCN) of the hypothalamus (Sollars and Pickard, 2015). The SCN network autonomously generates a circadian rhythm and transmits this temporal information to peripheral oscillators that are present in virtually all other cell types in the body. The SCN is synchronized to the external environment by light input that is transmitted from the retina directly to the SCN through a neural pathway called the retinal hypothalamic tract (RHT) (Hughes et al., 2015).

Within the retina, light is perceived by a subgroup of retinal ganglion cells that express the photopigment melanopsin, which renders them intrinsically photosensitive. Modulated by input from rods and cones (Van Diepen et al., 2013; Barrionuevo et al., 2014; Spitschan et al., 2014), these intrinsically photosensitive retinal ganglion cells (ipRGCs) transmit non-visual light information not only to the SCN, but also to other brain areas involved in non-image forming functions such as the olivary pretectal nucleus, which is involved in the regulation of the pupillary light reflex (Chen et al., 2011; La Morgia et al., 2018).

CIRCADIAN ENTRAINMENT BY LIGHT-DARK CYCLES IN THE NEONATAL INTENSIVE CARE UNIT

Introducing a robust light-dark cycle in the NICU has been suggested as a strategy to entrain the circadian system in preterm infants, which may support growth and development as well as help prevent complications frequently experienced by the preterm infant such as disturbances in body temperature, sleep or feeding patterns (Morag and Ohlsson, 2016). Currently, lighting conditions in NICUs across the world are highly variable, owing to flexible guidelines (e.g., see Best et al., 2018). For example, the Consensus Committee for NICU Design, recommends illuminance levels to be between 10 and 600 lux in the NICU (White et al., 2013). NICUs can be distinguished by observing either constant light or constant near-darkness, with light levels below 20 lux throughout the 24-h period (Morag and Ohlsson, 2016).

Several studies have evaluated the effect of introducing a robust light-dark cycle ('cycled light') compared to either constant light or near-darkness on clinical outcomes in preterm infants in NICUs, such as weight gain. A systematic review by the Cochrane library concluded that cycled light seems to shorten the length of hospital stay, although the evidence is hampered by the small sample size and the inability to blind the intervention (Morag and Ohlsson, 2016). Cycled light may also improve other outcomes, such as weight gain and the incidence or retinopathy of prematurity (Morag and Ohlsson, 2016). Specifically, the clearest benefits were found in studies that compared exposure

to cycled light to exposure to constant light conditions in NICUs. Several studies reported that cycled light compared to continuous light was associated with improved weight gain (Mann et al., 1986; Miller et al., 1995; Vásquez-Ruiz et al., 2014; Farahani et al., 2018), although the magnitude of the effect is difficult to compare between the studies. For example, Farahani et al. (2018) found that infants in cycled light conditions gained significantly more weight between day 9 after birth and discharge from the NICU than infants in constant conditions (29 ± 7 g per day vs 15 ± 6 g, per day; mean ± SD), while Mann et al. (1986) found no difference in weight at discharge, but 3 months after discharge, infants that had been exposed to cycled light in the NICU were on average 500 g heavier than those exposed to continuous light. Furthermore, one study found that the length of the hospitalization period was significantly shorter in infants exposed to cycled light condition compared to those exposed to continuous light (34 ± 3 days vs 51 ± 5 days; mean ± SEM) (Vásquez-Ruiz et al., 2014). Another study found an effect of similar magnitude on hospitalization period (59 ± 28 days in the cycled light group vs 75 ± 25 days in the continuous light group), although this difference was not statistically significant (Miller et al., 1995). However, it should be noted that other studies did not find an effect of cycled light on hospitalization duration (Mann et al., 1986; Farahani et al., 2018; Moselhi Mater et al., 2019). Cycled light interventions in the NICU have also been reported to increase nighttime sleep duration (Guyer et al., 2015) and the ratio of daytime to nighttime activity (Blackburn and Patteson, 1991; Watanabe et al., 2013), to reduce or stabilize heart rate patterns (Blackburn and Patteson, 1991; Vásquez-Ruiz et al., 2014), and lower distress levels compared to continuous light (Moselhi Mater et al., 2019). Interestingly, one study reported a difference in morning and evening melatonin levels in infants exposed to cycled light but not in infants exposed to continuous light (Vásquez-Ruiz et al., 2014), suggesting that implementing a light-dark cycle promotes circadian entrainment. Although the long-term benefits of improved circadian entrainment in infants early in life remain to be investigated, improved circadian entrainment, provided that it leads to more robust sleep-wake cycles, would be of immediate benefit to the parents after the infant's release from the NICU.

Other studies compared outcomes in preterm infants exposed to cycled light compared to constant near-darkness. One study found that preterm infants receiving cycled light at birth or from gestational week 32 onward gained significantly more weight than those exposed to constant near-darkness until gestational week 36 (Brandon et al., 2002). However, most studies reported no significant effects on body weight at discharge or body weight gain (Boo et al., 2002; Rivkees et al., 2004; Guyer et al., 2012) and length of hospital stay (Brandon et al., 2002, 2017; Rivkees et al., 2004; Guyer et al., 2012). One underpowered study reported a clinically relevant, but not statistically significant effect of initiating a cycled light intervention at a gestational age of 28 weeks compared to cycled light started at 36 weeks on weight gain (mean weight gain of 193.8 g vs 176.3 g between gestational week 36 and 44) (Brandon et al., 2017). In addition, while a cycled light intervention did not affect the emergence of day/night differences in body temperature compared to constant near-darkness in preterm infants (Mirmiran et al., 2003), the development of distinct rest-activity cycles was accelerated in preterm infants exposed to cycled light compared to those exposed to constant near-darkness (Rivkees et al., 2004), although this effect was not observed in another study (Lebel et al., 2017). Finally, exposure to cycled light in the NICU reduced fussing and crying per 24 h after discharge to home compared to exposure to constant near-darkness (Guyer et al., 2012). Of note, the observation that some effects of cycled light interventions are only observed after discharge from the hospital highlight that long-term follow-up is essential to better understand the effects of cycled light in the NICU (Mann et al., 1986; Rivkees et al., 2004).

Altogether, the available literature provides a strong rationale to further evaluate strategies to improve circadian entrainment in NICUs. However, a more systematic approach is needed that considers the underlying physiological mechanisms by which cycled light may exert its beneficial effects. An important point of consideration is that light levels varied from study to study, and are often not precisely reported – if at all (**Figure 1**). This makes it hard to compare different studies and make recommendations regarding the optimal light levels. Therefore, future research is warranted to determine what lighting regimes, in terms of intensity and spectral composition, and at what developmental time point, lead to optimal clinical outcomes.

DEVELOPMENT OF THE CIRCADIAN SYSTEM, FROM LIGHT INPUT TO FUNCTIONAL OUTPUT

The use of cycled light as a strategy to promote circadian entrainment and improve clinical outcome should be considered in context of the marked developmental changes of the visual and circadian system that occur in preterm infants during their stay in the NICU. At different stages of gestation, the different anatomical structures of the visual and circadian systems develop (**Figure 2**). This starts on gestational day 17, when the first structures of the eye are formed (Van Cruchten et al., 2017). In infants born at term (between gestational week 37–41), the structural development of the eye takes place nearly completely *in utero*, although the further functional maturation is not completed until at least 4 years after birth (Hendrickson and Yuodelis, 1984).

The pupil can be viewed as the anatomical gateway that modulates the transmission of light from the environment to the circadian system. Its development starts around gestational week 17. However, its function in regulating the amount of light that reaches the retina develops only later in gestation. From 30 weeks onward preterm infants start to show slow alterations in pupil diameter, and from 34 weeks gestation they have a clear and fast pupil reflex to changes in illumination (Robinson and Fielder, 1990). However, as the babies are still developing, there might be some differences in thickness of the eyelids, which may affect the amount of light entering the eye. Robinson et al. (1991) showed that a higher percentage of red light penetrates the eyelid in prematurely born babies compared to adults, but how this changes over the course of development is unknown.

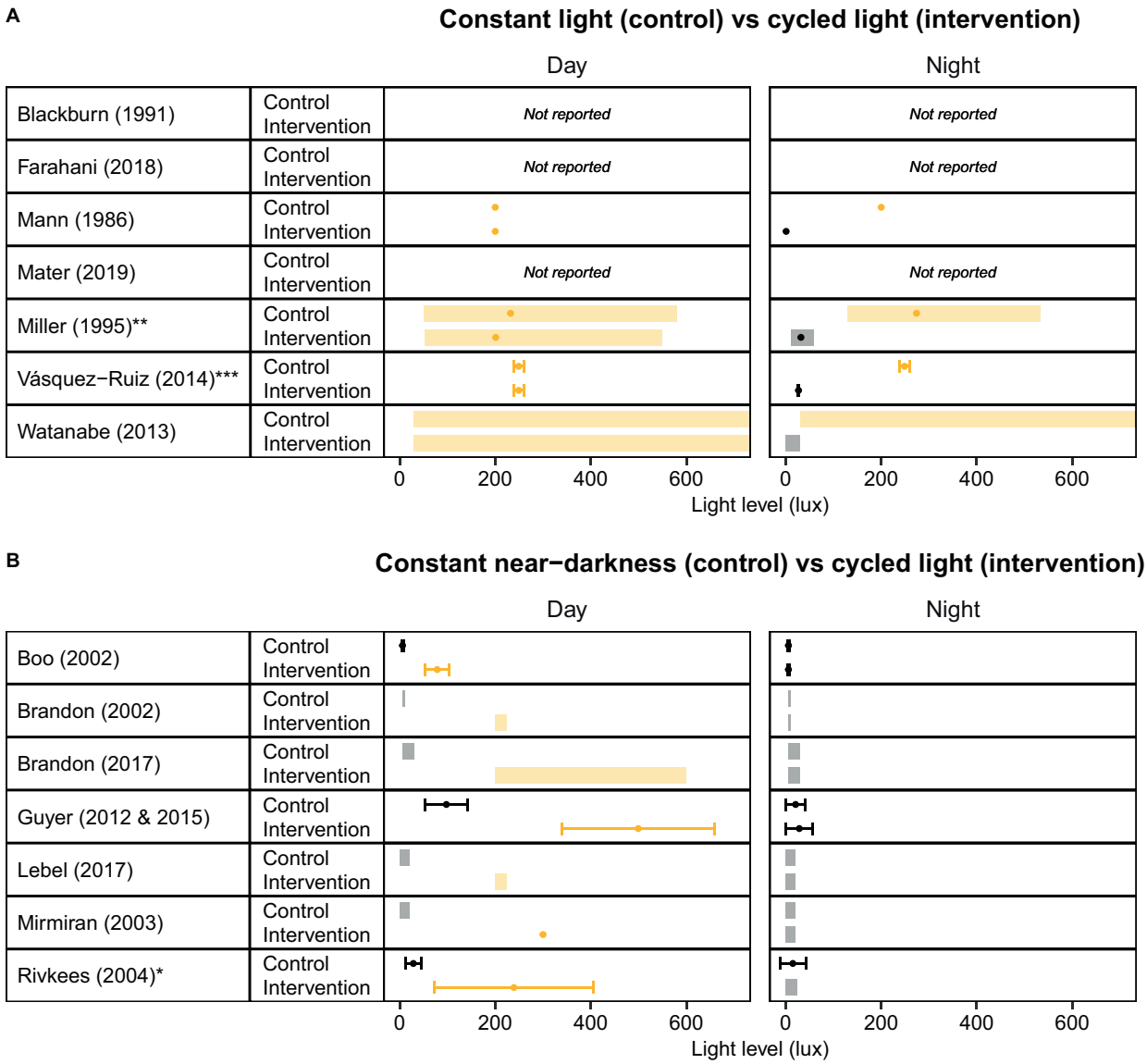

FIGURE 1 | Overview of light levels used in cycled light studies that have been conducted in Neonatal Intensive Care Units. Light levels reported in studies that investigated the effect of cycled light versus **(A)** constant light and **(B)** constant near-darkness. Values are depicted as ranges (shaded rectangles), means (dots), and/or standard deviations (error bars), depending on the values reported in the publication. Yellow/Orange colors indicate "light", Black/Gray colors indicate "darkness". *Standard errors reported in Rivkees et al. (2004) are converted to standard deviations by multiplying with the square root of the n per group. **Light intensities measured in the horizontal plane are reported here. ***Unclear whether standard deviations or standard errors are reported; using published values for error bars.

Secondly, the effect of light on circadian entrainment is influenced by the function of the different retinal cells. The retinal ganglion cells are formed from gestational week 7 onward, well-before the emergence of rods and cones between week 10 and 12 (Van Cruchten et al., 2017). Expression of melanopsin is present in human eye tissue at least by gestational week 8.6 (Tarttelin et al., 2003). Melanopsin may even be present earlier, since this was the earliest developmental timepoint that was included in the study by Tarttelin et al. (2003). For instance, in mice, melanopsin is expressed by embryonic day 10.5–11.5 in mice (equivalent to gestational week 4 in humans) (Tarttelin et al., 2003). This coincides with the emergence of retinal ganglion cells in mice, which occurs at an earlier developmental stage compared to humans (Tarttelin et al., 2003). Of note, while rod and cone photoreceptors only become functional two weeks after birth in mice, melanopsin-expressing retinal ganglion cells are light responsive immediately at birth (Sekaran et al., 2005), and possibly even earlier during gestation (Rao et al., 2013). This light response is mediated by melanopsin and, strikingly, was found to have a functional role for vascular patterning *in utero*: a higher degree of retinal vascular overgrowth was observed in pups reared in constant darkness during late gestation compared

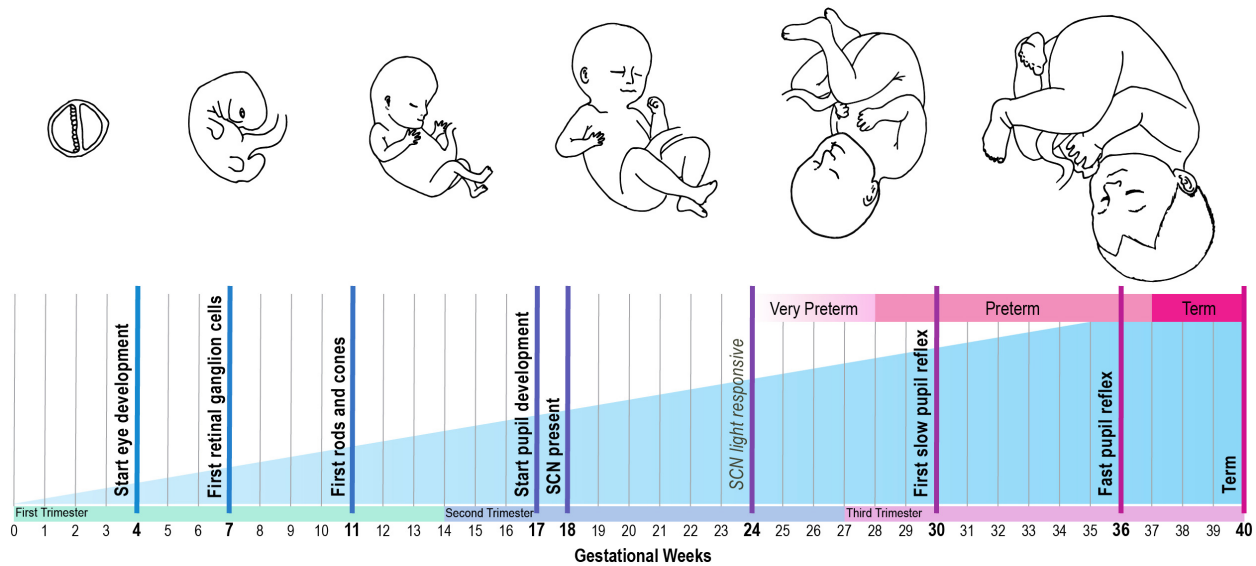

FIGURE 2 | Developmental timeline of the human circadian system, based on reviewed human and animal studies. Bold text: developmental time points that are obtained from human studies. Italic text: developmental time points that are inferred from animal studies, using the gestational age equivalent to humans.

to those reared in a light-dark cycle (Rao et al., 2013). This effect seems to be mediated by melanopsin, because a null-mutation in the melanopsin gene *Opn4* caused the same phenotype (Rao et al., 2013). These results suggest that light exposure *in utero* is already important for fetal eye development in mice. To what extent this applies to human fetal development remains to be investigated. However, these findings support the need to develop a clear mechanistic understanding of the effect of light-dark cycles on the development of the visual system in preterm infants at different developmental stages.

The ability of a neonate's circadian system to entrain to the environmental light-dark cycle also depends on the functionality of the RHT. To the best of our knowledge no studies are available on the development of the human RHT. However, it is known that the SCN is light responsive in baboons born at term and can be entrained to a light-dark cycle with a light intensity of 200 lux (Rivkees et al., 1997). Furthermore, the SCN in preterm baboons responds to light from a stage equivalent to 24 weeks of gestation in humans onward (Hao and Rivkees, 1999). As the fetal development of primates and human is similar (Stouffer and Woodruff, 2017), these results suggest the projections from the retina to the SCN via the RHT may be functional from 24 weeks of gestation onward in human development.

For entrainment of the neonate to be possible, the environmental light input must be processed by a functional SCN. At what stage the SCN develops during gestation in humans is largely unknown. However, it has been shown that the SCN is present at 18 weeks of gestation, using melatonin receptor- and D1 dopamine receptor labeling (Reppert et al., 1988; Rivkees and Lachowicz, 1997; Rivkees, 2007). In addition, studies in squirrel monkeys support these findings, with SCN neurogenesis during early gestation (Reppert and Schwartz, 1984). At the end of gestation, a clear day-night difference in SCN glucose utilization can be observed in these monkeys (Reppert and Schwartz, 1984). Since only 20% of the total cell number found in adulthood is present at term (Swaab, 1995), further maturation of the human SCN takes place after birth.

Once the individual components of the circadian system are formed, they generate an output in the form an approximately 24-h rhythm that is projected to other brain areas and peripheral organs, which regulate circadian rhythms both in behavior and hormone production. In term babies, 24 h sleep-wake rhythms are not yet apparent directly after birth, but these typically emerge between 7 and 16 weeks of age (Jenni et al., 2006). Around the same time, day-night differences can also be observed in hormone production, such as melatonin from 12 weeks of age (Kennaway et al., 1992). In addition to rhythms in hormone production, heart rate shows a clear difference between day and night from 7 weeks onward (Hoppenbrouwers et al., 2012), whereas day/night differences in body temperature only become apparent from 2 months of age (Petersen and Wailoo, 1994). Whether the developmental timeline of these rhythms is influenced by the postnatal environmental light-dark cycle in preterm infants is unclear, as reviewed above.

Together, these studies show that the initial structures of the eye and central clock are present at 24 weeks of gestation, and that further maturation of both the eye and the SCN takes place largely in the third trimester of pregnancy and in the first few years after birth. With most of the structures formed by 24 weeks of gestation, it is conceivable that in the case of preterm birth, environmental light input is conveyed by the eyes to an SCN that is – at least partly – functional. The physiological mechanisms underlying the seemingly beneficial effects of cycled light in the NICU, such as weight gain and length of hospital stay, remain to be elucidated, although it has been suggested that reduced (nighttime) activity and lower, more stable heart rate

rhythms, leading to reduced energy expenditure, may play a role (Miller et al., 1995).

DISCUSSION

As exposure to a bright day and dark night seems to positively influence weight gain, duration of hospital stay, and other clinically relevant measures, cycled light appears to be beneficial for the development of preterm babies. As the structures of the circadian system appear to be formed at 24 weeks, it is conceivable that the positive effects of cycled light are mediated through these structures. This fits with the striking observation that environmental light not only reaches the uterus in both sheep and mice (Parraguez et al., 1998; Rao et al., 2013) but also plays a role in retinal vascularization in the mouse fetus (Rao et al., 2013). To what extent light reaches the uterus in pregnant women, and whether light plays a functional role in developmental processes *in utero* in humans as well, are important questions that warrant further investigation.

In addition to the beneficial effects of cycled light, another topic that requires attention in future studies is the potential functional role of other environmental timing cues on circadian entrainment and clinical outcomes in the NICU, such as temperature and feeding cues. For example, the unborn fetus is exposed to fluctuations in maternal core body temperature *in utero*, which – in non-pregnant women – shows a circadian rhythm with an amplitude of around 0.4–0.5°C (Baker et al., 2001). Whether this rhythm persists during human pregnancy is unknown (Mark et al., 2017). Likewise, 24-h variations in the levels of circulating hormones, such as melatonin, may promote circadian entrainment of the unborn fetus (McCarthy et al., 2019). Furthermore, as a result of alternating periods of eating and fasting of the mother during pregnancy, the unborn fetus will be exposed to 24-h variations in nutrients, metabolites, and metabolic hormones, which may also function as timing cues for the circadian system (Wehrens et al., 2017; Lewis et al., 2020). In the NICU, where neonates typically receive intermittent or continuous feeding, this rhythmicity is largely lost. Therefore, optimizing 24 h rhythms in the environment – in the broadest sense – may be an opportunity to further improve a preterm infant's health and development.

Much remains unknown regarding the mechanisms underlying the effect of environmental light/dark cycles on clinical outcomes in preterm infants. Based on the developmental timeline of the visual and circadian system, it seems that prematurely born infants, even those born extremely preterm, are functionally capable to sense light to some degree, since most of the photoreceptors and opsins are present during early gestation. With the formation of both the RHT and the SCN during the second trimester, the circadian system is at least partially functional from gestational week 24 onward.

Taken together, as the survival rate of preterm infants continues to rise, it becomes increasingly important to focus on optimizing the NICU environment and thereby help improve preterm infants' health and wellbeing later in life. Several studies show beneficial effects of cycled light over constant light conditions, and a systematic review on the topic is cautiously positive (Morag and Ohlsson, 2016). For these findings to be implemented, larger studies are necessary, preferably with a long term follow-up and more precise reporting of experimental light conditions, such as the spectral composition of light. In this context, the minimal reporting guidelines for studies involving lighting interventions recently developed by Spitschan et al. (2019) may be helpful. In parallel, fundamental research should focus on providing a mechanistic understanding of these findings. Furthermore, the effect of other rhythmic timing cues such as temperature and feeding on clinical outcomes in preterm infants are a promising avenue to investigate in future studies.

AUTHOR CONTRIBUTIONS

EH and LK wrote and revised the manuscript. JD and JM revised the manuscript. All authors contributed to the article and approved the submitted version.

FUNDING

This work was supported by the Velux Stiftung (grant number 1131 to JM), the Netherlands Organization for Scientific Research (NWO; grant number ALWOP.389 to JM), and the European Research Council (ERC) under the European Union's Horizon 2020 Research and Innovation Program (grant number 834513 Diurnal health ERC-2018-ADG to JM).

ACKNOWLEDGMENTS

The authors are grateful to Dr. Stephan Michel and Dr. Nicolette Ognjanovski for proofreading an earlier version of this manuscript.

REFERENCES

Andescavage, N. N., Du Plessis, A., McCarter, R., Serag, A., Evangelou, I., Vezina, G., et al. (2017). Complex trajectories of brain development in the healthy human fetus. *Cereb. Cortex* 27, 5274–5283. doi: 10.1093/cercor/bhw306

Aucott, S., Donohue, P. K., Atkins, E., and Allen, M. C. (2002). Neurodevelopmental care in the NICU. *Ment. Retard. Dev. Disabil. Res. Rev.* 8, 298–308. doi: 10.1002/mrdd.10040

Baker, F. C., Waner, J. I., Vieira, E. F., Taylor, S. R., Driver, H. S., and Mitchell, D. (2001). Sleep and 24 hour body temperatures: a comparison in young men, naturally cycling women and women taking hormonal contraceptives. *J. Physiol.* 530, 565–574. doi: 10.1111/j.1469-7793.2001.0565k.x

Barrionuevo, P. A., Nicandro, N., McAnany, J. J., Zele, A. J., Gamlin, P., and Cao, D. (2014). Assessing rod, cone, and melanopsin contributions to human pupil flicker responses. *Investig. Ophthalmol. Vis. Sci.* 55, 719–727. doi: 10.1167/iovs.13-13252

Bates, K., and Herzog, E. D. (2020). Maternal-fetal circadian communication during pregnancy. *Front. Endocrinol. (Lausanne)* 11:198. doi: 10.3389/fendo.2020.00198

Best, K., Bogossian, F., and New, K. (2018). Sensory exposure of neonates in single-room environments (SENSE): an observational study of light. *Arch. Dis.*

Child Fetal Neonatal. Ed. 103, F436–F440. doi: 10.1136/archdischild-2017-312977

Blackburn, S., and Patteson, D. (1991). Effects of cycled light on activity state and cardiorespiratory function in preterm infants. *J. Perinat. Neonatal Nurs.* 4, 47–54. doi: 10.1097/00005237-199103000-00009

Boo, N. Y., Chee, S. C., and Rohana, J. (2002). Randomized controlled study of the effects of different durations of light exposure on weight gain by preterm infants in a neonatal intensive care unit. *Acta Paediatr. Int. J. Paediatr.* 91, 674–679. doi: 10.1080/080352502760069106

Borniger, J. C., McHenry, Z. D., Abi Salloum, B. A., and Nelson, R. J. (2014). Exposure to dim light at night during early development increases adult anxiety-like responses. *Physiol. Behav.* 133, 99–106. doi: 10.1016/j.physbeh.2014.05.012

Brandon, D. H., Holditch-Davis, D., and Belyea, M. (2002). Preterm infants born at less than 31 weeks' gestation have improved growth in cycled light compared with continuous near darkness. *J. Pediatr.* 140, 192–199. doi: 10.1067/mpd.2002.121932

Brandon, D. H., Silva, S. G., Park, J., Malcolm, W., Kamhawy, H., and Holditch-Davis, D. (2017). Timing for the introduction of cycles light for extermely preterm infants: a randomized controlled trial. *Res. Nurses Heal.* 40, 294–310. doi: 10.1109/EMBC.2016.7590696.Upper

Bueno, C., and Menna-Barreto, L. (2016). Environmental factors influencing biological rhythms in newborns: from neonatal intensive care units to home. *Sleep Sci.* 9, 295–300. doi: 10.1016/j.slsci.2016.10.004

Cai, C., Vandermeer, B., Khurana, R., Nerenberg, K., Featherstone, R., Sebastianski, M., et al. (2019). The impact of occupational shift work and working hours during pregnancy on health outcomes: a systematic review and meta-analysis. *Am. J. Obstet. Gynecol.* 221, 563–576. doi: 10.1016/j.ajog.2019.06.051

Chen, S. K., Badea, T. C., and Hattar, S. (2011). Photoentrainment and pupillary light reflex are mediated by distinct populations of ipRGCs. *Nature* 476, 92–96. doi: 10.1038/nature10206

Cissé, Y. M., Russart, K. L. G., and Nelson, R. J. (2017a). Depressive-like behavior is elevated among offspring of parents exposed to dim light at night prior to mating. *Phychoneuroendocrinology* 83, 182–186. doi: 10.1016/j.physbeh.2017.03.040

Cissé, Y. M., Russart, K. L. G., and Nelson, R. J. (2017b). Parental exposure to dim light at night prior to mating alters offspring adaptive immunity. *Sci. Rep.* 7:45497. doi: 10.1038/srep45497

Dibner, C., Schibler, U., and Albrecht, U. (2010). The mammalian circadian timing system : organization and coordination of central and peripheral clocks. *Annu. Rev. Physiol.* 72, 517–549. doi: 10.1146/annurev-physiol-021909-135821

Farahani, E. A., Nourian, M., Ahmadi, F., and Kazemian, M. (2018). Comparing the effects of cycles and constant lighting on weight gain and length of stay in neonatal intensive care unit among premature neonates: a two-group randomized controlled clinical trial. *Nurs. Midwifery Stud.* 7, 93–99. doi: 10.4103/nms.nms

Fielder, A. R., and Moseley, M. J. (2000). Environmental light and the Preterm infant. *Semin. Perinatol.* 24, 291–298. doi: 10.1053/spen2000.8597

Guyer, C., Huber, R., Fontijn, J., Bucher, H. U., Nicolai, H., Werner, H., et al. (2012). Cycled light exposure reduces fussing and crying in very preterm infants. *Pediatrics* 130, e145–e151. doi: 10.1542/peds.2011-2671

Guyer, C., Huber, R., Fontijn, J., Bucher, H. U., Nicolai, H., Werner, H., et al. (2015). Very preterm infants show earlier emergence of 24-hour sleep-wake rhythms compared to term infants. *Early Hum. Dev.* 91, 37–42. doi: 10.1016/j.earlhumdev.2014.11.002

Hao, H., and Rivkees, S. A. (1999). The biological clock of very premature primate infants is responsive to light. *Proc. Natl. Acad. Sci. U.S.A.* 96, 2426–2429. doi: 10.1073/pnas.96.5.2426

Hay, W. W. (2017). Optimizing nutrition of the preterm infant. *Chin. J. Contemp. Pediatr.* 19, 1–21. doi: 10.7499/j.issn.1008-8830.2017.01.001

Hendrickson, A. E., and Yuodelis, C. (1984). The morphological development of the human fovea. *Ophthalmology* 91, 603–612. doi: 10.1016/S0161-6420(84)34247-6

Hoppenbrouwers, T., Oliveira, F., Sandarupa, S., Khoo, M., Neuman, M., and Ramanathan, R. (2012). The development of the circadian heart rate rhythm (CHR) in Asian infants. *Early Hum. Dev.* 88, 555–561. doi: 10.1016/j.earlhumdev.2011.12.031

Hughes, S., Jagannath, A., Hankins, M. W., Foster, R. G., and Peirson, S. N. (2015). *Photic Regulation of Clock Systems*, 1st Edn, Vol. 552. Amsterdam: Elsevier Inc. doi: 10.1016/bs.mie.2014.10.018

Jenni, O. G., Deboer, T., and Achermann, P. (2006). Development of the 24-h rest-activity pattern in human infants. *Infant Behav. Dev.* 29, 143–152. doi: 10.1016/j.infbeh.2005.11.001

Kennaway, D. J., Stamp, G. E., and Goble, F. C. (1992). Development of melatonin production in infants and the impact of prematurity. *J. Clin. Endocrinol. Metab.* 75, 367–369.

Kervezee, L., Shechter, A., and Boivin, D. B. (2018). Impact of shift work on the circadian timing system and health in women. *Sleep Med. Clin.* 13, 295–306. doi: 10.1016/j.jsmc.2018.04.003

La Morgia, C., Carelli, V., and Carbonelli, M. (2018). Melanopsin retinal ganglion cells and pupil: clinical implications for neuro-ophthalmology. *Front. Neurol.* 9:1047. doi: 10.3389/fneur.2018.01047

Lebel, V., Aita, M., Johnston, C., Heón, M., and Dupuis, F. (2017). Effects of cycled lighting versus continuous near darkness on physiological stability and motor activity level in preterm infants. *Adv. Neonatal Care* 17, 282–291. doi: 10.1097/ANC.0000000000000372

Lewis, P., Oster, H., Korf, H. W., Foster, R. G., and Erren, T. C. (2020). Food as a circadian time cue — evidence from human studies. *Nat. Rev. Endocrinol.* 16, 213–223. doi: 10.1038/s41574-020-0318-z

Man, G. C. W., Zhang, T., Chen, X., Wang, J., Wu, F., Liu, Y., et al. (2017). The regulations and role of circadian clock and melatonin in uterine receptivity and pregnancy—an immunological perspective. *Am. J. Reprod. Immunol.* 78:e12715. doi: 10.1111/aji.12715

Mann, N. P., Haddow, R., Stokes, L., Goodley, S., and Rutter, N. (1986). Effect of night and day on preterm infants in a newborn nursery: randomised trial. *Br. Med. J. (Clin. Res. Ed.)* 293, 1265–1267. doi: 10.1136/bmj.293.6557.1265

Mark, P. J., Crew, R. C., Wharfe, M. D., and Waddell, B. J. (2017). Rhythmic three-part harmony: the complex interaction of maternal, placental and fetal circadian systems. *J. Biol. Rhythms* 32, 534–549. doi: 10.1177/0748730417728671

Matthews, L. G., Walsh, B. H., Knutsen, C., Neil, J. J., Smyser, C. D., Rogers, C. E., et al. (2018). Brain growth in the NICU: critical periods of tissue-specific expansion. *Pediatr. Res.* 83, 976–981. doi: 10.1038/pr.2018.4

McCarthy, R., Jungheim, E. S., Fay, J. C., Bates, K., Herzog, E. D., and England, S. K. (2019). Riding the rhythm of melatonin through pregnancy to deliver on time. *Front. Endocrinol. (Lausanne)* 10:616. doi: 10.3389/fendo.2019.00616

Miller, C. L., White, R., Whitman, T. L., O'Callaghan, M. F., and Maxwell, S. E. (1995). The effects of cycled versus noncycled lighting on growth and development in preterm infants. *Infant Behav. Dev.* 18, 87–95. doi: 10.1016/0163-6383(95)90010-1

Mirmiran, M., Baldwin, R. B., and Ariagno, R. L. (2003). Circadian and sleep development in preterm infants occurs independently from the influences of environmental lighting. *Pediatr. Res.* 53, 933–938. doi: 10.1203/01.PDR.0000061541.94620.12

Morag, I., and Ohlsson, A. (2016). Cycled light in the intensive care unit for preterm and low birth weight infants. *Cochrane Database Syst. Rev.* 2016:CD006982. doi: 10.1002/14651858.CD006982.pub4

Moselhi Mater, E. A., Mahamud, H. S., and Mohamed, M. F. (2019). Effects of eye cover among high risk neonates at night shift on their distress levels. *J. Nurs. Educ. Pract.* 9:9. doi: 10.5430/jnep.v9n7p9

Parraguez, V. H., Sales, F., Valenzuela, G. J., Vergara, M., Catalán, L., and Serón-Ferré, M. (1998). Diurnal changes in light intensity inside the pregnant uterus in sheep. *Anim. Reprod. Sci.* 52, 123–130. doi: 10.1016/S0378-4320(98)00094-3

Petersen, S. A., and Wailoo, M. P. (1994). Interactions between infant care practices and physiological development in Asian infants. *Early Hum. Dev.* 38, 181–186. doi: 10.1016/0378-3782(94)90210-0

Platt, M. J. (2014). Outcomes in preterm infants. *Public Health* 128, 399–403. doi: 10.1016/j.puhe.2014.03.010

Rao, S., Chun, C., Fan, J., Kofron, J. M., Yang, M. B., Hegde, R. S., et al. (2013). A direct and melanopsin-dependent fetal light response regulates mouse eye development. *Nature* 494, 243–246. doi: 10.1038/nature11823

Reppert, S. M., and Schwartz, W. J. (1984). Functional activity of the suprachiasmatic nuclei in the fetal primate. *Neurosci. Lett.* 46, 145–149. doi: 10.1016/0304-3940(84)90432-4

Reppert, S. M., Weaver, D. R., Rivkees, S. A., and Stopa, E. G. (1988). Putative melatonin receptors in a human biological clock. *Science* 242, 78–81. doi: 10.1126/science.2845576

Rivkees, S. A. (2007). The development of circadian rhythms: from animals to humans. *Sleep Med. Clin.* 2, 331–341. doi: 10.1016/j.jsmc.2007.05.010

Rivkees, S. A., Hofman, P. L., and Fortman, J. (1997). Newborn primate infants are entrained by low intensity lighting. *Proc. Natl. Acad. Sci. U.S.A.* 94, 292–297. doi: 10.1073/pnas.94.1.292

Rivkees, S. A., and Lachowicz, J. E. (1997). Functional D1 and D5 dopamine receptors are expressed in the suprachiasmatic, supraoptic, and paraventricular nuclei of primates. *Synapse* 26, 1–10. doi: 10.1002/(SICI)1098-2396(199705)26:1<1::AID-SYN1>3.0.CO;2-D

Rivkees, S. A., Mayes, L., Jacobs, H., and Gross, I. (2004). Rest-activity patterns of premature infants are regulated by cycled lighting. *Pediatrics* 113, 833–840.

Robinson, J., Bayliss, S. C., and Fielder, A. R. (1991). Transmission of light across the adult and neonatal eyelid in vivo. *Vision Res.* 31, 1837–1840. doi: 10.1016/0042-6989(91)90031-Y

Robinson, J., and Fielder, A. R. (1990). Pupillary diameter and reaction to light in preterm neonates. *Arch. Dis. Child.* 65, 35–38. doi: 10.1136/adc.65.1_Spec_No.35

Salazar, E. R., Richter, H. G., Spichiger, C., Mendez, N., Halabi, D., Vergara, K., et al. (2018). Gestational chronodisruption leads to persistent changes in the rat fetal and adult adrenal clock and function. *J. Physiol.* 596, 5839–5857. doi: 10.1113/JP276083

Santos, J., Pearce, S. E., and Stroustrup, A. (2016). Impact of hospital-based environmental exposures on neurodevelopmental outcomes of preterm infants. *Curr. Opin. Pediatr.* 27, 254–260. doi: 10.1097/MOP.0000000000000190. Impact

Sekaran, S., Lupi, D., Jones, Sl, Sheely, C., Hattar, S., Yau, K. W., et al. (2005). Melanopsin dependent photoreception providec earliest light detection in the mammalian retina. *Curr. Biol.* 15, 1099–1107. doi: 10.1016/j.cub.2005.05.053

Serón-Ferré, M., Mendez, N., Abarzua-Catalan, L., Vilches, N., Valenzuela, F. J., Reynolds, H. E., et al. (2012). Circadian rhythms in the fetus. *Mol. Cell Endocrinol.* 349, 68–75. doi: 10.1016/j.mce.2011.07.039

Serón-Ferré, M., Torres-Farfán, C., Forcelledo, M. L., and Valenzuela, G. J. (2001). The development of circadian rhythms in the fetus and neonate. *Semin. Perinatol.* 25, 363–370. doi: 10.1053/sper.2001.29037

Smarr, B. L., Grant, A. D., Perez, L., Zucker, I., and Kriegsfeld, L. J. (2017). Maternal and early-life circadian disruption have long-lasting negative consequences on offspring development and adult behavior in mice. *Sci. Rep.* 7, 1–12. doi: 10.1038/s41598-017-03406-4

Sollars, P. J., and Pickard, G. E. (2015). The neurobiology of circadian rhythms. *Psychiatr. Clin. North Am.* 33, 395–401. doi: 10.1038/nbt.3121.ChIP-nexus

Spitschan, M., Jain, S., Brainard, D. H., and Aguirre, G. K. (2014). Opponent melanopsin and S-cone signals in the human pupillary light response. *Proc. Natl. Acad. Sci. U.S.A.* 111, 15568–15572. doi: 10.1073/pnas.1400942111

Spitschan, M., Stefani, O., Blattner, P., Gronfier, C., Lockley, S., and Lucas, R. (2019). How to report light exposure in human chronobiology and sleep research experiments. *Clocks Sleep* 1, 280–289. doi: 10.3390/clockssleep1030024

Stouffer, R. L., and Woodruff, T. K. (2017). Nonhuman primates: a vital model for basic and applied research on female reproduction, prenatal development, and women's health. *ILAR J.* 58, 281–294. doi: 10.1093/ilar/ilx027

Summa, K. C., Vitaterna, M. H., and Turek, F. W. (2012). Environmental perturbation of the Circadian clock disrupts pregnancy in the mouse. *PLoS One* 7:e37668. doi: 10.1371/journal.pone.0037668

Swaab, D. F. (1995). Development of the human hypothalamus. *Neurochem. Res.* 20, 509–519. doi: 10.1007/BF01694533

Symington, A. J., and Pinelli, J. (2006). Developmental care for promoting development and preventing morbidity in preterm infants. *Cochrane Database Syst. Rev.* 2006:CD001814. doi: 10.1002/14651858.cd001814.pub2

Tarttelin, E. E., Bellingham, J., Bibb, L. C., Foster, R. G., Hankins, M. W., Gregory-Evans, K., et al. (2003). Expression of opsin genes early in ocular development of humans and mice. *Exp. Eye Res.* 76, 393–396. doi: 10.1016/S0014-4835(02)00300-7

Twilhaar, E. S., Wade, R. M., De Kieviet, J. F., Van Goudoever, J. B., Van Elburg, R. M., and Oosterlaan, J. (2018). Cognitive outcomes of children born extremely or very preterm since the 1990s and associated risk factors: a meta-analysis and meta-regression. *JAMA Pediatr.* 172, 361–367. doi: 10.1001/jamapediatrics.2017.5323

Van Cruchten, S., Vrolyk, V., Perron Lepage, M. F., Baudon, M., Voute, H., Schoofs, S., et al. (2017). Pre- and postnatal development of the eye: a species comparison. *Birth Defects Res.* 109, 1540–1567. doi: 10.1002/bdr2.1100

van den Hoogen, A., Teunis, C. J., Shellhaas, R. A., Pillen, S., Benders, M., and Dudink, J. (2017). How to improve sleep in a neonatal intensive care unit: a systematic review. *Early Hum. Dev.* 113, 78–86. doi: 10.1016/j.earlhumdev.2017.07.002

Van Diepen, H. C., Ramkisoensing, A., Peirson, S. N., Foster, R. G., and Meijer, J. H. (2013). Irradiance encoding in the suprachiasmatic nuclei by rod and cone photoreceptors. *FASEB J.* 27, 4204–4212. doi: 10.1096/fj.13-233098

Vásquez-Ruiz, S., Maya-Barrios, J. A., Torres-Narváez, P., Vega-Martínez, B. R., Rojas-Granados, A., Escobar, C., et al. (2014). A light/dark cycle in the NICU accelerates body weight gain and shortens time to discharge in preterm infants. *Early Hum. Dev.* 90, 535–540. doi: 10.1016/j.earlhumdev.2014.04.015

Ward, R. M., and Beachy, J. C. (2003). Neonatal complications following preterm birth. *BJOG An. Int. J. Obstet. Gynaecol.* 110(Suppl. 20), 8–16. doi: 10.1016/S1470-0328(03)00012-0

Watanabe, S., Akiyama, S., Hanita, T., Li, H., Nakagawa, M., Kaneshi, Y., et al. (2013). Designing artificial environments for preterm infants based on circadian studies on pregnant uterus. *Front. Endocrinol. (Lausanne)* 4:113. doi: 10.3389/fendo.2013.00113

Wehrens, S. M. T., Christou, S., Isherwood, C., Middleton, B., Gibbs, M. A., Archer, S. N., et al. (2017). Meal timing regulates the human circadian system. *Curr. Biol.* 27, 1768–1775.e3. doi: 10.1016/j.cub.2017.04.059

White, R. D., Smith, J. A., and Shepley, M. M. (2013). Recommended standards for newborn ICU design, eighth edition. *J. Perinatol.* 33(Suppl. 1), S2–S16. doi: 10.1038/jp.2013.10

World Health Organization, (2012). *Born Too Soon the Global Action Report on Preterm Birth*. Geneva: World Health Organization.

Zeitlin, J., Ancel, P. Y., Delmas, D., Bréart, G., Papiernik, E., and Epipage and Mosaic Ile-de-France Groups. (2010). Changes in care and outcome of very preterm babies in the Parisian region between 1998 and 2003. *Arch. Dis. Child. Fetal Neonatal Ed.* 95, 188–193. doi: 10.1136/adc.2008.156745

Conflict of Interest: The authors declare that the research was conducted in the absence of any commercial or financial relationships that could be construed as a potential conflict of interest.

frontiers in Neuroscience

REVIEW
published: 23 March 2021
doi: 10.3389/fnins.2021.659974

Genesis of the Master Circadian Pacemaker in Mice

Arthur H. Cheng[1,2] and Hai-Ying Mary Cheng[1,2]**

[1] Department of Biology, University of Toronto Mississauga, Mississauga, ON, Canada, [2] Department of Cell and Systems Biology, University of Toronto, Toronto, ON, Canada

The suprachiasmatic nucleus (SCN) of the hypothalamus is the central circadian clock of mammals. It is responsible for communicating temporal information to peripheral oscillators via humoral and endocrine signaling, ultimately controlling overt rhythms such as sleep-wake cycles, body temperature, and locomotor activity. Given the heterogeneity and complexity of the SCN, its genesis is tightly regulated by countless intrinsic and extrinsic factors. Here, we provide a brief overview of the development of the SCN, with special emphasis on the murine system.

Keywords: suprachiasmatic nucleus, neurogenesis, development, neuronal differentiation, transcription factors, neuropeptides

OPEN ACCESS

Edited by:
Daisuke Ono,
Nagoya University, Japan

Reviewed by:
Michihiro Mieda,
Kanazawa University, Japan
Charles N. Allen,
Oregon Health and Science University, United States

****Correspondence:***
Arthur H. Cheng
ahh.cheng@mail.utoronto.ca
Hai-Ying Mary Cheng
haiying.cheng@utoronto.ca

Specialty section:
This article was submitted to Sleep and Circadian Rhythms, a section of the journal Frontiers in Neuroscience

Received: *28 January 2021*
Accepted: *04 March 2021*
Published: *23 March 2021*

Citation:
Cheng AH and Cheng H-YM (2021) Genesis of the Master Circadian Pacemaker in Mice. Front. Neurosci. 15:659974. doi: 10.3389/fnins.2021.659974

INTRODUCTION

On this rhythmic planet, we are surrounded by countless environmental oscillations of varying frequencies. The most notable of all rhythms is the 24 h day-night cycle, which results in predictable changes in the availability of light, warmth, and sustenance. In order to thrive, organisms must be able to anticipate and prepare for daily rhythmic events in the environment, rather than simply reacting to them upon their detection. From bacteria to humans, organisms evolved circadian clocks to keep track of time, enabling them to prepare for external challenges and opportunities through temporal coordination of behavior and physiology.

In mammals, circadian rhythms are driven by a hierarchy of tissue-specific oscillators throughout the body, orchestrated by a central circadian pacemaker, the hypothalamic suprachiasmatic nuclei (SCN). Individual SCN neurons synthesize neuropeptides and neurotransmitters to coordinate endogenous oscillations and entrainment at the tissue level (Aton et al., 2005; Maywood et al., 2011; Mieda et al., 2015). The SCN is unique within the clock hierarchy, as it is the only clock to respond to light directly (Morin and Allen, 2006). The SCN (oscillator) receives and integrates time cues (input) from the environment, and communicates temporal information to peripheral oscillators via humoral and endocrine signaling. Ultimately, the SCN coordinates and controls overt rhythms (outputs) such as sleep-wake cycles, body temperature, osmoregulation, hormone secretion, and gastrointestinal, hepatic, and cardiac functions (Roenneberg and Merrow, 2016). As the biological clock coordinates nearly all physiological processes, perturbation of the circadian system constitutes a risk factor for a myriad of disorders, including obesity, diabetes, cardiovascular disease, cancer, and neurodegeneration (Kurose et al., 2011; Uth and Sleigh, 2014; Broussard and Van Cauter, 2016; Melo et al., 2016; Khaper et al., 2018; Musiek et al., 2018). Conversely, many pathological conditions (e.g., Alzheimer's disease, cancer) contribute to circadian disruption, which further exacerbates them (Lim et al., 2014). By expanding our knowledge and mechanistic understanding of the circadian clock, we position ourselves to develop new strategies that leverage the circadian system to promote better physical and mental health.

TRANSCRIPTION-TRANSLATION FEEDBACK LOOP/THE MOLECULAR CLOCK

The molecular clock machinery relies on a series of transcription-translation feedback loops (TTFLs) that generate rhythmic expression of "clock genes" through a negative feedback mechanism. In mammals, the positive limb of the core feedback loop consists of the basic helix-loop-helix PAS transcription factors, Circadian locomotor output cycles kaput (CLOCK) and Brain and muscle ARNT-like protein 1 (BMAL1) (**Figure 1**). During the subjective day, CLOCK and BMAL1 dimerize and bind to the E-box elements in Period (*Per1*, *Per2*) and Cryptochrome (*Cry1*, *Cry2*) promoters, inducing their transcription (Shearman et al., 1997; Gekakis et al., 1998; Kume et al., 1999; Bunger et al., 2000; Vitaterna et al., 2006). During the subjective night, PER and CRY protein heterodimers translocate from the cytoplasm to the nucleus, where they repress their own gene transcription through inhibition of CLOCK:BMAL1 (Kume et al., 1999; Vitaterna et al., 1999; Zheng et al., 1999, 2001; Shearman et al., 2000). PER proteins are degraded during the late subjective night, but CRY continues to accumulate in the nucleus and maintains the repressive phase of the cycle (Ye et al., 2014). In the early subjective day, the degradation of CRY results in the derepression of CLOCK:BMAL1-mediated transcription and thus a new round of E-box-dependent gene expression (Gekakis et al., 1998; Kume et al., 1999). This core clock circuitry is regulated by secondary feedback loops. For example, the transcription of *Bmal1* is positively and negatively regulated by the nuclear orphan receptors, ROR (α, β, and γ) and REV-ERB (α and β), respectively, which are themselves E-box-containing genes and are therefore controlled by the primary feedback loop (Preitner et al., 2002; Sato et al., 2004; Guillaumond et al., 2005). Together, the primary and secondary TTFLs drive the ∼24 h oscillation of the molecular clock, while additional layers of regulation (described in the following sections) ensure its stability and robustness.

SCN STRUCTURE AND CONNECTIVITY

As it is currently understood, the SCN is responsible for interpreting photic and non-photic signals that it receives from afferent projections, and ultimately produces a coherent temporal output to peripheral oscillators through humoral and neuroendocrine mechanisms. Each individual SCN neuron harbors the clock machinery and is able to maintain robust molecular rhythms on a single-cell level. Through neuropeptide, neurotransmitter, and synaptic signaling, SCN neurons form an intricately connected oscillatory network with astounding precision and resilience.

The SCN is a pair of nuclei located in the anterior hypothalamus, situated directly dorsal to the optic chiasm and lateral to the third ventricle. It is comprised of approximately 20,000 heterogenous neurons that secrete dozens of neuropeptides, neurotransmitters, and cytokines, many of which can be at least partially co-expressed by certain populations of SCN neurons (**Figure 2**; Abrahamson and Moore, 2001; Cheng et al., 2002; Antle and Silver, 2005; Todd et al., 2020; Wen et al., 2020). The SCN is classically divided into two subregions, a light-responsive ventrolateral "core" and a rhythmic dorsomedial "shell," based on the neurochemical nature of cells in each area and its physiological function (Aton et al., 2005). SCN core neurons are characterized by expression of vasoactive intestinal peptide (VIP), gastrin releasing peptide (GRP), calbindin, calretinin, neuromedin S (NMS), and neurotensin (Abrahamson and Moore, 2001; Lee et al., 2015). In contrast, SCN shell neurons express arginine vasopressin (AVP), calbindin, NMS, angiotensin II, and met-enkephalin (Abrahamson and Moore, 2001; Lee et al., 2015). All SCN neurons synthesize γ-aminobutyric acid (GABA) as the main neurotransmitter in addition to the neuropeptidergic signals (Moore and Speh, 1993; Abrahamson and Moore, 2001).

In addition to neurons, astrocytes in the murine SCN also contribute to circadian timekeeping. Astrocytes have been shown to display daily rhythms in structural protein expression, morphology, metabolic function, and clock gene expression (Prolo et al., 2005; Becquet et al., 2008; Cheng et al., 2009; Burkeen et al., 2011). Astrocyte-specific ablation of *Bmal1* lengthens the period of clock gene oscillations and locomotor behavior (Barca-Mayo et al., 2017; Tso et al., 2017). Furthermore, excision of the short-period CK1ε tau mutation specifically from SCN astrocytes lengthens molecular and behavioral rhythms (Brancaccio et al., 2017; Tso et al., 2017). It has been shown that SCN astrocytes control circadian period by regulating GABA uptake and glutamatergic signaling (Barca-Mayo et al., 2017; Brancaccio et al., 2017, 2019). Recently, Sominsky et al. (2021) reported that microglia are another important component for maintaining clock gene expression and behavioral rhythms. By expressing the diphtheria toxin (DT) receptor specifically in fractalkine receptor-positive cells (*Cx3cr1*$^{+}$), 94% of SCN microglia was acutely ablated in transgenic Wistar rats (Sominsky et al., 2021). This resulted in pronounced disruption of behavioral rhythms, circadian temperature profiles, and *Per1* and BMAL1 expression (Sominsky et al., 2021).

As the master circadian clock, the SCN is intricately connected with many regions of the brain to regulate the phase and period of circadian rhythms. The SCN has three major afferent connections: retinohypothalamic tract (RHT) projections from the retina, geniculohypothalamic tract (GHT) projections from the intergeniculate leaflet (IGL), and serotonergic projections from the median raphe nucleus (MnR) in the brainstem (Meyer-Bernstein and Morin, 1996; Mintz et al., 1997; Abrahamson and Moore, 2001). Photic information received by intrinsically photosensitive retinal ganglion cells (ipRGCs) is delivered to the SCN through the RHT (Do and Yau, 2010). Although the terminal fields of the RHT can be found in all parts of the murine SCN, the core region has denser retinal innervation compare to the SCN shell (Morin et al., 2006). IpRGC input is essential for SCN light entrainment, which occurs through the release of glutamate, aspartate, and the neuropeptide pituitary adenylate cyclase-activating polypeptide (PACAP) (Chen et al., 1999; Guido et al., 1999; Kawaguchi et al., 2003; Hannibal et al., 2008). In contrast, the IGL innervates the SCN with neuropeptide

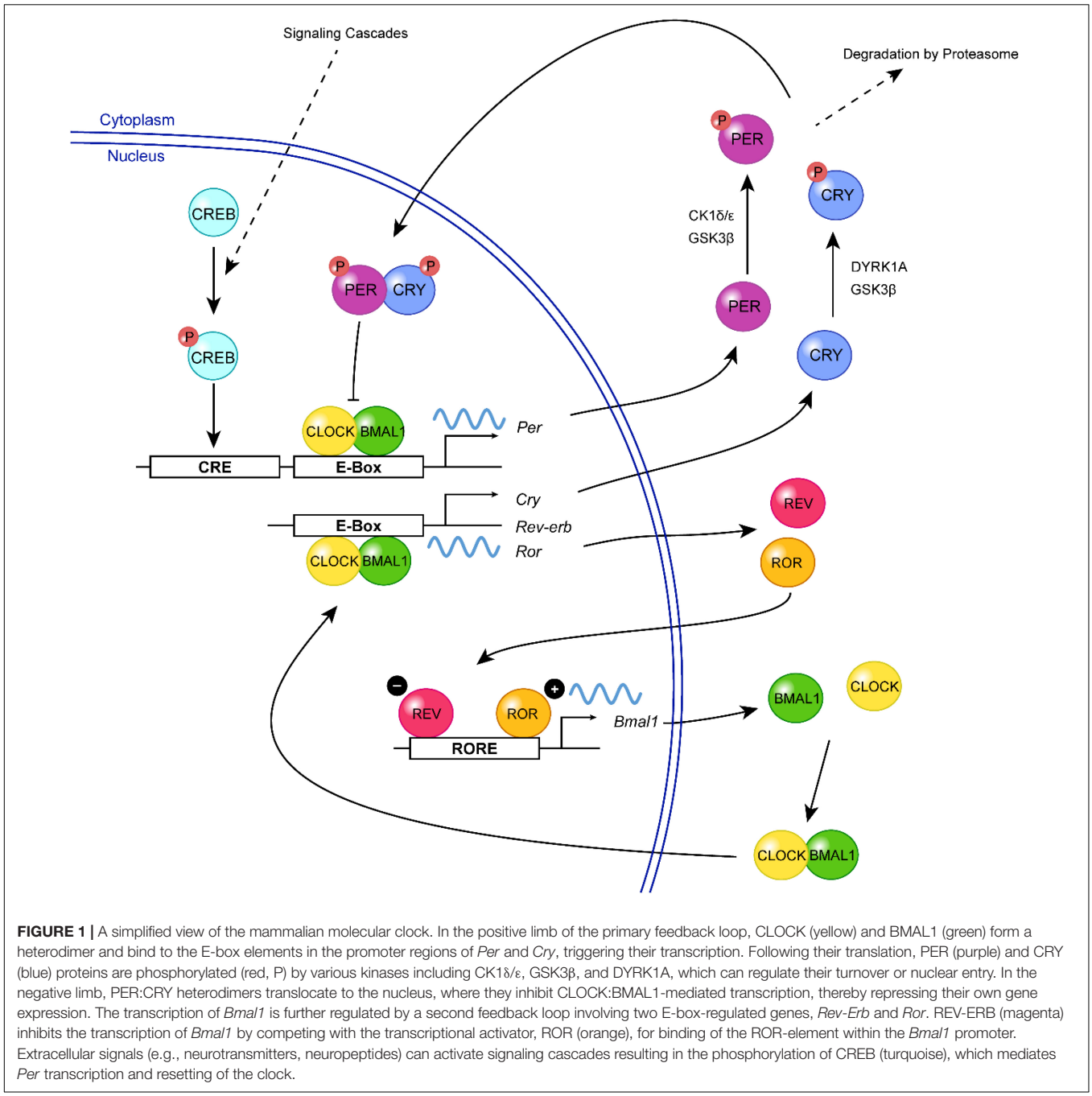

FIGURE 1 | A simplified view of the mammalian molecular clock. In the positive limb of the primary feedback loop, CLOCK (yellow) and BMAL1 (green) form a heterodimer and bind to the E-box elements in the promoter regions of *Per* and *Cry*, triggering their transcription. Following their translation, PER (purple) and CRY (blue) proteins are phosphorylated (red, P) by various kinases including CK1δ/ε, GSK3β, and DYRK1A, which can regulate their turnover or nuclear entry. In the negative limb, PER:CRY heterodimers translocate to the nucleus, where they inhibit CLOCK:BMAL1-mediated transcription, thereby repressing their own gene expression. The transcription of *Bmal1* is further regulated by a second feedback loop involving two E-box-regulated genes, *Rev-Erb* and *Ror*. REV-ERB (magenta) inhibits the transcription of *Bmal1* by competing with the transcriptional activator, ROR (orange), for binding of the ROR-element within the *Bmal1* promoter. Extracellular signals (e.g., neurotransmitters, neuropeptides) can activate signaling cascades resulting in the phosphorylation of CREB (turquoise), which mediates *Per* transcription and resetting of the clock.

Y (NPY) and GABA terminals (Moore et al., 2002). As with RHT terminals, NPY terminals are concentrated in the ventro-central region of the SCN and are sparser in the dorsomedial region (Morin et al., 2006). The IGL plays a significant role in relaying photic and non-photic information to the SCN, as either IGL lesions or NPY infusion into the SCN can alter circadian rhythms (Albers and Ferris, 1984; Pickard et al., 1987). The SCN also receives serotonergic projections from the MnR, where the plexus appears to be densest along the medial and ventral SCN border, grading to sparse innervation centrally and dorsolaterally (Morin et al., 2006). Notably, all three major SCN inputs significantly overlap in the core SCN, reflecting its key role in integrating luminance information from the retina and non-photic input from the midbrain arousal center during entrainment. In addition to these three major afferents, ∼35 brain regions have been shown to project to the SCN: these include other hypothalamic nuclei, the amygdalohippocampal zone, and brainstem nuclei (Krout et al., 2002). However, relatively few SCN afferent systems have been explored in terms of their rhythm-related functions. On the other hand, SCN efferents innervate ∼15 brain regions, likely carrying circadian rhythm phase information to distal targets. Notably, the SCN

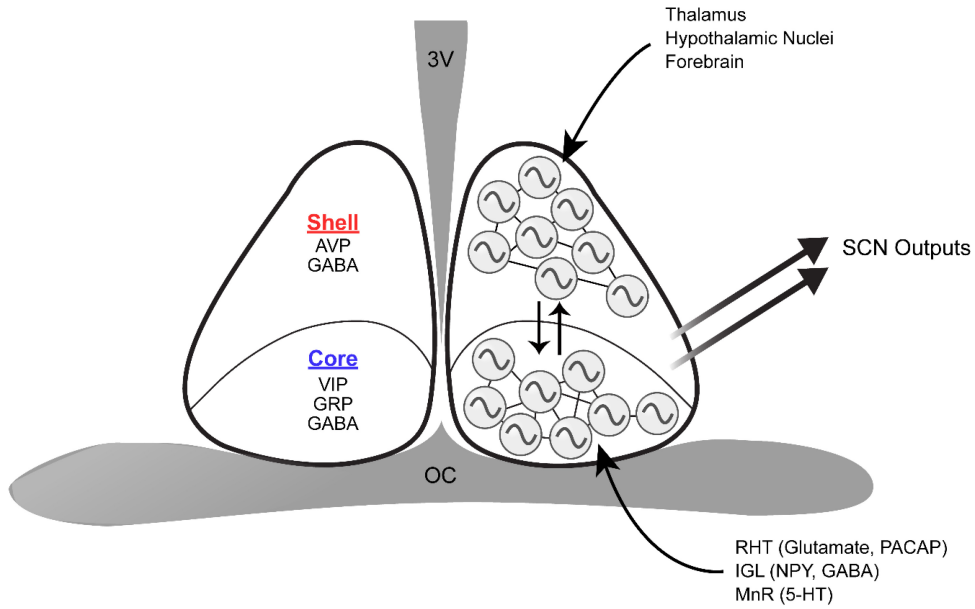

FIGURE 2 | Schematic of the structure and organization of the SCN. The dorsomedial SCN (shell) expresses AVP and GABA, whereas the ventrolateral SCN (core) synthesizes VIP, GRP, and GABA. The retinohypothalamic tract (RHT), intergeniculate leaflet (IGL), and median raphe nucleus (MnR) directly innervate the core. On the other hand, inputs from the thalamus, various hypothalamic nuclei, and the forebrain are mainly received in the shell. Core and shell SCN neurons are synchronized through various means of intercellular communication, and are thus capable of producing coherent outputs to peripheral clocks. 3V, third ventricle; OC, optic chiasm.

projects to many hypothalamic nuclei including the preoptic area, the paraventricular nucleus, the subparaventricular zone, the retrochiasmatic area, the dorsomedial and ventromedial nuclei, and the premammillary area (Watts and Swanson, 1987; Abrahamson and Moore, 2001). These efferent projections from the SCN have been implicated in circadian regulation of body temperature, locomotor activity, sleep-wake cycles, and feeding (Lu et al., 2001; Chou et al., 2003; Abrahamson and Moore, 2006). Neuropeptides such as prokineticin 2 (PROK2) have been shown to serve as functional outputs of the SCN, communicating phase information to other brain regions (Cheng et al., 2002). Mice deficient in either PROK2 or its cognate receptor, prokineticin receptor 2 (PROKR2), have a pronounced redistribution of locomotor activity from early night to late night with significantly dampened amplitude (Li et al., 2006; Prosser et al., 2007).

INTRA-SCN COMMUNICATION AND SIGNALING

In vivo or in organotypic cultures, oscillations of SCN neurons are synchronized and coherent, yet follow a consistent pattern of distinct phases and amplitudes. Bioluminescence imaging of SCN explants *in vitro* using *Per1*-LUC or PER2:LUC reporters have shown that the shell region has much more pronounced PER oscillations than the core (Yamaguchi et al., 2003). Circadian cycling of PER expression begins in the dorsomedial periventricular region of the shell, propagates ventrally and laterally to the center of the shell after 4–8 h, and ends in the ventral SCN after 12–15 h (Yamaguchi et al., 2003). However, a minority of cells have been shown to remain ∼12 h out-of-phase with the population mean, potentially allowing multiple, variously phased output signals to be generated (Herzog et al., 1997; Nakamura et al., 2001). This oscillation pattern is preserved from cycle-to-cycle, as well as after pharmacological manipulations that delay or stop the clock, suggesting that SCN coupling is mediated by specific neural circuits instead of a homogeneous coupling scheme (Liu et al., 1997). When challenged by an abrupt phase shift (jet lag), the shell and core SCN exhibit desynchronization and appear to be out-of-phase initially (Nagano et al., 2003; Albus et al., 2005; Nakamura et al., 2005). The phase of the ventral region, measured by either clock gene expression or impulse activity of SCN neurons, shifts rapidly, whereas the dorsal region requires more days to shift and to align with the ventral SCN (Nagano et al., 2003). This finding is consistent with the notion that the core SCN is the compartment that receives photic cues and directs resynchronization of the shell. When cultured at low density, individual SCN neurons can still express robust rhythms autonomously for weeks, showing that they do not require rhythmic input from other cells to oscillate (Welsh et al., 1995). However, dispersed clock cells in the same culture dish display rhythms with varying periods and progressively distinct phase relationships. Dissociating SCN cells thus removes the coupling forces that normally maintain intercellular synchrony at the tissue level.

Three modes of intercellular communication have been established to maintain network stability and coupling of the SCN: chemical synapses, electrical synapses (gap junctions), and paracrine signaling. The most common neurotransmitter

in the SCN is GABA, which is present in all SCN neurons (Moore and Speh, 1993). Although GABA usually elicits spontaneous inhibitory post-synaptic potentials, it may be excitatory in some instances (De Jeu and Pennartz, 2002; Albus et al., 2005; Hee et al., 2008). GABA-mediated excitation is most common at night in the dorsal region of the SCN, a process mediated by Na^+-K^+-Cl^- cotransporter 1 (NKCC1) and K^+-Cl^- cotransporters (KCCs) (De Jeu and Pennartz, 2002; Hee et al., 2008). In Syrian hamsters, blocking excitatory responses of GABA by inhibiting NKCC1 has been shown to attenuate light-induced phase delays during the early subjective night (McNeill et al., 2018). In the SCN, many cellular responses of GABA are driven by ionotropic $GABA_A$ and $G\alpha_{i/o}$−coupled $GABA_B$ receptors (Jiang et al., 1997b; Strecker et al., 1997; Liu and Reppert, 2000; Gribkoff et al., 2003; Belenky et al., 2008). $GABA_A$ receptor-mediated signaling causes phase shifts when applied to dissociated SCN neurons, and daily pulses of GABA synchronizes them (Liu and Reppert, 2000). In addition, GABA signaling is essential for shell and core re-synchronization after a jet lag treatment, as well as for modulating phase shifting responses after a light pulse (Ralph and Menaker, 1985, 1986, 1989; Gillespie et al., 1997, 1999; Albus et al., 2005; Albers et al., 2017). On the other hand, blocking both $GABA_A$ and $GABA_B$ receptors does not affect oscillatory amplitude and synchrony of neurons in SCN slices (Aton et al., 2006). Recently, Barca-Mayo et al. (2017) showed that astrocyte-mediated GABA signaling modulates clock gene expression of cortical neurons *in vitro* (Barca-Mayo et al., 2017).

It is widely accepted that communication between neurons is mediated primarily by Ca^{2+}-dependent synaptic transmission. However, when chemical synaptic transmission is blocked using Ca^{2+}-free medium, periodic and synchronized bursts of action potentials in a large population of SCN neurons can still be detected, indicating that mechanisms other than chemical synaptic transmission may modulate SCN synchrony (Bouskila and Dudek, 1993). It was also noted that metabolic rhythms in the embryonic SCN precede chemical synaptogenesis in rats, indicating that non-synaptic mechanisms may be important in coordinating circadian rhythms (Reppert and Schwartz, 1984). Subsequently, gap junctions (electrical synapses) have been identified in the SCN and found to mediate neuronal coupling (Jiang et al., 1997a; Colwell, 2000; Long et al., 2005; Rash et al., 2007; Wang et al., 2014). Gap junction channels allow the passage of ions and other small molecules between coupled cells and function to connect cells electrically and metabolically. They are formed by two hemichannels, each composed of 6 connexin proteins (Cheung et al., 2014). The majority of neuronal gap junctions in the SCN are miniature gap junctions that are composed of less than 50 connexons comprised primarily of connexin-36 (Cx36) subunits (Rash et al., 2007). Possibly due to the small number of large gap junctions and the predominance of mini-gap junctions, there is limited electrotonic coupling and coupling-mediated spike-for-spike synchronization between SCN neurons (Rash et al., 2007). Cx36 knockout mice have deficits in circadian behavior and electrical coupling between SCN neurons; however, the results are complicated by the global nature of the Cx36 ablation (Long et al., 2005). Blocking gap junctions in SCN slices with carbonoxolone also weakens synchrony of the SCN network (Wang et al., 2014).

The SCN expresses a plethora of neuropeptides, many of which are strongly implicated in SCN coupling. The core SCN and the most prevalent neuropeptide intrinsic to this region—VIP—are vital for maintaining coupling within the SCN. In mice, VIP is released rhythmically from the core and acts through the G-protein coupled, vasoactive intestinal peptide receptor 2 (VPAC2, also known as VIPR2), which is expressed in both the core and the shell SCN (Shinohara et al., 2000; Dardente et al., 2004). *Vip* or *Vpac2* knockout mice display weak behavioral rhythms and often become arrhythmic after a few days in constant darkness (Harmar et al., 2002; Colwell et al., 2003; Aton et al., 2005). Organotypic SCN slices from these mice show suppressed neuronal firing, low amplitude clock gene rhythms, and desynchrony among cells (Cutler et al., 2003; Aton et al., 2005; Brown et al., 2007; Hughes et al., 2008; Maywood et al., 2011). VIP evokes phase shifts in locomotor activity, AVP release, multiunit firing rate, and PER2:LUC rhythms in a phase- and dose-dependent manner (Piggins et al., 1995; Watanabe et al., 2000; Reed et al., 2001; An et al., 2011). Molecularly, VIP-mediated phase shifting requires PKA, PLC, and MAPK signaling pathways, which ultimately converge on the activation of CRE-mediated transcription of clock genes (Nielsen et al., 2002; Meyer-Spasche and Piggins, 2004). Furthermore, VIP has been shown to modulate the strength of electrical synapses, which in turn regulate intercellular coupling (Wang et al., 2014). Intriguingly, studies have demonstrated that VIP can promote network plasticity by destabilizing intercellular synchrony in addition to its role as a synchronizing factor. For instance, application of exogenous VIP at concentrations greater than 100 nM desynchronizes and broadens the phase distribution of cells within the SCN, in particular during the nadir of PER2 expression (An et al., 2013). When microinjected into the SCN during the early subjective day, a phase when VIP does not induce phase shifts, VIP accelerates entrainment of locomotor rhythms to an advanced LD cycle in a jet lag paradigm (An et al., 2013). Although $Vip^{-/-}$ and $Vpac2^{-/-}$ mice have weak behavioral rhythms in DD, their behavioral rhythmicity can be restored by long-term exposure to constant light (An et al., 2013; Hughes et al., 2015). Detailed analyses of $Vpac2^{-/-}$ mice revealed that exposure to LL diminishes the intercellular signaling deficit in these animals, resulting in both improved behavioral rhythms and increased cellular synchrony (Hughes et al., 2015). This is in stark contrast with the disruptive effect of LL on neuronal function and physiological rhythms in animals with a fully functional SCN, where the elevated level of VIP induced by LL might destabilize the circadian pacemaker (Ohta et al., 2005; An et al., 2011).

The core SCN also produces another type of neuropeptide that participates in maintaining cellular synchrony, behavioral rhythmicity, and entrainment—namely, GRP. In mice, GRP is expressed rhythmically under a light-dark cycle and act through the G-protein coupled receptor bombesin receptor 2 (BB2, also known as GRPR) (McArthur et al., 2000; Karatsoreos et al., 2006). Similar to VIP, application of exogenous GRP to the

SCN produces phase shifts in a phase-dependent manner both *in vitro* and *in vivo* (Piggins et al., 1995; McArthur et al., 2000; Aida et al., 2002). This light-like response to GRP stimulation is accompanied by the upregulation of *Per1* and c-Fos expression in the dorsal SCN (Aida et al., 2002). GRP can also act as a secondary synchronizing neuropeptide when VIP-VPAC2 signaling is defective, since addition of GRP to *Vpac2*$^{-/-}$ SCN explants can transiently restore network synchrony (Brown et al., 2005; Maywood et al., 2011). Recent single cell RNAseq studies have found that GRP-expressing neurons are a subpopulation of VIP neurons: approximately one-quarter of VIP^{+} cells in the SCN co-express GRP (Todd et al., 2020; Wen et al., 2020).

Neuropeptides expressed by the shell SCN have also been shown to modulate circadian timekeeping. The most prevalent neuropeptide expressed by the shell is AVP. *Avp* is rhythmically expressed in mice, as its promoter contains E-box motifs for CLOCK:BMAL1 transactivation (Jin et al., 1999). When the AVP receptors *V1a* and *V1b* are genetically ablated, mutant mice become resistant to jetlag, re-entraining abruptly to shifts in the light-dark cycles (Yamaguchi et al., 2013). Examination of clock gene expression coupled with bioluminescence imaging of SCN explants revealed that *V1a*$^{-/-}$*V1b*$^{-/-}$ SCN neurons show severely permutated phase order, and loss of intercellular synchrony following phase resetting (Yamaguchi et al., 2013). These results suggest that AVP-mediated interneuronal communication provides buffering toward abrupt external perturbations, and disruption of AVP-V1a/b signaling leads to a weakened oscillator. A mouse model with *Bmal1* deletion specifically in AVPergic neurons shows enhanced re-entrainment and lengthened behavioral period, possibly due to the combined attenuation of *Avp*, *Prok2*, and *Rgs16* expression in the SCN shell of these conditional knockout mice (Mieda et al., 2015). Deletion of CK1δ in AVP neurons also results in lengthened behavioral period and altered spatiotemporal pattern of PER2:LUC oscillations in SCN slices, indicating that AVP neurons can regulate SCN pacemaking (Mieda et al., 2016).

The majority of VIP^{+} and AVP^{+} neurons co-express the neuropeptide neuromedin S (NMS) (Todd et al., 2020; Wen et al., 2020). Although mice lacking NMS retain normal circadian rhythms *in vivo*, blocking vesicular transmission from NMS^{+} neurons disrupted the network synchrony of the SCN (Lee et al., 2015). Manipulating the expression of core clock genes, such as *Bmal1* and *Per2*, within NMS-expressing neurons is sufficient to disrupt molecular oscillations and behavioral rhythms (Lee et al., 2015). Conversely, overexpression of the *Clock*Δ*19* transgene in NMS-expressing neurons can lengthen circadian period *in vivo*, indicating that periodicity is dictated by this subset of SCN neurons (Lee et al., 2015). Similar pace-setting effects have been reported for DRD1a^{+} cells in the SCN, which represent ∼60% of all SCN cells (Smyllie et al., 2016). When floxed *Ck1ε*^{Tau} alleles are excised from DRD1a^{+} neurons, ∼60% of the *Drd1a*$^{cre/+}$*:Ck1ε*$^{Tau/Tau}$ temporally chimeric mice exhibited a free-running period that resembles wildtype animals (*Ck1ε*$^{WT/WT}$), whereas ∼30% of the chimeric mice displayed a short period similar to *Ck1ε*$^{Tau/Tau}$ animals (Smyllie et al., 2016). The majority of chimeric SCN slices also displayed significantly lengthened PER2:LUC period, suggesting that DRD1a^{+} cells play a dominant role in period determination within the SCN (Smyllie et al., 2016).

EMBRYONIC DEVELOPMENT OF THE HYPOTHALAMUS

Hypothalamic histogenesis follows the same general pattern as that observed in other neural tube-derived brain regions, with dividing progenitors residing in the ventricular zone and producing neuronal and glial precursors that migrate laterally into the parenchyma (Bedont and Blackshaw, 2015; Xie and Dorsky, 2017). It was originally thought that hypothalamic development follows an outside−in pattern, where lateral hypothalamic nuclei are generated first and displaced outward by medial nuclei that are born later (Shimada and Nakamura, 1973; Altman and Bayer, 1978). However, more recent research has found that in some hypothalamic regions, including the arcuate nucleus and dorsolateral anterior hypothalamus, cells occupying different medial-lateral locations are born during the same interval (Markakis and Swanson, 1997; Padilla et al., 2010).

After neural plate formation following gastrulation, diffusible morphogens generated by the mesodermal domains such as the notochord and prechordal plate (PCP) begin patterning the developing nervous system, including the presumptive hypothalamus. These morphogenic cues modulate important processes during hypothalamic induction and the establishment of regional identity (Bedont and Blackshaw, 2015). Sonic hedgehog (SHH) is a lipid−linked polypeptide signal that is first released from the prechordal plate, is necessary for induction of the hypothalamus, and drives *Shh* expression in the ventral diencephalon (Shimamura and Rubenstein, 1997). Through a Glioma associated oncogene(GLI)-mediated signaling cascade, PCP-derived SHH activates markers of hypothalamic identity along the overlying ventral diencephalic midline (Dale et al., 1997; Motoyama et al., 2003; Manning et al., 2006). Studies have shown that SOX2 and SOX3 can activate and maintain *Shh* transcription in the hypothalamic neuroepithelium through direct binding to the long-range Shh forebrain enhancer-2 (SBE2), whereas T-box transcription factors 2 (TBX2) and TBX3 repress *Shh* in the caudal hypothalamus by sequestering SOX2 away from the SBE2 (Zhao et al., 2012; Trowe et al., 2013). Sineoculis homeobox homolog 3 (SIX3) likewise targets the SBE2 to directly activate *Shh* transcription (Geng et al., 2008; Jeong et al., 2008). Using the *Nkx2.1-cre* mouse line, selective deletion of *Shh* from the basal plate domain of the developing hypothalamus results in ablation of markers of tuberal and anterior hypothalamic nuclei, along with thinning of the telencephalic and hypothalamic neuroepithelium (Shimogori et al., 2010). *Shh* deletion in the zona limitans interthalamica (ZLI) leads to a complete loss of prethalamic markers such as LIM homeobox 1 (*Lhx1)* and Gastrulation brain homeobox 2 (*Gbx2)* (Szabó et al., 2009a,b). *Shh* expression is also dependent on Retina and anterior neural fold homeobox (*Rax)*,

as $Rax^{-/-}$ mouse embryos show a downregulation of *Shh* expression in the dorsomedial portion of the hypothalamus along with underdevelopment of the hypothalamic neuroepithelium (Orquera et al., 2016).

In addition to SHH, modulators of Wingless/Int-1 (WNT) signaling also regulate the patterning of the diencephalon and hypothalamus (Bedont and Blackshaw, 2015). The WNTs are a diverse family of secreted, palmitoleoylated signaling glycoproteins well known for their role in regulating anteroposterior patterning (Mikels and Nusse, 2006). WNTs released by the posterior neurectoderm and somites promote hindbrain fate, whereas the PCP and anterior neurectoderm produce WNT inhibitors to antagonize WNT signaling. *Wnt8b* is expressed in the mouse posterior hypothalamus beginning at ∼ E8.5, consistent with a role in patterning (Braun et al., 2003; Shimogori et al., 2010; Martinez-Ferre et al., 2013). *Wnt7a* and *Wnt7b* are expressed selectively in prethalamic and hypothalamic GABAergic neuronal progenitors around E12.5, suggesting a role in interneuron development; however, their function has not been well characterized (Shimogori et al., 2010). When the transcriptional repressor of WNT targets, Transcription factor 7-like 1 (*Tcf7l1),* is conditionally knocked out in the mouse hypothalamus and pituitary, the developing hypothalamus is posteriorized (Gaston-Massuet et al., 2016). In contrast, loss-of-function of β-catenin (encoded by *Ctnnb1*) results in the anteriorization of the hypothalamus as seen in *Foxd1-Cre;* $Ctnnb1^{lox/lox}$ and *Nkx2.1-Cre;* $Ctnnb1^{lox/lox}$ mice (Newman et al., 2018b). Loss of SIX3, a direct *Wnt1* repressor, results in rostral expansion of caudal diencephalic markers as well as prosencephalon truncation (Lagutin et al., 2003). Lastly, *Lhx2*, a potential upstream inhibitor of WNT signaling (Peukert et al., 2011), has also been shown to play a role in the patterning of the telencephalic-optic-hypothalamic field and to specify SCN neurons at the expense of neuroendocrine fates (Roy et al., 2013).

EMBRYONIC DEVELOPMENT OF THE SCN

SCN neurogenesis begins at ∼60% of gestation in rodents (E12 for mice) (**Figure 3A**; Shimada and Nakamura, 1973; Antle et al., 2005; Kabrita and Davis, 2008). By ∼70% of gestation (E13.5), most ventrolateral neurons have already been produced, while dorsomedial neurogenesis is still underway. The final major burst of SCN neurogenesis (including a number of ventrolateral neurons) occurs at ∼80% of gestation (E15). Neurogenesis in the SCN along its rostral/caudal axis also shows heterochronicity, with neurogenesis in the medial SCN peaking at E12, in the caudal SCN peaking at E13.5, and in the rostral SCN peaking at E14. After immature SCN neurons are generated, they will continue to develop and ultimately express signature neuropeptides such as VIP, GRP, and AVP. Consistent with the regional differences in the peak timing of neurogenesis, cell types that are concentrated in the core SCN (e.g., VIP, GRP, and calbindin expressing cells) are mostly born early. In comparison, AVP neurons of the shell SCN are generated consistently during the period of neurogenesis that extends into later embryonic ages, with those in the middle-posterior regions generated prior to those situated in the anterior pole (Antle et al., 2005). It has been suggested that SCN core and shell neurons derive from distinct progenitor pools in the neuroepithelium (Altman and Bayer, 1986), but the precise mechanisms that regulate cell−type differences in the timing of SCN neurogenesis are not well understood.

SCN development is modulated by morphogen signaling. For instance, the WNT receptor frizzled 5 (*Fzd5*) is detected at E10.5–13.5 in mitotic cells (VanDunk et al., 2011). *Fzd5* is later downregulated, coinciding with the induction of distal-less homeobox 2 (*Dlx2*), which is a selector gene important for GABAergic neuron development (Pla et al., 2018). In addition, members of the fibroblast growth factor (*Fgf*) family are known to control the development of the hypothalamus and the SCN (Tsai et al., 2011). *Fgf8*, one of the 22 *Fgf* ligands, is expressed in the developing hypothalamus by E9.5 in developing mouse embryos, with robust expression in regions surrounding the optic chiasm (Fon Tacer et al., 2010). In homozygous *Fgf8* hypomorphic mice (∼54% reduction of *Fgf8* mRNA) at postnatal day (P)0, SCN volume as well as the expression of AVP and VIP are severely reduced, indicating that normal SCN development relies heavily on *Fgf8* signaling (Brooks et al., 2010; Tsai et al., 2011; Miller et al., 2016). Furthermore, hypomorphism in the cognate tyrosine kinase receptor of FGF8, *Fgfr1*, also causes reduction in VIP expression but does not affect SCN volume. The lesser dependence of SCN development on *Fgfr1* suggests possible compensation by other FGF receptors, as *Fgfr1*, *2*, and *3* are all expressed along the proliferative ventricular zone, but *Fgf8* is the only ligand expressed robustly in the ventral diencephalon near the presumptive SCN (Wanaka et al., 1990; Crossley and Martin, 1995; Belluardo et al., 1997; Bansal et al., 2003). Hence, the consequence of *Fgf8* expression deficit is more severe, as other compensatory factors may not be available during SCN development.

NEURONAL DIFFERENTIATION IN THE DEVELOPING SCN

Many transcription factors such as *Rax*, forkhead box D1 (*Foxd1)*, *Nkx2.2*, *Lhx2*, *Six3*, *Six6*, and ventral anterior homeobox 1 (*Vax1*) are expressed in the ventral anterior hypothalamic neuroepithelium prior to the onset of SCN neurogenesis, although expression of many of these factors become restricted to specific anatomical regions or is lost entirely as the SCN develops (Shimogori et al., 2010; VanDunk et al., 2011).

A subset of these genetic markers such as *Lhx2*, *Rax*, *Foxd1*, and *Nkx2.2* are expressed transiently in the ventral anterior hypothalamus and are gradually lost as the SCN develops. *Foxd1* is broadly expressed in the developing hypothalamus from E11.5 to E13.5 and has been shown to be necessary for SCN development (Newman et al., 2018a). At the early stages of SCN neurogenesis, *Foxd1*-deficient mice display mild developmental deficits, with reduced expression of *Vax1* and *Six3* and a decrease in cellular proliferation (Newman et al., 2018a).

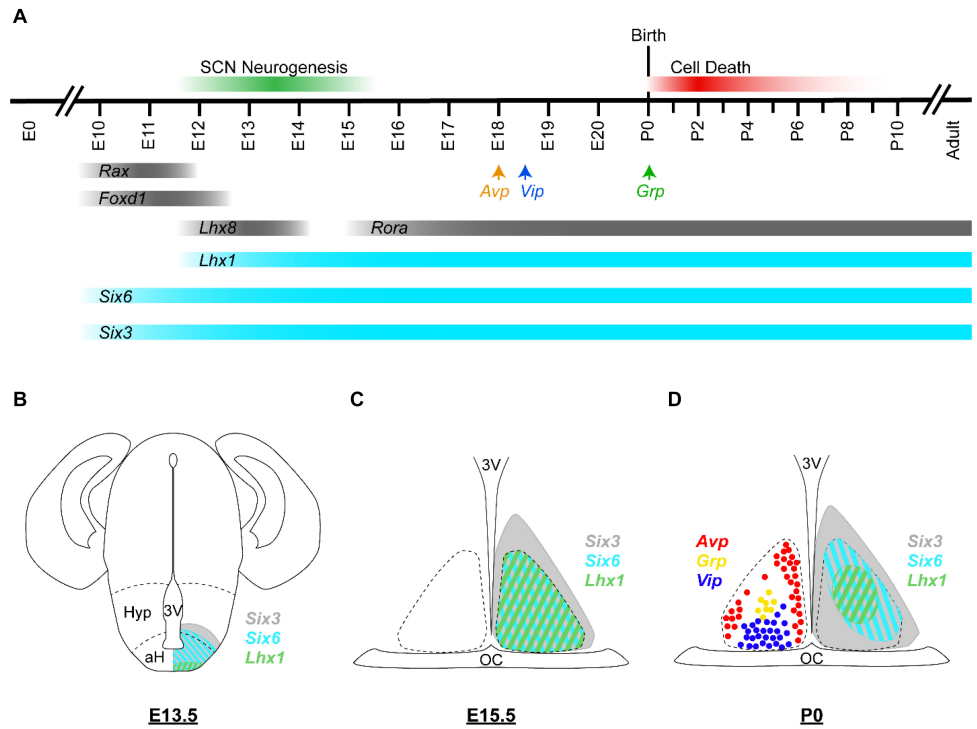

FIGURE 3 | Embryonic development of the murine SCN. **(A)** Developmental timeline of the murine SCN. In mice, SCN neurogenesis begins around E12 and is considered complete by E15 (green bar). *Avp*, *Vip*, and *Grp* transcripts are first detected in the developing SCN at E18, E18.5, and P0, respectively (arrows). Many SCN cells are lost during P0–P8 by apoptotic cell death (red bar). Expression timeline of selected hypothalamus- and SCN-enriched transcription factors are shown; those with known developmental functions are depicted in turquoise and the others are depicted in gray. **(B–D)** Schematic illustrations of the murine brain/SCN showing the spatiotemporal expression patterns of *Six3* (gray), *Six6* (turquoise), and *Lhx1* (green) at **(B)** E13.5, **(C)** E15.5, and **(D)** P0. Cells expressing *Avp* (red), *Grp* (yellow), and *Vip* (blue) at P0 are depicted as colored circles. Dashed lines in **(A)** indicate the boundaries of the anterior hypothalamus (aH) and the hypothalamus (Hyp). Dashed lines in **(C,D)** indicate the margins of the SCN. Expression data are from Shimogori et al. (2010), VanDunk et al. (2011), Bedont et al. (2014), Newman et al. (2018a); unpublished observation (AH Cheng and HYM Cheng). 3V, third ventricle; OC, optic chiasm.

By P0.5, more severe defects are observed in the SCN of *Foxd1*-deficient mice, including reduced expression of genetic markers and agenesis (Newman et al., 2018a). *Rax* is expressed in the murine ventral hypothalamus between E10.5 and E12.5 (Pak et al., 2014). Deletion of *Rax* prior to E8.5 disrupts *Shh* expression and is accompanied by a patterning defect of the mediobasal hypothalamus as described in the previous section, whereas later deletion causes misspecification of ventral medial hypothalamic nucleus (VMH) neurons (Lu et al., 2013; Orquera et al., 2016). *Lhx2* is required for specification of the SCN, as $Lhx2^{-/-}$ mice lack expression of multiple central anterior markers at E12.5, including *Lhx1 and Vax1* (Roy et al., 2013). In contrast to many early anterior hypothalamic markers that are down-regulated in the SCN later in development, *Six3* and *Six6* expression in the SCN persists throughout the lifespan (Shimogori et al., 2010; VanDunk et al., 2011; Clark et al., 2013). Both *Six3* and *Six6* are required for initial SCN specification, as both *Nestin-cre;* $Six3^{fl/fl}$ and $Six6^{-/-}$ mice fail to form a morphologically recognizable SCN or to express SCN-specific markers (VanDunk et al., 2011; Clark et al., 2013). Collectively, these observations suggest that early genetic markers have a long-lasting impact on SCN development by regulating the activation of other transcription factors. Moreover, they may be able to prime the activation of *cis*-regulatory elements that control the expression of cell type-specific genes during differentiation.

Downstream of *Six3* and *Six6*, *Lhx1* is a crucial regulator of SCN terminal differentiation (**Figure 3**; Bedont et al., 2014). *Lhx1* is considered to be the only known transcription factor involved in SCN differentiation and the earliest selective marker expressed throughout the developing SCN (VanDunk et al., 2011; Bedont et al., 2014). *Six3-cre;* $Lhx1^{fl/fl}$ SCN retains expression and proper compartmentalization of most markers initially expressed prior to E16.5, but neuropeptides with important roles in circadian function, including VIP, GRP, and AVP, are absent in the adult SCN (Bedont et al., 2014). By P4, significantly fewer SCN neurons are present in *Lhx1*-deficient SCN due to increased cell death from P0 to P4 (Bedont et al., 2014). Through bioinformatic and luciferase analyses, LHX1 has been shown to directly regulate the expression of *Vip* and potentially *Nms*, *Prok2*, and *proenkephalin* (Bedont et al., 2014; Hatori et al., 2014). Given that *Lhx1* is first detectable at E11.5, the relatively normal development of *Lhx1*-deficient SCN from E11.5 to E16.5 suggests that *Lhx1* is not necessary for early cell fate decisions or regional patterning of the SCN. Instead, *Lhx1* is likely regulating terminal differentiation of SCN neurons. It is also possible that the loss of *Lhx1* is compensated by one or more factors during this

period; one potential candidate is *Lhx8*, an *Lhx1* homolog that is co-expressed with LHX1 in the SCN from E11.5 to E16.5 (Shimogori et al., 2010). Alternatively, *Creb3l1,* an *Lhx1*-regulated gene, is a regulator of AVP expression in the SCN, although its role in SCN development has yet to be explored (Greenwood et al., 2014; Hatori et al., 2014).

Zfhx3 is another genetic marker with known roles in certain aspects of SCN function. *Zfhx3* is highly and almost exclusively expressed in the adult SCN (Lein et al., 2007). While the constitutive knockout of *Zfhx3* results in preweaning sublethality in heterozygous mice and the dominant missense mutation of *Zfhx3*, *Short circuit* (*Sci)*, is homozygous perinatal lethal, adult mice with a single allele of *Sci* show downregulated neuropeptide expression and shortened period of wheel-running activity (Parsons et al., 2015). Furthermore, ablating *Zfhx3* in adult mice using a tamoxifen-inducible transgenic line recapitulated the circadian behavioral deficit in $Zfhx3^{Sci/+}$ mice, indicating that *Zfhx3* acts to regulate SCN function in adulthood by activating transcription at AT motifs (Parsons et al., 2015; Wilcox et al., 2017). Its function in the developing SCN remains unclear.

The clock gene *Rora* is expressed in the ventral SCN starting at E14.5, throughout the SCN at E17.5, and in a pattern more restricted to the SCN shell by P21 (VanDunk et al., 2011; Newman et al., 2018a). Staggerer mice ($Rora^{sg/sg}$) containing a deletion of the fifth exon of *Rora* have a morphologically normal SCN with nominal VIP and AVP expression; however, more characterization is necessary to conclude the function (or the lack thereof) of *Rora* during SCN development, as only the expression of VIP and AVP were examined in $Rora^{sg/sg}$ mice (VanDunk et al., 2011).

NEURONAL LOSS, GLIAL DEVELOPMENT, AND SYNAPTOGENESIS

A large number of SCN neurons are lost during the perinatal period through the activation of caspases and pro-apoptotic proteins of the Bcl-2 family. However, the mechanisms that initiate apoptosis in SCN neurons are largely unclear. SCN cell death begins as synapse formation increases, with substantial death between P1–P7 in mice (Ahern et al., 2013; Mosley et al., 2017). SCN neuronal survival might be dependent on intercellular communication, as apoptotic neurons are isolated from the neuronal clusters (Moore and Bernstein, 1989). Although peak cell death occurs in the murine SCN by P7, an additional 20% of cells are lost by adulthood (Bedont et al., 2014).

It has been estimated that the adult rat SCN contains at least 10^8 synapses with the majority of these being intra-SCN connections (Güldner, 1976; van den Pol, 1980; Moore and Bernstein, 1989). Anatomical studies investigating synaptology in the rat or hamster SCN have revealed important insights on the timing of synapse formation within the SCN (Lenn et al., 1977; Moore and Bernstein, 1989; Laemle et al., 1991; Speh and Moore, 1993). Extensive studies in rats demonstrated that synaptic development is largely a postnatal event with a spike of synaptogenesis occurring between P4 and P10 (Moore and Bernstein, 1989). At E19, 2 days after the end of rat SCN neurogenesis, the neuropil surrounding SCN neurons is sparse and contains large and medium-sized dendritic profiles (Moore and Bernstein, 1989). Immature synapses with very few synaptic vesicles are also present at this time (Lenn et al., 1977; Moore and Bernstein, 1989). Synaptic number and diversity gradually increase from E21 to P2, and then expand rapidly from P2 to P10 (Moore and Bernstein, 1989). Another 30% of the synapses are formed after P10 (Moore and Bernstein, 1989). The window of SCN synaptogenesis overlaps with the arrival of prominent afferent projections. For both mice and rats, terminals from the RHT begin to sparsely innervate the ventrolateral SCN ipsilaterally at birth, followed by the first appearance of contralateral projections in the ventromedial SCN at P4 (McNeill et al., 2011). By P10, the morphology of the axon terminals and the density of the RHT projections are considered to be adult-like (McNeill et al., 2011). Other SCN afferents such as the raphe nuclei and the IGL also innervate the nuclei postnatally and slowly mature in the following weeks (Takatsuji et al., 1995; Migliarini et al., 2013).

Similar to other brain regions, astrogliogenesis follows neurogenesis in the SCN, with the astrocyte marker glial fibrillary acidic protein (GFAP) first detectable shortly before birth, at E15 in hamsters and E20 in rats (Botchkina and Morin, 1995; Munekawa et al., 2000). In both species, there is a postnatal increase in $GFAP^+$ processes that complements the decreasing expression of vimentin (a marker of radial glia) (Botchkina and Morin, 1995; Munekawa et al., 2000). The first major increase in GFAP expression within the SCN, indicative of astrocytic maturation, occurs around P3-P4 in rats (Munekawa et al., 2000).

EXPRESSION OF CLOCK GENES AND NEUROPEPTIDES

During late gestation, circadian rhythms of clock gene expression gradually emerge in a staggered fashion. PER proteins are generally considered to be the earliest core clock components to exhibit rhythmicity. PER2:LUC rhythms are detected as early as E13.5 in SCN slice cultures, but histological data collected from *in vivo* studies have placed the onset of *Per2* and PER2 rhythm at a later stage, around E17 (Shimomura et al., 2001; Ansari et al., 2009; Wreschnig et al., 2014; Landgraf et al., 2015; Carmona-Alcocer et al., 2018). Per1 gene and protein expression begin to show daily oscillations at around the same developmental age as *Per2*, or ∼E18 (Shimomura et al., 2001; Ansari et al., 2009). In comparison, *Cry1* and *Cry2* show robust rhythmicity after birth, with *Cry1*, CRY1, and CRY2 beginning to oscillate at P1, P10, and P2, respectively (Ansari et al., 2009; Huang et al., 2010). In contrast to the highly dynamic expression of PER and CRY, CLOCK and BMAL1 are constitutively expressed in the adult or developing murine SCN, respectively (Von Gall et al., 2003; Ansari et al., 2009). CLOCK is detectable at low levels at E18 and gradually rises to reach adult-level expression by P10 (Ansari et al., 2009). On the other hand, BMAL1 is robustly expressed in a large proportion of SCN cells at E18 and remains at a constantly high level during later developmental stages (Ansari et al., 2009). However, rhythmic *Bmal1* expression in the SCN can be detected

at ∼P3 (Huang et al., 2010). The transcriptional activator of *Bmal1*, *Rora,* is first expressed at E13.5 and is found throughout the murine SCN by E17.5; therefore, *Rora* might contribute to the expression of BMAL1 at E18 (Ansari et al., 2009; VanDunk et al., 2011).

In mice, *Vip* expression is first detected ∼3.5 days after the end of neurogenesis in the SCN core, at E18.5 (Kabrita and Davis, 2008; VanDunk et al., 2011). VPAC2 and VIP reach detectable levels shortly after birth (P0 to P2) (Carmona-Alcocer et al., 2018). Further increases in the level of VIP expression as well as VIP-containing projections have been reported as the SCN matures (Herzog et al., 2000). Similarly, *Avp* is first detected in the murine SCN at E18 and robust expression of AVP is evident by P0 (Hyodo et al., 1992; VanDunk et al., 2011; Bedont et al., 2014). AVP expression continues to rise as the animal matures to ∼P30, at which point an adult level of expression is achieved (Herzog et al., 2000).

Intriguingly, mature SCN neurons continue to express genes that are commonly associated with maintenance of the stem cell states, even though the SCN does not undergo adult neurogenesis. These genes include doublecortin-like (DCL), transportin 1, *Six3*, *Lhx1*, and *Sox2* (Sato et al., 2011; VanDunk et al., 2011; Saaltink et al., 2012; Hoefflin and Carter, 2014; Brown et al., 2017; Beligala et al., 2018; Cheng et al., 2019). SCN neurons also conspicuously exhibit low levels of NeuN, a marker for mature neurons (Morin et al., 2011). This raises the possibility that SCN neurons are not fully committed to a differentiated state, thus retaining a degree of plasticity that presumably allows it to rearrange neuronal circuitry in order to entrain and adapt to a dynamic environment. It is also possible that SCN neurons have "re-purposed" these stem cell or developmental genes for circadian rhythm regulation once their canonical role has been fulfilled.

AUTHOR CONTRIBUTIONS

AHC wrote the manuscript. H-YMC edited the manuscript. Both authors contributed to the article and approved the submitted version.

FUNDING

H-YMC was supported by the Canadian Institutes of Health Research and the Natural Sciences and Engineering Research Council (NSERC) of Canada. AHC was supported by the NSERC post-graduate scholarship.

REFERENCES

Abrahamson, E. E., and Moore, R. Y. (2001). Suprachiasmatic nucleus in the mouse: retinal innervation, intrinsic organization and efferent projections. *Brain Res.* 916, 172–191. doi: 10.1016/s0006-8993(01)02890-6

Abrahamson, E. E., and Moore, R. Y. (2006). Lesions of suprachiasmatic nucleus efferents selectively affect rest-activity rhythm. *Mol. Cell. Endocrinol.* 252, 46–56. doi: 10.1016/j.mce.2006.03.036

Ahern, T. H., Krug, S., Carr, A. V., Murray, E. K., Fitzpatrick, E., Bengston, L., et al. (2013). Cell death atlas of the postnatal mouse ventral forebrain and hypothalamus: Effects of age and sex. *J. Comp. Neurol.* 521, 2551–2569. doi: 10.1002/cne.23298

Aida, R., Moriya, T., Araki, M., Akiyama, M., Wada, K., Wada, E., et al. (2002). Gastrin-releasing peptide mediates photic entrainable signals to dorsal subsets of suprachiasmatic nucleus via induction of Period gene in mice. *Mol. Pharmacol.* 61, 26–34. doi: 10.1124/mol.61.1.26

Albers, H. E., and Ferris, C. F. (1984). Neuropeptide Y: role in light-dark cycle entrainment of hamster circadian rhythms. *Neurosci. Lett.* 50, 163–168. doi: 10.1016/0304-3940(84)90480-4

Albers, H. E., Walton, J. C., Gamble, K. L., McNeill, J. K., and Hummer, D. L. (2017). The dynamics of GABA signaling: Revelations from the circadian pacemaker in the suprachiasmatic nucleus. *Front. Neuroendocrinol.* 44:35–82. doi: 10.1016/j.yfrne.2016.11.003

Albus, H., Vansteensel, M. J., Michel, S., Block, G. D., and Meijer, J. H. (2005). A GABAergic mechanism is necessary for coupling dissociable ventral and dorsal regional oscillators within the circadian clock. *Curr. Biol.* 15, 886–893. doi: 10.1016/j.cub.2005.03.051

Altman, J., and Bayer, S. A. (1978). Development of the diencephalon in the rat. I. Autoradiographic study of the time of origin and settling patterns of neurons of the hypothalamus. *J. Comp. Neurol.* 182, 945–971. doi: 10.1002/cne.901820511

Altman, J., and Bayer, S. A. (1986). *The Development of the Rat Hypothalamus*. Berlin: Springer.

An, S., Harang, R., Meeker, K., Granados-Fuentes, D., Tsai, C. A., Mazuski, C., et al. (2013). A neuropeptide speeds circadian entrainment by reducing intercellular synchrony. *Proc. Natl. Acad. Sci. U.S.A.* 110, E4355–E4361.

An, S., Irwin, R. P., Allen, C. N., Tsai, C., and Herzog, E. D. (2011). Vasoactive intestinal polypeptide requires parallel changes in adenylate cyclase and phospholipase C to entrain circadian rhythms to a predictable phase. *J. Neurophysiol.* 105, 2289–2296. doi: 10.1152/jn.00966.2010

Ansari, N., Agathagelidis, M., Lee, C., Korf, H.-W., and von Gall, C. (2009). Differential maturation of circadian rhythms in clock gene proteins in the suprachiasmatic nucleus and the pars tuberalis during mouse ontogeny. *Eur. J. Neurosci.* 29, 477–489. doi: 10.1111/j.1460-9568.2008.06605.x

Antle, M. C., LeSauter, J., and Silver, R. (2005). Neurogenesis and ontogeny of specific cell phenotypes within the hamster suprachiasmatic nucleus. *Dev. Brain Res.* 157, 8–18. doi: 10.1016/j.devbrainres.2005.02.017

Antle, M. C., and Silver, R. (2005). Orchestrating time: arrangements of the brain circadian clock. *Trends Neurosci.* 28, 145–151. doi: 10.1016/j.tins.2005.01.003

Aton, S. J., Colwell, C. S., Harmar, A. J., Waschek, J., and Herzog, E. D. (2005). Vasoactive intestinal polypeptide mediates circadian rhythmicity and synchrony in mammalian clock neurons. *Nat. Neurosci.* 8, 476–483. doi: 10.1038/nn1419

Aton, S. J., Huettner, J. E., Straume, M., and Herzog, E. D. (2006). GABA and Gi/o differentially control circadian rhythms and synchrony in clock neurons. *Proc. Natl. Acad. Sci. U.S.A.* 103, 19188–19193. doi: 10.1073/pnas.0607466103

Bansal, R., Lakhina, V., Remedios, R., and Tole, S. (2003). Expression of FGF receptors 1, 2, 3 in the embryonic and postnatal mouse brain compared with Pdgfra, Olig2 and Plp/dm20: Implications for oligodendrocyte development. *Dev. Neurosci.* 25, 83–95. doi: 10.1159/000072258

Barca-Mayo, O., Pons-Espinal, M., Follert, P., Armirotti, A., Berdondini, L., and De Pietri Tonelli, D. (2017). Astrocyte deletion of Bmal1 alters daily locomotor activity and cognitive functions via GABA signalling. *Nat. Commun.* 8, 1–14.

Becquet, D., Girardet, C., Guillaumond, F., François-Bellan, A.-M., and Bosler, O. (2008). Ultrastructural plasticity in the rat suprachiasmatic nucleus. Possible involvement in clock entrainment. *Glia* 56, 294–305. doi: 10.1002/glia.20613

Bedont, J. L., and Blackshaw, S. (2015). Constructing the suprachiasmatic nucleus: a watchmaker's perspective on the central clockworks. *Front. Syst. Neurosci.* 9:74. doi: 10.3389/fnsys.2015.00074

Bedont, J. L., LeGates, T. A., Slat, E. A., Byerly, M. S., Wang, H., Hu, J., et al. (2014). Lhx1 Controls Terminal Differentiation and Circadian Function of the Suprachiasmatic Nucleus. *Cell Rep.* 7, 609–622. doi: 10.1016/j.celrep.2014.03.060

Belenky, M. A., Yarom, Y., and Pickard, G. E. (2008). Heterogeneous expression of γ-aminobutyric acid and γ-aminobutyric acid-associated receptors and

transporters in the rat suprachiasmatic nucleus. *J. Comp. Neurol.* 506, 708–732. doi: 10.1002/cne.21553

Beligala, D. H., De, A., and Geusz, M. E. (2018). A meta-analysis characterizing stem-like gene expression in the suprachiasmatic nucleus and its circadian clock. *Biomed Res. Int.* 2018:3610603.

Belluardo, N., Wu, G., Mudo, G., Hansson, A. C., Pettersson, R., and Fuxe, K. (1997). Comparative localization of fibroblast growth factor receptor-1, -2, and -3 mRNAs in the rat brain: In situ hybridization analysis. *J. Comp. Neurol.* 379, 226–246. doi: 10.1002/(sici)1096-9861(19970310)379:2<226::aid-cne5>3.0.co;2-5

Botchkina, G. I., and Morin, L. P. (1995). Ontogeny of radial glia, astrocytes and vasoactive intestinal peptide immunoreactive neurons in hamster suprachiasmatic nucleus. *Dev. Brain Res.* 86, 48–56. doi: 10.1016/0165-3806(95)00017-8

Bouskila, Y., and Dudek, F. E. (1993). Neuronal synchronization without calcium-dependent synaptic transmission in the hypothalamus. *Proc. Natl. Acad. Sci. U.S.A.* 90, 3207–3210. doi: 10.1073/pnas.90.8.3207

Brancaccio, M., Edwards, M. D., Patton, A. P., Smyllie, N. J., Chesham, J. E., Maywood, E. S., et al. (2019). Cell-autonomous clock of astrocytes drives circadian behavior in mammals. *Science* 363, 187–192. doi: 10.1126/science.aat4104

Brancaccio, M., Patton, A. P., Chesham, J. E., Maywood, E. S., and Hastings, M. H. (2017). Astrocytes control circadian timekeeping in the suprachiasmatic nucleus via glutamatergic signaling. *Neuron* 93, 1420–1435.e5.

Braun, M. M., Etheridge, A., Bernard, A., Robertson, C. P., and Roelink, H. (2003). Wnt signaling is required at distinct stages of development for the induction of the posterior forebrain. *Development* 130, 5579–5587. doi: 10.1242/dev.00685

Brooks, L. R., Chung, W. C. J., and Tsai, P.-S. (2010). Abnormal hypothalamic oxytocin system in fibroblast growth factor 8-deficient mice. *Endocrine* 38, 174–180. doi: 10.1007/s12020-010-9366-9

Broussard, J. L., and Van Cauter, E. (2016). Disturbances of sleep and circadian rhythms. *Curr. Opin. Endocrinol. Diabetes Obes.* 23, 353–359.

Brown, L. A., Williams, J., Taylor, L., Thomson, R. J., Nolan, P. M., Foster, R. G., et al. (2017). Meta-analysis of transcriptomic datasets identifies genes enriched in the mammalian circadian pacemaker. *Nucleic Acids Res.* 45, 9860–9873. doi: 10.1093/nar/gkx714

Brown, T. M., Colwell, C. S., Waschek, J. A., and Piggins, H. D. (2007). Disrupted neuronal activity rhythms in the suprachiasmatic nuclei of vasoactive intestinal polypeptide-deficient mice. *J. Neurophysiol.* 97, 2553–2558. doi: 10.1152/jn.01206.2006

Brown, T. M., Hughes, A. T., and Piggins, H. D. (2005). Gastrin-releasing peptide promotes suprachiasmatic nuclei cellular rhythmicity in the absence of vasoactive intestinal polypeptide-VPAC2 receptor signaling. *J. Neurosci.* 25, 11155–11164. doi: 10.1523/jneurosci.3821-05.2005

Bunger, M. K., Wilsbacher, L. D., Moran, S. M., Clendenin, C., Radcliffe, L. A., Hogenesch, J. B., et al. (2000). Mop3 is an essential component of the master circadian pacemaker in mammals. *Cell* 103, 1009–1017. doi: 10.1016/s0092-8674(00)00205-1

Burkeen, J. F., Womac, A. D., Earnest, D. J., and Zoran, M. J. (2011). Mitochondrial calcium signaling mediates rhythmic extracellular ATP accumulation in suprachiasmatic nucleus astrocytes. *J. Neurosci.* 31, 8432–8440. doi: 10.1523/jneurosci.6576-10.2011

Carmona-Alcocer, V., Abel, J. H., Sun, T. C., Petzold, L. R., Doyle, F. J., Simms, C. L., et al. (2018). Ontogeny of circadian rhythms and synchrony in the suprachiasmatic nucleus. *J. Neurosci.* 38, 1326–1334. doi: 10.1523/jneurosci.2006-17.2017

Chen, D., Buchanan, G. F., Ding, J. M., Hannibal, J., and Gillette, M. U. (1999). Pituitary adenylyl cyclase-activating peptide: a pivotal modulator of glutamatergic regulation of the suprachiasmatic circadian clock. *Proc. Natl. Acad. Sci. U.S.A.* 96, 13468–13473. doi: 10.1073/pnas.96.23.13468

Cheng, A. H., Bouchard-Cannon, P., Hegazi, S., Lowden, C., Fung, S. W., Chiang, C. K., et al. (2019). SOX2-dependent transcription in clock neurons promotes the robustness of the central circadian pacemaker. *Cell Rep.* 26, 3191–3202.e8.

Cheng, H. Y. M., Alvarez-Saavedra, M., Dziema, H., Choi, Y. S., Li, A., and Obrietan, K. (2009). Segregation of expression of mPeriod gene homologs in neurons and glia: Possible divergent roles of mPeriod1 and mPeriod2 in the brain. *Hum. Mol. Genet.* 18, 3110–3124. doi: 10.1093/hmg/ddp252

Cheng, M. Y., Bullock, C. M., Li, C., Lee, A. G., Bermak, J. C., Belluzzi, J., et al. (2002). Prokineticin 2 transmits the behavioural circadian rhythm of the suprachiasmatic nucleus. *Nature* 417, 405–410. doi: 10.1038/417405a

Cheung, G., Chever, O., and Rouach, N. (2014). Connexons and pannexons: Newcomers in neurophysiology. *Front. Cell. Neurosci.* 8:348. doi: 10.3389/fncel.2014.00348

Chou, T. C., Scammell, T. E., Gooley, J. J., Gaus, S. E., Saper, C. B., and Lu, J. (2003). Critical role of dorsomedial hypothalamic nucleus in a wide range of behavioral circadian rhythms. *J. Neurosci.* 23, 10691–10702. doi: 10.1523/jneurosci.23-33-10691.2003

Clark, D. D., Gorman, M. R., Hatori, M., Meadows, J. D., Panda, S., and Mellon, P. L. (2013). Aberrant Development of the suprachiasmatic nucleus and circadian rhythms in mice lacking the homeodomain protein Six6. *J. Biol. Rhythms* 28, 15–25. doi: 10.1177/0748730412468084

Colwell, C. S. (2000). Rhythmic coupling among cells in the suprachiasmatic nucleus. *J. Neurobiol.* 43, 379–388. doi: 10.1002/1097-4695(20000615)43:4<379::aid-neu6>3.0.co;2-0

Colwell, C. S., Michel, S., Itri, J., Rodriguez, W., Tam, J., Lelievre, V., et al. (2003). Disrupted circadian rhythms in VIP- and PHI-deficient mice. *Am. J. Physiol. Regul. Integr. Comp. Physiol.* 285, 939–949.

Crossley, P. H., and Martin, G. R. (1995). The mouse Fgf8 gene encodes a family of polypeptides and is expressed in regions that direct outgrowth and patterning in the developing embryo. *Development* 121, 439–451.

Cutler, D. J., Haraura, M., Reed, H. E., Shen, S., Sheward, W. J., Morrison, C. F., et al. (2003). The mouse VPAC 2 receptor confers suprachiasmatic nuclei cellular rhythmicity and responsiveness to vasoactive intestinal polypeptide in vitro. *Eur. J. Neurosci.* 17, 197–204. doi: 10.1046/j.1460-9568.2003.02425.x

Dale, J. K., Vesque, C., Lints, T. J., Sampath, T. K., Furley, A., Dodd, J., et al. (1997). Cooperation of BMP7 and SHH in the induction of forebrain ventral midline cells by prechordal mesoderm. *Cell* 90, 257–269. doi: 10.1016/s0092-8674(00)80334-7

Dardente, H., Menet, J. S., Challet, E., Tournier, B. B., Pévet, P., and Masson-Pévet, M. (2004). Daily and circadian expression of neuropeptides in the suprachiasmatic nuclei of nocturnal and diurnal rodents. *Mol. Brain Res.* 124, 143–151. doi: 10.1016/j.molbrainres.2004.01.010

De Jeu, M., and Pennartz, C. (2002). Circadian modulation of GABA function in the rat suprachiasmatic nucleus: excitatory effects during the night phase. *J. Neurophysiol.* 87, 834–844. doi: 10.1152/jn.00241.2001

Do, M. T. H., and Yau, K.-W. (2010). Intrinsically Photosensitive Retinal Ganglion Cells. *Physiol. Rev.* 90, 1547–1581.

Fon Tacer, K., Bookout, A. L., Ding, X., Kurosu, H., John, G. B., Wang, L., et al. (2010). Research resource: comprehensive expression atlas of the fibroblast growth factor system in adult mouse. *Mol. Endocrinol.* 24, 2050–2064. doi: 10.1210/me.2010-0142

Gaston-Massuet, C., McCabe, M. J., Scagliotti, V., Young, R. M., Carreno, G., Gregory, L. C., et al. (2016). Transcription factor 7-like 1 is involved in hypothalamo-pituitary axis development in mice and humans. *Proc. Natl. Acad. Sci. U.S.A.* 113, E548–E557.

Gekakis, N., Staknis, D., Nguyen, H. B., Davis, F. C., Wilsbacher, L. D., King, D. P., et al. (1998). Role of the CLOCK protein in the mammalian circadian mechanism. *Science* 280, 1564–1569. doi: 10.1126/science.280.5369.1564

Geng, X., Speirs, C., Lagutin, O., Inbal, A., Liu, W., Solnica-Krezel, L., et al. (2008). Haploinsufficiency of Six3 Fails to activate sonic hedgehog expression in the ventral forebrain and causes holoprosencephaly. *Dev. Cell* 15, 236–247. doi: 10.1016/j.devcel.2008.07.003

Gillespie, C. F., Mintz, E. M., Marvel, C. L., Huhman, K. L., and Albers, H. E. (1997). GABA(A) and GABA(B) agonists and antagonists alter the phase-shifting effects of light when microinjected into the suprachiasmatic region. *Brain Res.* 759, 181–189. doi: 10.1016/s0006-8993(97)00235-7

Gillespie, C. F., Van Der Beek, E. M., Mintz, E. M., Mickley, N. C., Jasnow, A. M., Huhman, K. L., et al. (1999). GABAergic regulation of light-induced c-Fos immunoreactivity within the suprachiasmatic nucleus. *J. Comp. Neurol.* 411, 683–692. doi: 10.1002/(sici)1096-9861(19990906)411:4<683::aid-cne12>3.0.co;2-j

Greenwood, M., Bordieri, L., Greenwood, M. P., Rosso Melo, M., Colombari, D. S. A., Colombari, E., et al. (2014). Transcription factor CREB3L1 regulates vasopressin gene expression in the rat hypothalamus. *J. Neurosci.* 34, 3810–3820. doi: 10.1523/jneurosci.4343-13.2014

Gribkoff, V. K., Pieschl, R. L., and Dudek, F. E. (2003). GABA receptor-mediated inhibition of neuronal activity in rat SCN in vitro: Pharmacology and influence of circadian phase. *J. Neurophysiol.* 90, 1438–1448. doi: 10.1152/jn.01082.2002

Guido, M. E., De Guido, L., Goguen, D., Robertson, H. A., and Rusak, B. (1999). Differential effects of glutamatergic blockade on circadian and photic regulation of gene expression in the hamster suprachiasmatic nucleus. *Mol. Brain Res.* 67, 247–257. doi: 10.1016/s0169-328x(99)00074-1

Guillaumond, F., Dardente, H., Giguère, V., and Cermakian, N. (2005). Differential control of Bmal1 circadian transcription by REV-ERB and ROR nuclear receptors. *J. Biol. Rhythms* 20, 391–403. doi: 10.1177/0748730405277232

Güldner, F. H. (1976). Synaptology of the rat suprachiasmatic nucleus. *Cell Tissue Res.* 165, 509–544.

Hannibal, J., Brabet, P., and Fahrenkrug, J. (2008). Mice lacking the PACAP type I receptor have impaired photic entrainment and negative masking. *Am. J. Physiol. Integr. Comp. Physiol.* 295, R2050–R2058.

Harmar, A. J., Marston, H. M., Shen, S., Spratt, C., West, K. M., Sheward, W. J., et al. (2002). The VPAC(2) receptor is essential for circadian function in the mouse suprachiasmatic nuclei. *Cell* 109, 497–508. doi: 10.1016/s0092-8674(02)00736-5

Hatori, M., Gill, S., Mure, L. S., Goulding, M., O'leary, D. D. M., and Panda, S. (2014). Lhx1 maintains synchrony among circadian oscillator neurons of the SCN. *Elife* 3, 1–16.

Hee, J. C., Lee, C. J., Schroeder, A., Yoon, S. K., Seung, H. J., Jeong, S. K., et al. (2008). Excitatory actions of GABA in the suprachiasmatic nucleus. *J. Neurosci.* 28, 5450–5459. doi: 10.1523/jneurosci.5750-07.2008

Herzog, E. D., Geusz, M. E., Khalsa, S. B. S., Straume, M., and Block, G. D. (1997). Circadian rhythms in mouse suprachiasmatic nucleus explants on multimicroelectrode plates. *Brain Res.* 757, 285–290. doi: 10.1016/s0006-8993(97)00337-5

Herzog, E. D., Grace, M. S., Harrer, C., Williamson, J., Shinohara, K., and Block, G. D. (2000). The role of Clock in the developmental expression of neuropeptides in the suprachiasmatic nucleus. *J. Comp. Neurol.* 424, 86–98. doi: 10.1002/1096-9861(20000814)424:1<86::aid-cne7>3.0.co;2-w

Hoefflin, S., and Carter, D. A. (2014). Neuronal expression of SOX2 is enriched in specific hypothalamic cell groups. *J. Chem. Neuroanat.* 61, 153–160. doi: 10.1016/j.jchemneu.2014.09.003

Huang, J., Lu, C., Chen, S., Hua, L., and Qian, R. (2010). Postnatal ontogenesis of clock genes in mouse suprachiasmatic nucleus and heart. *Lipids Health Dis.* 9, 2–7. doi: 10.1007/3-540-27789-7_2

Hughes, A. T. L., Croft, C. L., Samuels, R. E., Myung, J., Takumi, T., and Piggins, H. D. (2015). Constant light enhances synchrony among circadian clock cells and promotes behavioral rhythms in VPAC2-signaling deficient mice. *Sci. Rep.* 5:14044.

Hughes, A. T. L., Guilding, C., Lennox, L., Samuels, R. E., McMahon, D. G., and Piggins, H. D. (2008). Live imaging of altered period1 expression in the suprachiasmatic nuclei of Vipr2-/- mice. *J. Neurochem.* 106, 1646–1657. doi: 10.1111/j.1471-4159.2008.05520.x

Hyodo, S., Yamada, C., Takezawa, T., and Urano, A. (1992). Expression of provasopressin gene during ontogeny in the hypothalamus of developing mice. *Neuroscience* 46, 241–250. doi: 10.1016/0306-4522(92)90024-v

Jeong, Y., Leskow, F. C., El-Jaick, K., Roessler, E., Muenke, M., Yocum, A., et al. (2008). Regulation of a remote Shh forebrain enhancer by the Six3 homeoprotein. *Nat. Genet.* 40, 1348–1353. doi: 10.1038/ng.230

Jiang, Z. G., Yang, Y. Q., and Allen, C. N. (1997a). Tracer and electrical coupling of rat suprachiasmatic nucleus neurons. *Neuroscience* 77, 1059–1066. doi: 10.1016/s0306-4522(96)00539-8

Jiang, Z. G., Yang, Y. Q., Liu, Z. P., and Allen, C. N. (1997b). Membrane properties and synaptic inputs of suprachiasmatic nucleus neurons in rat brain slices. *J. Physiol.* 499, 141–159. doi: 10.1113/jphysiol.1997.sp021917

Jin, X., Shearman, L. P., Weaver, D. R., Zylka, M. J., de Vries, G. J., and Reppert, S. M. (1999). A molecular mechanism regulating rhythmic output from the suprachiasmatic circadian clock. *Cell* 96, 57–68. doi: 10.1016/s0092-8674(00)80959-9

Kabrita, C. S., and Davis, F. C. (2008). Development of the mouse suprachiasmatic nucleus: Determination of time of cell origin and spatial arrangements within the nucleus. *Brain Res.* 1195, 20–27. doi: 10.1016/j.brainres.2007.12.020

Karatsoreos, I. N., Romeo, R. D., McEwen, B. S., and Silver, R. (2006). Diurnal regulation of the gastrin-releasing peptide receptor in the mouse circadian clock. *Eur. J. Neurosci.* 23, 1047–1053. doi: 10.1111/j.1460-9568.2006.04633.x

Kawaguchi, C., Tanaka, K., Isojima, Y., Shintani, N., Hashimoto, H., Baba, A., et al. (2003). Changes in light-induced phase shift of circadian rhythm in mice lacking PACAP. *Biochem. Biophys. Res. Commun.* 310, 169–175. doi: 10.1016/j.bbrc.2003.09.004

Khaper, N., Bailey, C. D. C., Ghugre, N. R., Reitz, C., Awosanmi, Z., Waines, R., et al. (2018). Implications of disturbances in circadian rhythms for cardiovascular health: A new frontier in free radical biology. *Free Radic. Biol. Med.* 119, 85–92. doi: 10.1016/j.freeradbiomed.2017.11.006

Krout, K., Kawano, J., Mettenleiter, T., and Loewy, A. (2002). CNS inputs to the suprachiasmatic nucleus of the rat. *Neuroscience* 110, 73–92. doi: 10.1016/s0306-4522(01)00551-6

Kume, K., Zylka, M. J., Sriram, S., Shearman, L. P., Weaver, D. R., Jin, X., et al. (1999). mCRY1 and mCRY2 are essential components of the negative limb of the circadian clock feedback loop. *Cell* 98, 193–205. doi: 10.1016/s0092-8674(00)81014-4

Kurose, T., Yabe, D., and Inagaki, N. (2011). Circadian rhythms and diabetes. *J. Diabetes Investig.* 2, 176–177.

Laemle, L. K., Repke, K. B., Hawkes, R., and Rice, F. L. (1991). Synaptogenesis in the rat suprachiasmatic nucleus: a light microscopic immunocytochemical survey. *Brain Res.* 544, 108–117. doi: 10.1016/0006-8993(91)90891-x

Lagutin, O. V., Zhu, C. C., Kobayashi, D., Topczewski, J., Shimamura, K., Puelles, L., et al. (2003). Six3 repression of Wnt signaling in the anterior neuroectoderm is essential for vertebrate forebrain development. *Genes Dev.* 17, 368–379. doi: 10.1101/gad.1059403

Landgraf, D., Achten, C., Dallmann, F., and Oster, H. (2015). Embryonic development and maternal regulation of murine circadian clock function. *Chronobiol. Int.* 32, 416–427. doi: 10.3109/07420528.2014.986576

Lee, I. T., Chang, A. S., Manandhar, M., Shan, Y., Fan, J., Izumo, M., et al. (2015). Neuromedin s-producing neurons act as essential pacemakers in the suprachiasmatic nucleus to couple clock neurons and dictate circadian rhythms. *Neuron* 85, 1086–1102. doi: 10.1016/j.neuron.2015.02.006

Lein, E. S., Hawrylycz, M. J., Ao, N., Ayres, M., Bensinger, A., Bernard, A., et al. (2007). Genome-wide atlas of gene expression in the adult mouse brain. *Nature* 445, 168–176.

Lenn, N. J., Beebe, B., and Moore, R. Y. (1977). Postnatal development of the suprachiasmatic hypothalamic nucleus of the rat. *Cell Tissue Res.* 178, 463–475.

Li, J.-D., Hu, W.-P., Boehmer, L., Cheng, M. Y., Lee, A. G., Jilek, A., et al. (2006). Attenuated Circadian rhythms in mice lacking the prokineticin 2 Gene. *J. Neurosci.* 26, 11615–11623. doi: 10.1523/jneurosci.3679-06.2006

Lim, M. M., Gerstner, J. R., and Holtzman, D. M. (2014). The sleep-wake cycle and Alzheimer's disease: what do we know? *Neurodegener. Dis. Manag.* 4, 351–362. doi: 10.2217/nmt.14.33

Liu, C., and Reppert, S. M. (2000). GABA synchronizes clock cells within the suprachiasmatic circadian clock. *Neuron* 25, 123–128. doi: 10.1016/s0896-6273(00)80876-4

Liu, C., Weaver, D. R., Strogatz, S. H., and Reppert, S. M. (1997). Cellular construction of a circadian clock: Period determination in the suprachiasmatic nuclei. *Cell* 91, 855–860. doi: 10.1016/s0092-8674(00)80473-0

Long, M. A., Jutras, M. J., Connors, B. W., and Burwell, R. D. (2005). Electrical synapses coordinate activity in the suprachiasmatic nucleus. *Nat. Neurosci.* 8, 61–66. doi: 10.1038/nn1361

Lu, F., Kar, D., Gruenig, N., Zhang, Z. W., Cousins, N., Rodgers, H. M., et al. (2013). Rax is a selector gene for mediobasal hypothalamic cell types. *J. Neurosci.* 33, 259–272. doi: 10.1523/jneurosci.0913-12.2013

Lu, J., Zhang, Y. H., Chou, T. C., Gaus, S. E., Elmquist, J. K., Shiromani, R., et al. (2001). Contrasting effects of ibotenate lesions of the paraventricular nucleus and subparaventricular zone on sleep-wake cycle and temperature regulation. *J. Neurosci.* 21, 4864–4874. doi: 10.1523/jneurosci.21-13-04864.2001

Manning, L., Ohyama, K., Saeger, B., Hatano, O., Wilson, S. A., Logan, M., et al. (2006). Regional morphogenesis in the hypothalamus: a BMP-Tbx2 pathway coordinates fate and proliferation through Shh downregulation. *Dev. Cell* 11, 873–885. doi: 10.1016/j.devcel.2006.09.021

Markakis, E. A., and Swanson, L. W. (1997). Spatiotemporal patterns of secretomotor neuron generation in the parvicellular neuroendocrine system. *Brain Res. Rev.* 24, 255–291. doi: 10.1016/s0165-0173(97)00006-4

Martinez-Ferre, A., Navarro-Garberi, M., Bueno, C., and Martinez, S. (2013). Wnt signal specifies the intrathalamic limit and its organizer properties by regulating Shh induction in the alar plate. *J. Neurosci.* 33, 3967–3980. doi: 10.1523/jneurosci.0726-12.2013

Maywood, E. S., Chesham, J. E., O'Brien, J. A., and Hastings, M. H. (2011). A diversity of paracrine signals sustains molecular circadian cycling in suprachiasmatic nucleus circuits. *Proc. Natl. Acad. Sci. U.S.A.* 108, 14306–14311. doi: 10.1073/pnas.1101767108

McArthur, A. J., Coogan, A. N., Ajpru, S., Sugden, D., Biello, S. M., and Piggins, H. D. (2000). Gastrin-releasing peptide phase-shifts suprachiasmatic nuclei neuronal rhythms in vitro. *J. Neurosci.* 20, 5496–5502. doi: 10.1523/jneurosci.20-14-05496.2000

McNeill, D. S., Sheely, C. J., Ecker, J. L., Badea, T. C., Morhardt, D., Guido, W., et al. (2011). Development of melanopsin-based irradiance detecting circuitry. *Neural Dev.* 6:8. doi: 10.1186/1749-8104-6-8

McNeill, J. K., Walton, J. C., and Albers, H. E. (2018). Functional significance of the excitatory effects of GABA in the suprachiasmatic nucleus. *J. Biol. Rhythms* 33, 376–387. doi: 10.1177/0748730418782820

Melo, M. C. A., Garcia, R. F., Linhares Neto, V. B., Sá, M. B., de Mesquita, L. M. F., de Araújo, C. F. C., et al. (2016). Sleep and circadian alterations in people at risk for bipolar disorder: a systematic review. *J. Psychiatr. Res.* 83, 211–219. doi: 10.1016/j.jpsychires.2016.09.005

Meyer-Bernstein, E. L., and Morin, L. P. (1996). Differential serotonergic innervation of the suprachiasmatic nucleus and the intergeniculate leaflet and its role in circadian rhythm modulation. *J. Neurosci.* 16, 2097–2111. doi: 10.1523/jneurosci.16-06-02097.1996

Meyer-Spasche, A., and Piggins, H. D. (2004). Vasoactive intestinal polypeptide phase-advances the rat suprachiasmatic nuclei circadian pacemaker in vitro via protein kinase A and mitogen-activated protein kinase. *Neurosci. Lett.* 358, 91–94. doi: 10.1016/j.neulet.2003.12.114

Mieda, M., Okamoto, H., and Sakurai, T. (2016). Manipulating the Cellular circadian period of arginine vasopressin neurons alters the behavioral circadian period. *Curr. Biol.* 26, 2535–2542. doi: 10.1016/j.cub.2016.07.022

Mieda, M., Ono, D., Hasegawa, E., Okamoto, H., Honma, K.-I., Honma, S., et al. (2015). Cellular clocks in AVP neurons of the SCN are critical for interneuronal coupling regulating circadian behavior rhythm. *Neuron* 85, 1103–1116. doi: 10.1016/j.neuron.2015.02.005

Migliarini, S., Pacini, G., Pelosi, B., Lunardi, G., and Pasqualetti, M. (2013). Lack of brain serotonin affects postnatal development and serotonergic neuronal circuitry formation. *Mol. Psychiatry* 18, 1106–1118. doi: 10.1038/mp.2012.128

Mikels, A. J., and Nusse, R. (2006). Wnts as ligands: Processing, secretion and reception. *Oncogene* 25, 7461–7468. doi: 10.1038/sj.onc.1210053

Miller, A. V., Kavanaugh, S. I., and Tsai, P. S. (2016). Disruption of the suprachiasmatic nucleus in fibroblast growth factor signaling-deficient mice. *Front. Endocrinol. (Lausanne)* 7:11. doi: 10.3389/fendo.2016.00011

Mintz, E. M., Gillespie, C. F., Marvel, C. L., Huhman, K. L., and Albers, H. E. (1997). Serotonergic regulation of circadian rhythms in Syrian hamsters. *Neuroscience* 79, 563–569. doi: 10.1016/s0306-4522(96)00696-3

Moore, R. Y., and Bernstein, M. E. (1989). Synaptogenesis in the rat suprachiasmatic nucleus demoinstrated by electron microscopy and synapsin I immunoreactivity. *J. Neurosci.* 9, 2151–2162. doi: 10.1523/jneurosci.09-06-02151.1989

Moore, R. Y., and Speh, J. C. (1993). GABA is the principal neurotransmitter of the circadian system. *Neurosci. Lett.* 150, 112–116. doi: 10.1016/0304-3940(93)90120-a

Moore, R. Y., Speh, J. C., and Leak, R. K. (2002). Suprachiasmatic nucleus organization. *Cell Tissue Res.* 309, 89–98.

Morin, L. P., and Allen, C. N. (2006). The circadian visual system, 2005. *Brain Res. Rev.* 51, 1–60. doi: 10.1016/j.brainresrev.2005.08.003

Morin, L. P., Hefton, S., and Studholme, K. M. (2011). Neurons identified by NeuN/Fox-3 immunoreactivity have a novel distribution in the hamster and mouse suprachiasmatic nucleus. *Brain Res.* 1421, 44–51.

Morin, L. P., Shivers, K. Y., Blanchard, J. H., and Muscat, L. (2006). Complex organization of mouse and rat suprachiasmatic nucleus. *Neuroscience* 137, 1285–1297. doi: 10.1016/j.neuroscience.2005.10.030

Mosley, M., Shah, C., Morse, K. A., Miloro, S. A., Holmes, M. M., Ahern, T. H., et al. (2017). Patterns of cell death in the perinatal mouse forebrain. *J. Comp. Neurol.* 525, 47–64. doi: 10.1002/cne.24041

Motoyama, J., Milenkovic, L., Iwama, M., Shikata, Y., Scott, M. P., and Hui, C. C. (2003). Differential requirement for Gli2 and Gli3 in ventral neural cell fate specification. *Dev. Biol.* 259, 150–161. doi: 10.1016/s0012-1606(03)00159-3

Munekawa, K., Tamada, Y., Iijima, N., Hayashi, S., Ishihara, A., Inoue, K., et al. (2000). Development of astroglial elements in the suprachiasmatic nucleus of the rat: with special reference to the involvement of the optic nerve. *Exp. Neurol.* 166, 44–51. doi: 10.1006/exnr.2000.7490

Musiek, E. S., Bhimasani, M., Zangrilli, M. A., Morris, J. C., Holtzman, D. M., and Ju, Y.-E. S. (2018). Circadian Rest-activity pattern changes in aging and preclinical Alzheimer disease. *JAMA Neurol.* 75:582. doi: 10.1001/jamaneurol.2017.4719

Nagano, M., Adachi, A., Nakahama, K., Nakamura, T., Tamada, M., Meyer-Bernstein, E., et al. (2003). An abrupt shift in the day/night cycle causes desynchrony in the mammalian circadian center. *J. Neurosci.* 23, 6141–6151. doi: 10.1523/jneurosci.23-14-06141.2003

Nakamura, W., Honma, S., Shirakawa, T., and Honma, K. (2001). Regional pacemakers composed of multiple oscillator neurons in the rat suprachiasmatic nucleus. *Eur. J. Neurosci.* 14, 666–674. doi: 10.1046/j.0953-816x.2001.01684.x

Nakamura, W., Yamazaki, S., Takasu, N. N., Mishima, K., and Block, G. D. (2005). Differential response of Period 1 expression within the suprachiasmatic nucleus. *J. Neurosci.* 25, 5481–5487. doi: 10.1523/jneurosci.0889-05.2005

Newman, E. A., Kim, D. W., Wan, J., Wang, J., Qian, J., and Blackshaw, S. (2018a). Foxd1 is required for terminal differentiation of anterior hypothalamic neuronal subtypes. *Dev. Biol.* 439, 102–111. doi: 10.1016/j.ydbio.2018.04.012

Newman, E. A., Wu, D., Taketo, M. M., Zhang, J., and Blackshaw, S. (2018b). Canonical Wnt signaling regulates patterning, differentiation and nucleogenesis in mouse hypothalamus and prethalamus. *Dev. Biol.* 442, 236–248. doi: 10.1016/j.ydbio.2018.07.021

Nielsen, H. S., Hannibal, J., and Fahrenkrug, J. (2002). Vasoactive intestinal polypeptide induces *per1* and *per2* gene expression in the rat suprachiasmatic nucleus late at night. *Eur. J. Neurosci.* 15, 570–574. doi: 10.1046/j.0953-816x.2001.01882.x

Ohta, H., Yamazaki, S., and McMahon, D. G. (2005). Constant light desynchronizes mammalian clock neurons. *Nat. Neurosci.* 8, 267–269. doi: 10.1038/nn1395

Orquera, D. P., Nasif, S., Low, M. J., Rubinstein, M., and de Souza, F. S. J. (2016). Essential function of the transcription factor Rax in the early patterning of the mammalian hypothalamus. *Dev. Biol.* 416, 212–224. doi: 10.1016/j.ydbio.2016.05.021

Padilla, S. L., Carmody, J. S., and Zeltser, L. M. (2010). Pomc-expressing progenitors give rise to antagonistic neuronal populations in hypothalamic feeding circuits. *Nat. Med.* 16, 403–405. doi: 10.1038/nm.2126

Pak, T., Yoo, S., Miranda-Angulo, A. M., Wang, H., and Blackshaw, S. (2014). Rax-CreERT2knock-in mice: a tool for selective and conditional gene deletion in progenitor cells and radial glia of the retina and hypothalamus. *PLoS One* 9:e90381. doi: 10.1371/journal.pone.0090381

Parsons, M. J., Brancaccio, M., Sethi, S., Maywood, E. S., Satija, R., Edwards, J. K., et al. (2015). The regulatory factor ZFHX3 Modifies circadian function in SCN via an AT motif-driven axis. *Cell* 162, 607–621. doi: 10.1016/j.cell.2015.06.060

Peukert, D., Weber, S., Lumsden, A., and Scholpp, S. (2011). Lhx2 and Lhx9 determine neuronal differentiation and compartition in the caudal forebrain by regulating Wnt signaling. *PLoS Biol.* 9:e1001218. doi: 10.1371/journal.pbio.1001218

Pickard, G. E., Ralph, M. R., and Menaker, M. (1987). The Intergeniculate leaflet partially mediates effects of light on circadian rhythms. *J. Biol. Rhythms* 2, 35–56. doi: 10.1177/074873048700200104

Piggins, H., Antle, M., and Rusak, B. (1995). Neuropeptides phase shift the mammalian circadian pacemaker. *J. Neurosci.* 15, 5612–5622. doi: 10.1523/jneurosci.15-08-05612.1995

Pla, R., Stanco, A., Howard, M. A., Rubin, A. N., Vogt, D., Mortimer, N., et al. (2018). Dlx1 and Dlx2 promote interneuron GABA synthesis, synaptogenesis, and dendritogenesis. *Cereb. Cortex* 28, 3797–3815. doi: 10.1093/cercor/bhx241

Preitner, N., Damiola, F., Luis-Lopez-Molina Zakany, J., Duboule, D., Albrecht, U., and Schibler, U. (2002). The orphan nuclear receptor REV-ERBα controls circadian transcription within the positive limb of the mammalian circadian oscillator. *Cell* 110, 251–260. doi: 10.1016/s0092-8674(02)00825-5

Prolo, L. M., Takahashi, J. S., and Herzog, E. D. (2005). Circadian rhythm generation and entrainment in astrocytes. *J. Neurosci.* 25, 404–408. doi: 10.1523/jneurosci.4133-04.2005

Prosser, H. M., Bradley, A., Chesham, J. E., Ebling, F. J. P., Hastings, M. H., and Maywood, E. S. (2007). Prokineticin receptor 2 (Prokr2) is essential for the regulation of circadian behavior by the suprachiasmatic nuclei. *Proc. Natl. Acad. Sci. U.S.A.* 104, 648–653. doi: 10.1073/pnas.0606884104

Ralph, M. R., and Menaker, M. (1985). Bicuculline blocks circadian phase delays but not advances. *Brain Res.* 325, 362–365. doi: 10.1016/0006-8993(85)90341-5

Ralph, M. R., and Menaker, M. (1986). Effects of diazepam on circadian phase advances and delays. *Brain Res.* 372, 405–408. doi: 10.1016/0006-8993(86)91154-6

Ralph, M. R., and Menaker, M. (1989). GABA regulation of circadian responses to light. I. Involvement of GABA(A)-benzodiazepine and GABA(B) receptors. *J. Neurosci.* 9, 2858–2865. doi: 10.1523/jneurosci.09-08-02858.1989

Rash, J. E., Olson, C. O., Pouliot, W. A., Davidson, K. G. V., Yasumura, T., Furman, C. S., et al. (2007). Connexin36 vs. connexin32, "miniature" neuronal gap junctions, and limited electrotonic coupling in rodent suprachiasmatic nucleus. *Neuroscience* 149, 350–371. doi: 10.1016/j.neuroscience.2007.06.052

Reed, H. E., Meyer-Spasche, A., Cutler, D. J., Coen, C. W., and Piggins, H. D. (2001). Vasoactive intestinal polypeptide (VIP) phase-shifts the rat suprachiasmatic nucleus clock in vitro. *Eur. J. Neurosci.* 13, 839–843. doi: 10.1046/j.0953-816x.2000.01437.x

Reppert, S. M., and Schwartz, W. J. (1984). The suprachiasmatic characterization nuclei of the fetal rat: of a functional circadian. *J. Neurosci.* 4, 1677–1682. doi: 10.1523/jneurosci.04-07-01677.1984

Roenneberg, T., and Merrow, M. (2016). The circadian clock and human health. *Curr. Biol.* 26, R432–R443.

Roy, A., de Melo, J., Chaturvedi, D., Thein, T., Cabrera-Socorro, A., Houart, C., et al. (2013). LHX2 is necessary for the maintenance of optic identity and for the progression of optic morphogenesis. *J. Neurosci.* 33, 6877–6884. doi: 10.1523/jneurosci.4216-12.2013

Saaltink, D. J., Håvik, B., Verissimo, C. S., Lucassen, P. J., and Vreugdenhil, E. (2012). Doublecortin and doublecortin-like are expressed in overlapping and non-overlapping neuronal cell population: implications for neurogenesis. *J. Comp. Neurol.* 520, 2805–2823. doi: 10.1002/cne.23144

Sato, M., Mizoro, Y., Atobe, Y., Fujimoto, Y., Yamaguchi, Y., Fustin, J. M., et al. (2011). Transportin 1 in the mouse brain: appearance in regions of neurogenesis, cerebrospinal fluid production/sensing, and circadian clock. *J. Comp. Neurol.* 519, 1770–1780. doi: 10.1002/cne.22600

Sato, T. K., Panda, S., Miraglia, L. J., Reyes, T. M., Rudic, R. D., McNamara, P., et al. (2004). A functional genomics strategy reveals rora as a component of the mammalian circadian clock. *Neuron* 43, 527–537. doi: 10.1016/j.neuron.2004.07.018

Shearman, L. P., Sriram, S., Weaver, D. R., Maywood, E. S., Chaves, I., Zheng, B., et al. (2000). Interacting molecular loops in the mammalian circadian clock. *Science* 288, 1013–1019. doi: 10.1126/science.288.5468.1013

Shearman, L. P., Zylka, M. J., Weaver, D. R., Kolakowski, L. F., and Reppert, S. M. (1997). Two period homologs: Circadian expression and photic regulation in the suprachiasmatic nuclei. *Neuron* 19, 1261–1269. doi: 10.1016/s0896-6273(00)80417-1

Shimada, M., and Nakamura, T. (1973). Time of neuron origin in mouse hypothalamic nuclei. *Exp. Neurol.* 41, 163–173. doi: 10.1016/0014-4886(73)90187-8

Shimamura, K., and Rubenstein, J. L. R. (1997). Inductive interactions direct early regionalization of the mouse forebrain. *Development* 124, 2709–2718.

Shimogori, T., Lee, D. A., Miranda-Angulo, A., Yang, Y., Wang, H., Jiang, L., et al. (2010). A genomic atlas of mouse hypothalamic development. *Nat. Neurosci.* 13, 767–775. doi: 10.1038/nn.2545

Shimomura, H., Moriya, T., Sudo, M., Wakamatsu, H., Akiyama, M., Miyake, Y., et al. (2001). Differential daily expression of Per1 and Per2 mRNA in the suprachiasmatic nucleus of fetal and early postnatal mice. *Eur. J. Neurosci.* 13, 687–693. doi: 10.1046/j.0953-816x.2000.01438.x

Shinohara, K., Funabashi, T., Mitushima, D., and Kimura, F. (2000). Effects of gap junction blocker on vasopressin and vasoactive intestinal polypeptide rhythms in the rat suprachiasmatic nucleus in vitro. *Neurosci. Res.* 38, 43–47. doi: 10.1016/s0168-0102(00)00141-3

Smyllie, N. J., Chesham, J. E., Hamnett, R., Maywood, E. S., and Hastings, M. H. (2016). Temporally chimeric mice reveal flexibility of circadian period-setting in the suprachiasmatic nucleus. *Proc. Natl. Acad. Sci. U.S.A.* 113, 3657–3662. doi: 10.1073/pnas.1511351113

Sominsky, L., Dangel, T., Malik, S., De Luca, S. N., Singewald, N., and Spencer, S. J. (2021). Microglial ablation in rats disrupts the circadian system. *FASEB J.* 35, 1–10.

Speh, J. C., and Moore, R. Y. (1993). Retinohypothalamic tract development in the hamster and rat. *Dev. Brain Res.* 76, 171–181. doi: 10.1016/0165-3806(93)90205-o

Strecker, G. J., Wuarin, J. P., and Dudek, F. E. (1997). GABAA-mediated local synaptic pathways connect neurons in the rat suprachiasmatic nucleus. *J. Neurophysiol.* 78, 2217–2220. doi: 10.1152/jn.1997.78.4.2217

Szabó, N. E., Zhao, T., Çankaya, M., Theil, T., Zhou, X., and Alvarez-Bolado, G. (2009a). Role of neuroepithelial Sonic hedgehog in hypothalamic patterning. *J. Neurosci.* 29, 6989–7002. doi: 10.1523/jneurosci.1089-09.2009

Szabó, N. E., Zhao, T., Zhou, X., and Alvarez-Bolado, G. (2009b). The Role of sonic hedgehog of neural origin in thalamic differentiation in the mouse. *J. Neurosci.* 29, 2453–2466. doi: 10.1523/jneurosci.4524-08.2009

Takatsuji, K., Oyamada, H., and Tohyama, M. (1995). Postnatal development of the substance P-, neuropeptide Y- and serotonin-containing fibers in the rat suprachiasmatic nucleus in relation to development of the retino-hypothalamic projection. *Dev. Brain Res.* 84, 261–270. doi: 10.1016/0165-3806(94)00209-i

Todd, W. D., Venner, A., Anaclet, C., Broadhurst, R. Y., De Luca, R., Bandaru, S. S., et al. (2020). Suprachiasmatic VIP neurons are required for normal circadian rhythmicity and comprised of molecularly distinct subpopulations. *Nat. Commun.* 11:4410.

Trowe, M.-O., Zhao, L., Weiss, A.-C., Christoffels, V., Epstein, D. J., and Kispert, A. (2013). Inhibition of Sox2-dependent activation of Shh in the ventral diencephalon by Tbx3 is required for formation of the neurohypophysis. *Development* 140, 2299–2309. doi: 10.1242/dev.094524

Tsai, P.-S., Brooks, L. R., Rochester, J. R., Kavanaugh, S. I., and Chung, W. C. J. (2011). Fibroblast growth factor signaling in the developing neuroendocrine hypothalamus. *Front. Neuroendocrinol.* 32:95–107. doi: 10.1016/j.yfrne.2010.11.002

Tso, C. F., Simon, T., Greenlaw, A. C., Puri, T., Mieda, M., and Herzog, E. D. (2017). Astrocytes regulate daily rhythms in the suprachiasmatic nucleus and behavior. *Curr. Biol.* 27, 1055–1061. doi: 10.1016/j.cub.2017.02.037

Uth, K., and Sleigh, R. (2014). Deregulation of the circadian clock constitutes a significant factor in tumorigenesis: a clockwork cancer. Part II. In vivo studies. *Biotechnol. Biotechnol. Equip.* 28, 379–386. doi: 10.1080/13102818.2014.925298

van den Pol, A. N. (1980). The hypothalamic suprachiasmatic nucleus of rat: Intrinsic anatomy. *J. Comp. Neurol.* 191, 661–702. doi: 10.1002/cne.901910410

VanDunk, C., Hunter, L. A., and Gray, P. A. (2011). Development, Maturation, and necessity of transcription factors in the mouse suprachiasmatic nucleus. *J. Neurosci.* 31, 6457–6467. doi: 10.1523/jneurosci.5385-10.2011

Vitaterna, M. H., Ko, C. H., Chang, A. M., Buhr, E. D., Fruechte, E. M., Schook, A., et al. (2006). The mouse Clock mutation reduces circadian pacemaker amplitude and enhances efficacy of resetting stimuli and phase-response curve amplitude. *Proc. Natl. Acad. Sci. U.S.A.* 103, 9327–9332. doi: 10.1073/pnas.0603601103

Vitaterna, M. H., Selby, C. P., Todo, T., Niwa, H., Thompson, C., Fruechte, E. M., et al. (1999). Differential regulation of mammalian Period genes and circadian rhythmicity by cryptochromes 1 and 2. *Proc. Natl. Acad. Sci. U.S.A.* 96, 12114–12119. doi: 10.1073/pnas.96.21.12114

Von Gall, C., Noton, E., Lee, C., and Weaver, D. R. (2003). Light does not degrade the constitutively expressed BMAL1 protein in the mouse suprachiasmatic nucleus. *Eur. J. Neurosci.* 18, 125–133. doi: 10.1046/j.1460-9568.2003.02735.x

Wanaka, A., Johnson, E. M., and Milbrand, J. (1990). Localization of FGF receptor mRNA in the adult rat central nervous system by in situ hybridization. *Neuron* 5, 267–281. doi: 10.1016/0896-6273(90)90164-b

Wang, M. H., Chen, N., and Wang, J. H. (2014). The coupling features of electrical synapses modulate neuronal synchrony in hypothalamic superachiasmatic nucleus. *Brain Res.* 1550, 9–17. doi: 10.1016/j.brainres.2014.01.007

Watanabe, K., Vanecek, J., and Yamaoka, S. (2000). In vitro entrainment of the circadian rhythm of vasopressin-releasing cells in suprachiasmatic nucleus by vasoactive intestinal polypeptide. *Brain Res.* 877, 361–366. doi: 10.1016/s0006-8993(00)02724-4

Watts, A. G., and Swanson, L. W. (1987). Efferent projections of the suprachiasmatic nucleus: II. Studies using retrograde transport of fluorescent

dyes and simultaneous peptide immunohistochemistry in the rat. *J. Comp. Neurol.* 258, 230–252. doi: 10.1002/cne.902580205

Welsh, D. K., Logothetis, D. E., Meister, M., and Reppert, S. M. (1995). Individual neurons dissociated from rat suprachiasmatic nucleus express independently phased circadian firing rhythms. *Neuron* 14, 697–706. doi: 10.1016/0896-6273(95)90214-7

Wen, S., Ma, D., Zhao, M., Xie, L., Wu, Q., Gou, L., et al. (2020). Spatiotemporal single-cell analysis of gene expression in the mouse suprachiasmatic nucleus. *Nat. Neurosci.* 23, 456–467. doi: 10.1038/s41593-020-0586-x

Wilcox, A. G., Vizor, L., Parsons, M. J., Banks, G., and Nolan, P. M. (2017). Inducible knockout of mouse Zfhx3 emphasizes its key role in setting the pace and amplitude of the adult circadian clock. *J. Biol. Rhythms* 32, 433–443. doi: 10.1177/0748730417722631

Wreschnig, D., Dolatshad, H., and Davis, F. C. (2014). Embryonic development of circadian oscillations in the mouse hypothalamus. *J. Biol. Rhythms* 29, 299–310. doi: 10.1177/0748730414545086

Xie, Y., and Dorsky, R. I. (2017). Development of the hypothalamus: conservation, modification and innovation. *Development* 144, 1588–1599. doi: 10.1242/dev.139055

Yamaguchi, S., Isejima, H., Matsuo, T., Okura, R., Yagita, K., Kobayashi, M., et al. (2003). Synchronization of cellular clocks in the suprachiasmatic nucleus. *Science* 302, 1408–1412. doi: 10.1126/science.1089287

Yamaguchi, Y., Suzuki, T., Mizoro, Y., Kori, H., Okada, K., Chen, Y., et al. (2013). Mice genetically deficient in vasopressin V1a and V1b receptors are resistant to jet lag. *Science* 342, 85–90. doi: 10.1126/science.1238599

Ye, R., Selby, C. P., Chiou, Y., Ozkan-Dagliyan, I., Gaddameedhi, S., and Sancar, A. (2014). Dual modes of CLOCK:BMAL1 inhibition mediated by Cryptochrome and Period proteins in the mammalian circadian clock. *Genes Dev.* 28, 1989–1998. doi: 10.1101/gad.249417.114

Zhao, L., Zevallos, S. E., Rizzoti, K., Jeong, Y., Lovell-Badge, R., and Epstein, D. J. (2012). Disruption of SoxB1-dependent sonic hedgehog expression in the hypothalamus causes septo-optic dysplasia. *Dev. Cell* 22, 585–596. doi: 10.1016/j.devcel.2011.12.023

Zheng, B., Albrecht, U., Kaasik, K., Sage, M., Lu, W., Vaishnav, S., et al. (2001). Nonredundant roles of the mPer1 and mPer2 genes in the mammalian circadian clock. *Cell* 105, 683–694. doi: 10.1016/s0092-8674(01)00380-4

Zheng, B., Larkin, D. W., Albrecht, U., Sun, Z. S., Sage, M., Eichele, G., et al. (1999). The mPer2 gene encodes a functional component of the mammalian circadian clock. *Nature* 400, 169–173. doi: 10.1038/22118

Conflict of Interest: The authors declare that the research was conducted in the absence of any commercial or financial relationships that could be construed as a potential conflict of interest.

frontiers in Neuroscience

MINI REVIEW
published: 16 April 2021
doi: 10.3389/fnins.2021.659883

Chrono-Nutrition Has Potential in Preventing Age-Related Muscle Loss and Dysfunction

Shinya Aoyama, Yasukazu Nakahata and Kazuyuki Shinohara**

Graduate School of Biomedical Sciences, Nagasaki University, Nagasaki, Japan

The mammalian circadian clock systems regulate the day–night variation of several physiological functions such as the sleep/wake cycle and core body temperature. Disturbance in the circadian clock due to shiftwork and chronic jetlag is related to the risk of several disorders such as metabolic syndrome and cancer. Recently, it has been thought that shiftwork increases the risk of sarcopenia which is characterized by age-related decline of muscle mass and its dysfunctions including muscle strength and/or physical performance. First, we summarize the association between circadian rhythm and the occurrence of sarcopenia and discuss its mechanistic insight by focusing on the muscle function and molecular clock gene in knockout or mutant mice. The clock gene knockout or mutant mice showed early aging phenotypes, including low survival rate and muscle loss. It suggests that improvement in the disturbance of the circadian clock plays an important role in the aging process of healthy muscles. Nutritional intake has the potential to augment muscle growth and entrain the peripheral clock. Second, we discuss the potential of chrono-nutrition in preventing aging-related muscle loss and dysfunction. We also focus on the effects of time-restricted feeding (TRF) and the distribution of protein intake across three meals.

Keywords: circadian rhythm, sarcopenia, nutrition, aging, muscle, chrono-nutrition

OPEN ACCESS

Edited by:
Takahiro J. Nakamura, Meiji University, Japan

Reviewed by:
Hideaki Oike, National Agriculture and Food Research Organization (NARO), Japan
Elizabeth Anne Schroder, University of Kentucky, United States

****Correspondence:***
Kazuyuki Shinohara
kazuyuki@nagasaki-u.ac.jp
Shinya Aoyama
aoyamas@nagasaki-u.ac.jp

Specialty section:
This article was submitted to Sleep and Circadian Rhythms, a section of the journal Frontiers in Neuroscience

Received: *28 January 2021*
Accepted: *26 March 2021*
Published: *16 April 2021*

Citation:
Aoyama S, Nakahata Y and Shinohara K (2021) Chrono-Nutrition Has Potential in Preventing Age-Related Muscle Loss and Dysfunction. Front. Neurosci. 15:659883. doi: 10.3389/fnins.2021.659883

INTRODUCTION

Several physiological functions such as sleep/wake cycle exhibit day–night variation. Most of the physiological events based on day–night variations are regulated by the circadian clock systems consisting of transcriptional and translational negative feedback loop of core clock genes. The heterodimer of brain and muscle ARNT-like 1 (BMAL1) and circadian locomotor output cycle kaput (CLOCK) induces the transcription of *Period1/2* (*Per1/2*) and *Cryptochrome1/2* (*Cry1/2*) by binding to E-box-binding site within promoter regions of *Per1/2* and *Cry1/2* (Gekakis et al., 1998). After their transcription and translation, PER1/2 and CRY1/2 inhibits its own transcription mediated by the BMAL1 and CLOCK complex. PER1/2 and CRY1/2 are also degraded by post-translational modifications such as phosphorylation and ubiquitination (Busino et al., 2007). However, the transcriptions of *Bmal1* and *Clock* are suppressed and activated by *nuclear receptor subfamily 1, group D* (*Rev-erbα*), and *RAR-related orphan receptor* (*Rors*), respectively, by binding to the ROR-responsive element (Preitner et al., 2002; Sato et al., 2004). The transcriptions of *Rev-erbα* and *Rors* are regulated by binding to the E-box-binding elements of the BMAL1 and CLOCK complex (Preitner et al., 2002; Sato et al., 2004). The clock genes are expressed in the whole

body, and the negative feedback loop in several tissues regulates the tissue-dependent day–night variations of physiological functions (Zhang et al., 2014). The mammalian circadian clock system is divided into two layers, namely, the central clock in the suprachiasmatic nucleus (SCN) of the hypothalamus and peripheral clock in the peripheral tissue, including brain areas other than the SCN, liver, skeletal muscle, and so on. Light stimulates SCN neuronal activity, which acts as the main entrainer of the central clock in the SCN. The central clock synchronizes the peripheral clocks through the neural and endocrine signaling pathways such as the sympathetic nervous system and glucocorticoid signaling (Schibler et al., 2003; Shibata, 2004). The peripheral clocks are entrained not only by stimulus from the central clock but also by other factors such as a meal, exercise, and stress in a central clock-independent manner (Tahara and Shibata, 2013). Although exercise, insulin, glucocorticoid and hypoxia entrain the muscle clock, the muscle clock is less susceptible to feeding-dependent entrainment than the liver clock (Harfmann et al., 2015; Oishi et al., 2017; Peek et al., 2017). Such rhythmic regulation changes with life stages. In the older adults, the amplitude of many physiological rhythms such as waking activity dampens and some of them exhibit phase shifts (Hood and Amir, 2017). The analysis of clock gene knockout mice suggests that aging is accelerated due to the circadian clock disturbance (Kondratov et al., 2006). Sarcopenia, which is one of the common diseases among older adults, is muscle dysfunctions due to aging. In recently, some studies show the disturbance of sleep and circadian rhythms relates to the risk of sarcopenia (Piovezan et al., 2015; Choi et al., 2020). Herein, we discuss the following two topics: (1) the association between circadian rhythm and age-related muscle loss and dysfunction in human which are diurnal (day active) and discuss mechanistic insights focusing on the molecular clock gene using knockout or mutant mice models which are nocturnal animal (night active), and (2) the potential of chrono-nutrition in preventing age-related muscle loss and dysfunction.

CIRCADIAN RHYTHM AND SARCOPENIA

Human Study

Sarcopenia is characterized by age-related muscle loss and its dysfunctions such as strength and/or physical performance (Chen et al., 2014). Its pathogenesis is complex and includes multiple factors such as age-related decline of hormonal and metabolic system, malnutrition and so on (Chen et al., 2014). Recently, it is reported that sleep is also play a partial role in the aging of healthy skeletal muscle, such as sarcopenia and metabolic dysfunction. Longer sleep duration (>9 h) leads to a higher risk of sarcopenia than optimal sleep duration (approximately 7 h) (Kwon et al., 2017). A similar association was observed in postmenopausal women (Fex et al., 2012). Another study showed that the prevalence of sarcopenia in older adults is higher with shorter sleep duration (<6 h) and longer (>8 h) sleep duration (Hu et al., 2017; Rubio-Arias et al., 2019). A U-shaped relationship between sleep duration and the prevalence of sarcopenia was observed. These associations between sleep duration and the prevalence of sarcopenia remained after adjusting for confounding factors including age, BMI, physical activity, smoking, energy intake and so on (Hu et al., 2017; Kwon et al., 2017). Although mechanistic insight of association between sleep duration and sarcopenia remains unclear, insulin resistance, chronic inflammation and anabolic hormone could be possible link between sleep duration and sarcopenia (Patel et al., 2009; Piovezan et al., 2015; Smiley et al., 2019). In addition to sleep duration, sleep quality, assessed using the Pittsburgh Sleep Quality Index (PSQI), was also associated with sarcopenia (Buchmann et al., 2016; Lucassen et al., 2017). As with the relationship between sleep duration and sarcopenia, the PSQI score was still associated with muscle mass after adjusting for age, physical activity, HOMA-IR and testosterone (Buchmann et al., 2016). Frailty is an age-related clinical state that indicates a decline in physiological function and enhanced vulnerability to stressors. Physical functions such as grip strength and gait speed are also included in the sarcopenia diagnostic criteria. Similar to the relationship between sleep duration and sarcopenia, shorter (<6 h) and longer (>8 h) sleep duration significantly increased the risk of frailty (Pourmotabbed et al., 2020). Additionally, the risk of frailty is increased by other sleep parameters such as daytime sleepiness, sleep-disordered breathing, and prolonged sleep latency (Endeshaw et al., 2009; Ensrud et al., 2009, 2012; Vaz Fragoso et al., 2009; Nakakubo et al., 2019). These data suggest that adequate sleep might have preventive effects on the development of sarcopenia. Chronotype is also related to the prevalence of sarcopenia. Yu et al. reported that the evening chronotype was associated with an increased risk of sarcopenia in older men, independent of sleep duration (Yu et al., 2015). Recently, an analysis of the data of 9105 Korean people including non-shift workers and shift workers reported that shift workers had a higher risk of sarcopenia (Choi et al., 2019). Further analysis showed that a shift worker with an irregular schedule had the highest risk of sarcopenia (Choi et al., 2019). These data suggest that inadequate sleep and disturbance of circadian clocks were related with the risk of sarcopenia.

Animal Study

Although human studies have suggested that low sleep quality and shiftwork, which cause disturbance of the circadian rhythm, are risk factors for sarcopenia, the underlying mechanism is not yet fully understood. Evidence from animal studies may support the mechanistic insight connecting the relationship between disturbance of the circadian clock and occurrence of sarcopenia (Chatterjee and Ma, 2016; Aoyama and Shibata, 2017). Whole-body *Bmal1*-knockout mice exhibited early age-related muscle loss (Kondratov et al., 2006). Similar findings were observed in *Clock mutant* mice and *Rev-erb*α knockout mice (Andrews et al., 2010; Mayeuf-Louchart et al., 2017). It was expected that the muscle clock was contributed to muscle volume from the results of the restored body weight loss in muscle-specific *Bmal1* rescue in whole-body *Bmal1* knockout mice (muscle mass was not evaluated) (McDearmon et al., 2006). However now it is thought that its contribution to age-related muscle loss is small because muscle loss was not observed in muscle-specific *Bmal1*-knockout

mice in contrast to whole-body *Bmal1*-knockout mice (Dyar et al., 2014; Schroder et al., 2015). In the discrepancy of phenotype between muscle-specific *Bmal1* rescued mice and muscle-specific *Bmal1* knockout mice, prevention of body weight loss by muscle-specific *Bmal1* rescue may be explained by restoration of locomotor activity (McDearmon et al., 2006). Although the muscle-specific *Bmal1* knockout mice showed the normal locomotor activity (Hodge et al., 2015), they also had gait issues similar to that observed in aging humans (Schroder et al., 2015). The broader impacts of intrinsic muscle clock on musculoskeletal system might contribute to in turn locomotor activity through improvement of gait. In addition to muscle-specific effects, it is suggested that the timing of *Bmal1* expression is key to development aging. In tamoxifen-inducible whole-body *Bmal1*-knockout mice, the deletion of *Bmal1* after muscle development (>3 months old) did not affect body weight loss and some early aging phenotypes such as glucose intolerance (Yang et al., 2016). These data suggest that *Bmal1* expression during development is important for maintaining muscle volume. On the other hand, the muscle-specific *Bmal1*-knockout mice also exhibited lower muscle strength, a shift to oxidative fiber type and muscle fibrosis (Dyar et al., 2014; Schroder et al., 2015). It suggests that the intrinsic muscle molecular clock affects muscle quality rather than muscle mass. Skeletal muscle has a key role of whole-body energy metabolism (Zurlo et al., 1990). Intrinsic muscle clock controls the day-night variations of glucose, amino acids and lipid metabolism, and muscle-specific *Bmal1* knockout mice show the glucose intolerance and insulin resistance (Dyar et al., 2014, 2018; Harfmann et al., 2016). Considering that insulin resistance and diabetes are one of the risk factors of sarcopenia, the metabolic dysfunctions due to disturbance of muscle clock may encourage the development of sarcopenic phenotypes such as a decline of muscle strength. Taken together, the muscle clock affects the quality of skeletal muscle such as a shift of muscle fiber type and muscle strength while the molecular clock in non-muscle fiber cell such as myogenic progenitors may contribute to age-related muscle decline shown in whole-body *Bmal1* knockout mice.

THE ROLE OF MOLECULAR CLOCK ON MUSCLE GROWTH AND MYOGENESIS

Muscle Protein Synthesis and Degradation

The balance between muscular protein synthesis and degradation is important for the regulation of skeletal muscle mass and strength. *Atrogin1* (*F-box protein 32*) and *Muscle RING-finger protein-1* (*Murf1*) are rhythmic genes found in the circadian transcriptome (McCarthy et al., 2007; Miller et al., 2007; Dyar et al., 2015). These genes are E3 ubiquitin ligase and the key genes in the progression of muscle atrophy, and each knockout mouse shows resistance to denervated muscle atrophy (Bodine et al., 2001). The day–night variation of *Atrogin1* was also observed in the hindlimb unloading-induced muscle atrophy model but not in hindlimb unloaded *Clock mutant* mice (Aoyama et al., 2018). Dyar et al. reported that *Murf1* transcription was downregulated by *Rev-erbα* and its expression was found to be reduced due to the rescue of *Rev-erbα* in muscle-specific *Bmal1*-knockout mice (Dyar et al., 2018). These data suggest that a circadian clock is associated with muscle atrophy. Muscle protein synthesis is important for muscle growth and repair after exercise-induced muscle hypertrophy. The mTOR pathway is the key signaling pathway in protein synthesis, and this pathway is activated by resistance exercise training and nutrition such as amino acids (Stokes et al., 2018). Lipton et al. reported that phosphorylation of BMAL1 by S6K (ribosomal S6 protein kinase), which is a substrate of mTOR, regulates the day–night variation of translation in the liver (Lipton et al., 2015). The results of circadian transcriptomics and metabolomics of muscle-specific *Bmal1*-knockout mice revealed that amino acid metabolism was dramatically reprogrammed by the loss of muscle *Bmal1* (Dyar et al., 2018). Indeed, the translation level, which was assessed with puromycin-labeled peptides, was found to be altered in the muscle-specific *Bmal1*-knockout mice (Dyar et al., 2018). These results indicate that the circadian clock controls the day–night variation in muscle protein synthesis. It is possible that the day–night variation in muscle protein synthesis depends on the fasting/feeding cycle and locomotor activity rhythm rather than the direct regulation of the muscle clock because muscle protein synthesis shows a higher response to feeding and physical activity. In recent years, Kelu et al. (2020) reported that muscle exhibited day–night differences in growth independent of physical activity and feeding in zebrafish which was diurnal. Muscle anabolism is activated during the day, while the muscle catabolism is high during the night. Such day–night variation remained in the inactive muscle and under the no-feeding condition. However, the day–night variation in muscle growth disappeared due to clock disruption. Taken together, the circadian clock regulates the day–night variation in muscle growth, and this is augmented by locomotor activity rhythm and the feeding/fasting cycle.

Myogenesis

Myofilament architecture was disrupted in the skeletal muscle of *Bmal1*-knockout mice and *Clock mutant* mice (Andrews et al., 2010). *Myod* is one of the key genes participating in muscle myogenesis, the process of myotube formation from satellite cells and myoblast cells. The day–night variation in *Myod* was observed in the skeletal muscle of wild-type mice but not in *Clock mutant* mice (Andrews et al., 2010). Its rhythmic expression is regulated by the BMAL1 and CLOCK complex (Andrews et al., 2010). Chatterjee et al. (2013, 2015) reported the role of *Bmal1* in myogenesis. Suppressed expression of myogenic genes such as *Myod*, *Myog*, and *Myf5* and impairment of myogenesis were observed in the myoblasts of *Bmal1*-knockout mice (Chatterjee et al., 2013). In addition, the authors reported the *in vivo* function of *Bmal1* in skeletal muscle regeneration (Chatterjee et al., 2015). Freeze- or cardiotoxin-induced muscle regeneration was suppressed by the depletion of *Bmal1* (Chatterjee et al., 2015). Recently, there has been evidence for the potential of *Rev-erbα* in preventing myogenesis through augmented satellite cell expansion and myogenic progression (Chatterjee et al., 2019).

In addition, CRY1 and CRY2 regulate the proliferation and differentiation of muscle satellite cells negatively and positively, respectively. The CRY2-dependent acceleration of muscle cell differentiation was controlled by the rhythmic expression of *CyclinD1* and *Tmem176b* due to binding to BCLAF1 (Lowe et al., 2018). These results indicate that the myogenic process is regulated by the circadian clock (**Figure 1**). In recent study, MYOD1 regulates not only the myogenesis but also the amplitude of *Bmal1* and clock-controlled genes such as *Tcap* (Hodge et al., 2019). Considering the role of intrinsic muscle clock in muscle strength and metabolism, *Myod1* is one of therapeutic target as a daily maintenance of skeletal muscle functions. Recently, in satellite cells, aging reprogrammed the expression profile of rhythmic genes without any change in clock gene expression (Solanas et al., 2017). Although the physiological effects caused by aging-related reprogramming are fully unclear, these data may help to understand the mechanism underlying the relationship between the occurrence of sarcopenia and disturbance in the circadian rhythm.

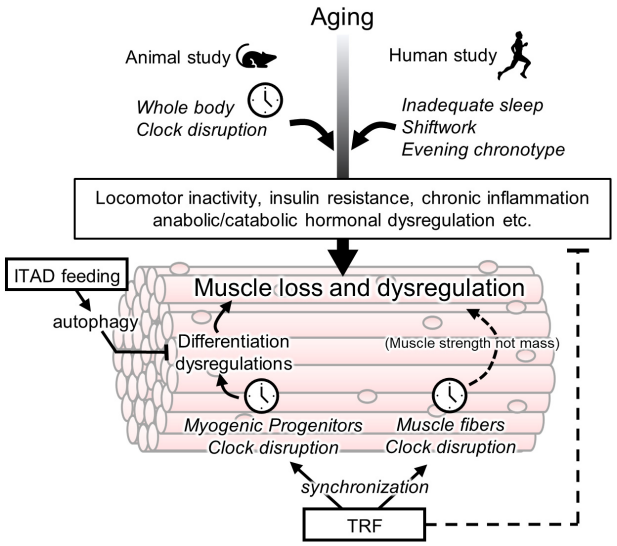

FIGURE 1 | Association between circadian clock and age-related muscle loss and targets of chrono-nutrition. Age-related muscle loss is accelerated by a disturbance of a circadian clock in the animal and human studies. Its disturbance may be involved in early onset of sarcopenia via several non-muscular rhythmic functions such as a locomotor activity and insulin resistance. The muscle fiber clock has a impact on the age-related weakness of muscle strength. The circadian clock in myogenic progenitors controls muscle differentiation however its involvement in sarcopenia is unclear yet. The isocaloric twice-a-day (ITAD) feeding promotes the myogenesis via the activation of autophagy in myogenic progenitor cells. The time-restricted feeding (TRF) may have a potential for prevention of age-related muscle dysfunctions via entrainment of the peripheral clock including muscle fiber and progenitor cells. In addition to the role of TRF as an entrainer, TRF also maintains the daily homeostasis of metabolism such as prevention of insulin resistance.

THERAPEUTIC POTENTIAL OF CHRONO-NUTRITION AGAINST ARE-RELATED MUSCLE DYSFUNCTIONS

Time-restricted feeding (TRF), which is restricted only to the eating time window but not calorie restriction, has strong preventive or therapeutic potential for metabolic dysfunction such as obesity and insulin resistance (Longo and Panda, 2016; Manoogian and Panda, 2017; Chaix et al., 2019). In *Drosophila*, TRF improves obesity-induced muscle dysfunction, including sarcomere disorganization, mitochondrial function, and insulin resistance (Villanueva et al., 2019) (**Figure 1**). In that study, TRF was also effective in the constant light-induced muscle dysfunction (Villanueva et al., 2019). TRF also attenuated age-related decline of cardiac muscle function in *Drosophila* (Manoogian and Panda, 2017). Martinez-Lopez et al. reported the beneficial effects of an isocaloric twice-a-day (ITAD) feeding model, which has two eating windows (Martinez-Lopez et al., 2017). ITAD feeding increased type IIB fibers, which are glycolytic muscle fibers (Martinez-Lopez et al., 2017). Moreover, an increase in myogenic genes was observed in the ITAD-fed mice, suggesting that ITAD feeding enhanced myogenesis of glycolytic muscle fibers. In addition, ITAD feeding prevented age-related metabolic defects such as glucose intolerance and mitochondrial dysfunction (Martinez-Lopez et al., 2017). These beneficial effects of ITAD feeding were not observed in myogenic progenitor-specific *Atg7*-knockout mice (Martinez-Lopez et al., 2017). Autophagy of myogenic progenitor cells is required for glycolytic muscle fiber expansion due to ITAD feeding (**Figure 1**). These data suggest that intermittent fasting-induced autophagy within a day is one of the key beneficial effects of time-controlled feeding such as TRF and ITAD feeding. Other animal studies have shown a difference between the TRF conducted during the active phase (night time) and that conducted during the rest phase (day time) (Abe et al., 2019; Aoyama et al., 2019). The TRF conducted during the active phase has beneficial effects on muscle growth and muscular protein synthesis compared with that conducted during the rest phase (Abe et al., 2019; Aoyama et al., 2019). Taken together, considering that muscle loss is particularly observed in glycolytic muscle fibers of patients with sarcopenia, ITAD feeding during the active phase may be an effective nutritional intervention for the prevention of sarcopenia.

A few human studies have shown the effects of TRF on skeletal muscle function in young and older adults. The TRF induced between 0800 and 1400 improved the 24-h glucose levels and increased the expression of the anti-aging gene *SIRT1* and the autophagy gene *LC3A* in the blood compared with the TRF induced between 0800 and 2000 (Jamshed et al., 2019). In terms of skeletal muscle function, 2 weeks of TRF induced between 0800 and 1600 improves insulin and anabolic responses in the skeletal muscle of healthy young men (Jones et al., 2020). Indeed, TRF increased the skeletal muscle uptake of glucose and branched-chain amino acids (BCAAs) (Jones et al., 2020). The effects of TRF in men who are overweight/obese have been elucidated using the circadian transcriptome of skeletal muscle (Lundell et al., 2020). TRF conducted for 8 h stimulated rhythmicity of

amino acid metabolites and its transporter expression without perturbing the expression of molecular clock genes (Lundell et al., 2020). Additionally, considering that the transcriptomics and metabolomics data from human skeletal muscle after acute sleep loss suggest the muscle degradation according to the change of circadian clock expression (Cedernaes et al., 2018), synchronization of the muscle clock by TRF may suppress muscle degradation due to sleep loss. In older overweight adults, a 4-week TRF intervention resulted in body weight loss, although improvements in cognitive and physical function were not observed in this pilot study (Anton et al., 2019). Although few studies have reported about the effects of TRF on muscle function in older adults, evidence of the TRF effects focusing on skeletal muscle function in human studies is increasing.

Protein intake is important for maintaining balance between muscle protein synthesis and protein degradation. Dietary protein and amino acids act not only as a source of body protein but also as activators of mTOR signaling. Compared with young adults, a higher amount of dietary protein was required in older adults for a greater response to muscle protein synthesis (Fujita and Volpi, 2006), suggesting that the sensitivity of amino acids in the skeletal muscle decreased with aging. Considering the reduction in meal size in elderly people, we need ingenuity to take enough amount of protein across the three meals. A diet survey conducted in several countries showed that protein intake at breakfast was at a low level, and the daily distribution of protein was skewed (National Center for Health Statistics About the National Health and Nutrition Exmaination Survey (NHANES), 2012; Tieland et al., 2015; Ishikawa-Takata and Takimoto, 2018). Some human and animal studies have shown that even distribution of dietary protein across the three meals increased muscle protein synthesis and muscle mass compared with the skewed distribution, which indicates a low protein meal at breakfast (Mamerow et al., 2014; Norton L.E. et al., 2016). Another report showed that protein supplementation at breakfast and lunch for 24 weeks increased whole-body lean tissue mass in healthy older adults (Norton C. et al., 2016). The distribution of dietary protein is associated with muscle strength and frailty (Bollwein et al., 2013; Farsijani et al., 2017). In addition to muscle function, dietary protein has the potential to entrain peripheral clocks through the regulation of insulin growth factor-1 and glucagon signaling in an animal study (Ikeda et al., 2018). Tahara et al. (2017) reported age-related changes in peripheral clock entrainment according to feeding, and aged mice were susceptible to the feeding-induced phase shift of peripheral clocks such as the kidney and submandibular gland. In other words, a high protein meal at breakfast may have two effects on the prevention of sarcopenia: (1) augmentation of muscle growth and (2) improvement of the disrupted circadian clock through entrainment of peripheral clocks.

SUMMARY AND PERSPECTIVES

In this review, we confirmed that inadequate sleep and shiftwork, which disturbs the circadian clock, were risk factors for sarcopenia and frailty. Considering that age-related muscle loss is observed in the whole body but not muscle-specific disruption of the molecular clock, it is suggested that the risk of sarcopenia may be increased due to the disturbance of the circadian clock in non-muscle tissues such as the SCN or myogenic progenitor cells. On the other hand, the broader impact of muscle clock on the musculoskeletal system such as muscle strength and gait might also have a role in preventing a sarcopenia as these changes of musculoskeletal system might precede the loss of muscle mass. Further studies are warranted to gain a clearer understanding of the mechanism underlying the interaction between circadian clock disturbance and age-related muscle dysfunction. We also discussed the potential of chrono-nutrition in preventing muscle aging in terms of two aspects: (1) to consider adequate timing or distribution of protein intake in a day and (2) to reset the peripheral clock. Although there is evidence for the beneficial effect of scheduled controlled feeding such as TRF in human and animal studies, the role of a circadian clock in the effects of chrono-nutrition on muscle health is not fully understood. Further research is needed to reveal the mechanism and elucidate the anti-aging effects of chrono-nutrition in older subjects who experience disturbance in the circadian rhythm, such as shift workers.

AUTHOR CONTRIBUTIONS

SA was involved in conceptualizing and writing the manuscript. KS and YN were involved in conceptualizing and editing the manuscript. All authors contributed to the article and approved the submitted version.

FUNDING

This research was supported in part by the Nutrition and Food Science Fund of Japan Society of Nutrition and Food Science and the Japan Society for the Promotion of Science (JSPS) KAKENHI (grant number 20K19710).

ACKNOWLEDGMENTS

We would like to thank Editage (http://www.editage.com) for editing and reviewing this manuscript for English language.

REFERENCES

Abe, T., Kazama, R., Okauchi, H., and Oishi, K. (2019). Food deprivation during active phase induces skeletal muscle atrophy via IGF-1 reduction in mice. *Arch. Biochem. Biophys.* 677:108160. doi: 10.1016/j.abb.2019.108160

Andrews, J. L., Zhang, X., McCarthy, J. J., McDearmon, E. L., Hornberger, T. A., Russell, B., et al. (2010). CLOCK and BMAL1 regulate MyoD and are necessary for maintenance of skeletal muscle phenotype and function. *Proc. Natl. Acad. Sci. U.S.A.* 107, 19090–19095. doi: 10.1073/pnas.1014523107

Anton, S. D., Lee, S. A., Donahoo, W. T., McLaren, C., Manini, T., Leeuwenburgh, C., et al. (2019). The effects of time restricted feeding on overweight, older adults: a pilot study. *Nutrients* 11:1500. doi: 10.3390/nu11071500

Aoyama, S., Kojima, S., Sasaki, K., Ishikawa, R., Tanaka, M., Shimoda, T., et al. (2018). Day-night oscillation of atrogin1 and timing-dependent preventive

effect of weight-bearing on muscle atrophy. *EBioMedicine* 37, 499–508. doi: 10.1016/j.ebiom.2018.10.057

Aoyama, S., Kojima, S., Sasaki, K., Shimoda, T., Takahashi, K., Hirooka, R., et al. (2019). Effects of day-time feeding on murine skeletal muscle growth and synthesis. *J. Nutr. Int. Metab.* 17:100099. doi: 10.1016/j.jnim.2019.100099

Aoyama, S., and Shibata, S. (2017). The role of circadian rhythms in muscular and osseous physiology and their regulation by nutrition and exercise. *Front. Neurosci.* 11:63. doi: 10.3389/fnins.2017.00063

Bodine, S. C., Latres, E., Baumhueter, S., Lai, V. K., Nunez, L., Clarke, B. A., et al. (2001). Identification of ubiquitin ligases required for skeletal muscle atrophy. *Science* 294, 1704–1708. doi: 10.1126/science.1065874

Bollwein, J., Diekmann, R., Kaiser, M. J., Bauer, J. M., Uter, W., Sieber, C. C., et al. (2013). Distribution but not amount of protein intake is associated with frailty: a cross-sectional investigation in the region of Nurnberg. *Nutr. J.* 12:109.

Buchmann, N., Spira, D., Norman, K., Demuth, I., Eckardt, R., and Steinhagen-Thiessen, E. (2016). Sleep, muscle mass and muscle function in older people. *Dtsch. Arztebl. Int.* 113, 253–260.

Busino, L., Bassermann, F., Maiolica, A., Lee, C., Nolan, P. M., Godinho, S. I., et al. (2007). SCFFbxl3 controls the oscillation of the circadian clock by directing the degradation of cryptochrome proteins. *Science* 316, 900–904. doi: 10.1126/science.1141194

Cedernaes, J., Schönke, M., Westholm, J. O., Mi, J., Chibalin, A., Voisin, S., et al. (2018). Acute sleep loss results in tissue-specific alterations in genome-wide DNA methylation state and metabolic fuel utilization in humans. *Sci. Adv.* 4:eaar8590. doi: 10.1126/sciadv.aar8590

Chaix, A., Manoogian, E. N. C., Melkani, G. C., and Panda, S. (2019). Time-restricted eating to prevent and manage chronic metabolic diseases. *Annu. Rev. Nutr.* 39, 291–315. doi: 10.1146/annurev-nutr-082018-124320

Chatterjee, S., and Ma, K. (2016). Circadian clock regulation of skeletal muscle growth and repair. *F1000Res.* 5:1549. doi: 10.12688/f1000research.9076.1

Chatterjee, S., Nam, D., Guo, B., Kim, J. M., Winnier, G. E., Lee, J., et al. (2013). Brain and muscle Arnt-like 1 is a key regulator of myogenesis. *J. Cell Sci.* 126, 2213–2224. doi: 10.1242/jcs.120519

Chatterjee, S., Yin, H., Li, W., Lee, J., Yechoor, V. K., and Ma, K. (2019). The nuclear receptor and clock repressor Rev-erbα suppresses myogenesis. *Sci. Rep.* 9, 4585–4585.

Chatterjee, S., Yin, H., Nam, D., Li, Y., and Ma, K. (2015). Brain and muscle Arnt-like 1 promotes skeletal muscle regeneration through satellite cell expansion. *Exp. Cell Res.* 331, 200–210. doi: 10.1016/j.yexcr.2014.08.041

Chen, L.-K., Liu, L.-K., Woo, J., Assantachai, P., Auyeung, T.-W., Bahyah, K. S., et al. (2014). Sarcopenia in Asia: consensus report of the asian working group for sarcopenia. *J. Am. Med. Dir. Assoc.* 15, 95–101.

Choi, Y., Cho, J., No, M. H., Heo, J. W., Cho, E. J., Chang, E., et al. (2020). Re-setting the circadian clock using exercise against sarcopenia. *Int. J. Mol. Sci.* 21:3106. doi: 10.3390/ijms21093106

Choi, Y. I., Park, D. K., Chung, J.-W., Kim, K. O., Kwon, K. A., and Kim, Y. J. (2019). Circadian rhythm disruption is associated with an increased risk of sarcopenia: a nationwide population-based study in Korea. *Sci. Rep.* 9:12015.

Dyar, K. A., Ciciliot, S., Tagliazucchi, G. M., Pallafacchina, G., Tothova, J., Argentini, C., et al. (2015). The calcineurin-NFAT pathway controls activity-dependent circadian gene expression in slow skeletal muscle. *Mol. Metab.* 4, 823–833. doi: 10.1016/j.molmet.2015.09.004

Dyar, K. A., Ciciliot, S., Wright, L. E., Bienso, R. S., Tagliazucchi, G. M., Patel, V. R., et al. (2014). Muscle insulin sensitivity and glucose metabolism are controlled by the intrinsic muscle clock. *Mol. Metab.* 3, 29–41. doi: 10.1016/j.molmet.2013.10.005

Dyar, K. A., Hubert, M. J., Mir, A. A., Ciciliot, S., Lutter, D., Greulich, F., et al. (2018). Transcriptional programming of lipid and amino acid metabolism by the skeletal muscle circadian clock. *PLoS Biol.* 16:e2005886. doi: 10.1371/journal.pbio.2005886

Endeshaw, Y. W., Unruh, M. L., Kutner, M., Newman, A. B., and Bliwise, D. L. (2009). Sleep-disordered breathing and frailty in the cardiovascular health study cohort. *Am. J. Epidemiol.* 170, 193–202. doi: 10.1093/aje/kwp108

Ensrud, K. E., Blackwell, T. L., Ancoli-Israel, S., Redline, S., Cawthon, P. M., Paudel, M. L., et al. (2012). Sleep disturbances and risk of frailty and mortality in older men. *Sleep Med.* 13, 1217–1225. doi: 10.1016/j.sleep.2012.04.010

Ensrud, K. E., Blackwell, T. L., Redline, S., Ancoli-Israel, S., Paudel, M. L., Cawthon, P. M., et al. (2009). Sleep disturbances and frailty status in older community-dwelling men. *J. Am. Geriatr. Soc.* 57, 2085–2093. doi: 10.1111/j.1532-5415.2009.02490.x

Farsijani, S., Payette, H., Morais, J. A., Shatenstein, B., Gaudreau, P., and Chevalier, S. (2017). Even mealtime distribution of protein intake is associated with greater muscle strength, but not with 3-y physical function decline, in free-living older adults: the quebec longitudinal study on nutrition as a determinant of successful aging (NuAge study). *Am. J. Clin. Nutr.* 106, 113–124. doi: 10.3945/ajcn.116.146555

Fex, A., Barbat-Artigas, S., Dupontgand, S., Filion, M.-E., Karelis, A. D., and Aubertin-Leheudre, M. (2012). Relationship between long sleep duration and functional capacities in postmenopausal women. *J. Clin. Sleep Med.* 08, 309–313. doi: 10.5664/jcsm.1922

Fujita, S., and Volpi, E. (2006). Amino acids and muscle loss with aging. *J. Nutr.* 136, 277s–280s.

Gekakis, N., Staknis, D., Nguyen, H. B., Davis, F. C., Wilsbacher, L. D., King, D. P., et al. (1998). Role of the CLOCK protein in the mammalian circadian mechanism. *Science* 280, 1564–1569. doi: 10.1126/science.280.5369.1564

Harfmann, B. D., Schroder, E. A., and Esser, K. A. (2015). Circadian rhythms, the molecular clock, and skeletal muscle. *J. Biol. Rhythms* 30, 84–94. doi: 10.1177/0748730414561638

Harfmann, B. D., Schroder, E. A., Kachman, M. T., Hodge, B. A., Zhang, X., and Esser, K. A. (2016). Muscle-specific loss of Bmal1 leads to disrupted tissue glucose metabolism and systemic glucose homeostasis. *Skelet Muscle* 6:12.

Hodge, B. A., Wen, Y., Riley, L. A., Zhang, X., England, J. H., Harfmann, B. D., et al. (2015). The endogenous molecular clock orchestrates the temporal separation of substrate metabolism in skeletal muscle. *Skelet Muscle* 5:17.

Hodge, B. A., Zhang, X., Gutierrez-Monreal, M. A., Cao, Y., Hammers, D. W., Yao, Z., et al. (2019). MYOD1 functions as a clock amplifier as well as a critical co-factor for downstream circadian gene expression in muscle. *eLife* 8:e43017.

Hood, S., and Amir, S. (2017). The aging clock: circadian rhythms and later life. *J. Clin. Invest.* 127, 437–446. doi: 10.1172/jci90328

Hu, X., Jiang, J., Wang, H., Zhang, L., Dong, B., and Yang, M. (2017). Association between sleep duration and sarcopenia among community-dwelling older adults: a cross-sectional study. *Medicine* 96:e6268. doi: 10.1097/md.0000000000006268

Ikeda, Y., Kamagata, M., Hirao, M., Yasuda, S., Iwami, S., Sasaki, H., et al. (2018). Glucagon and/or IGF-1 production regulates resetting of the liver circadian clock in response to a protein or amino acid-only diet. *EBioMedicine* 28, 210–224. doi: 10.1016/j.ebiom.2018.01.012

Ishikawa-Takata, K., and Takimoto, H. (2018). Current protein and amino acid intakes among Japanese people: analysis of the 2012 National Health and Nutrition Survey. *Geriatr. Gerontol. Int.* 18, 723–731. doi: 10.1111/ggi.13239

Jamshed, H., Beyl, R. A., Della Manna, D. L., Yang, E. S., Ravussin, E., and Peterson, C. M. (2019). Early time-restricted feeding improves 24-Hour glucose levels and affects markers of the circadian clock, aging, and autophagy in humans. *Nutrients* 11:1234. doi: 10.3390/nu11061234

Jones, R., Pabla, P., Mallinson, J., Nixon, A., Taylor, T., Bennett, A., et al. (2020). Two weeks of early time-restricted feeding (eTRF) improves skeletal muscle insulin and anabolic sensitivity in healthy men. *Am. J. Clin. Nutr.* 112, 1015–1028. doi: 10.1093/ajcn/nqaa192

Kelu, J. J., Pipalia, T. G., and Hughes, S. M. (2020). Circadian regulation of muscle growth independent of locomotor activity. *Proc. Natl. Acad. Sci. U.S.A.* 117, 31208–31218. doi: 10.1073/pnas.2012450117

Kondratov, R. V., Kondratova, A. A., Gorbacheva, V. Y., Vykhovanets, O. V., and Antoch, M. P. (2006). Early aging and age-related pathologies in mice deficient in BMAL1, the core componentof the circadian clock. *Genes Dev.* 20, 1868–1873. doi: 10.1101/gad.1432206

Kwon, Y. J., Jang, S. Y., Park, E. C., Cho, A. R., Shim, J. Y., and Linton, J. A. (2017). Long sleep duration is associated with sarcopenia in korean adults based on data from the 2008-2011 KNHANES. *J. Clin. Sleep Med.* 13, 1097–1104. doi: 10.5664/jcsm.6732

Lipton, J. O., Yuan, E. D., Boyle, L. M., Ebrahimi-Fakhari, D., Kwiatkowski, E., Nathan, A., et al. (2015). The circadian protein BMAL1 regulates translation in response to S6K1-Mediated phosphorylation. *Cell* 161, 1138–1151. doi: 10.1016/j.cell.2015.04.002

Longo, V. D., and Panda, S. (2016). Fasting, circadian rhythms, and time-restricted feeding in healthy lifespan. *Cell Metab.* 23, 1048–1059. doi: 10.1016/j.cmet.2016.06.001

Lowe, M., Lage, J., Paatela, E., Munson, D., Hostager, R., Yuan, C., et al. (2018). Cry2 is critical for circadian regulation of myogenic differentiation by bclaf1-mediated mRNA Stabilization of Cyclin D1 and Tmem176b. *Cell Rep.* 22, 2118–2132. doi: 10.1016/j.celrep.2018.01.077

Lucassen, E. A., de Mutsert, R., le Cessie, S., Appelman-Dijkstra, N. M., Rosendaal, F. R., and van Heemst, D. (2017). Poor sleep quality and later sleep timing are risk factors for osteopenia and sarcopenia in middle-aged men and women: the NEO study. *PLoS One* 12:e0176685. doi: 10.1371/journal.pone.0176685

Lundell, L. S., Parr, E. B., Devlin, B. L., Ingerslev, L. R., Altıntaş, A., Sato, S., et al. (2020). Time-restricted feeding alters lipid and amino acid metabolite rhythmicity without perturbing clock gene expression. *Nat. Commun.* 11:4643.

Mamerow, M. M., Mettler, J. A., English, K. L., Casperson, S. L., Arentson-Lantz, E., Sheffield-Moore, M., et al. (2014). Dietary protein distribution positively influences 24-h muscle protein synthesis in healthy adults. *J. Nutr.* 144, 876–880. doi: 10.3945/jn.113.185280

Manoogian, E. N. C., and Panda, S. (2017). Circadian rhythms, time-restricted feeding, and healthy aging. *Ageing Res. Rev.* 39, 59–67. doi: 10.1016/j.arr.2016.12.006

Martinez-Lopez, N., Tarabra, E., Toledo, M., Garcia-Macia, M., Sahu, S., Coletto, L., et al. (2017). System-wide benefits of intermeal fasting by autophagy. *Cell Metab.* 26, 856.e5–871.e5.

Mayeuf-Louchart, A., Thorel, Q., Delhaye, S., Beauchamp, J., Duhem, C., Danckaert, A., et al. (2017). Rev-erb-alpha regulates atrophy-related genes to control skeletal muscle mass. *Sci. Rep.* 7:14383.

McCarthy, J. J., Andrews, J. L., McDearmon, E. L., Campbell, K. S., Barber, B. K., Miller, B. H., et al. (2007). Identification of the circadian transcriptome in adult mouse skeletal muscle. *Phys. Genomics* 31, 86–95. doi: 10.1152/physiolgenomics.00066.2007

McDearmon, E. L., Patel, K. N., Ko, C. H., Walisser, J. A., Schook, A. C., Chong, J. L., et al. (2006). Dissecting the functions of the mammalian clock protein BMAL1 by tissue-specific rescue in mice. *Science* 314, 1304–1308. doi: 10.1126/science.1132430

Miller, B. H., McDearmon, E. L., Panda, S., Hayes, K. R., Zhang, J., Andrews, J. L., et al. (2007). Circadian and CLOCK-controlled regulation of the mouse transcriptome and cell proliferation. *Proc. Natl. Acad. Sci. U.S.A.* 104, 3342–3347. doi: 10.1073/pnas.0611724104

Nakakubo, S., Doi, T., Makizako, H., Tsutsumimoto, K., Kurita, S., Kim, M., et al. (2019). Association of sleep condition and social frailty in community-dwelling older people. *Geriatr. Gerontol. Int.* 19, 885–889. doi: 10.1111/ggi.13734

National Center for Health Statistics About the National Health and Nutrition Exmaination Survey (NHANES) (2012). *What We Eat in America*. Washington, DC: U.S. Department of Agriculture. (NHANES 2009-2010).

Norton, C., Toomey, C., McCormack, W. G., Francis, P., Saunders, J., Kerin, E., et al. (2016). Protein supplementation at breakfast and lunch for 24 weeks beyond habitual intakes increases whole-body lean tissue mass in healthy older adults. *J. Nutr.* 146, 65–69. doi: 10.3945/jn.115.219022

Norton, L. E., Wilson, G. J., Moulton, C. J., and Layman, D. K. (2016). Meal distribution of dietary protein and leucine influences long-term muscle mass and body composition in adult rats. *J. Nutr.* 147, 195–201. doi: 10.3945/jn.116.231779

Oishi, K., Yasumoto, Y., Higo-Yamamoto, S., Yamamoto, S., and Ohkura, N. (2017). Feeding cycle-dependent circulating insulin fluctuation is not a dominant Zeitgeber for mouse peripheral clocks except in the liver: differences between endogenous and exogenous insulin effects. *Biochem. Biophys. Res. Commun.* 483, 165–170. doi: 10.1016/j.bbrc.2016.12.173

Patel, S. R., Zhu, X., Storfer-Isser, A., Mehra, R., Jenny, N. S., Tracy, R., et al. (2009). Sleep duration and biomarkers of inflammation. *Sleep* 32, 200–204. doi: 10.1093/sleep/32.2.200

Peek, C. B., Levine, D. C., Cedernaes, J., Taguchi, A., Kobayashi, Y., Tsai, S. J., et al. (2017). Circadian clock interaction with HIF1α mediates oxygenic metabolism and anaerobic glycolysis in skeletal muscle. *Cell Metab.* 25, 86–92.

Piovezan, R. D., Abucham, J., Dos Santos, R. V., Mello, M. T., Tufik, S., and Poyares, D. (2015). The impact of sleep on age-related sarcopenia: possible connections and clinical implications. *Ageing Res. Rev.* 23, 210–220. doi: 10.1016/j.arr.2015.07.003

Pourmotabbed, A., Boozari, B., Babaei, A., Asbaghi, O., Campbell, M. S., Mohammadi, H., et al. (2020). Sleep and frailty risk: a systematic review and meta-analysis. *Sleep Breath* 24, 1187–1197. doi: 10.1007/s11325-020-02061-w

Preitner, N., Damiola, F., Lopez-Molina, L., Zakany, J., Duboule, D., Albrecht, U., et al. (2002). The orphan nuclear receptor REV-ERBalpha controls circadian transcription within the positive limb of the mammalian circadian oscillator. *Cell* 110, 251–260. doi: 10.1016/s0092-8674(02)00825-5

Rubio-Arias, J., Rodríguez-Fernández, R., Andreu, L., Martínez-Aranda, L. M., Martínez-Rodriguez, A., and Ramos-Campo, D. J. (2019). Effect of sleep quality on the prevalence of sarcopenia in older adults: a systematic review with meta-analysis. *J. Clin. Med.* 8:2156. doi: 10.3390/jcm8122156

Sato, T. K., Panda, S., Miraglia, L. J., Reyes, T. M., Rudic, R. D., McNamara, P., et al. (2004). A functional genomics strategy reveals Rora as a component of the mammalian circadian clock. *Neuron* 43, 527–537. doi: 10.1016/j.neuron.2004.07.018

Schibler, U., Ripperger, J., and Brown, S. A. (2003). Peripheral circadian oscillators in mammals: time and food. *J. Biol. Rhythms* 18, 250–260. doi: 10.1177/0748730403018003007

Schroder, E. A., Harfmann, B. D., Zhang, X., Srikuea, R., England, J. H., Hodge, B. A., et al. (2015). Intrinsic muscle clock is necessary for musculoskeletal health. *J. Physiol.* 593, 5387–5404. doi: 10.1113/jp271436

Shibata, S. (2004). Neural regulation of the hepatic circadian rhythm. *Anat. Record Part A Discov. Mol. Cell. Evol. Biol.* 280, 901–909. doi: 10.1002/ar.a.20095

Smiley, A., King, D., and Bidulescu, A. (2019). The association between sleep duration and metabolic syndrome: the NHANES 2013/2014. *Nutrients* 11:2582. doi: 10.3390/nu11112582

Solanas, G., Peixoto, F. O., Perdiguero, E., Jardí, M., Ruiz-Bonilla, V., Datta, D., et al. (2017). Aged stem cells reprogram their daily rhythmic functions to adapt to stress. *Cell* 170, 678.e20–692.e20.

Stokes, T., Hector, A. J., Morton, R. W., McGlory, C., and Phillips, S. M. (2018). Recent perspectives regarding the role of dietary protein for the promotion of muscle hypertrophy with resistance exercise training. *Nutrients* 10:180. doi: 10.3390/nu10020180

Tahara, Y., and Shibata, S. (2013). Chronobiology and nutrition. *Neuroscience* 253, 78–88. doi: 10.1016/j.neuroscience.2013.08.049

Tahara, Y., Takatsu, Y., Shiraishi, T., Kikuchi, Y., Yamazaki, M., Motohashi, H., et al. (2017). Age-related circadian disorganization caused by sympathetic dysfunction in peripheral clock regulation. *NPJ Aging Mech. Dis.* 3:16030.

Tieland, M., Borgonjen-Van den Berg, K. J., Van Loon, L. J., and de Groot, L. C. (2015). Dietary protein intake in dutch elderly people: a focus on protein sources. *Nutrients* 7, 9697–9706. doi: 10.3390/nu7125496

Vaz Fragoso, C. A., Gahbauer, E. A., Van Ness, P. H., and Gill, T. M. (2009). Sleep-wake disturbances and frailty in community-living older persons. *J. Am. Geriatr. Soc.* 57, 2094–2100. doi: 10.1111/j.1532-5415.2009.02522.x

Villanueva, J. E., Livelo, C., Trujillo, A. S., Chandran, S., Woodworth, B., Andrade, L., et al. (2019). Time-restricted feeding restores muscle function in *Drosophila* models of obesity and circadian-rhythm disruption. *Nat. Commun.* 10:2700.

Yang, G., Chen, L., Grant, G. R., Paschos, G., Song, W. L., Musiek, E. S., et al. (2016). Timing of expression of the core clock gene Bmal1 influences its effects on aging and survival. *Sci. Transl. Med.* 8:324ra316.

Yu, J. H., Yun, C. H., Ahn, J. H., Suh, S., Cho, H. J., Lee, S. K., et al. (2015). Evening chronotype is associated with metabolic disorders and body composition in middle-aged adults. *J. Clin. Endocrinol. Metab.* 100, 1494–1502. doi: 10.1210/jc.2014-3754

Zhang, R., Lahens, N. F., Ballance, H. I., Hughes, M. E., and Hogenesch, J. B. (2014). A circadian gene expression atlas in mammals: implications for biology and medicine. *Proc. Natl. Acad. Sci. U.S.A.* 111, 16219–16224. doi: 10.1073/pnas.1408886111

Zurlo, F., Larson, K., Bogardus, C., and Ravussin, E. (1990). Skeletal muscle metabolism is a major determinant of resting energy expenditure. *J. Clin. Invest.* 86, 1423–1427. doi: 10.1172/jci114857

Conflict of Interest: The authors declare that the research was conducted in the absence of any commercial or financial relationships that could be construed as a potential conflict of interest.

frontiers in Neuroscience

ORIGINAL RESEARCH
published: 24 May 2021
doi: 10.3389/fnins.2021.647589

Attenuated SIRT1 Activity Leads to PER2 Cytoplasmic Localization and Dampens the Amplitude of *Bmal1* Promoter-Driven Circadian Oscillation

Atsushige Ashimori[1,2,3], Yasukazu Nakahata[1,2], Toshiya Sato[4], Yuichiro Fukamizu[4], Takaaki Matsui[1], Hikari Yoshitane[5], Yoshitaka Fukada[5], Kazuyuki Shinohara[2] and Yasumasa Bessho[1]*

[1] Laboratory of Gene Regulation Research, Division of Biological Science, Graduate School of Science and Technology, Nara Institute of Science and Technology, Nara, Japan, [2] Department of Neurobiology and Behavior, Graduate School of Biomedical Sciences, Nagasaki University, Nagasaki, Japan, [3] Department of Ophthalmology, Graduate School of Medicine, Yamaguchi University, Yamaguchi, Japan, [4] Research and Development Division, Mitsubishi Corporation Life Sciences Limited, Tokyo, Japan, [5] Department of Biological Sciences, School of Science, The University of Tokyo, Tokyo, Japan

OPEN ACCESS

Edited by:
Takahiro J. Nakamura, Meiji University, Japan

Reviewed by:
Yoshiki Tsuchiya, Kyoto Prefectural University of Medicine, Japan
Shihoko Kojima, Virginia Tech, United States

***Correspondence:**
Yasukazu Nakahata
yasu-nakahata@nagasaki-u.ac.jp

Specialty section:
This article was submitted to Sleep and Circadian Rhythms, a section of the journal Frontiers in Neuroscience

Received: *30 December 2020*
Accepted: *08 April 2021*
Published: *24 May 2021*

Citation:
Ashimori A, Nakahata Y, Sato T, Fukamizu Y, Matsui T, Yoshitane H, Fukada Y, Shinohara K and Bessho Y (2021) Attenuated SIRT1 Activity Leads to PER2 Cytoplasmic Localization and Dampens the Amplitude of Bmal1 Promoter-Driven Circadian Oscillation. Front. Neurosci. 15:647589. doi: 10.3389/fnins.2021.647589

The circadian clock possesses robust systems to maintain the rhythm approximately 24 h, from cellular to organismal levels, whereas aging is known to be one of the risk factors linked to the alternation of circadian physiology and behavior. The amount of many metabolites in the cells/body is altered with the aging process, and the most prominent metabolite among them is the oxidized form of nicotinamide adenine dinucleotide (NAD^+), which is associated with posttranslational modifications of acetylation and poly-ADP-ribosylation status of circadian clock proteins and decreases with aging. However, how low NAD^+ condition in cells, which mimics aged or pathophysiological conditions, affects the circadian clock is largely unknown. Here, we show that low NAD^+ in cultured cells promotes PER2 to be retained in the cytoplasm through the NAD^+/SIRT1 axis, which leads to the attenuated amplitude of *Bmal1* promoter-driven luciferase oscillation. We found that, among the core clock proteins, PER2 is mainly affected in its subcellular localization by NAD^+ amount, and a higher cytoplasmic PER2 localization was observed under low NAD^+ condition. We further found that NAD^+-dependent deacetylase SIRT1 is the regulator of PER2 subcellular localization. Thus, we anticipate that the altered PER2 subcellular localization by low NAD^+ is one of the complex changes that occurs in the aged circadian clock.

Keywords: circadian clock, PER2, NAD^+, SIRT1, subcelluar localization

INTRODUCTION

The oxidized form of nicotinamide adenine dinucleotide (NAD^+) found in all living cells plays critical roles in a wide range of physiological processes. NAD^+ acts as a coenzyme for enzymes which are involved in energy metabolism and homeostasis pathways such as glycolysis, TCA cycle, and oxidative phosphorylation (Campbell, 1995). NAD^+ also acts as a co-substrate for enzymes

such as sirtuins (SIRTs) and poly(ADP-ribose) polymerases (PARPs) to regulate a wide array of cellular processes such as survival/cell death, circadian clock, and aging (Imai and Guarente, 2014; Verdin, 2015). In mammals, cellular NAD^+ is primarily biosynthesized by the NAD^+ salvage pathway, in which nicotinamide phosphoribosyltransferase (NAMPT) is the rate-limiting enzyme and converts nicotinamide into nicotinamide mononucleotide (NMN), the NAD^+ precursor (Revollo et al., 2007; Imai and Guarente, 2014; Nakahata and Bessho, 2016).

NAD^+ amount declines during the aging process, causing defects in nuclear and mitochondrial functions and resulting in many age-associated diseases (Gomes et al., 2013; Mouchiroud et al., 2013). Intriguingly, administration of NAD^+ precursors such as NMN and nicotinamide riboside (NR) can ameliorate many age-associated pathologies, thereby leading to healthy longevity (Yoshino et al., 2018; Custodero et al., 2020; Hong et al., 2020). Similar to organismal aging, NAD^+ amount is also reported to decline with cellular aging, i.e., cellular senescence (Khaidizar et al., 2017). Overexpression of NAMPT in primary fibroblast cells delays the onset of replicative senescence (van der Veer et al., 2007; Khaidizar et al., 2017) and confers a protective effect against stress-induced premature senescence (Nuriliani et al., 2020). These reports demonstrate that a decline in NAD^+ is one of the causes to induce cellular senescence as well as organismal aging.

NAD^+ in cells and organs demonstrates circadian oscillation due to the circadian clock regulation of *Nampt* gene expression (Nakahata et al., 2009; Ramsey et al., 2009). Moreover, NAD^+ is associated with the transcriptional regulation of circadian clock genes through the regulation of SIRT1, SIRT6, and PARP1 activities (Asher et al., 2008, 2010; Nakahata et al., 2008; Masri et al., 2014). These findings demonstrate that circadian clock and NAD^+ metabolism are mutually regulated (Imai, 2010; Nakahata and Bessho, 2016). Since NAD^+ amount declines with senescence/aging, circadian clock properties are expected to be altered by senescence/aging. Indeed, circadian clocks in primary cells, tissues, and animals show altered circadian properties by senescence/aging. The circadian amplitude at the transcriptional (Kunieda et al., 2006; Nakamura et al., 2015; Ahmed et al., 2019), neural activity (Nakamura et al., 2011), and locomotor activity levels (Pittendrigh and Daan, 1974; Witting et al., 1994; Valentinuzzi et al., 1997; Sellix et al., 2012) declines with aging. The period of circadian genes alters with senescence/aging in primary human fibroblasts and *ex vivo* mouse SCN slices (Nakamura et al., 2015; Ahmed et al., 2019), although it is still controversial at the organismal level (Valentinuzzi et al., 1997; Aujard et al., 2001; Kolker et al., 2004). However, only a few researches have looked into the molecular mechanisms of how the circadian clock is affected by senescence/aging (Chang and Guarente, 2014; Zwighaft et al., 2015; Levine et al., 2020).

We have reported that a decline in NAD^+ keeps activating the transcription of E-box-regulated circadian clock genes *via* hyperacetylation of lysine 9/14 residues on histone H3, due to the inactivation of NAD^+-dependent deacetylase, SIRT1 (Nakahata et al., 2008). In addition to that report, some investigators have also demonstrated that NAD^+ regulates other circadian clock components: SIRT1 deacetylates PER2, resulting in its stabilization (Asher et al., 2008); SIRT1 deacetylates PGC1α to activate *Bmal1* transcription (Chang and Guarente, 2014); PARP-1, an NAD^+-dependent ADP-ribosyltransferase, poly(ADP-ribosyl)ates CLOCK (Asher et al., 2010); and the inhibitor of SIRT1 changes the ratio of PER2 subcellular localization (Miki et al., 2012).

The aforementioned findings prompted us to reveal the molecular mechanisms of how NAD^+ amount, especially low NAD^+, affects the circadian clock system, which might give some hints to unravel molecular links between aging and circadian clock. In this study, we reduced intracellular NAD^+ amount by inhibiting NAMPT enzymatic activity and found that it attenuates the amplitude of *Bmal1* promoter-driven luciferase oscillation and promotes cytoplasmic localization of PER2, leading to attenuated CRY/PER-dependent repression, thereby enhancing E-box-regulated circadian gene expressions. At the molecular level, we revealed that the translocation of PER2 with low NAD^+ is dependent upon SIRT1 activity, but not PARP1 activity.

MATERIALS AND METHODS

Reagents, Antibodies, and Plasmids

FK866, GMX1778, nicotinamide, EX-527, and PJ34 were purchased from the Axon Medchem, AdipoGen Life Sciences, Sigma, Cayman Chemical, and Abcam, respectively. Nicotinamide mononucleotide (NMN) was provided by the Mitsubishi Corporation Life Sciences Limited, Japan. Anti-Per2 (PM083), anti-Lamin B1 (PM064), anti-Myc-tag (M047-3), and anti-DDDDK-tag (M185-3) were purchased from the MBL, Japan. Anti-α-tubulin (T6074) and the secondary anti-mouse antibody Alexa Fluor Plus 488 (A32723) were purchased from the Sigma-Aldrich and Thermo Fisher Scientific, respectively. PAR/pADPr antibody was purchased from the R&D Systems. Anti-Bmal1 (ab93806) and anti-acetyl Bmal1 (Lys538) were purchased from the Abcam and Merck, respectively. Secondary anti-mouse (NA931V) or rabbit (NA934) antibodies conjugated with HRP were purchased from the GE Healthcare. Myc-mClock/pcDNA3 was subcloned from Myc-mClock/pSG5 as described (Doi et al., 2006). 5xMyc-mCry1-Flag/pCS2 and Myc-mBmal1/pcDNA3 were described as previously (Hirayama et al., 2007). Flag-hRORα1/pcDNA3, Flag-hRORγ/pcDNA3, Flag-mRev-erbα/pcDNA3, and Flag-mRev-erbβ/pcDNA3 were inserted a single Flag epitope into hRORα1/pcDNA3, hRORγ/pcDNA3, mRev-erbα/pcDNA3, and mRev-erbβ/pcDNA3, respectively, provided by Akashi and Takumi (2005). Flag-mCry1/pcDNA3, 2xMyc-Per2-NLS/pcDNA3, and 2xMyc-Per2-NES/pcDNA3 were kind gifts of Akashi et al. (2014). pLLX-shRNA and pLLX-scrambled shRNA were kindly provided by ME Greenberg (Zhou et al., 2006).

Cell Culture

NIH3T3 cells were cultured in DMEM–4.5 g/L glucose (Nacalai Tesque, Japan) supplemented with 10% FBS (Sigma) and antibiotics (100 units/ml penicillin, 100 μg/ml streptomycin, Nacalai Tesque, Japan) at 37°C and 5% CO_2 in a humidified

incubator. Cells were treated with FK866/GMX1778 with or without 1 mM nicotinamide mononucleotide for 24 h and harvested for measuring NAD^+ amount, performing qPCR, immunofluorescence, and western blotting. For experiments analyzing circadian oscillations of clock genes, luciferase, and PER2 protein, cells were pretreated with FK866 for 24 h before Dex synchronization and also treated with FK866 after synchronization.

Quantification of Intracellular NAD^+ by HPLC

NAD^+ was measured by an HPLC system, an Agilent 1260 Infinity Binary LC System with guard (Polaris C18-A, MetaGuard, 5 μm, 4.6 mm; A2000MG, Agilent) and analytical (Polaris 5 C18-A 4.6 × 150 mm; A2000150 × 046, Agilent) columns, following the protocol reported previously (Yoshino and Imai, 2013; Khaidizar et al., 2017).

SDS-PAGE, Western Blotting Analysis, RNA Extraction, and qPCR

Protocols for SDS-PAGE, western blotting analysis, RNA extraction, and qPCR were followed as described previously (Khaidizar et al., 2017). Protein measurement was performed using 660 Protein Assay Reagent (Thermo Fisher Scientific) according to the manufacturer's instruction. The sequences for qPCR primers are shown in **Supplementary Table 1**.

Real-Time Luciferase Monitoring Assay

The method was described previously (Ahmed et al., 2019).

Immunofluorescence

NIH3T3 cells were seeded on a sterilized cover glass (Matsunami; 24 × 24 mm; thickness no. 1) placed on a six-well plate so as to have 4×10^5 cells/well as a single experiment. Cells were co-transfected with indicated expression vectors using FuGENE HD (Promega) and cultured for 48 h. The cells after washing twice with phosphate buffered saline (PBS) were fixed with 1 ml of 4% paraformaldehyde for 15 min with shaking at room temperature. Then, cells were washed three times with PBS and permeabilized with 1 ml of 0.5% Triton X-100 for 10 min with shaking at room temperature. After blocking the cells with 1% bovine serum albumin (BSA) for 30 min at room temperature, the cells were washed three times with PBS and incubated with Myc antibody diluted with 1% BSA/PBS for 1 h at room temperature. Then, cells were incubated with secondary antibody conjugated with Alexa Fluor Plus 488 diluted with 1% BSA/PBS for 1 h at room temperature. Nuclei were also stained with 1 μg/ml Hoechst 33342 (Nacalai Tesque, Japan) to justify subcellular localizations of clock proteins. Fluorescent images were acquired with a confocal laser scanning microscope (ZEISS; LSM 700), and subcellular localizations of clock proteins were counted at least 100 cells. We interpreted the result for nuclear localization of PER2/CRY1 (N) as positive when fluorescence intensity of PER2/CRY1 signal that overlapped with Hoechst 33342 signal was higher than the fluorescence intensity of PER2/CRY1 in the cytoplasm (**Supplementary Figure 1**). Meanwhile, we interpreted the result for cytoplasmic localization of PER2/CRY1 (C) as positive when PER2/CRY1 signal that did not overlap with Hoechst 33342 signal exhibited higher fluorescence intensity than PER2/CRY1 signal intensity that overlapped with Hoechst 33342 signal. Finally, we interpreted the result for nuclear and cytoplasm localization of PER2/CRY1 (N + C) as positive when PER2/CRY1 fluorescence signal at both nucleus and cytoplasm had the same intensities. We performed the experiments independently for at least three times and showed the data as mean ± SEM.

Nuclear Extract From NIH3T3 Cells

NIH3T3 cells treated with or without 7.5 nM FK866 for 24 h in a 10-cm dish were synchronized with 100 μM dexamethasone for 1 h. Synchronized cells after 24–44 h were collected every 4 h. Cells were washed twice with PBS and harvested by cell scrapers, centrifuged at 300 × *g* for 5 min at 4°C, and resuspended in 50 μl lysis buffer [10 mM HEPES (pH 7.9), 1.5 mM $MgCl_2$, 10 mM KCl]. Cells were vortexed for 10 s and allowed to stand on ice for 10 min, and the same step was repeated again to extract cell components other than the nuclear fraction. The nuclear fraction was washed three times with lysis buffer, added with 50 μl RIPA buffer [50 mM Tris–HCl (pH 7.4), 150 mM $NaCl_2$, 1 mM EDTA, 0.2% SDS, 1% NP-40], vortexed for 30 s, and then allowed to stand on ice for 20 min. The nuclear fraction was centrifuged at 15,000 × *g* for 5 min at 4°C, and the supernatant was collected as a nuclear extract. Total cell extract was obtained by extracting cells with RIPA buffer.

Dual-Luciferase Promoter Assay

NIH3T3 cells seeded in a 24-well plate were co-transfected with 500 ng of *Per1* firefly reporter, 50 ng of *EF1a Renilla* reporter, and indicated expression vectors using FuGENE HD (Roche). Samples were prepared using a Dual-Luciferase promoter assay kit (Promega) according to their instructions and analyzed by a multiwell luminescence measurement plate reader (Mithras, LB940). Firefly luciferase activity of the reporter was normalized by the activity of *Renilla* luciferase under control of EF1α promoter.

Establishment of Sirt1 Knockdown Cell

To establish Sirt1 knockdown cells, lentivirus vector pLLX-shRNA (Zhou et al., 2006), which expresses GFP and a puromycin resistant gene, was used. After virus infection to *Bmal1*-luc/NIH3T3 (Yoshitane et al., 2012), cells were selected by puromycin for 1 week and confirmed by GFP fluorescence (all cells were ∼100% GFP positive). Three different target sequences for mouse *Sirt1* and scramble sequence are shown in **Supplementary Table 2**.

Statistics

Values are reported as mean ± SEM. Statistical differences were determined by a Student's two-tailed *t*-test. Statistical significance is displayed as $^*p < 0.05$, $^{**}p < 0.01$, or $^{***}p < 0.001$.

RESULTS

To investigate how the circadian clock system is affected by low NAD^+ in cells, we first evaluated how much NAD^+ was decreased by the inhibition of the rate-limiting enzyme, NAMPT, in the NAD^+ salvage pathway (**Figure 1A**). We used FK866 (Hasmann and Schemainda, 2003) to inhibit the NAMPT activity and found that 2.0, 5.0, and 7.5 nM FK866 treatment decreased NAD^+ to approximately 50, 33, and 25%, respectively (**Figure 1B**). In addition, the acetylated form of BMAL1, which has been reported to be increased by FK866 treatment (Nakahata et al., 2009), was increased by FK866 treatment in a dose-dependent manner (**Supplementary Figure 2A**). We further confirmed that the effect of FK866 treatment at 7.5 nM on NAD^+ amount was abrogated by the co-treatment with the NAD^+ precursor, NMN (**Figure 1C**). A similar tendency was observed by another NAMPT inhibitor, GMX1778 (Watson et al., 2009) (**Supplementary Figures 3A,B**). We then performed a real-time luciferase assay to address whether circadian clock properties are affected by low NAD^+. To address that, we used NIH3T3 cells stably expressing *Bmal1* promoter-driven *luciferase* (Yoshitane et al., 2012). The amplitude, which was defined in this study as the height from the first peak to the first trough, of *Bmal1* promoter-driven luciferase oscillation was attenuated in FK866-treated cells, compared with that in control cells (**Figures 1D,E**). A delayed phase was also observed in FK866-treated *Bmal1*-luc oscillation. Intriguingly, the attenuated amplitude and delayed phase were abrogated in FK866 and NMN co-treated cells, indicating that the amplitude and phase are regulated by NAD^+ amount. The reason why these alterations were abrogated after 60 h Dex treatment is presumably due to the recovery of intracellular NAD^+ amount (**Supplementary Figure 4**). We further checked endogenous circadian gene expressions in unsynchronized cells with low NAD^+. Among core circadian genes, E-box-regulated genes, such as *Rev-erbα*, *Rev-erbβ*, *Per1*, and *Per2*, were upregulated; however, the RORE-regulated gene, *Bmal1*, was downregulated (**Figure 1F**). Moreover, these alterations were abrogated in FK866 and NMN co-treated cells, indicating that the alterations of these genes are regulated by NAD^+ amount. Furthermore, we demonstrated that circadian profiles of endogenous *Bmal1* and *Rev-erbα* transcripts were also affected, lower *Bmal1* and higher *Rev-erbα*, in synchronized cells with low NAD^+ (**Figure 1G**). These results demonstrate that low NAD^+ alters transcript levels of not only E-box-regulated genes as we have reported previously (Nakahata et al., 2008), but also RORE-regulated genes, which presumably regulate the amplitude of circadian clocks.

As our previous studies have demonstrated that the circadian gene expressions are epigenetically regulated by NAD^+-dependent deacetylases, SIRT1 and SIRT6 (Nakahata et al., 2008; Masri et al., 2014), in this study, we sought to find out whether the properties of circadian clock proteins, such as protein stability and subcellular localization, are regulated by NAD^+ amount. First, whether low NAD^+ affects protein stability of clock proteins was investigated using cycloheximide, which is an inhibitor of protein biosynthesis due to its prevention in translational elongation. However, the stabilities of CLOCK, BMAL1, PER2, and CRY1 were not significantly affected by low NAD^+ (**Supplementary Figure 5**). Next, whether low NAD^+ affects subcellular localization of clock proteins was investigated

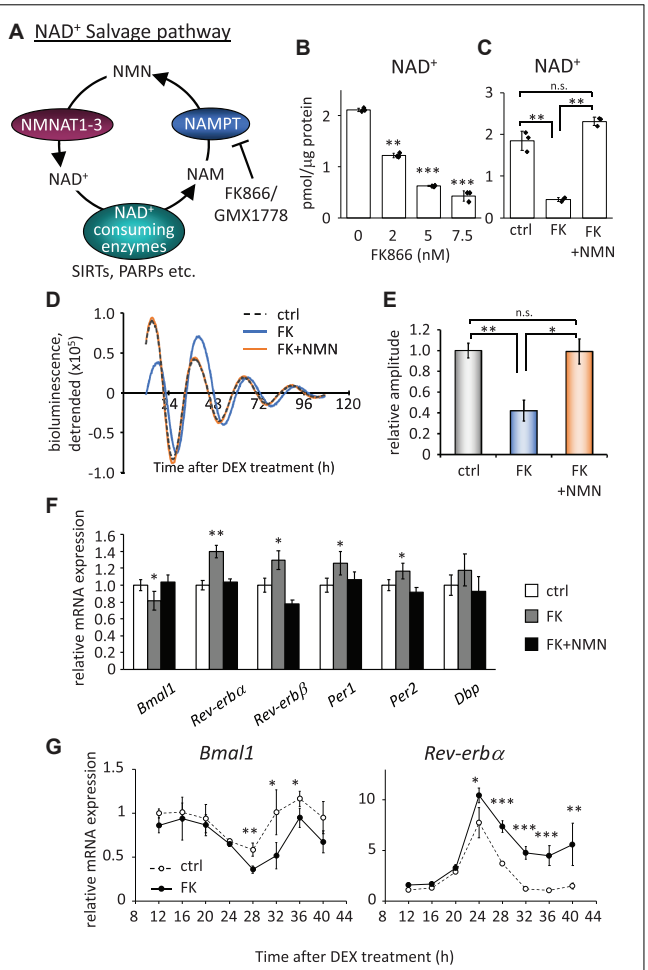

FIGURE 1 | FK866 changes the expression levels of circadian genes, which is abrogated by co-treatment with NMN. **(A)** Scheme of the NAD^+ salvage pathway. NAM, nicotinamide; NMN, nicotinamide mononucleotide; NAMPT, nicotinamide phosphoribosyltransferase; NMNAT1-3, nicotinamide mononucleotide adenylyltransferase 1-3. **(B)** NAD^+ amount after 24 h treatment of FK866 at indicated concentrations was measured by HPLC. NAD^+ amount was normalized by protein amount. **(C)** NAD^+ amount after 24 h treatment of 7.5 nM FK866 with or without 1 mM NMN was measured by HPLC. NAD^+ amount was normalized by protein amount. **(D)** *Bmal1*-luc oscillation patterns in NIH3T3 cells treated with FK866 with or without NMN were monitored by using a real-time luciferase monitoring system. One representative result is shown for each condition. **(E)** Relative amplitudes were analyzed. In this study, the amplitude was defined as the height from the first peak to the first trough. The value of control (ctrl) was set to 1. **(F)** Circadian gene expression levels after treatment with 7.5 nM FK866 alone or 7.5 nM FK866 and 1 mM NMN were quantified by qPCR. Each sample was normalized by the amount of 18S rRNA. Each gene expression level in untreated cells (ctrl) was set to 1. **(G)** Circadian profiles of *Bmal1* and *Rev-erbα* synchronized by DEX were quantified. Each sample was normalized by 18S rRNA. Time 12 of control cells was set to 1 for each gene. All data represented here, except **(E)** ($n = 4$), are the mean ± SEM of three independent samples. $^*p < 0.05$, $^{**}p < 0.01$, and $^{***}p < 0.001$, compared to each of the untreated control by Student's two-tailed *t*-test.

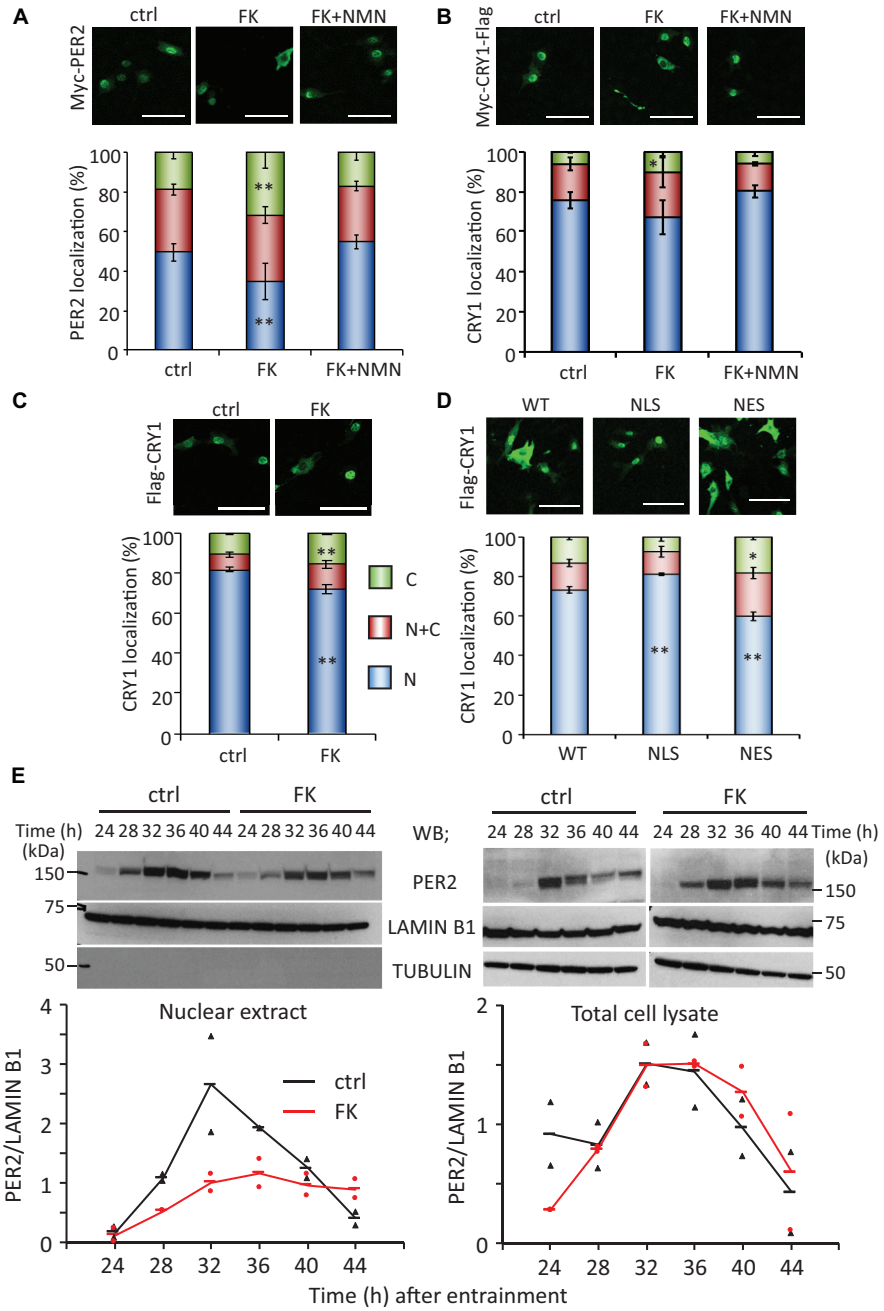

FIGURE 2 | FK866 changes PER2 subcellular localization, which is abrogated by co-treatment with NMN. [**(A–D)**, top] NIH3T3 cells expressing Myc-PER2 **(A)**, Myc-CRY1-Flag **(B)**, or Myc-PER2/Flag-CRY1 **(C)** were immunostained with antibody to Myc or Flag (top). Cells were either untreated (ctrl) or treated with 7.5 nM FK866 (FK) or 7.5 nM FK866 and 1 mM NMN (FK + NMN). NIH3T3 cells expressing Flag-CRY1 and either Myc-PER2-WT, Myc-PER2-NLS, or Myc-PER2-NES were immunostained with antibody to Flag **(D)**. The representative images were captured by a confocal laser scanning microscope. White scale bars represent 100 μm. [**(A–D)**, bottom] Subcellular localizations were counted and quantified; N, nucleus; C, cytoplasm; N + C, both nucleus and cytoplasm. The data represented are the mean ± SEM of at least three independent samples. $^{*}p < 0.05$, $^{**}p < 0.01$, compared to each subcellular localization in control cells by Student's two-tailed *t*-test. **(E)** PER2 protein levels in nuclear extract and total cell lysate were detected under the 7.5 nM FK866-treated condition (top). PER2 protein levels were quantified using ImageJ software (bottom). Each sample was normalized by LAMIN B1 protein level. TUBULIN was used to confirm fractionation. The data represented as filled circle and triangle are individual data of two independent samples and bars are the average of two samples.

(**Figures 2A,B** and **Supplementary Figure 6**). Among clock proteins tested in this study, subcellular localization of PER2 was clearly affected by FK866 treatment (**Figure 2A**). Cytoplasmic and nuclear PER2 under control condition were 18.8 ± 3.4 and 49.3 ± 4.2%, respectively, whereas cytoplasmic and nuclear PER2 under FK866-treated condition were 32.0 ± 7.9% ($p = 5.1 \times 10^{-3}$,

compared with cytoplasmic PER2 under control condition) and 34.5 ± 9.2% ($p = 3.8 \times 10^{-3}$, compared with nuclear PER2 under control condition), respectively. Furthermore, GMX1778 treatment also changed the ratio of PER2 subcellular localization from 22.2 ± 0.5 to 26.3 ± 0.1% in the cytoplasm ($p = 1.0 \times 10^{-4}$) and from 62.0 ± 1.9 to 50.0 ± 0.6% in the nucleus ($p = 2.0 \times 10^{-4}$) (**Supplementary Figure 7**). Importantly, the effect of FK866 or GMX1778 on PER2 subcellular localization was abrogated when cells were treated with both FK866 and NMN or GMX1778 and NMN (**Figure 2A** and **Supplementary Figure 7**). These results indicate that PER2 subcellular localizations are controlled by intracellular NAD$^+$ amount; lower NAD$^+$ promotes the translocation of PER2 from the nucleus to the cytoplasm. Similarly, cytoplasmic and nuclear CRY1 under control condition were 6.3 ± 0.9 and 75.6 ± 3.9%, respectively, while cytoplasmic and nuclear CRY1 under FK866-treated condition were 10.6 ± 2.8% ($p = 0.026$, compared with cytoplasmic CRY1 under control condition) and 67.1 ± 8.5% ($p = 0.12$, compared with nuclear CRY1 under control condition), respectively (**Figure 2B**), indicating the similarity to the change in PER2 by FK866 treatment. These results prompted us to investigate whether the increase in PER2 cytoplasmic localization triggered by FK866 induces the increase in CRY1 cytoplasmic localization, because it is well known that PER2 determines CRY1 localization (Albrecht et al., 2007). Cytoplasmic localizations of CRY1 co-expressing PER2 with or without FK866 were 15.4 ± 0.7 and 10.8 ± 0.8% ($p = 4.8 \times 10^{-3}$) and nuclear localizations were 71.8 ± 2.2 and 81.7 ± 1.3% ($p = 8.6 \times 10^{-3}$), respectively (**Figure 2C**). The alteration of CRY1 subcellular localization by FK866 treatment was more when PER2 was co-expressed, suggesting that the alteration of PER2 subcellular localization leads to that of CRY1.

To confirm whether the changes in PER2 subcellular localization alter CRY1 subcellular localizations, PER2 wild type (WT), C-terminal-tagged nuclear localization signal (-NLS), or C-terminal-tagged nuclear export signal (-NES) (Akashi et al., 2014) was co-expressed with CRY1. Similar to a previous report (Akashi et al., 2014), nuclear localizations of PER2-WT, PER2-NLS, and PER2-NES without CRY1 were 59.1 ± 2.1, 73.6 ± 1.3, and 37.0 ± 4.7%, respectively (**Supplementary Figure 8A**). As expected, subcellular localizations of CRY1 were followed by those of PER2. Compared with the ratio of nuclear CRY1 co-expressing with PER2-WT (73.1 ± 1.6%), the ratio of nuclear CRY1 was increased (81.1 ± 0.7%, $p = 0.011$) when PER2-NLS was co-expressed, whereas the ratio of nuclear CRY1 was decreased (59.8 ± 2.2%, $p = 0.008$) when PER2-NES was co-expressed (**Figure 2D**). These results are consistent with previous reports that PER2 determines CRY1 localization (Albrecht et al., 2007). Even when CRY1 was co-expressed with these PER2s, PER2 subcellular localizations were not affected (**Supplementary Figure 8B**). The results of **Figures 2A–D** suggest that localization of PER2 is directly affected by intracellular NAD$^+$ amount and the intracellular localization of CRY1 follows that of PER2.

Since PER2 protein amount and subcellular localization show time-of-day variations, whether circadian subcellular localization of PER2 is affected by NAD$^+$ amount was next investigated (**Figure 2E**). Although nuclear localization of PER2 clearly showed the time-of-day variation under the control condition as reported previously (Lee et al., 2001; Yagita et al., 2001), the nuclear accumulation of PER2 was reduced, but still showed circadian oscillation, under the FK866-treated condition (**Figure 2E**, left panel). Intriguingly, PER2 in total cell lysate under the FK866-treated condition was comparable with that under the control condition (**Figure 2E**, right panels), suggesting that the reduction of PER2 nuclear localization under the FK866-treated condition is not due to the reduction of PER2, but the decrease in PER2 nuclear entry and/or the increase in PER2 nuclear export.

CRY acts as a transcriptional repressor with PER against CLOCK/BMAL1-dependent, namely E-box-regulated, transcriptions. As the decrease in nuclear localization of PER2 by FK866 suggested the attenuation of PER/CRY-dependent repression against E-box-regulated genes, we next addressed that possibility. To address that, luciferase reporter assay using *Per1* promoter that possesses several E-boxes was assessed using PER2-NES, which mimics PER2 subcellular localizations under the FK866-treated condition. As reported previously, *Per1* promoter activity was activated by CLOCK/BMAL1 and this activation was repressed by CRY1 (**Figure 3**). When PER2-NES was co-expressed, the repression by CRY1 against CLOCK/BMAL1-dependent *Per1* expression was attenuated; namely, the luciferase intensities were increased in a PER2-NES dose-dependent manner (**Figure 3**). On the other hand, when PER2-WT or PER2-NLS was co-expressed, the repression by CRY1 was not affected. The results from **Figures 2E**, **3** indicate that PER2 subcellular localization determines PER/CRY-dependent repression potential, and support that the mechanism

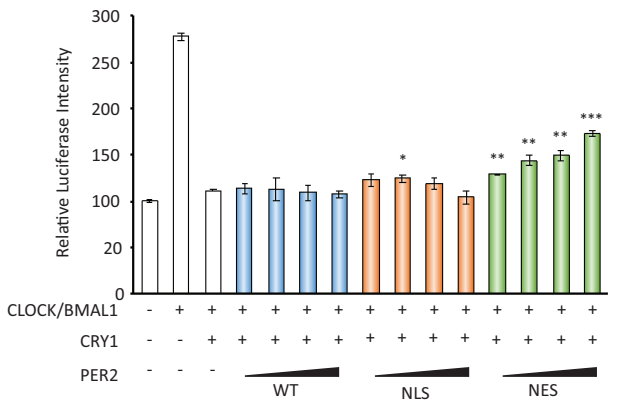

FIGURE 3 | PER2 subcellular localization affects *Per1* gene expression. The effects of PER2-WT, PER2-NLS, and PER2-NES on per1 luciferase activity are shown; 100 ng of CLOCK, 100 ng of BMAL1, 10 ng of CRY1, 500 ng of *Per1* firefly reporter, and 50 ng of *EF1a Renilla* reporter were co-transfected in NIH3T3 cells. Indicated amounts of PER2-WT, PER2-NLS, or PER2-NES were also co-transfected in NIH3T3 cells. Firefly luciferase intensity was normalized by *Renilla* luciferase intensity. Basal *per1* promoter activity (far left bar) was set to 100. The data represented are the mean ± SEM of three independent samples. $^*p < 0.05$, $^{**}p < 0.01$, and $^{***}p < 0.001$, compared with the sample with CLOCK/BMAL1 and CRY1, the third bar from left, by Student's two-tailed *t*-test.

of upregulation of E-box-regulated genes under the FK866-treated condition (**Figure 1C**) is due to the preferential cytoplasmic localization of PER2 with CRY1.

Finally, to investigate the molecular mechanisms of how PER2 subcellular localization is regulated, we pharmacologically inhibited NAD$^+$-dependent enzymes, SIRT1 and PARP1. The SIRT1 inhibitors, 10 mM nicotinamide (NAM) or 5 μM EX-527 (Bitterman et al., 2002; Napper et al., 2005), significantly increased cytoplasmic PER2 from 24.1 ± 1.3 to 39.5 ± 0.5% ($p = 4.0 \times 10^{-4}$) and 33.5 ± 2.1% ($p = 1.9 \times 10^{-4}$), respectively, and decreased nuclear PER2 from 42.7 ± 5.5 to 28.7 ± 3.8% ($p = 3.0 \times 10^{-4}$) and 30.5 ± 4.2% ($p = 1.8 \times 10^{-4}$), respectively (**Figure 4A**), showing the same tendency when treated by FK866 (**Figure 2A**). Both 10 mM NAM and 5 μM EX-527 were confirmed to be effective to inhibit SIRT1 deacetylate activity against BMAL1 (Nakahata et al., 2008; **Supplementary Figures 2A,B**). However, the PARP1 inhibitor, PJ34 (Abdelkarim et al., 2001), did not change both cytoplasmic and nuclear PER2 populations [17.3 ± 3.8% (p = 0.56) and 54.6 ± 3.3% (p = 0.10), respectively] (**Figure 4**), and even 10 μM PJ34 was confirmed to be effective to reduce poly-ADP-ribosylation (**Supplementary Figure 2C**). As FK866 treatment attenuated the amplitude of *Bmal1*-luc circadian oscillation (**Figures 1D,E**), we further investigated whether SIRT1 deacetylation activity is involved in the regulation of amplitude of *Bmal1*-luc circadian oscillation. NAM or EX-527 treatment attenuated the amplitude of *Bmal1*-luc circadian oscillation (**Figures 4B,C,E**). Intriguingly, a delayed phase was observed only in cells treated with 10 mM NAM, the concentration at which the enzymatic activity of SIRT1 and also others such as SIRT2 and PARP1 is inhibited (Virág and Szabó, 2002; Peck et al., 2010). However, a delayed phase was not observed in cells treated with 5 μM EX-527, the concentration at which the enzymatic activity of SIRT1 is specifically inhibited (Peck et al., 2010), suggesting that SIRT1 deacetylation activity is involved in the amplitude regulation and other enzymes inhibited by NAM are involved in the phase regulation. *Sirt1*-knockdown cells also demonstrated the attenuated *Bmal1*-luc amplitude, but not a delayed phase (**Figure 4D**). Knockdown efficiencies against *Sirt1* and circadian oscillation patterns of other *Sirt1* knockdown cell lines are shown in **Supplementary Figure 9**. These results demonstrate that the NAD$^+$/SIRT1 axis regulates PER2 subcellular localization, which further affects the amplitude of the circadian clock.

To further investigate whether the acetylation status of lysine 680 residue of PER2, where PER2 is acetylated and deacetylated by SIRT1 (Levine et al., 2020), affects its subcellular localization, we analyzed subcellular localizations of lysine 680 residue mutants of PER2 (**Figure 5**). Non-acetyl mimetic PER2^{K680R} mutant only slightly increased in the cytoplasmic population of PER2, compared with the cytoplasmic population of PER2^{WT} (p = 0.010). Moreover, acetyl mimetic PER2^{K680Q} had no effect on PER2 subcellular localization. These mutant PER2 experiments suggest that K680 of PER2 is not the responsible lysine to regulate subcellular localization by SIRT1, although we cannot deny the possibility that acetyl mimetic mutant of PER2^{K680Q} does not completely substitute the functions of acetyl-K680 of PER2.

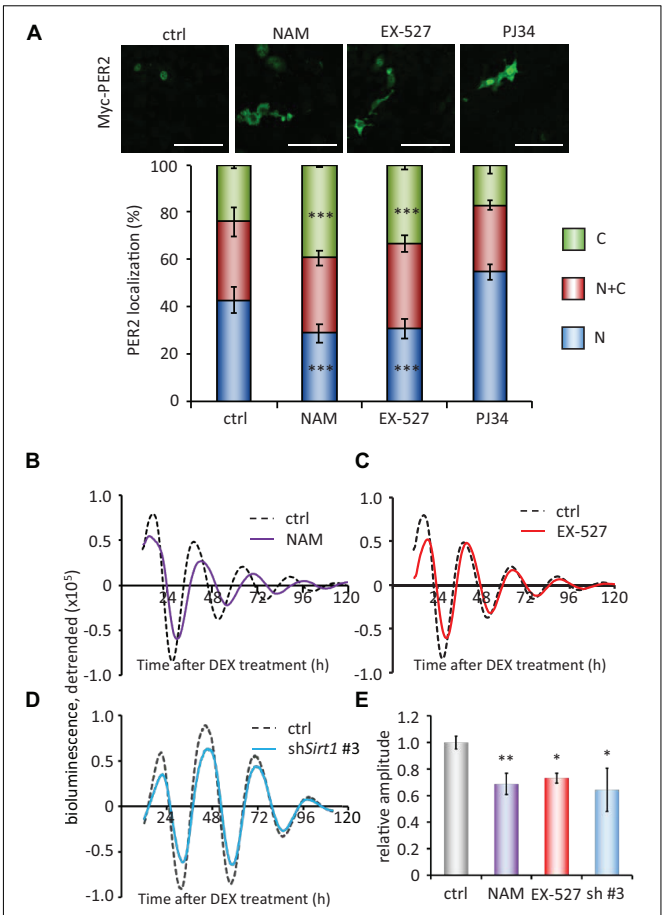

FIGURE 4 | SIRT1 inhibitors, but not PARP1 inhibitor, regulate PER2 localization and attenuate the amplitude. **(A)** NIH3T3 cells expressing Myc-PER2 were immunostained with antibody to Myc. Cells were either untreated (ctrl), treated with 10 mM nicotinamide (NAM), 5 μM EX-527 or 10 μM PJ34 (top). The representative images were captured by a confocal laser scanning microscope. White scale bars represent 100 μm. (Bottom) Subcellular localizations were quantified; N, nucleus; C, cytoplasm; N + C, both nucleus and cytoplasm. The data represented are the mean ± SEM of independent three samples. ***$p < 0.001$, compared to each subcellular localization in control (ctrl) cells by Student's two-tailed t test. **(B,C)** *Bmal1*-luc oscillation patterns in NIH3T3 cells treated with either NAM or EX-527 were monitored by using a real-time luciferase monitoring system. One representative result is shown for each condition. **(D)** *Bmal1*-luc oscillation patterns in WT (ctrl) or *Sirt1* knockdown (sh*Sirt1* #3) NIH3T3 cells were monitored by using a real-time luciferase monitoring system. One representative result is shown for each condition. **(E)** Relative amplitudes were analyzed. The value of control (ctrl) was set to 1. The data represented are the mean ± SEM of independent 8, 5, 3 or 3 samples for the control, NAM, EX-627, or sh*Sirt1* #3, respectively. *$p < 0.05$, **$p < 0.01$, compared to the control (ctrl) by Student's two-tailed t-test.

DISCUSSION

In this study, we found that low intracellular NAD$^+$, which was induced by the pharmacological inhibition of NAMPT, promoted PER2 subcellular localization from the nucleus to the cytoplasm and increased and decreased the expressions of E-box- and RORE-regulated circadian genes, respectively, leading to

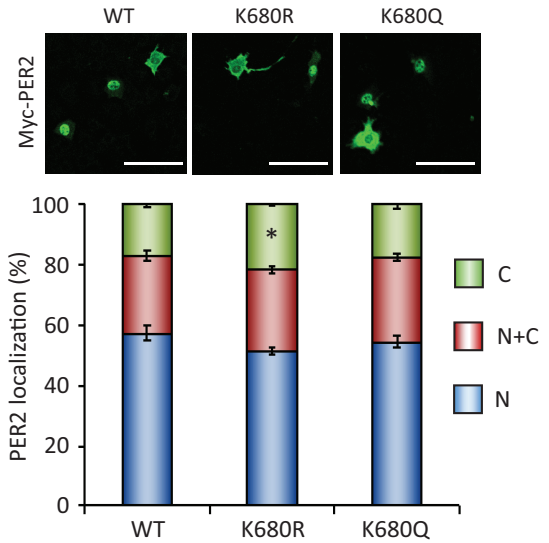

FIGURE 5 | PER2^{K680} mutants have no effects on PER2 subcellular localizations. NIH3T3 cells expressing either Myc-PER2-WT (WT), Myc-PER2^{K680R} (KR) or Myc-PER2^{K680Q} (KQ) were immunostained with antibody to Myc (top). The representative images were captured by a confocal laser scanning microscope. White scale bars represent 100 μm. (bottom) Subcellular localizations were quantified; N, nucleus; C, cytoplasm; N + C, both nucleus and cytoplasm. The data represented are the mean ± SEM of three independent samples. *$p < 0.05$, compared to each subcellular localization in WT cells by Student's two-tailed *t*-test.

the attenuated *Bmal1*-luc circadian oscillation. Furthermore, we demonstrated that SIRT1 was responsible for NAD$^+$-dependent PER2 subcellular regulation, and suggested that lysine 680 residue on PER2 is not responsible for SIRT1-regulated PER2 subcellular localization.

Since several lines of evidence indicate that a decline in NAD$^+$ is a hallmark of senescence/aging (Braidy et al., 2011; Yoshino et al., 2011; Canto et al., 2012; Massudi et al., 2012; Camacho-Pereira et al., 2016; Zhang et al., 2016; Khaidizar et al., 2017), in this study, we used NAMPT inhibitors, FK866 and GMX1778, to reduce intracellular NAD$^+$, which, we expect, mimics cellular senescence. However, many other physiological events and metabolites such as AMP/ATP ratio and polyamines are known to be changed with senescence/aging (James et al., 2015; Zwighaft et al., 2015). An increase in the AMP/ATP ratio promotes AMP-activated protein kinase (AMPK), which acts as a sensor of the reduced energetic state and further activates catabolic pathways while inhibiting anabolic ones (Hardie, 2003; Garcia and Shaw, 2017). Meanwhile, it has been reported that mTOR, which is an intracellular nutrient sensor for high cellular energy state and associated with autophagy, is also upregulated during senescence (Herranz et al., 2015; Laberge et al., 2015; Nacarelli and Sell, 2017). These signaling molecules have been reported to be involved in the circadian clock. AMPK is a rhythmically expressed kinase and phosphorylates CK1ε, resulting in enhanced phosphorylation and degradation of PER2 (Um et al., 2007; Sahar and Sassone-Corsi, 2012) and CRY1 (Lamia et al., 2011; Sahar and Sassone-Corsi, 2012; Jordan and Lamia, 2013). mTOR perturbation, such as RNAi knockdown or mTOR inhibitors, alters circadian rhythms in fibroblast, SCN, and animal behaviors (Zhang et al., 2009; Ramanathan et al., 2018). Several lines of evidence mentioned here imply that the altered aforementioned signaling pathways during senescence may affect circadian clock properties, although it is largely unknown whether these pathways alter circadian clock properties in senescent cells. We recently demonstrated that altered circadian properties such as period extension and phase delay occur in senescent human cells (Ahmed et al., 2019, 2021). Therefore, we assume that these circadian alterations in senescent cells will be useful indexes to evaluate whether low NAD$^+$ or other conditions are sufficient for the circadian clock to mimic senescent condition.

Real-time luciferase monitoring assay revealed that the attenuated amplitude of *Bmal1*-luc oscillations was observed by either NAMPT inhibitors, FK866 and GMX1778; Sirtuins and PARPs broad inhibitor, NAM; SIRT1-specific inhibitor, EX-527; or *Sirt1* knockdown. However, the delayed phase of *Bmal1*-luc oscillations was not observed by SIRT1-specific inhibitor, EX-527, or *Sirt1* knockdown. These results indicate that SIRT1 deacetylation activity is involved in amplitude regulation, but not in phase regulation. This is supported by the report that circadian profiles of *Dbp* and *Per2* in *Sirt1*$^{-/-}$ cells showed higher amplitude and no delayed phase (Nakahata et al., 2008). In contrast, delayed phases were observed with FK866, GMX1778, or NAM treatment, suggesting that NAD$^+$-dependent enzymes other than SIRT1 are involved in the phase regulation. The investigation to address which enzyme is associated with phase regulation will be needed to understand the mechanisms of how circadian clocks work in senescent cells. Actually, we have recently shown that senescent cells possess altered circadian clocks with a prolonged period and delayed phase (Ahmed et al., 2019, 2021).

In this study, we investigated whether acetylation of lysine 680 residue on PER2 is responsible for PER2 subcellular localization; however, neither acetyl mimetic mutant (K680Q) nor non-acetyl mimetic mutant (K680R) of PER2 changed subcellular localization such as low NAD$^+$ or SIRT1 inhibitor-treated conditions. Levine and coworkers recently reported that PER2 is acetylated on K680, which is deacetylated by SRIT1; furthermore, FK866 treatment increases PER2 phosphorylation at numerous sites (Levine et al., 2020). This suggests that acetylation of K680 or other lysine residues of PER2 might be a trigger for subsequent phosphorylation(s), which might determine PER2 subcellular localization. Our current results cannot deny the possibility that acetyl mimetic mutant PER2^{K680Q} may not trigger subsequent phosphorylation(s) because of differences of three-dimensional structures triggered by the acetylated form of lysine residue and substituted glutamine residue. Further experiments including structural biological experiments will be needed to elucidate which lysine residue is responsible for subcellular localization of PER2 regulated by SIRT1.

Our current results suggest that PER/CRY-dependent repression against E-box-regulated genes might be dependent on the NAD$^+$/SIRT1 axis. Intriguingly, we have reported that SIRT1 deacetylates lysine 9/14 residues of histone H3 on the promoters of E-box-regulated genes to repress their

expressions epigenetically (Nakahata et al., 2008). These results imply that the NAD$^+$/SIRT1 axis coordinates the transcriptional repression of E-box-regulated genes by different ways. In addition to the coordinated mechanisms for E-box-regulated genes, RORE-regulated genes might also be coordinated by the NAD$^+$/SIRT1 axis. It has been reported that NAD$^+$ activates *Bmal1* transcription by SIRT1 through the deacetylation of PGC1α (Chang and Guarente, 2014), while we demonstrated in this study that the low NAD$^+$ condition increased *Rev-erbα/β* which in turn might repress *Bmal1* gene expression. These coordinated *Bmal1* gene regulations by the NAD$^+$/SIRT1 axis presumably regulate the amplitude of *Bmal1* circadian oscillation, namely the low NAD$^+$ condition or decreased SIRT1 activity attenuates the amplitude of *Bmal1* circadian oscillation. Therefore, these coordinated transcriptional regulations of E-box- and RORE-regulated circadian genes by the NAD$^+$/SIRT1 axis might interlock circadian negative feedback loops.

In addition to our finding that low NAD$^+$ retains PER2 in the cytoplasm, some studies have demonstrated that the NAD$^+$/SIRT1 axis regulates PER2 properties; PER2 in *Sirt1*$^{-/-}$ cells is more stable (Asher et al., 2008) and localizes predominantly in the nucleus (Levine et al., 2020), while PER2 in nicotinamide-treated cells localizes predominantly in the cytoplasm (Miki et al., 2012). Our pharmacologically conducted results were consistent with the results pharmacologically performed by Miki and colleagues, but not with the results performed genetically. These conflicting results by pharmacological (acute) and genetical (chronic) approaches suggest the possibility that responses of molecular clock are different at early and chronic senescence/aging phases. This possibility is worth verifying so further experiments using different stages of senescent cells/aging animals will be needed to reveal this possibility.

DATA AVAILABILITY STATEMENT

The raw data supporting the conclusions of this article will be made available by the authors, without undue reservation.

AUTHOR CONTRIBUTIONS

AA performed and analyzed the experiments. YN designed the research and wrote the manuscript. TS, YuF, HY, and YoF provided the reagents. KS assisted with the experiments and reviewed the manuscript. TM and YB designed the research and reviewed the manuscript. All authors contributed to the article and approved the submitted version.

FUNDING

This work was supported by the JSPS KAKENHI Grant Number 17K08569 (YN).

ACKNOWLEDGMENTS

We thank Dr. R. Ahmed for her critical comments on the manuscript.

SUPPLEMENTARY MATERIAL

The Supplementary Material for this article can be found online at: https://www.frontiersin.org/articles/10.3389/fnins.2021.647589/full#supplementary-material

Supplementary Figure 1 | Representative Immunofluorescence images. N, nucleus; C, cytoplasm; N + C, nuclear and cytoplasm. We interpreted a result for nuclear localization of PER2/CRY1 (N) as positive when fluorescence intensity (Alexa Fluor Plus 488) of PER2/CRY1 signal that overlapped with Hoechst 33342 signal was higher than the fluorescence intensity of PER2/CRY1 in the cytoplasm Meanwhile, we interpreted a result for cytoplasmic localization of PER2/CRY1 (C) as positive when PER2/CRY1 signal that did not overlap with Hoechst 33342 signal exhibited higher fluorescence intensity than PER2/CRY1 signal intensity that overlapped with Hoechst 33342 signal. Finally, we interpreted a result for nuclear and cytoplasm localization of PER2/CRY1 (N + C) as positive when PER2/CRY1 fluorescence signal at both nucleus and cytoplasm had the same intensities.

Supplementary Figure 2 | Confirmations of inhibitors by western blotting. **(A)** NIH3T3 cells were treated with FK866 or EX-527 at indicated concentrations for 24 h. Total cell extracts were immunoblotted with antibodies against acetylated form of BMAL1 (Ac-BMAL1) or BMAL1. **(B)** NIH3T3 cells were treated with 10 mM NAM for 24 h. Total cell extracts from NIH3T3 (left and middle lanes) and mouse embryonic fibroblast derived from *Sirt1*$^{-/-}$ without any treatment (right lane) were immunoblotted with antibodies against acetylated form of BMAL1 (Ac-BMAL1) or BMAL1. **(C)** NIH3T3 cells were treated with 10 μM PJ34 for 24 h. Total cell extracts were immunoblotted with antibodies against poly ADP-ribosylation (PAR/pADPr), PARP1 or TUBLIN.

Supplementary Figure 3 | GMX1778 decreases in NAD$^+$ in cells. **(A)** NAD$^+$ amount after 24 h treatment of GMX1778 at indicated concentrations were measured by HPLC. NAD$^+$ amount was normalized by protein amount. **(B)** NAD$^+$ amount after 24 h treatment of 75 nM GMX1778 with or without 1mM NMN were measured by HPLC. NAD$^+$ amount was normalized by protein amount. **(C)** *Bmal1*-luc oscillation patterns treated with GMX1778 with or without NMN were monitored by using a real-time luciferase monitoring system. **(D)** Relative amplitudes were analyzed. The value of control (ctrl) was set to 1. All data represented in **Supplementary Figure 3** are the mean ± SEM of independent three samples. $^{**}p < 0.01$ and $^{***}p < 0.001$, compared to each of the untreated control by Student's two-tailed *t*-test, n.s., means not significant.

Supplementary Figure 4 | Effects of FK866 or GMX1778 on intracellular NAD$^+$ amount. NIH3T3 were treated with NAMPT inhibitors, FK866 or GMX1778, throughout this experiment.

Supplementary Figure 5 | FK866 has no effect on stabilities of clock proteins. NIH3T3 cells expressing Myc-CLOCK **(A)**, Myc-BMAL1 **(B)**, Myc-PER2 **(C),** or Myc-CRY1 **(D)** were treated with cycloheximide (CHX) at 100 μg/ml. At indicated times, cells were lysed and protein extracts were immunoblotted with antibody to Myc (top) and antibody to Tubulin (middle) as loading control. Cells were either untreated (ctrl) or treated with 7.5 nM FK866. The results are representative of three independent experiments. (Bottom) The immunoblots were quantified by densitometric analysis. The graph shows the percentage of protein amount relative to time 0 (100%). Myc-tagged proteins were normalized by each Tubulin amount.

Supplementary Figure 6 | FK866 has no effect on subcellular localizations of CLOCK, BMAL1, RORα/γ and REV-ERVα/β. NIH3T3 cells expressing Myc-CLOCK **(A)**, Myc-BMAL1 **(B)**, Flag-RORα **(C)**, Flag-RORγ **(D)**, Flag-REV-ERBα **(E)**, or Flag-REV-ERBβ **(F)** were immunostained with antibody to Myc or DDDDK (top). Cells were untreated (ctrl), treated with 7.5 nM FK866 (FK) or 7.5 nM FK866 & 1 mM NMN (FK + NMN). The representative images were captured by a confocal laser scanning microscope. (bottom) Subcellular localizations were quantified; N, nucleus; C, cytoplasm; N + C, both nucleus and

cytoplasm. White scale bars represent 100 μm. The data represented are the mean ± SEM of three independent samples.

Supplementary Figure 7 | GMX1778 changes PER2 subcellular localization, which is abrogated by co-treatment with NMN. (top) NIH3T3 cells expressing indicated Myc-PER2 were immunostained with antibody to Myc. Cells were untreated (ctrl), treated with 75 nM GMX1778 (GMX) or 75 nM GMX1778 & 1 mM NMN (GMX + NMN). The representative images were captured by a confocal laser scanning microscope. White scale bars represent 100 μm. (bottom) Subcellular localizations were quantified; N, nucleus; C, cytoplasm; N + C, both nucleus and cytoplasm. The data represented are the mean ± SEM of three independent samples. $^{***}p < 0.001$, compared to each subcellular localization in control cells by Student's two-tailed *t*-test.

Supplementary Figure 8 | CRY1 did not alter PER2 subcellular localization. **(A)** Subcellular localizations of either PER2-WT, PER2-NLS, or PER2-NES were quantified; N, nucleus; C, cytoplasm; N + C, both nucleus and cytoplasm. **(B)** Subcellular localizations of either PER2-WT, PER2-NLS, or PER2-NES were quantified when CRY1 was co-expressed. The data represented are the mean ± SEM of three independent samples. $^{*}p < 0.05$, $^{**}p < 0.01$, and $^{***}p < 0.001$, compared to each subcellular localization in cells expressing PER2-WT by Student's two-tailed *t*-test.

Supplementary Figure 9 | *Sirt1* knockdown attenuates the amplitude of *Bmal1*-luc oscillation. **(A)** Knockdown efficiencies against *Sirt1* were analyzed by qPCR. *Sirt1* amount in control (scramble) was set to 1. The data represented are the mean ± SEM of independent three samples. **(B)** *Bmal1*-luc oscillation patterns in *Sirt1* knockdown (sh*Sirt1* #1 or #2) NIH3T3 cells were monitored by using a real-time luciferase monitoring system. **(C)** Relative amplitudes were analyzed. The value of control (ctrl) was set to 1. The data represented are the mean ± SEM of independent 8, 3, or 3 samples for control, sh*Sirt1* #1 or #2, respectively. $^{**}p < 0.01$, compared to control cells by Student's two-tailed *t*-test, n.s., means not significant.

Supplementary Table 1 | Primer sequences for qPCR.

Supplementary Table 2 | Oligonucleotide sequences for knockdown against *Sirt1*.

REFERENCES

Abdelkarim, G. E., Gertz, K., Harms, C., Katchanov, J., Dirnagl, U., Szabó, C., et al. (2001). Protective effects of PJ34, a novel, potent inhibitor of poly(ADP-ribose) polymerase (PARP) in in vitro and in vivo models of stroke. *Int. J. Mol. Med.* 7, 255–260.

Ahmed, R., Ashimori, A., Iwamoto, S., Matsui, T., Nakahata, Y., and Bessho, Y. (2019). Replicative senescent human cells possess altered circadian clocks with a prolonged period and delayed peak-time. *Aging* 11, 950–973. doi: 10.18632/aging.101794

Ahmed, R., Nakahata, Y., Shinohara, K., and Bessho, Y. (2021). Cellular senescence triggers altered circadian clocks with a prolonged period and delayed phases. *Front. Neurosci.* 15:638122. doi: 10.3389/fnins.2021.638122

Akashi, M., and Takumi, T. (2005). The orphan nuclear receptor RORalpha regulates circadian transcription of the mammalian core-clock Bmal1. *Nat. Struct. Mol. Biol.* 12, 441–448. doi: 10.1038/nsmb925

Akashi, M., Okamoto, A., Tsuchiya, Y., Todo, T., Nishida, E., and Node, K. (2014). A positive role for period in mammalian circadian gene expression. *Cell Rep.* 7, 1056–1064. doi: 10.1016/j.celrep.2014.03.072

Albrecht, U., Bordon, A., Schmutz, I., and Ripperger, J. (2007). The multiple facets of Per2. *Cold Spring Harb Symp. Quant. Biol.* 72, 95–104. doi: 10.1101/sqb.2007.72.001

Asher, G., Gatfield, D., Stratmann, M., Reinke, H., Dibner, C., Kreppel, F., et al. (2008). SIRT1 regulates circadian clock gene expression through PER2 deacetylation. *Cell* 134, 317–328. doi: 10.1016/j.cell.2008.06.050

Asher, G., Reinke, H., Altmeyer, M., Gutierrez-Arcelus, M., Hottiger, M. O., and Schibler, U. (2010). Poly(ADP-ribose) polymerase 1 participates in the phase entrainment of circadian clocks to feeding. *Cell* 142, 943–953. doi: 10.1016/j.cell.2010.08.016

Aujard, F., Herzog, E. D., and Block, G. D. (2001). Circadian rhythms in firing rate of individual suprachiasmatic nucleus neurons from adult and middle-aged mice. *Neuroscience* 106, 255–261. doi: 10.1016/s0306-4522(01)00285-8

Bitterman, K. J., Anderson, R. M., Cohen, H. Y., Latorre-Esteves, M., and Sinclair, D. A. (2002). Inhibition of silencing and accelerated aging by nicotinamide, a putative negative regulator of yeast sir2 and human SIRT1. *J. Biol. Chem.* 277, 45099–45107. doi: 10.1074/jbc.M205670200

Braidy, N., Guillemin, G. J., Mansour, H., Chan-Ling, T., Poljak, A., and Grant, R. (2011). Age related changes in NAD+ metabolism oxidative stress and Sirt1 activity in wistar rats. *PLoS One* 6:e19194. doi: 10.1371/journal.pone.0019194.t001

Camacho-Pereira, J., Tarrago, M. G., Chini, C. C., Nin, V., Escande, C., Warner, G. M., et al. (2016). CD38 dictates age-related NAD decline and mitochondrial dysfunction through an SIRT3-dependent mechanism. *Cell Metab.* 23, 1127–1139. doi: 10.1016/j.cmet.2016.05.006

Campbell, M. K. (1995). *Biochemistry*, 2nd Edn. Philadelphia: Saunders College Publishing.

Canto, C., Houtkooper, R. H., Pirinen, E., Youn, D. Y., Oosterveer, M. H., Cen, Y., et al. (2012). The NAD(+) precursor nicotinamide riboside enhances oxidative metabolism and protects against high-fat diet-induced obesity. *Cell Metab.* 15, 838–847. doi: 10.1016/j.cmet.2012.04.022

Chang, H. C., and Guarente, L. (2014). SIRT1 and other sirtuins in metabolism. *Trends Endocrinol. Metab.* 25, 138–145. doi: 10.1016/j.tem.2013.12.001

Custodero, C., Saini, S. K., Shin, M. J., Jeon, Y. K., Christou, D. D., McDermott, M. M., et al. (2020). Nicotinamide riboside-A missing piece in the puzzle of exercise therapy for older adults? *Exp. Gerontol.* 137:110972. doi: 10.1016/j.exger.2020.110972

Doi, M., Hirayama, J., and Sassone-Corsi, P. (2006). Circadian regulator CLOCK is a histone acetyltransferase. *Cell* 125, 497–508. doi: 10.1016/j.cell.2006.03.033

Garcia, D., and Shaw, R. J. (2017). AMPK: mechanisms of cellular energy sensing and restoration of metabolic balance. *Mol. Cell* 66, 789–800. doi: 10.1016/j.molcel.2017.05.032

Gomes, A. P., Price, N. L., Ling, A. J., Moslehi, J. J., Montgomery, M. K., Rajman, L., et al. (2013). Declining NAD(+) induces a pseudohypoxic state disrupting nuclear-mitochondrial communication during aging. *Cell* 155, 1624–1638. doi: 10.1016/j.cell.2013.11.037

Hardie, D. G. (2003). Minireview: the AMP-activated protein kinase cascade: the key sensor of cellular energy status. *Endocrinology* 144, 5179–5183. doi: 10.1210/en.2003-0982

Hasmann, M., and Schemainda, I. (2003). FK866, a highly specific noncompetitive inhibitor of nicotinamide phosphoribosyltransferase, represents a novel mechanism for induction of tumor cell apoptosis. *Cancer Res.* 63, 7436–7442.

Herranz, N., Gallage, S., Mellone, M., Wuestefeld, T., Klotz, S., Hanley, C. J., et al. (2015). mTOR regulates MAPKAPK2 translation to control the senescence-associated secretory phenotype. *Nat. Cell Biol.* 17, 1205–1217. doi: 10.1038/ncb3225

Hirayama, J., Sahar, S., Grimaldi, B., Tamaru, T., Takamatsu, K., Nakahata, Y., et al. (2007). CLOCK-mediated acetylation of BMAL1 controls circadian function. *Nature* 450, 1086–1090. doi: 10.1038/nature06394

Hong, W., Mo, F., Zhang, Z., Huang, M., and Wei, X. (2020). Nicotinamide mononucleotide: a promising molecule for therapy of diverse diseases by targeting NAD+ metabolism. *Front. Cell Dev. Biol.* 8:246. doi: 10.3389/fcell.2020.00246

Imai, S. (2010). "Clocks" in the NAD World: NAD as a metabolic oscillator for the regulation of metabolism and aging. *Biochim. Biophys. Acta* 1804, 1584–1590. doi: 10.1016/j.bbapap.2009.10.024

Imai, S., and Guarente, L. (2014). NAD+ and sirtuins in aging and disease. *Trends Cell Biol.* 24, 464–471. doi: 10.1016/j.tcb.2014.04.002

James, E. L., Michalek, R. D., Pitiyage, G. N., de Castro, A. M., Vignola, K. S., Jones, J., et al. (2015). Senescent human fibroblasts show increased glycolysis and redox homeostasis with extracellular metabolomes that overlap with those of irreparable DNA damage, aging, and disease. *J. Proteome Res.* 14, 1854–1871. doi: 10.1021/pr501221g

Jordan, S. D., and Lamia, K. A. (2013). AMPK at the crossroads of circadian clocks and metabolism. *Mol. Cell Endocrinol.* 366, 163–169. doi: 10.1016/j.mce.2012.06.017

Khaidizar, F. D., Nakahata, Y., Kume, A., Sumizawa, K., Kohno, K., Matsui, T., et al. (2017). Nicotinamide phosphoribosyltransferase delays cellular senescence by upregulating SIRT1 activity and antioxidant gene expression in mouse cells. *Genes Cells* 22, 982–992. doi: 10.1111/gtc.12542

Kolker, D. E., Vitaterna, M. H., Fruechte, E. M., Takahashi, J. S., and Turek, F. W. (2004). Effects of age on circadian rhythms are similar in wild-type and heterozygous Clock mutant mice. *Neurobiol. Aging* 25, 517–523. doi: 10.1016/j.neurobiolaging.2003.06.007

Kunieda, T., Minamino, T., Katsuno, T., Tateno, K., Nishi, J., Miyauchi, H., et al. (2006). Cellular senescence impairs circadian expression of clock genes in vitro and in vivo. *Circ. Res.* 98, 532–539. doi: 10.1161/01.RES.0000204504.25798.a8

Laberge, R. M., Sun, Y., Orjalo, A. V., Patil, C. K., Freund, A., Zhou, L., et al. (2015). MTOR regulates the pro-tumorigenic senescence-associated secretory phenotype by promoting IL1A translation. *Nat. Cell Biol.* 17, 1049–1061. doi: 10.1038/ncb3195

Lamia, K. A., Papp, S. J., Yu, R. T., Barish, G. D., Uhlenhaut, N. H., Jonker, J. W., et al. (2011). Cryptochromes mediate rhythmic repression of the glucocorticoid receptor. *Nature* 480, 552–556. doi: 10.1038/nature10700

Lee, C., Etchegaray, J. P., Cagampang, F. R., Loudon, A. S., and Reppert, S. M. (2001). Posttranslational mechanisms regulate the mammalian circadian clock. *Cell* 107, 855–867. doi: 10.1016/s0092-8674(01)00610-9

Levine, D. C., Hong, H., Weidemann, B. J., Ramsey, K. M., Affinati, A. H., Schmidt, M. S., et al. (2020). NAD(+) controls circadian reprogramming through PER2 nuclear translocation to counter aging. *Mol. Cell* 78, 835–849.e7. doi: 10.1016/j.molcel.2020.04.010

Masri, S., Rigor, P., Cervantes, M., Ceglia, N., Sebastian, C., Xiao, C., et al. (2014). Partitioning circadian transcription by SIRT6 leads to segregated control of cellular metabolism. *Cell* 158, 659–672. doi: 10.1016/j.cell.2014.06.050

Massudi, H., Grant, R., Braidy, N., Guest, J., Farnsworth, B., and Guillemin, G. J. (2012). Age-associated changes in oxidative stress and NAD+ metabolism in human tissue. *PLoS One* 7:e42357. doi: 10.1371/journal.pone.0042357

Miki, T., Xu, Z., Chen-Goodspeed, M., Liu, M., Van Oort-Jansen, A., Rea, M. A., et al. (2012). PML regulates PER2 nuclear localization and circadian function. *EMBO J.* 31, 1427–1439. doi: 10.1038/emboj.2012.1

Mouchiroud, L., Houtkooper, R. H., and Auwerx, J. (2013). NAD(+) metabolism: a therapeutic target for age-related metabolic disease. *Crit. Rev. Biochem. Mol. Biol.* 48, 397–408. doi: 10.3109/10409238.2013.789479

Nacarelli, T., and Sell, C. (2017). Targeting metabolism in cellular senescence, a role for intervention. *Mol. Cell Endocrinol.* 455, 83–92. doi: 10.1016/j.mce.2016.08.049

Nakahata, Y., and Bessho, Y. (2016). The circadian NAD+ metabolism: impact on chromatin remodeling and aging. *BioMed. Res. Int.* 2016:3208429. doi: 10.1155/2016/3208429

Nakahata, Y., Kaluzova, M., Grimaldi, B., Sahar, S., Hirayama, J., Chen, D., et al. (2008). The NAD+-dependent deacetylase SIRT1 modulates CLOCK-mediated chromatin remodeling and circadian control. *Cell* 134, 329–340. doi: 10.1016/j.cell.2008.07.002

Nakahata, Y., Sahar, S., Astarita, G., Kaluzova, M., and Sassone-Corsi, P. (2009). Circadian control of the NAD+ salvage pathway by CLOCK-SIRT1. *Science* 324, 654–657. doi: 10.1126/science.1170803

Nakamura, T. J., Nakamura, W., Tokuda, I. T., Ishikawa, T., Kudo, T., Colwell, C. S., et al. (2015). Age-related changes in the circadian system unmasked by constant conditions. *eNeuro* 2. doi: 10.1523/ENEURO.0064-15.2015 [Epub ahead of print].

Nakamura, T. J., Nakamura, W., Yamazaki, S., Kudo, T., Cutler, T., Colwell, C. S., et al. (2011). Age-related decline in circadian output. *J. Neurosci.* 31, 10201–10205. doi: 10.1523/JNEUROSCI.0451-11.2011

Napper, A. D., Hixon, J., McDonagh, T., Keavey, K., Pons, J. F., Barker, J., et al. (2005). Discovery of indoles as potent and selective inhibitors of the deacetylase SIRT1. *J. Med. Chem.* 48, 8045–8054.

Nuriliani, A., Nakahata, Y., Ahmed, R., Khaidizar, F. D., Matsui, T., and Bessho, Y. (2020). Over-expression of nicotinamide phosphoribosyltransferase in mouse cells confers protective effect against oxidative and ER stress-induced premature senescence. *Genes Cells* 25, 593–602. doi: 10.1111/gtc.12794

Peck, B., Chen, C. Y., Ho, K. K., Di Fruscia, P., Myatt, S. S., Coombes, R. C., et al. (2010). SIRT inhibitors induce cell death and p53 acetylation through targeting both SIRT1 and SIRT2. *Mol. Cancer Ther.* 9, 844–855. doi: 10.1158/1535-7163.MCT-09-0971

Pittendrigh, C. S., and Daan, S. (1974). Circadian oscillations in rodents: a systematic increase of their frequency with age. *Science* 186, 548–550. doi: 10.1126/science.186.4163.548

Ramanathan, C., Kathale, N. D., Liu, D., Lee, C., Freeman, D. A., Hogenesch, J. B., et al. (2018). mTOR signaling regulates central and peripheral circadian clock function. *PLoS Genet.* 14:e1007369. doi: 10.1371/journal.pgen.1007369

Ramsey, K. M., Yoshino, J., Brace, C. S., Abrassart, D., Kobayashi, Y., Marcheva, B., et al. (2009). Circadian clock feedback cycle through NAMPT-mediated NAD+ biosynthesis. *Science* 324, 651–654. doi: 10.1126/science.1171641

Revollo, J. R., Korner, A., Mills, K. F., Satoh, A., Wang, T., Garten, A., et al. (2007). Nampt/PBEF/Visfatin regulates insulin secretion in beta cells as a systemic NAD biosynthetic enzyme. *Cell Metab.* 6, 363–375. doi: 10.1016/j.cmet.2007.09.003

Sahar, S., and Sassone-Corsi, P. (2012). Regulation of metabolism: the circadian clock dictates the time. *Trends Endocrinol. Metab.* 23, 1–8. doi: 10.1016/j.tem.2011.10.005

Sellix, M. T., Evans, J. A., Leise, T. L., Castanon-Cervantes, O., Hill, D. D., DeLisser, P., et al. (2012). Aging differentially affects the re-entrainment response of central and peripheral circadian oscillators. *J. Neurosci.* 32, 16193–16202. doi: 10.1523/JNEUROSCI.3559-12.2012

Um, J. H., Yang, S., Yamazaki, S., Kang, H., Viollet, B., Foretz, M., et al. (2007). Activation of 5'-AMP-activated kinase with diabetes drug metformin induces casein kinase Iepsilon (CKIepsilon)-dependent degradation of clock protein mPer2. *J. Biol. Chem.* 282, 20794–20798. doi: 10.1074/jbc.C700070200

Valentinuzzi, V. S., Scarbrough, K., Takahashi, J. S., and Turek, F. W. (1997). Effects of aging on the circadian rhythm of wheel-running activity in C57BL/6 mice. *Am. J. Physiol.* 273, R1957–R1964.

van der Veer, E., Ho, C., O'Neil, C., Barbosa, N., Scott, R., Cregan, S. P., et al. (2007). Extension of human cell lifespan by nicotinamide phosphoribosyltransferase. *J. Biol. Chem.* 282, 10841–10845. doi: 10.1074/jbc.C700018200

Verdin, E. (2015). NAD? in aging, metabolism, and neurodegeneration. *Science* 350, 1208–1213. doi: 10.1126/science.aac4854

Virág, L., and Szabó, C. (2002). The therapeutic potential of poly(ADP-Ribose) polymerase inhibitors. *Pharmacol. Rev.* 54, 375–429. doi: 10.1124/pr.54.3.375

Watson, M., Roulston, A., Belec, L., Billot, X., Marcellus, R., Bedard, D., et al. (2009). The small molecule GMX1778 is a potent inhibitor of NAD+ biosynthesis: strategy for enhanced therapy in nicotinic acid phosphoribosyltransferase 1-deficient tumors. *Mol. Cell Biol.* 29, 5872–5888. doi: 10.1128/MCB.00112-09

Witting, W., Mirmiran, M., Bos, N. P., and Swaab, D. F. (1994). The effect of old age on the free-running period of circadian rhythms in rat. *Chronobiol. Int.* 11, 103–112. doi: 10.3109/07420529409055896

Yagita, K., Tamanini, F., van Der Horst, G. T., and Okamura, H. (2001). Molecular mechanisms of the biological clock in cultured fibroblasts. *Science* 292, 278–281. doi: 10.1126/science.1059542

Yoshino, J., and Imai, S. (2013). Accurate measurement of nicotinamide adenine dinucleotide (NAD(+)) with high-performance liquid chromatography. *Methods Mol. Biol.* 1077, 203–215. doi: 10.1007/978-1-62703-637-5_14

Yoshino, J., Baur, J. A., and Imai, S. I. (2018). NAD(+) intermediates: the biology and therapeutic potential of NMN and NR. *Cell Metab.* 27, 513–528. doi: 10.1016/j.cmet.2017.11.002

Yoshino, J., Mills, K. F., Yoon, M. J., and Imai, S. (2011). Nicotinamide mononucleotide, a key NAD(+) intermediate, treats the pathophysiology of diet- and age-induced diabetes in mice. *Cell Metab.* 14, 528–536. doi: 10.1016/j.cmet.2011.08.014

Yoshitane, H., Honma, S., Imamura, K., Nakajima, H., Nishide, S. Y., Ono, D., et al. (2012). JNK regulates the photic response of the mammalian circadian clock. *EMBO Rep.* 13, 455–461. doi: 10.1038/embor.2012.37

Zhang, E. E., Liu, A. C., Hirota, T., Miraglia, L. J., Welch, G., Pongsawakul, P. Y., et al. (2009). A genome-wide RNAi screen for modifiers of the circadian clock in human cells. *Cell* 139, 199–210. doi: 10.1016/j.cell.2009.08.031

Zhang, H., Ryu, D., Wu, Y., Gariani, K., Wang, X., Luan, P., et al. (2016). NAD+ repletion improves mitochondrial and stem cell function and enhances life span in mice. *Science* 352, 1436–1443. doi: 10.1126/science.aaf2693

Zhou, Z., Hong, E. J., Cohen, S., Zhao, W. N., Ho, H. Y., Schmidt, L., et al. (2006). Brain-specific phosphorylation of MeCP2 regulates activity-dependent Bdnf transcription, dendritic growth, and spine maturation. *Neuron* 52, 255–269. doi: 10.1016/j.neuron.2006.09.037

Zwighaft, Z., Aviram, R., Shalev, M., Rousso-Noori, L., Kraut-Cohen, J., Golik, M., et al. (2015). Circadian clock control by polyamine levels through a mechanism that declines with age. *Cell Metab.* 22, 874–885. doi: 10.1016/j.cmet.2015.09.011

Conflict of Interest: TS and YF were employed by the Mitsubishi Corporation Life Sciences Limited. The remaining authors declare that the research was conducted in the absence of any commercial or financial relationships that could be construed as a potential conflict of interest.

Advantages of publishing in Frontiers

OPEN ACCESS
Articles are free to read for greatest visibility and readership

FAST PUBLICATION
Around 90 days from submission to decision

HIGH QUALITY PEER-REVIEW
Rigorous, collaborative, and constructive peer-review

TRANSPARENT PEER-REVIEW
Editors and reviewers acknowledged by name on published articles

Frontiers
Avenue du Tribunal-Fédéral 34
1005 Lausanne | Switzerland

Visit us: www.frontiersin.org
Contact us: frontiersin.org/about/contact

REPRODUCIBILITY OF RESEARCH
Support open data and methods to enhance research reproducibility

DIGITAL PUBLISHING
Articles designed for optimal readership across devices

FOLLOW US
@frontiersin

IMPACT METRICS
Advanced article metrics track visibility across digital media

EXTENSIVE PROMOTION
Marketing and promotion of impactful research

LOOP RESEARCH NETWORK
Our network increases your article's readership